THE RELATIONSHIP BETWEEN MASTICATORY STRESS AND PROGNATHISM:

A FINITE ELEMENT AND MORPHOMETRIC STUDY

by

Michelle L. Patriquin

Submitted in fulfillment of the requirements for the degree PhD Anatomy

In the Faculty of Health Sciences

University of Pretoria

Pretoria

October 2013

Declaration

I declare that the dissertation that I am hereby submitting to the University of Pretoria for the PhD degree in Anatomy is my own work and that I have never before submitted it to any other tertiary institution for any degree.

_____
Michelle L. Patriquin

_____ day of _____ 2013

ABSTRACT

Mechanical forces, such as mastication, influence morphological characteristics of the cranium. With varying degrees of prognathism found within and between populations, the ability to accommodate masticatory stress may vary, and this will have profound effects on final craniofacial form. The purpose of this research is a two-fold examination of mid-facial prognathism in modern African males. First, an osteometric and morphological examination of specific areas of the cranium involved in the masticatory apparatus was performed, and its relationship with prognathism assessed. Second, finite element analysis (FEA) was used to interpret the distribution of stress during mastication and the contribution of prognathism to this stress distribution. Two diametrically opposed facial forms (prognathic and orthognathic) were modelled to observe variation in displacement, pressure, and Von Mises stress patterns using linear elastic homogenous isotropic material properties.

Boundary conditions simulating muscle contraction of the masseter, medial pterygoid, and temporalis were attributed to the models. A vertical compressive bite-force was applied at the left central incisor and the first molar, respectively. With the use of FEA, differences in the pattern and magnitude of Von Mises stress were noted under simulated mastication. The prognathic model consistently experienced more stress for a molar and incisal bite-force than the orthognathic model. More specifically, the prognathic model accommodated for larger areas of Von Mises stress in the regions of the zygomatic arch, nasal aperture, margins of the orbits, and in the inter-orbital area. As individual muscle forces were modeled, the temporalis and medial pterygoid caused the greatest difference in the stress at the articular eminence between the working and balancing sides. These

muscles and their forces should be further investigated to understand their role in temporomandibular joint disorders.

Several cranial dimensions were shown to increase or decrease with prognathism. The relationship between the gnathic index and facial parameters were statistically significant for nine cranial and seven dental dimensions. The orthognathic group showed a larger inter-orbital dimension with a subsequent decrease in stress in that area. The upper facial index, maxillary molar crown area and the dental arcade shape demonstrated statistically significant shape changes associated with the degree of prognathism. Morphological analysis did not show a significant distribution in browridge expression and robusticity as a means to accommodate masticatory stress. Stress distribution patterns were correlated with osteometric data and showed a significant difference in inter-orbital breadth between the two groups.

Mechanical action of mastication may influence prognathic more than orthognatic facial forms. An orthognatic facial form is biomechanically more efficient under masticatory stress. Mechanical loading during mastication greatly influences the morphological patterns of the facial skeleton. Further investigation into patterns of stress is necessary when changes to the masticatory apparatus arises from clinical involvement, trauma, or as a means to avoid or predict failure in the underlying skeletal architecture.

Table of Contents

List of Tables

APPENDICIES

List of Figures

Acknowledgements

I would like to thank the faculty and staff of the Department of Anatomy at the University of Pretoria for their help and administrative assistance during my time at the university and allowing me access to the skeletal collection. Also, I appreciated the second opportunity to collect metric and morphological data from the Raymond Dart Collection at the University of the Witwatersrand. A few specific people need to be thanked from the University of Petoria. Firstly, I want to thank Prof Becker for his help with the statistical analysis for this project and Jolandie Myburgh for her time dedicated to data collection for inter-observer error analysis. Also, I want to thank Jaco Jansen Van Rensburg for developing the digital finite element models and running the analysis. Computer tomography (CT) scans of the prognathic and orthognathic skull used in the finite element analysis were performed by Labuschagne and Partners at Little Company of Mary Hospital, Pretoria. I thank them for their contribution to this research.

Most importantly I need to thank my supervisors Prof S Kok (Department of Mechanical and Aeronautical Engineering) and Prof M Steyn (Department of Anatomy). I have known Prof Steyn for 14 years. I did my MSc with her and she allowed me the opportunity to come back to South Africa and do a PhD under her supervision. This work would not have been completed without her continued support over the years. I partially attribute both my professional and academic success to our relationship and my experience working and learning from her. I hope the future holds new projects and collaborative efforts!

CHAPTER 1

INTRODUCTION

Over the years, physical anthropologists have observed, measured and defined facial prognathism. Furthermore, the degree of facial prognathism has been applied to unknown skeletal remains as a means to differentiate among population groups. Prognathism is an important feature biomechanically because the regions that make up the sub-nasal prognathism house portions of the masticatory apparatus. Although prognathism can be observed and measured, of interest is the important sub-nasal region that includes the maxilla, mandible and teeth, which can be externally influenced by a specific diet through the process of masticatory muscle activity. Changes in facial morphology due to the degree of prognathism may cause the craniofacial skeleton to accommodate for masticatory stress in different ways and potentially dictate changes in craniofacial morphology. An important morphological characteristic, like prognathism, may be biomechanically linked to changes in the craniofacial skeleton over time. The current study examines the influences of facial prognathism on the process of mastication and other cranial dimensions and morphological characteristics of the mid-face and jaw.

Prognathism is described as the degree of projection of the mid-face away from the rest of the cranium (De Villiers, 1968). In contrast, the orthognathic facial form is described as presenting in profile with a vertical appearance, where the maxilla and mandible are set under the orbits and do not project forward. An evolutionary trend in the craniofacial form of humans has been the decrease in the projection of the sub-nasal area. Over thousands of

years, from early *Homo* to modern humans, less prognathism and a more vertically positioned facial morphology has developed. Although the orthognathic profile has become recognized as a more modern craniofacial expression, a range in the degree of expression from prognathic to orthognathic exists globally in modern populations (Lewis, 1942; Birkby, 1966; Howells, 1973; El-Najjar and McWilliams, 1978; Krogman and İşcan, 1986; İşcan and Steyn, 1999; İşcan *et al.*, 2000).

Mastication is the process involved in breaking down food into smaller pieces to increase surface area, which aids in digestion and the extraction of nutrients (Anderson and Matthews, 1976). The methods/details of mastication have changed over generations because of modifications in diet. The diet of early *Homo* was of a much harder consistency than a modern, processed diet. With the invention of fire, the tenderizing of meat and the onset of agriculture, the quality of human diets became softer and less demanding on the masticatory system (Larsen, 1995).

The components of the masticatory apparatus are teeth housed in the maxilla and mandible, muscles that move the jaws and the skull where the process takes place. The muscles of the masticatory system are used to create the action of chewing. Depending on what is being chewed, they need to exert a larger or smaller force. The areas of attachment of these muscles and the force applied to the teeth while biting creates a pattern of strain in the craniofacial skeleton. As force is applied through mastication, modifications to the bony architecture of the craniofacial skeleton must accommodate for these experienced strains.

Bone is a biological tissue, it composition and thickness altered by body processes and effects (Clarke, 2008). Where strain is larger, this may induce bone production to accommodate mechanical reaction forces, and, therefore, less strain will be experienced

over time. The areas of decreased strain may also modify in structure and undergo resorption to decrease bone density. As a consequence, an increased strain will occur in that area. Although maintaining a homeostatic state is often noted for physiological processes, in reality, bone achieves the same practice to ensure that it experiences an optimal amount of strain with the use of the least amount of material.

Variations in the facial skeleton and how it has evolved over time have been the focus of extensive research (e.g., Björk, 1950; Glanville, 1969; Wei, 1969; Robertson, 1979; Rak, 1986; Brown and Maeda, 2004; Weaver *et al.*, 2007; Lieberman, 2008; Baab *et al.*, 2010). Because of the mechanical function that the cranium has to accommodate for and the changes in morphology and complex geometry of the crania, it is difficult to attribute changes to any one process or stimulus. The variation in populations and craniofacial form through the fossil record has been attributed to geography, cold adaptation, gene flow, and mechanical factors, for example. The present study examined only the degree of prognathism, and how it has influenced other cranial measurements or morphological characteristics as it functions in mastication.

Finite element analysis is an engineering technique used examine how structures respond when external forces are applied. With the development of this powerful software, and its use in anthropological research, obtaining experimental data about stress distribution in the skull has been made more readily available. The complex, bony geometry of the skull has previously made it difficult to model. Now, using computed tomography scans and three-dimensional software, a finite element analysis can be run on dry skulls of modern humans or fossils to obtain information of the skull accommodation for strain produced through mastication.

Chapter 1
INTRODUCTION

The process of finite element analysis takes a complex structure like the skull and uses a three dimensional model consisting of a number of finite elements which represent the complex geometry with a high degree of accuracy. In model creation, the researcher defines material properties of the bone and boundary conditions, which give a realistic magnitude and direction of force for muscle attachments and imposed external forces, such as those acting on the teeth during mastication. Previous researchers have used finite element analysis to obtain strain data from human and non-human skulls and observed stress patterns in response to a determined factor (Tanne *et al.*, 1988; Motoyoshi *et al.*, 2002; Mota *et al.*, 2003; Provatidis *et al.*, 2007; Röhrle and Pullan, 2007). In general, finite element results depend on the magnitude of the force being applied, location of the force and the material properties attributed to the model itself.

How the face withstands the forces of mastication is not completely understood, and the mechanisms whereby the process of mastication produce stress in different facial forms and those with varying degrees of prognathism in modern humans has yet to be addressed. Due to the need of the facial skeleton to accommodate for strain due to mastication, it stands to reason that varying degrees of prognathism may produce different patterns of compression and tension stress, which correspond to the structural differences in geometry.

The aims of this project were to record osteometric and morphological data from three distinct facial form groups (orthognathic, mesognathic, prognathic) in order to determine size and shape differences among the groups. Two skulls representing opposite ends of the prognathic scale were chosen from the data set to undergo finite element analysis, while simulating a molar and incisor bite force. Patterns of stress, the specific areas where the stress was observed, and its magnitude were compared between the two facial

forms. The results of the finite element analysis, along with the metric and morphological data, were used to interpret observations and draw conclusions with regard to the morphological characteristics of the skull related to changes in prognathism and to interpret which of these are related to masticatory stress.

The following hypotheses were tested:

A. Null hypothesis: The location and magnitude of the bone strain in the crania of the prognathic facial form will be identical to that in the orthognathic facial form. This hypothesis will be rejected if finite element analysis indicates significantly different strain patterns between prognathic and orthognathic crania.

B. Null hypothesis: No relationship exists between degree of prognathism and other cranial characteristics such as the size of the teeth, the degree of development of the brow ridges and cranial shape. This hypothesis will be rejected if statistically significant differences (in the case of size-based characteristics) and significant correlations (in the case of morphological characteristics) are found.

CHAPTER 2

LITERATURE REVIEW

Mastication involves the collaborative effort of several elements of the skull and the coordinated contraction and relaxation of the associated muscles. Several factors affect the efficiency and the forces applied through the cycles of mastication. Characteristics such as strength of the masticatory muscles, their attachment sites and how they influence the underlying architecture of bone, craniofacial morphology, teeth and changes made to accommodate the mechanical needs of the system all need to be investigated in order to understand the process of mastication. The following literature review focuses on the morphology of the skull of modern human populations and addresses these and other elements of mastication and craniofacial morphology individually. Finally, a description of the finite element analysis method is included with examples of how this powerful modeling tool is being widely used in current biological anthropology research.

2.1 BONE

Bone is a complex living tissue that has the ability, like other tissues, to change, repair and modify its structure. Bone functions in support, protection, as a system of levers for movement, blood production and as a calcium reserve (Young *et al.*, 2006; Silverthorn, 2007; DiGangi and Moore 2013). Development and growth of the bones takes place in either of two ways: intramembranous ossification or endochondral ossification. Endochondral ossification is found in the formation of the long bones (i.e. femur, humerus), however, the flat bones and those of the skull are formed through the process of

intramembranous ossification. A precursor to the development of this type of bone is the fibrous membrane of periosteum where the cells which perform osteogenesis are found. This membrane contains the cells responsible for bone formation (osteoblasts) and bone resorption (osteoclasts). The osteoblasts are found in a continuous layer on bone surfaces, performing deposition to function in the reconstruction and remodelling of bone, whereas osteoclasts are initiated in response to a decrease in use and/or strain and begin remodelling through resorption (Cowin, 1989; White, 2000).

There are two types of bone in the human skeleton, a spongy bone in appearance called trabecular bone, and a hard compact bone known as cortical bone. Both types of bone vary structurally and in their primary functions. Their specific structure is related to their function where the hard compact bone provides a mechanical and protective function throughout the skeleton and the trabecular bone serves in a metabolic capacity (Cullinane and Einhorn, 2002). When looking at the flat bones of the skull, it is easy to see the hard cortical bone located on the outer surfaces and sandwiched between is the softer trabecular bone.

The bones of the skull are deformable and can be acted on by forces. In response to these forces over time bone can begin remodelling to a stress history (Frost, 2003; Ruff *et al.*, 2006). Depending on the activities, the stimulus will initiate an increase in bone formation where there is a deployment of a new bone matrix and/or a resorption of existing bone (Figure 1). Regardless of its creation or destruction, bone must remodel in order to efficiently and successfully support the loads to which it is being continuously exposed.

Postnatal ontogeny is characterized by shape changes which occur between birth and adulthood. These shape changes occur, in part, in response to the mechanical demands

which initiate the remodelling of bone surfaces of the craniofacial skeleton (Cobb and O'Higgins, 2004). For example, the growth and change in the maxilla over time is dictated by the eruption of dentition as well as by the forces of mastication. The growth of the maxilla is directed forward to accommodate the changing dentition. The consistent growth and remodelling of the maxilla during this time causes a process of deposition on the surface and resorption of inner surfaces (Enlow and Bang, 1965).

Specific adaptations to stress can vary throughout the skeleton depending on the composition of cortical and trabecular bone, anatomical location and the bone's specific function. The trabecular bone of the skeleton is first to react to the decrease in mechanical needs and suffers a greater loss in density. The amount of trabecular bones varies from one area of the skull to another and therefore affects the mechanical properties and stiffness of the bones in this area (Smith and Suggs, 1976). Structurally, compact bone covers the skull inside and out and the trabecular bone found between the layers increases further away from the cranial sutures. The mechanical properties of compact bone are much more uniform than those of trabecular bone as one might expect, due to the matrix structure of trabecular bone (McElhaney *et al.*, 1970). Cortical bone can also undergo a loss of bone mass but this is often a more prolonged loss of tissue.

Research suggests that the role of mastication forces acting on the skull dictates skull shape more than any other external force (Preuschoft and Witzel, 2005). Bones of the cranium vary in architecture to accommodate the stress and strain produced by the cycles of mastication (Wroe *et al.*, 2007). The muscles of mastication change with force and intensity and the skull is optimized to meet its mechanical needs during feeding. Smith *et al.* (2007) found that temporal bone morphology varied among modern human populations

throughout the world. Although their study focused on climate changes, they noted that neural evolution and mechanical stresses caused by the availability of certain foods also played a significant role in the observed temporal bone variation.

2.1.1 WOLFF'S LAW AND BONE REMODELLING

The functional adaptation to a mechanical loading history is a specific property of bone. Throughout the literature, Wolff's Law is generalized as bone's ability to adapt to mechanical loads. Wolff's law simply states that the form and function of bone changes, along with its internal and external architecture as dictated by external forces imposed upon it (Wolff, 1892). The amount of strain a specific bone can withstand varies throughout the skeleton. Strain (ϵ) is the amount of deformation of the material that occurs as a result of the stress imposed upon it. Bone can withstand a certain amount of strain before it initiates the production of new bone, or conversely the lack of strain triggers the resorption of bone in areas of less strain (Frost, 2003; Ichim *et al.*, 2006).

The craniofacial skeleton deforms under mechanical stress and irrespective of whether stress is distant or next to the loading site, it is capable of inducing cortical bone remodelling to accommodate the amount of mechanical stress it incurs. Due to variation between skulls of individuals, environments and species, there is no overall pattern observed in the deformation of the skull under mechanical stress and often individual bones experience different amounts of stress from contracting muscles of the masticatory system (Herring and Ochareon, 2005). When investigating the mechanical properties of cranial bone, McElhaney *et al.* (1970) found that cranial bone appears to be stiffer in the transverse or tangent direction in macaque's (McElhaney *et al.*, 1970). Primate faces are thought to

have adapted to withstand lower stress more often and avoid fatigue as opposed to high stress fewer times a day as in the feeding routine of carnivores (Ross and Metzger, 2004).

The cranial morphology of an individual is expected to be related to the mechanical loading history. If morphology varies between two craniofacial forms, its mechanical history may be the primary stimulus for this variation. When investigating the degree of remodeling, comparisons between the stress distributions among individuals may highlight their functional adaptation to the mechanical stress they must withstand on a regular basis.

2.2 CRANIOFACIAL DEVELOPMENT AND PROGNATHISM

Facial structure and dentition have undergone considerable changes over time. Upon visual inspection, one of the most noticeable morphological characteristics of the human skull is the presence, in varying degrees, of sub-nasal prognathism (Figure 2). Prognathism is a characteristic of the skull that can be both observed and measured. Prognathism occurs when one or both jaws in the sub-nasal facial region are projected forward, away from the cranium (Figure 3). Maxillary alveolar prognathism, which is of importance to this study, has been previously defined by Björk (1950) as the angle formed by the cranial base and a line through both cranial landmarks nasion and prosthion.

Differences in prognathism and its expression can be observed in the fossil record of primates, hominids and modern humans. Björk (1950) proposed that a reduction in prognathism was brought about by an increase in brain volume which corresponded to an increase in the brain case size and a more prominent forehead in modern humans. Reduction of prognathism may also be caused by a deflection of the cranial base which occurs in connection with an upright posture, causing the forward displacement of the spinal column under the skull. A decrease in prognathism can occur in the face by a

retraction of the snout and a corresponding increase in the breadth of the jaws and skull. These three factors of brain size, cranial base deflection, and shortening of the jaws may occur independently but all contribute to a more orthognathic facial form. These where the reasons proposed by Björk (1950) for the degree of prognathism within a population, and its variation is mainly due to the individual size and shape of the cranial base found throughout a population.

Previous research has found statistical correlations between the expression of the prognathic facial form and other cranial characteristics, for example, a reduction in prognathism is accompanied by a reduced facial height and orbit breadth and an increase in orbit height. However, a long mandibular ramus height and a long maxillary base length with maxillary protrusion are associated with increased prognathism (Wei, 1969; Brown and Maeda, 2004). Prognathic individuals are said to have longer jaws in relation to their cranial base length, which itself is flatter, and the foramen magnum is positioned more posteriorly. With a decrease in the degree of prognathism, the jaws shorten, accompanied by a forward movement of the posterior region of the cranial base (Björk, 1950).

The growth of the facial skeleton has been mapped and differences between human and primate skeletons have been observed. Areas of progressive resorption have been recorded in the human skull in the area of the maxilla and zygomatic bones. The downward direction of growth of the nasal area results in a lesser degree of prognathism. Unlike other mammals, the human maxillary region grows downward instead of forward as seen in others species (Brodie, 1953; Enlow, 1966a, 1966b). An increase in prognathism is the result of new bone deposition during the maxillary growth in an inferior-anterior direction.

The Neandertal craniofacial form shows a classic case of prognathism with the protrusion of the maxillary region outward and away from the neurocranium (Trinkaus, 1987; Demes, 1987; Spencer and Demes, 1993; Weaver *et al.*, 2007). The overall shape is that of a more robust individual. Modern humans, however, show a more orthognathic facial form where the maxilla and mandible are positioned under the face and are more vertically set. The face appears flat and has a more gracile expression (Figure 4). Although the modern human face has become more orthognathic than that of earlier hominids, varying degrees in the expression of prognathism can be found throughout world populations (Björk, 1950; Wei, 1969; Robertson, 1979; Brown and Maeda, 2004).

Besides basic craniometry, there are other, more sophisticated methods that can be utilized to investigate shape differences in the human crania, more specifically geometric morphometrics (Viðarsdóttir *et al.,* 2002; Perez *et al.,* 2004; Bastir and Rosas, 2006). Analyzing the morphology of human anatomical features is one of the fundamental aspects of human biology and research. Particularly, geometric morphometrics is concerned with shape variation that can be seen from definable landmark points (Rohlf, 1998; Richtsmeier *et al.,* 2002; Zelditch *et al.,* 2004; Adams *et al.,* 2004; Slice, 2007; Milleroecker and Gunz, 2009). These three-dimensional landmark coordinates can undergo multivariate statistical analysis to determine patterns and variations in shape of anatomical features. The information obtained from geometric morphometric analyses allows researchers to look at variability in patterns and shapes while drawing conclusions on the ontogeny of the shape differences between and within human populations.

The degree of prognathism can be population specific and characteristic of some groups. These differences in craniofacial form develop through a facial shape template already present at birth and emphasized during the growth period (Viðarsdóttir *et al.*, 2002). During growth several bones grow independently as dictated by the genetics of the individual and local factors. Viðarsdóttir *et al.* (2002) observed differences in face shape present in infancy and tried to account for the adult variation in shape and size of the face. There were no differences between populations in their ontogenetic trajectories. The authors noted there is no indication that modern human infants from diverse groups share a common facial form and that much of the diversity among adults is present early in development.

Palaeoamericans have long narrow neurocrania, low projecting faces and low wide orbits and noses (Jantz and Owsley, 2001). These characteristics can be found among Africans and among the first modern humans (Neves *et al.*, 2007). Population variability in craniofacial forms has been documented extensively throughout the literature for years (Lewis, 1942; Birkby, 1966; Howells, 1973; El-Najjar and McWilliams, 1978; Krogman and İşcan, 1986; İşcan and Steyn, 1999; İşcan *et al.*, 2000).

Prognathism has been looked at in many ways and has been of interest to evolutionary biologists and dental practitioners alike (Glanville, 1969; Rak, 1986; Weaver *et al.*, 2007). The history of prognathism has been debated in the literature as to the reason and ontogeny of its expression. The literature suggests that the system is said to be more efficiently equipped in producing bite force at the incisors (Rak, 1986; Demes, 1987; Trinkaus, 1987) or molars (Spencer and Demes, 1993; Antón, 1996). During facial growth the anterior dentition migrates both forward and downward, away from the cranium and

the masticatory muscles, causing a prognathic individual to have to exert a greater muscle force for incisal biting than an orthognathic individual (Russell, 1982). Correlations between masticatory muscles, function and facial morphology have been observed and a positive correlation has been shown between the masseter muscle activity during chewing and facial prognathism (Ingervall, 1976).

Regardless of the degree of expression, the prognathic and orthognathic facial forms must function during mastication to support the forces of mastication with the appropriate buttressing to allow the system to work efficiently and without structural failure. Therefore, various degrees of buttressing are thought to be present to accommodate bone stress in the skull for mastication (Rak, 1983).

2.3 MASTICATION

Mastication is the first step in the digestive process. The action of mastication is the process of grinding, chewing and breaking food particles down into smaller manageable pieces in order to increase their surface areas and aid in the digestive process (van der Bilt *et al.*, 2006). The main elements involved in the mechanical action of mastication are the muscles, their underlying bone and the teeth.

The mandible, which is attached to the skull itself through the temporomandibular joint, acts as a Class III lever during mastication (Hylander, 1975; Kieser, 1999; Pileicikiene and Surna, 2004). The bite force is dependent on the relative length of the moment arm. In the case of the masticatory system, the moment arm is the distance from the bite force on the tooth in the dental arcade to the temporomandibular joint which acts as the fulcrum of the lever system. The cranium works in conjunction with the mandible to produce the cycles of mastication. The temporalis, masseter and medial pterygoid muscles exert an

adducting movement on the mandible to create the bite force necessary for mastication (Osborn and Baragar, 1985; Osborn, 1996; Daegling and Hotzman, 2003; Daegling, 2007).

2.3.1 MUSCLES OF MASTICATION

The masticatory muscles which create the cycles of chewing have corresponding skeletal attachments with the skull, maxilla, and mandible. Each of these muscles acts on the underlying bone to create mechanical stress due to forces required for mastication. It is the job of the bone in the craniofacial area to accommodate and support the load created by the bite force during the cycles of mastication (Demes, 1987; Kiliaridis, 1995; Vargervik, 1997; Herring and Ochareon, 2005) . Highest strengths in the skull occur at the insertion points of the masticatory muscles (Demes, 1982). Three muscles of the masticatory system namely the temporalis, masseter and medial pterygoid are used in elevation of the mandible (Fehrenbach and Herring, 1996). These muscles must move the lever or mandible in this case, to complete the cycles of mastication.

Innervation of the muscles of mastication by the nervous system does not take place equally across muscles fibres or across time during the cycles of mastication. It has been documented that muscle strength changes with the length of the muscles themselves (Koolstra and van Eijden, 1992). Several factors of the muscles also contribute to the force of contraction, for example, muscle fibre length, sacromere length and the directional orientation of the fibres themselves (Blanksma *et al.*, 1997).

Previous research has shown that masticatory muscle volumes correlate to the corresponding skeletal attachments (Gionhaku and Lowe, 1989; Antón, 1996; Kitai *et al.*, 2002; Goto *et al.*, 2006). A healthy masticatory system can be determined from size, length, volume and cross-sectional area of the masticatory muscles themselves or by taking cranial

and facial dimensions (Ringqvist, 1973; Demes and Creel, 1988; Hannam and Wood, 1989; Koolstra and van Eijden, 1992; Antón, 1996; Lahr and Wright, 1996; Tuxen *et al.*, 1999; Kitai *et al.*, 2002). The greater the bite force, the greater the diameter and cross sectional area of muscle fibres (Tuxen *et al.*, 1999). Various adaptations to the masticatory apparatus cause differences in the dominant muscle being used at any given time during the cycle of mastication (Koolstra and van Eijden, 1995; Blanksma *et al.*, 1997; Herring, 2007). A decrease in the muscle mass, volume or their visible attachment areas may be indicative of an individual missing substantial dentition and therefore, has a decreased bite force.

As mentioned before, three main muscles of the masticatory system will be of interest. They are the masseter, temporalis and medial pterygoid (Standring, 2004; Matshes *et al.*, 2005). The masseter muscle is most commonly divided into the deep and superficial portions. The superficial masseter originates at the anterior and inferior ⅔ margin of the zygomatic arch and inserts at the angle of the mandible (Figure 5). The deep head (much smaller) of the masseter originates on the posterior ⅓ of the medial surface of the zygomatic arch and inserts at the ramus of the mandible (Figure 5) (Fehrenbach and Herring, 1996). Masseter muscle thickness has been found to be positively correlated with mandibular ramus height, therefore, muscle morphology influences mandibular morphology (Kubota *et al.*, 1998). This phenomenon is easy to understand taking Wolff's Law (1892) into account, and also the fact that the masseter's insertion point on the mandible influences the bone morphology and is a reflection of the muscle's activity.

The temporalis muscle (Figure 6), characterised by its fan shape, encompasses the temporal fossa on the lateral sides of the skull and inserts on the coronoid process of the mandible (Osborn and Baragar, 1985). It is divided into an anterior portion and posterior

region which is more shallow (Fehrenbach and Herring, 1996; Blanksma *et al.*, 1997). The medial pterygoid muscle (Figure 7) which is used in jaw elevation has an origin at the pterygoid fossa of the sphenoid bone and inserts at the angle on the medial side of the mandible (Fehrenbach and Herring, 1996).

The size of a muscle is thought to be indicative of its maximum force. It is these muscles which function in creating differences in facial dimensions (Weijs and Hillen, 1986). It is the maximal muscle force which imposes changes over time in the underlying bony structures to create changes in facial morphology (Raadsheer *et al.*, 1996; Goto *et al.*, 2006). For example, muscle thickness has been shown to effect mandibular ramus morphology (Kubota *et al.*, 1998). Kitai *et al.,* (2002) found significant correlations between temporal and masseter cross-sectional volume and cross-section areas. The volume of muscle was positively correlated with bizygomatic arch and temporal fossa width. These results were consistent with previous work suggesting the wider the mandibular elevator muscles, the wider the transverse head dimensions (Weijs and Hillen, 1984; Kitai *et al.*, 2002). Temporal fossa width was correlated with temporal and masseter volumes but not with the cranial width (Kitai *et al.*, 2002). Muscles of mastication have evolved with dental morphology reflecting the needs of the system to endure more or less mechanical strain (Herring, 2007).

An increase in the bite force can only occur if there is an increase in muscle mass, changes in the lever arm system to generate greater forces, and an increase in the structural capabilities of the system to support the muscles during action (Herrel *et al.*, 2007). The muscle's force of contraction is not the only factor determining what force is used during the cycle of mastication. The periodontal ligament (PDL), alveolar bone surrounding the teeth and the point of load bearing also dictate what force is exerted by using a feedback

loop receiving messages from mechanoreceptors and nociceptors. Other receptors also monitor stress to protect the teeth from potentially damaging force loads (Paphangkorakit and Osborn, 1998).

2.3.2 TEETH

Housed within the maxilla and mandible are the teeth. Teeth are the hardest structures found within the body (Brkic *et al.*, 2006; Low *et al.*, 2008). As much as the muscles move the levers to create the action and force of mastication, the teeth play an important role by creating the rigid occlusal surface in which the force is applied to whatever is being chewed.

The greater the occlusal surface in an individual, the greater bite force (perpendicular to the occlusal plane) they are capable of creating and withstanding (Demes and Creel, 1988). In edentulous individuals and those experiencing the effects of osteoporosis due to age, both circumstances can result in a significantly reduced bite force due to resorption of bone and the lack of occlusal area (Agarwal and Grynpas, 1996).

The forces of mastication change in magnitude throughout the dental arcade. Posterior teeth, where the larger bite force is located, have a greater occlusal surface area to support such mechanical actions. The surface area of the teeth plays a role in determining the force of contraction of masticatory muscle. Surface areas of the teeth, like that of the molars, are created to endure larger compressive loads than that of the incisors. The location of the molars in closer proximity to the masseter and medial pterygoid muscles creates the greater force at the point of the shorter lever arm (Pileicikiene and Surna, 2004).

The occlusal force and facial morphology has also been shown to have relationships. The ability to produce a high magnitude for a molar bite is thought to be brought about by

the anterior migration of the masticatory muscles and/or the posterior migration of the dentition (Spencer, 1998). There is an increase in bite force acting perpendicular to the occlusal plane of the maxilla because of a decrease in length of the mandibular lever. Koolstra *et al,* (1988) showed the greatest bite force at the second molar over all other dentition. A correlation between incisor and molar bite force was recorded and found to be associated with a long mandible and a small gonial angle. The incisor bite force was significantly correlated with mandibular prognathism. The authors speculate that the strong correlation between bite force and the size of the mandible is due to the positive correlation between the bone and the size of the masticatory muscles (Ringqvist, 1973).

The investigation into changes in hominid dentition seen over time has shown a trend in the decrease in the overall size and the number of teeth (Demes and Creel, 1988). The anterior teeth have decreased in size, postcanine teeth have decreased in number and size and have become more adapted to grinding (Wolpoff, 1996; Oettle *et al.,* 2009). The presence or absence of modern human third molars is a perfect example of how a decrease in size and presence has occurred over time. It is not unusual to find a full set of molar dentition in early hominid fossils, but modern humans often do not have the eruption of third molars or they are removed due to the complications in their presence. Regardless of the muscle forces acting on the jaws, if there are not enough teeth to support a high bite force then, due to disuse, the subsequent muscle attachments will have a decrease in buttressing at the site of muscle attachment (Benjamin *et al.*, 2006). This is why, when investigating masticatory forces, a sample with a consistent minimum number for dentition should be used.

Occlusal force and facial dimensions have been investigated and thought to vary between dolichofacial (long faced) and brachyfacial (short faced) individuals (Proffit *et al.,* 1983). The differences observed in occlusal forces may simply be a case of physics and the lengthening of the lever arm and decreasing the amount of force which can be generated. Research has shown a correlation between the lengthening of facial dimensions found in dolichofacial individuals with the decrease in bite force on the occlusal surface (Proffit *et al.*, 1983).

2.4 EVOLUTION OF CRANIOFACIAL MORPHOLOGY FOR MASTICATION

Functional morphology implies an investigative look at the adaptation of biological forms to suit functionality (Ross, 1999). Adaptations such as these can be found in the masticatory system as diets changed over time. Cranial morphology has been used to reconstruct a time line for evolutionary biologists. Some researchers believe that changes are due to climate adaptation (Harvati and Weaver, 2006) but others agree that the change in diet and mechanical needs of the skulls have produced the greatest change (Robinson, 1954, 1962, 1963, 1967; Jolly, 1970; Ward and Molnar, 1980; Grine, 1981; Rak, 1983; Rak, 1985; Teaford and Ungar, 2000; Ungar, 2004; Lieberman *et al.*, 2004; Scott *et al., 2005*).

The *Australopithecines* are the first hominid ancestors recorded approximately four million years ago through the fossil record. Characteristics of this early ancestor as compared to modern humans were a powerful masticatory system, smaller brain, large robust face and mandible, very pronounced prognathism and significantly larger incisors and canines (Wolpoff, 1996). The more recent Neandertals exhibited the characteristic large browridges, low sloping foreheads, increased brain size, a larger nasal aperture, anterior dentition and mandible with its pronounced forward mid-facial projection

(Wolpoff, 1996; Park, 1996). The robust skull of earlier hominids was necessary for the large muscle attachments needed to move the powerful jaws during mastication. Muscles of mastication at that time must have been much larger, considering the diet of early hominids and the use of their anterior dentition as tools (Johnson and Moore, 1997).

The difference in craniofacial forms can be attributed in some ways to the changes in demand of the masticatory system over time. Neandertal's robust skull was necessary to accommodate the large masticatory muscles. The rough diet of Neandertals necessitated the large occlusal area provided by the full molar set in the dentition and a large bite force. The presence of prognathism in Neandertals allowed for the increased space needed to house and support the large teeth (Spencer and Demes, 1993; Wolpoff, 1996). The modern facial form evolved while exploiting new food sources, preparation techniques and agriculture. The modern facial form is more gracile in appearance with a vertical forehead, smaller anterior teeth, stronger presence of a chin on the mandible, long narrow brain case for increased brain size and a less prognathic facial form (Park, 1996).

The changes in diet, creation of tools and the preparing of food created less and less demands on the masticatory system for modern humans. As a result of the decreased demands the face retracted under the skull due to the need for less space for dentition and became characterized as orthognathic. The large masticatory muscles of the Neandertal used in elevating the mandible underwent an anterior migration to decrease the lever arm and to maintain the large bite force at the anterior dentition. The teeth became smaller and fewer due to the decreased demand in bite force and the unnecessary occlusal area. The skull of modern humans appears much more gracile because of the decrease in size and necessity of the large masticatory muscles.

The foundations which support the mechanical stress of mastication are not all the same. Craniofacial morphology has been studied in several species of primates, early hominids and groups of modern *Homo sapiens* (e.g., Moss and Young, 1960; Spencer and Demes, 1993;Lahr and Wright, 1996; Hennessy and Stringer, 2002; De Greef and Williems, 2005; O'Higgins *et al.*, 2006; Harvati and Weaver, 2006; Bruner and Manzi, 2007; Neves *et al.*, 2007). Differences in the skulls of primates and hominids have been documented as variations in the masticatory needs of each group. Dentition, diet and culture are determining factors which make the differences in the groups very pronounced (Lucas *et al.*, 1985; Demes and Creel, 1988; Usui *et al.*, 2004; Smith *et al.*, 2007). Primate and hominid groups where diets necessitate greater bite force would naturally have larger teeth in greater numbers, and the large muscle attachments to move the powerful jaws (Demes and Creel, 1988).

Structural similarities have been documented between Neandertals and modern humans in their masticatory muscle morphology (Antón, 1996). Mapping these muscles can be difficult but their similarities have been noted between modern humans and earlier hominids by observing markings left on bones by muscle attachments. These muscle markings on the bone, at the point of attachment of the muscles, reflect muscle force and/or direction of force. It is this masticatory muscle activity which is thought to have driven the evolution of the facial form. The strength of the muscles in creating forces during mastication at the anterior teeth is thought to vary in facial forms. Like the lever arm mechanics in other biomechanical systems, the longer lever arm created by the prognathic face is thought to have decreased force production at the anterior teeth - the region farthest away on the lever arm of mastication. The arrangement of the muscles in relation

to the dental arcade were previously orientated for the greatest force posteriorly; over time this has changed (Spears and Macho, 1998). Molars have become specialized in their function and the first molars seem to now be suited for the highest force loads and varying degree of functions (Spears and Macho, 1998).

Adaptations, like those of the masticatory system occur in response to the need for modifications in a biological form because of changes in its function over time. The reproductive success of a species selects for these new modifications in the system and in turn increases its fitness and reproductive success. Darwin in his "Origin of Species" uses these principles to explain natural selection and its role in evolving species (Ross, 1999). It is thought that the masticatory system and the structures involved in mastication are extremely susceptible to homoplasy because of its adaptation over time to varying feeding behaviours (Collard and Wood, 2001).

2.5 FINITE ELEMENT ANALYSIS

Finite element analysis is a mathematical modeling tool most often used by engineers to solve complex structural problems. With the increased availability of finite element analysis software and inter-disciplinary collaborations, its applications have recently been more used in the fields of biomechanics, functional morphology and anthropology. The application of the finite element method now allows routine analysis on complex geometries like that found in the human skull.

2.5.1 WHAT IS FINITE ELEMENT ANALYSIS?

The finite element method is a mathematical way to find approximate numerical solutions to problems which might otherwise be difficult to solve by practical scientific methods. The use of finite element analysis technology in anthropology is relatively new,

although the finite element analysis (FEA) method has been used in structural engineering to determine stress and deformation in materials other than bone for decades (Sarraj *et al.*, 2007; Predan *et al.*, 2007). This is also the case in orthodontic research when both orthodontic implants and bone are modeled together (Geng *et al.*, 2001; Provatidis *et al.*, 2007; Chatvanitkul and Lertchirakarn, 2010). The mathematics and numerical procedures behind the analysis can be found in a variety of textbooks but will not be gone into detail here (Zienkiewicz and Taylor, 2000; Chandrupatla and Belegundu, 2002). Rayfield (2007) describes a comprehensive review of the FEA method as it applies to anthropological and biomechanical studies.

The finite element method is well proven and is used often in biomechanics and on human bone to help determine bone stress patterns within the skeleton (Camacho *et al.*, 1997). One important use of finite element analysis is in determining stress distribution in the skull and brain tissues due to high impact (Chu *et al.*, 1994; Kleiven and von Holst, 2002; Zong *et al.*, 2006). Using a finite element model subject to the load case of interest and simplified with adequate material properties, produces a pattern of the stress and deformation in relation to a set variable.

2.5.2 STRESS DEFINITIONS

Externally applied forces to bone can be oriented in many directions to create stress (Cowin, 1989; Cullinane and Einhorn, 2002). Force is an action of one object against another and is recorded as a unit of Newtons (N). The stress on a bone is the transmitted force divided by the cross sectional area. Stress and the distortion of bone can be recorded throughout the skeleton as forces are applied. There are three type of stress which can be recorded in response to a force. Tension deformation is produced when forces are acting in

opposite directions (Cowin, 1989; Cullinane and Einhorn, 2002). Often with tension one can visualize the lengthening or stretching of a material (Figure 8). Compression works in the opposite direction of tension as two forces are directed towards each other in the same plane (Cowin, 1989; Cullinane and Einhorn, 2002). Deformation can be thought of as a shortening and widening of the material where forces are applied (Figure 8). Shear forces act on a material at an angle causing the material to rub against each other at angles (Cowin, 1989; Cullinane and Einhorn, 2002) (Figure 8). Although it is possible to record individual reactions to a force, often a combination of all three reactions occurs in response to an applied force.

2.5.3 STRESS ANALYSIS AND VON MISES

Internal resistance to a force being applied is expressed as a level of stress (σ). Stress is equal in magnitude but opposite in direction to the force being applied and is distributed over a certain area, therefore, stress = σ = Newtons per metre squared (N/m^2) (Cullinane and Einhorn, 2002). Because multiple stress components can exist simultaneously in a material, there is a need to combine all components into a single quantity that can be used to compare the intensity of one stress field to another. One such popular measure is Von Mises stress. Von Mises stress is also used as a failure criterion for many materials (i.e. if the Von Mises stress exceeds some critical value the material fails). Displacement and Von Mises stress contours have been widely used for finite element studies in the literature to represent the results of how bone reacts under external force loads (Camacho *et al.*, 1997; Taddei *et al.*, 2004; Ross *et al.*, 2005; Liao *et al.*, 2007; Kupczik *et al.*, 2007; Boryor *et al.*, 2008; Dumont *et al.*, 2009). It is widely understood that bone and its microstructures evolve in accordance with mechanical stress experienced over a period

of time (Wolff, 1892; Ruff *et al.*, 2006; Reina *et al.*, 2007). The use of the finite element analysis method gives us a means to visualize the Von Mises stresses caused by the muscle's force loads while simulating a specific bite force.

2.5.4 PREVIOUS FEA WORK IN BIOLOGICAL ANTHROPOLOGY

Previous studies using finite element analysis have investigated the effects of loading on the skulls of humans (Tanne *et al.*, 1988; Motoyoshi *et al.*, 2002; Mota *et al.*, 2003; Provatidis *et al.*, 2007; Röhrle and Pullan, 2007), macaques (Strait *et al.,* 2005; Ross *et al.*, 2005; Richmond *et al.*, 2005; Strait *et al.*, 2007), bats (Dumont *et al.*, 2005), geckos (Herrel *et al.*, 2007) as well as the teeth (Spears and Macho, 1998; Cattaneo *et al.*, 2003), the periodontal ligament (Poiate *et al.*, 2009) and the human mandible (Liao *et al.*, 2007; Röhrle and Pullan, 2007) just to name a few. The masticatory system and their muscles of action have been previously modeled (Koolstra and van Eijden, 1995; Daegling and Hylander, 2000; Koolstra, 2003; Sellers and Crompton, 2004; Ross *et al.*, 2005; Strait *et al.*, 2005; Ichim *et al.*, 2006; Kupczik *et al.*, 2007).

Kupczik *et al.* (2007) investigated the zygomatic arch in macaques using finite element analysis. They observed that maximum principal strains occurred in the anterior region of the zygomatic arch and decreased posteriorly in macaques when modeling masticatory loads on the second molar. The authors also modified material properties and observed a decrease in the strain values produced by an increased stiffness of the bone properties (Kupczik *et al.*,2007).

Ichim *et al.* (2006) compared human mandibles with and without the presence of a chin for molar and incisal biting. The finite element results showed little difference in stress

distribution and the authors concluded that the development of the chin area is not related to the functional demands of the mandible.

While modeling skulls of two types of fruit bats with different feeding behaviours, Dumont *et al.* (2005) observed significant differences in stress distribution in the molar bite as compared to the incisal bite. In bats, where molar biting is a common feeding adaptation, bites on the anterior dentition achieved higher stress in the rostrum than was observed in the other species of fruit bats that normally use their anterior dentition for feeding. Therefore, atypical biting behaviour in the fruit bats caused the rostrum to accommodate for more stress from forces of mastication.

The comparison of bite forces within the dental arcade between *M. fascicularis* and *A. africanus* was investigated using finite element analysis by Strait *et al.,* (2009). Strait *et al.,* (2009) found differences between the two craniofacial forms with regard to stress distributions for different simulated bite forces. High strain density was observed in the zygomatic arches, orbital margins and the interorbital region of *A. africanus* (Figure 9). Tensile strain for premolar biting was greatest in the lateral orbital region and zygomatic arch (Figure 10). Compressive strain for *A. africanus* for a premolar bite show largest areas in the maxilla, interorbital region, lateral to nasal margins and the zygomatic arch (Figure 11). One set of results showed that for a molar bite, *A. africanus* had higher strains in the facial region than *M. fascicularis.* For a premolar bite both *M. fascicularis* and *A. africanus* showed an increase in stress in the area of the nasal margins.

When attempting an investigation involving finite element analysis several important questions must be asked regarding the selection of bone, material properties, model creation, for example, before an analysis can be completed. A summary of the process

showing the individual steps involved in a finite element analysis can be found in Figure 12 and will be explained in the following sections.

2.6 MODEL CREATION

It is at the time of model creation that the investigator must decide the degree of accuracy and the questions being asked by the proposed study (Zannoni *et al.*, 1998; Helgason *et al.*, 2008; Dumont *et al.*, 2009). The first questions one must ask when starting with a finite element analysis is what sort of morphology is being investigated or needs modeling? What degree of accuracy is needed in the model to reflect the appropriate morphological characteristics? There are several ways to generate a model. In cases when the object to be modeled is bone, a two or three dimensional model is most often used. The three dimensional models have a greater number of elements and increase the complexity which therefore increases the time to run the analysis. Depending on the size and shape of what is modeled, a micro computed tomography (CT) scan may be used which yields greater accuracy with much smaller slices at micrometers of thickness. The greater the number of slices obtained from the CT scan, the greater the accuracy of the model. It may not be feasible to use such an accurate scan due to the size of the structure and the limited capability of the computer processor available. Standard medical three dimensional CT scans are often used for finite element modeling with success (Camacho *et al.*, 1997; Sellers and Crompton, 2004; Ichim *et al.*, 2006; Kupczik *et al.*, 2007; Provatidis *et al.*, 2007; Boryor *et al.*, 2008). Medical CT scans are sufficiently accurate in modeling both the internal and external geometry of the skull for use in finite element analysis. Although medical CT scans are less detailed than the micro CT scans, the size and complex geometry of the skull and the available resources used in performing the analysis makes them adequate.

2.6.1 THRESHOLDING

After the scans have been taken it is necessary to refine them to exclude all unwanted data acquired in the scan. It is at this time the investigator identifies tissue boundaries and the material for which specific properties will be assigned. This is a process known as thresholding. It is basically the process of using a grey scale found in software such as Amira® 5.1 (Visage Imaging, 2009) and generating a three dimensional model from a stack of CT scans. The attenuation of the CT scan changes with the density of the material being scanned. With the grey scale one can adjust the field of view to extract specific parts of the model such as cortical bone, trabecular bone or teeth. When creating a model with homogenous material properties the thresholding can be done by eye to include all the necessary structural components of the model.

2.6.2 MESHING THE MODEL

After the three dimensional computer aided design (CAD) surface mesh model has been created, it is possible that imperfections have been created along the way. To accurately represent what it is you are trying to model, these 'holes' need to be fixed so as not to interfere with the final analysis. Mesh repairing and editing can be accomplished with the use of mesh editing software like VRMesh Studio (VirtualGrid, Seattle City, WA).

The repaired skull model then needs to be converted to a volumetric three dimensional mesh model which is used by the finite element software. The mesh model is made up of elements that the finite element software will use to apply loads and compute deformations when the analysis is run. TetGen (Numerical Mathematics and Scientific Computing, Berlin, Germany) is an example of a three dimensional mesh generator software used to create models with tetrahedral elements used in finite element analysis.

2.6.3 MATERIAL PROPERTIES

Bone is a biological tissue which can withstand various force loads imposed upon it. However, because of its varying structure, the way in which the tissues and materials act differs. Depending on the structure or thickness of a material, some materials will be able to withstand force loads more easily than others before a critical breaking point is reached. The specific way a tissue reacts is called its material behaviour. Material behaviour is modelled by making use of a constitutive equation. Many materials, including bone, can be modelled by Hooke's law. Hooke's law expresses the stress in the material as a function of the strain, making use of constants known as the material properties. Material properties have been determined for bone in various areas of the human skeleton and can be found extensively throughout the literature e.g. femur (Ashman *et al.,* 1984; Zannoni *et al.*, 1998), mandible (Liao *et al.*, 2007; Gröning *et al.*, 2009), bones of skull (Mota *et al.*, 2003; Peterson and Dechow, 2003; Provatidis *et al.*, 2007; Boryor *et al.*, 2008), cortical bone (Camacho *et al.*, 1997), trabecular bone (Boryor *et al.*, 2008), teeth (Tanne *et al.*, 1988), and sutures (Motoyoshi *et al.*, 2002). The forces of compression, tension and shear, act on bone and elicit a response. The material properties of a substance describe how it acts under these force conditions.

When describing the material properties of a structure the values of Young's modulus (E), Poisson's ratio (v) and shear modulus (G) are recorded. The Young's modulus tells us the degree of stiffness or elasticity of a material, sometimes called the elastic modulus. Young's modulus is the slope of the linear relationship between stress and strain. The unit of Young's modulus is Pascal (Pa) or Newton per metre squared (N/m^2). The higher the value of the Young's modulus, the stiffer the material is and the more it can withstand

forces applied to it without deformation. Steel would have a higher Young's modulus than rubber, for example.

Poisson's ratio is the ratio of the change in width over the change in length due to an axial force and is one of the tensile properties of a material. Poisson's ratio has a range of values from approximately zero (cork) to 0.3 (metals) and almost 0.5 (rubber). Shear modulus can tell you how a material can withstand shearing forces. Again, using the rubber and steel example, steel would have a much higher shear modulus than that of rubber.

Materials can either be isotropic or anisotropic in nature. An isotropic material responds identically if a test is repeated with a different material orientation. The previous examples used steel which can be regarded as an isotropic material. Anisotropic materials respond differently to a force acting upon it depending on the orientation of the material. Biological tissues like bone can be regarded as anisotropic materials. A special case of anisotropic is orthotrophy. Orthotropic materials have mutually orthogonal axes of rotational symmetry. An easy example of an orthotropic material is wood; one can visualize the longitudinal axis of the tree but also the concentric rings of the inner structure. Force applied to either of these areas would generate different resultant behaviour on the part of the wood.

Prior to creating an accurate model for finite element analysis, the appropriate material properties for the material or bone, in this case, being studied must be determined. Several authors (Koolstra, 2003; Cattaneo *et al.,* 2003; Richmond *et al.*, 2005; Strait *et al.,* 2005; Ross, 2005; Wang *et al.*, 2006; Liao *et al.*, 2007) have stated that the more accurate a model one can create using the proper material properties of the bone being investigated, the more accurate the results that can be achieved. Several authors have recorded the

variation in bone material properties both between bones and within bones themselves and patterns of variation are shape and function specific (McElhaney *et al.*, 1970; Dechow *et al.*, 1993; Wang *et al.*, 2006; Wang and Dechow, 2006). Significant differences have been found in cortical bone between species, between individuals and are area specific (Wang and Dechow, 2006). Therefore, bone being heterogeneous in nature and having the ability to have different material properties in various locations of the same bone, makes building an accurate model tedious and very time consuming.

2.6.4 BOUNDARY CONDITIONS

Boundary conditions can be defined as the forces and the displacement restrictions imposed on the finite element model in order to mimic those of real life. In the case of modeling masticatory forces, the muscles of the primary masticatory muscles (temporalis, masseter and medial pterygoid) need to be modeled in the areas of muscle origins on the skull. Information about the origins of these muscles can be obtained from cadaver dissections and the literature (Fried, 1980; Fehrenbach and Herring, 1996; Fehrenbach and Herring, 2007). It is not only important to correctly designate the areas of origin of the muscles, but also the magnitude of reaction forces on the balancing and working sides of the skull in response to a molar or incisal bite force.

Other constraints of the finite element model need to be applied as realistically as possible or as accurate as the analysis in question necessitates. In the case of the skull, a natural cycle of mastication would involve interaction of the mandible with the skull. In order to account for the articulation point in the model, boundary conditions are used to represent the area of the articular eminence for the condyles of the mandible. The occipital condyles are the other region of the skull which, in reality, articulates with the rest of the

skeleton. The regions of the left and right occipital condyle are constrained to prevent rigid body motion of the model.

2.7 TESTING OF THE HYPOTHESIS

Once a finite element model has been created and decisions as to the appropriate material properties, boundary constraints and imposed force loads were made, an analysis can be run to test a hypothesis which includes the variability of one characteristic. The current project applied the general rules of bone behavior and muscle activity in order to test a hypothesis about one characteristic, prognathism. Inferences can be made from the stress analysis on a modeled skull with regard to the change in the degree of prognathism testing the hypothesis that the location of bone stress in the crania of a prognathic facial form will vary from that in the orthognathic facial form.

Figure 1. Feedback loop expressing relationship of strain levels with bone deposition and resorption (modified from Ruff *et al.*, 2006).

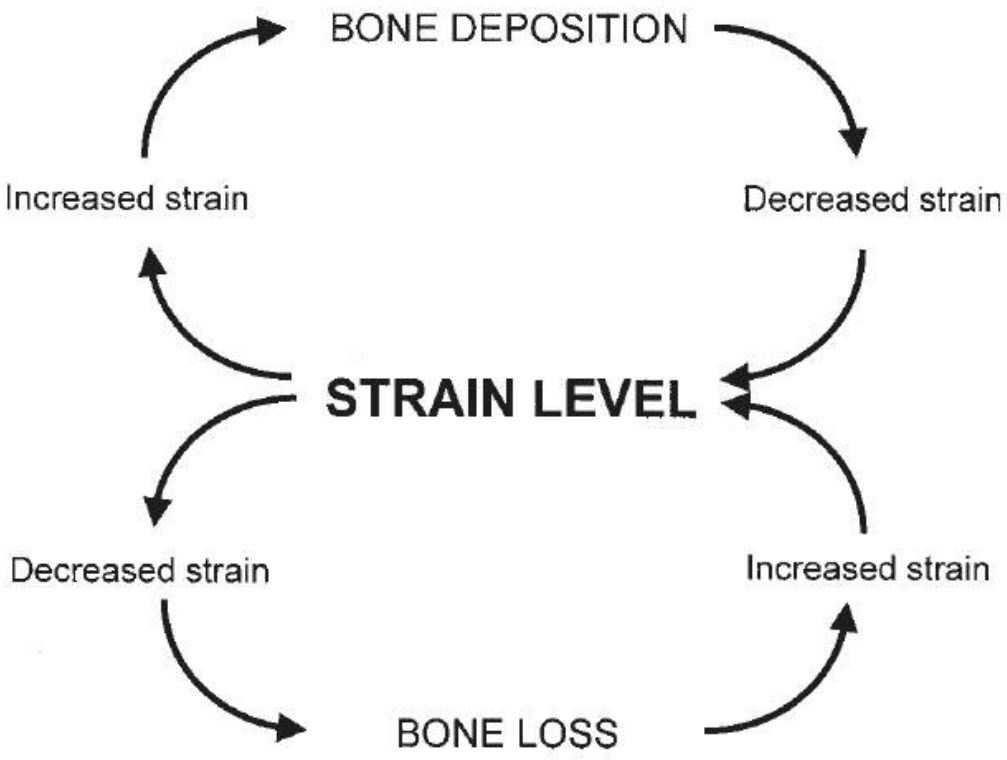

Figure 2. A characteristic African black skull on the left showing prognathism and a non-prognathic skull on the right characteristic of Europeans (adopted from Nott *et al.*, 1854).

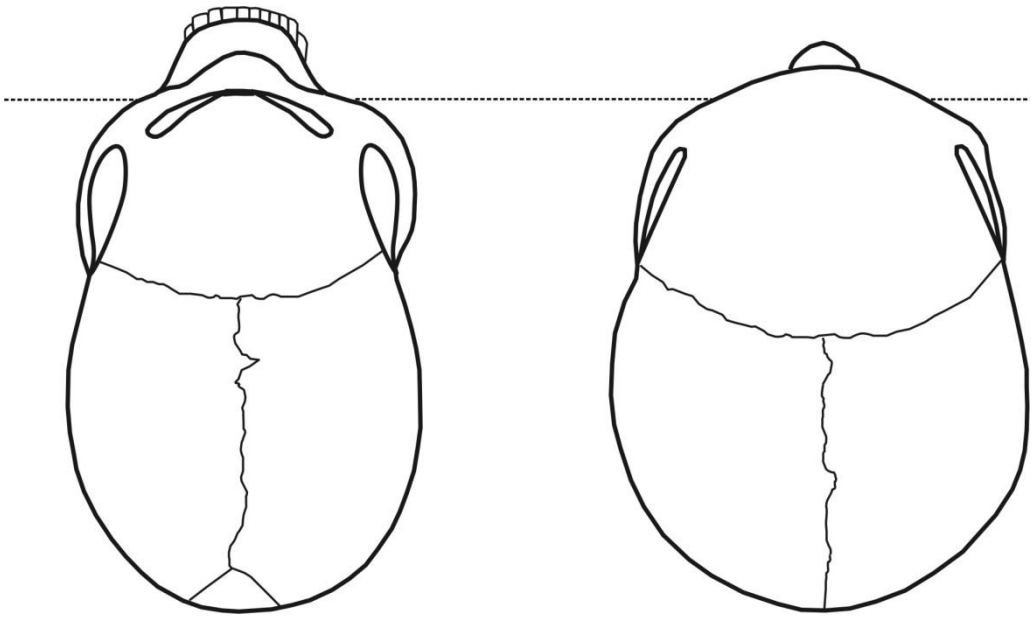

Figure 3. Prognathic skull (lateral view).

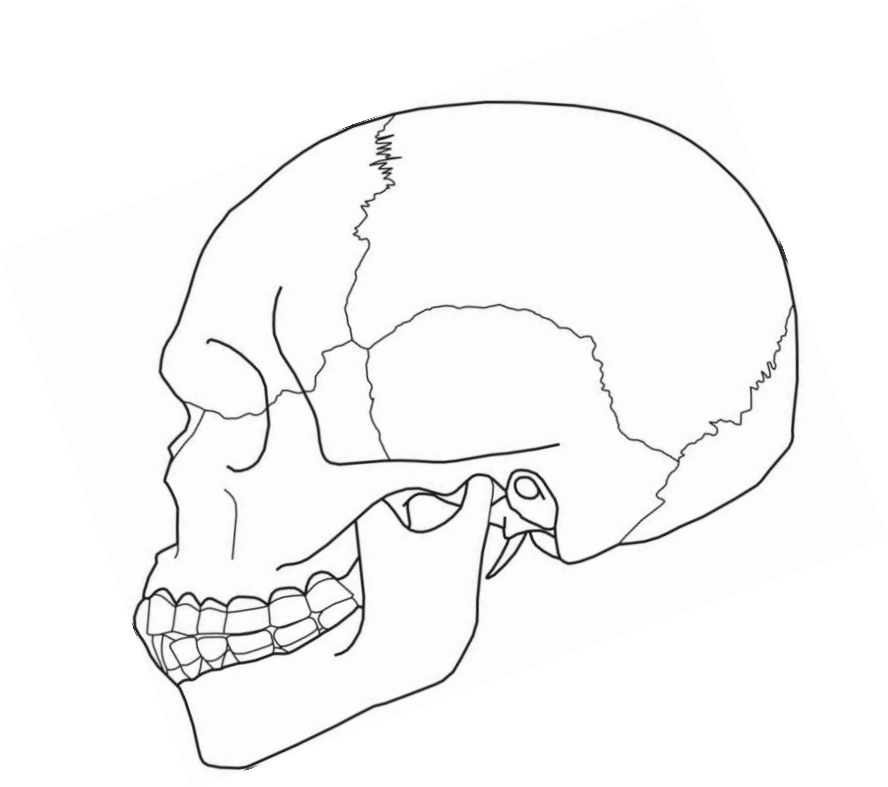

Figure 4. Non-prognathic skull (lateral view).

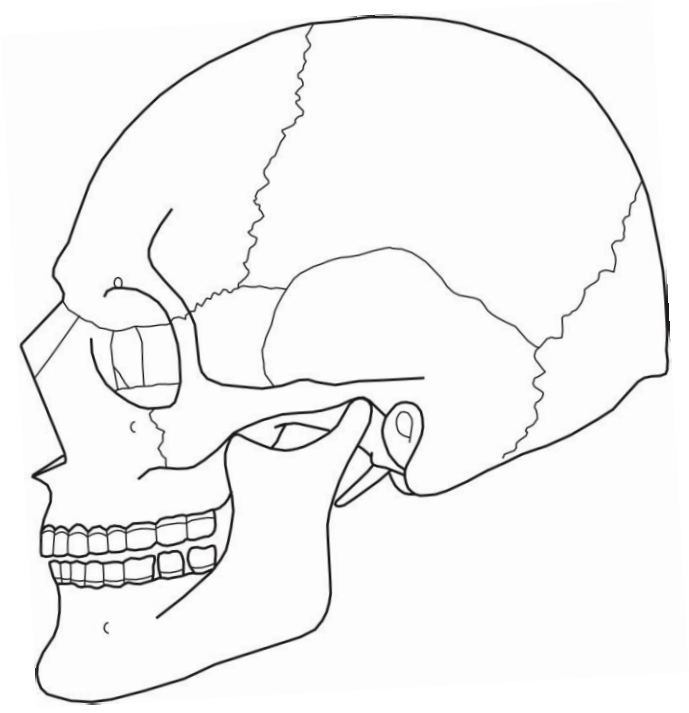

Figure 5. Lateral view showing masseter muscle origin and insertion. The deep head takes its origin at the posterior region of the zygomatic arch and the superficial masseter at the anterior 2/3 of the zygomatic arch (adapted from McMinn and Hutchings, 1988).

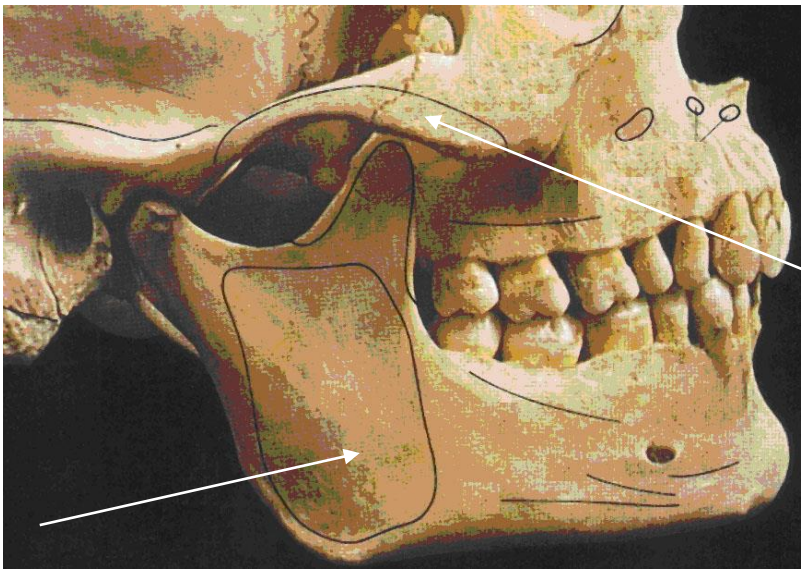

Figure 6. Lateral view showing temporalis muscle (modified from Standring, 2004).

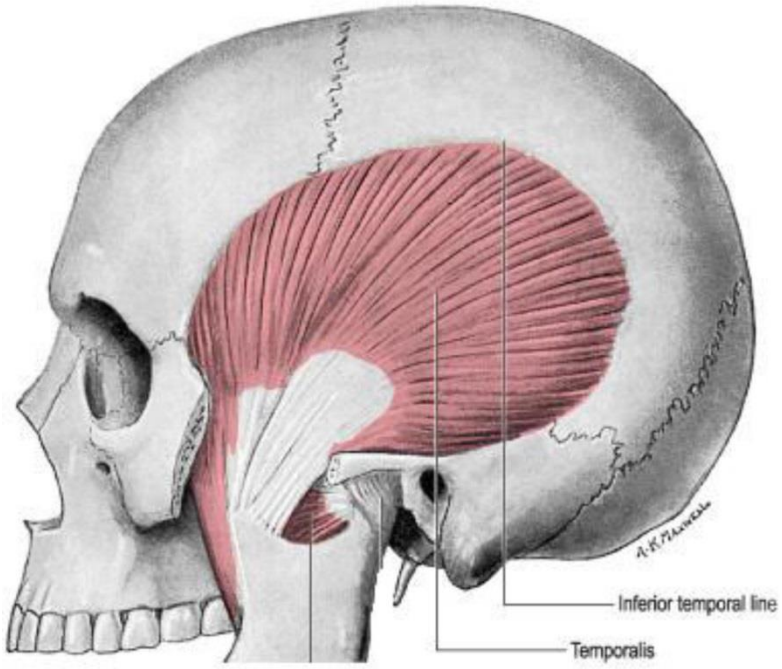

Figure 7. Lateral view showing medial pterygoid muscle (modified from Standring, 2004).

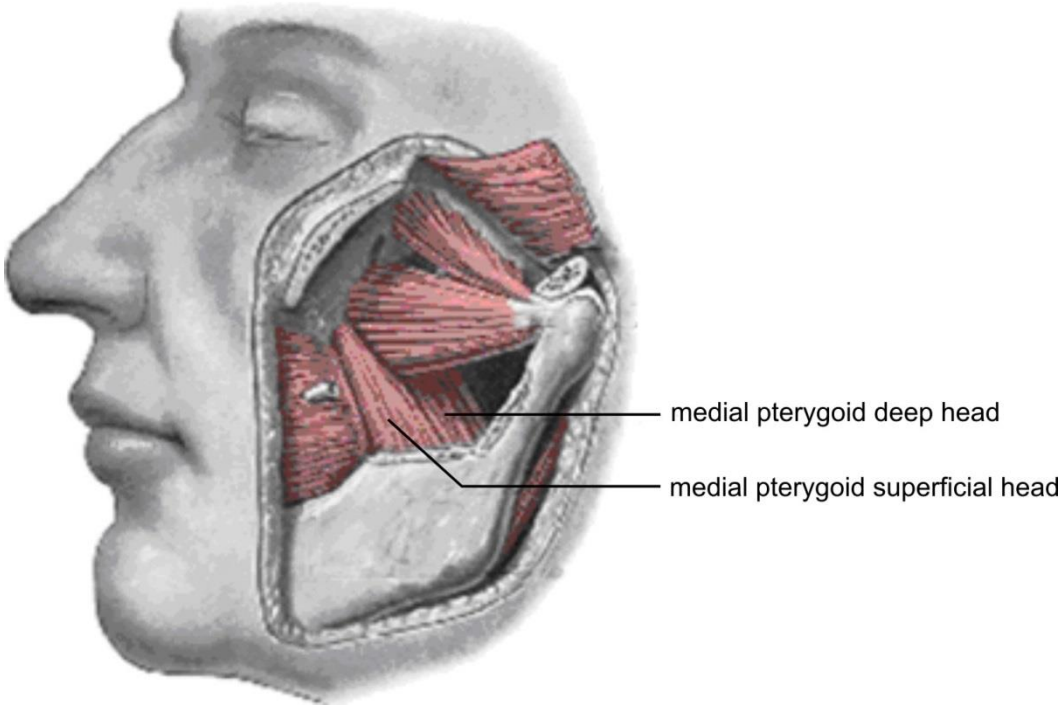

Figure 8. Compression, tension and shear forces.

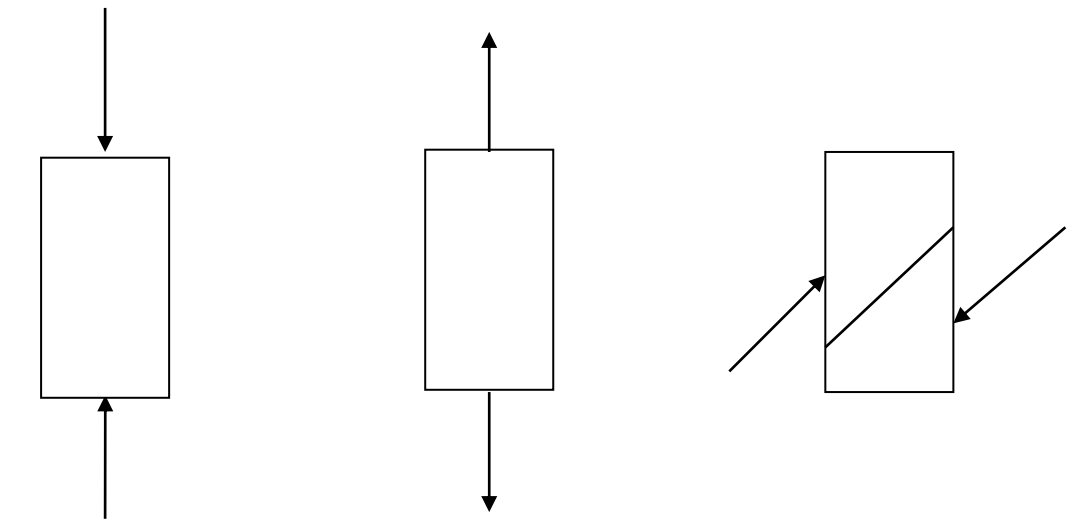

Figure 9. *Australopithecus africanus* strain energy density patterns observed from finite element analysis results for maximal molar bite (Strait *et al.,* 2009).

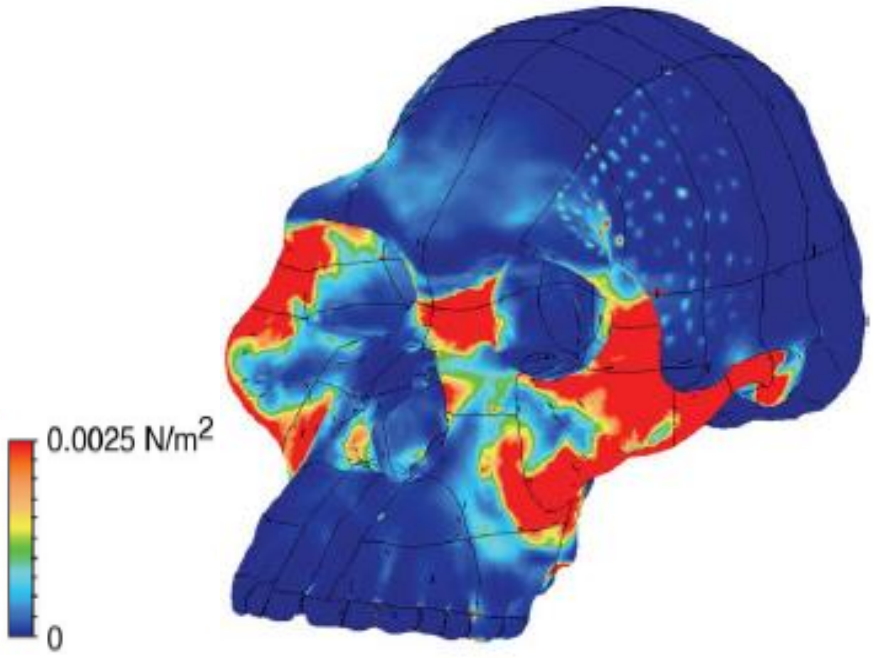

Figure 10. *Australopithecus africanus* principal strain tension maximal premolar biting (Strait *et al.,* 2009).

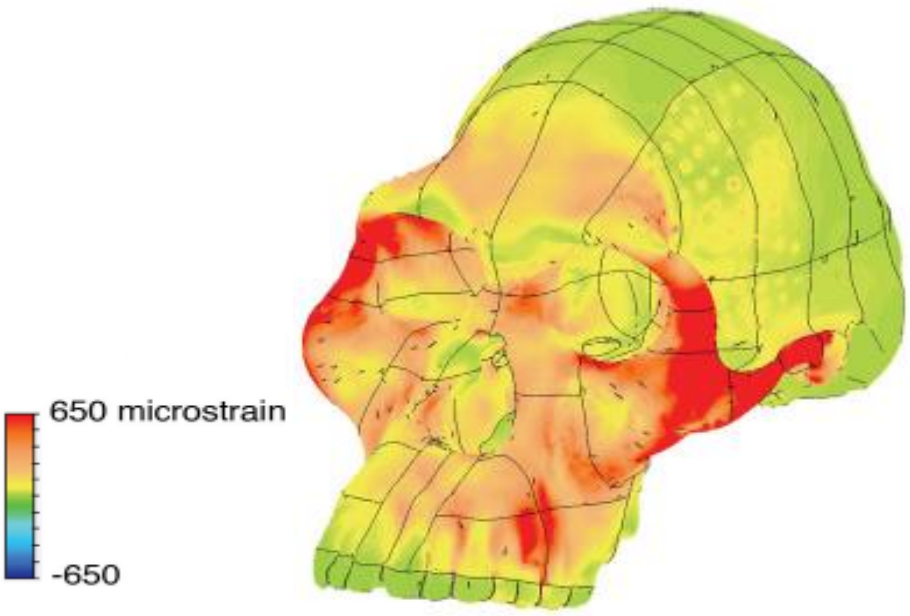

Figure 11. *Australopithecus africanus* principal strain compression maximal premolar biting (Strait *et al.,* 2009).

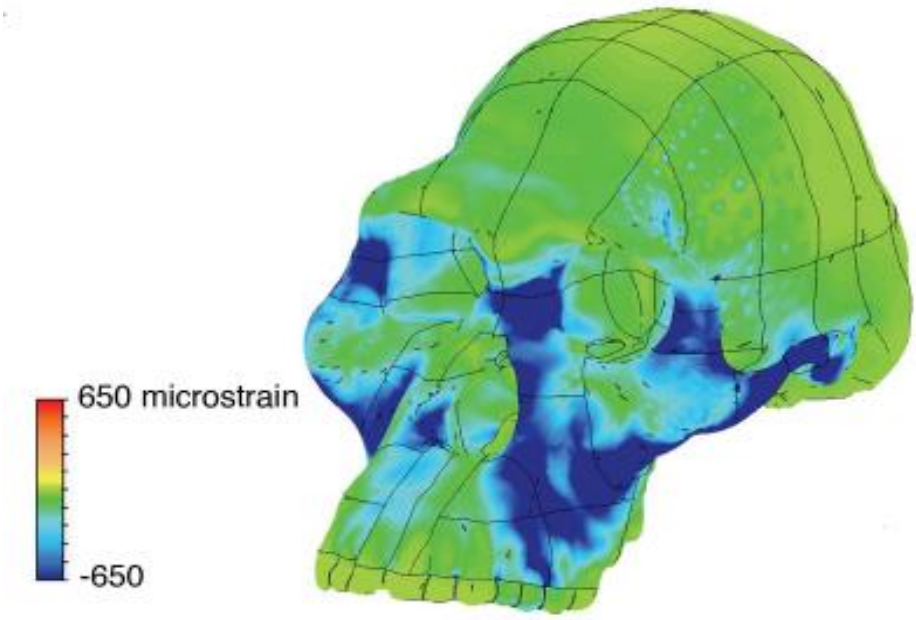

Figure 12. Stepwise description of the process of finite element analysis of human skulls.

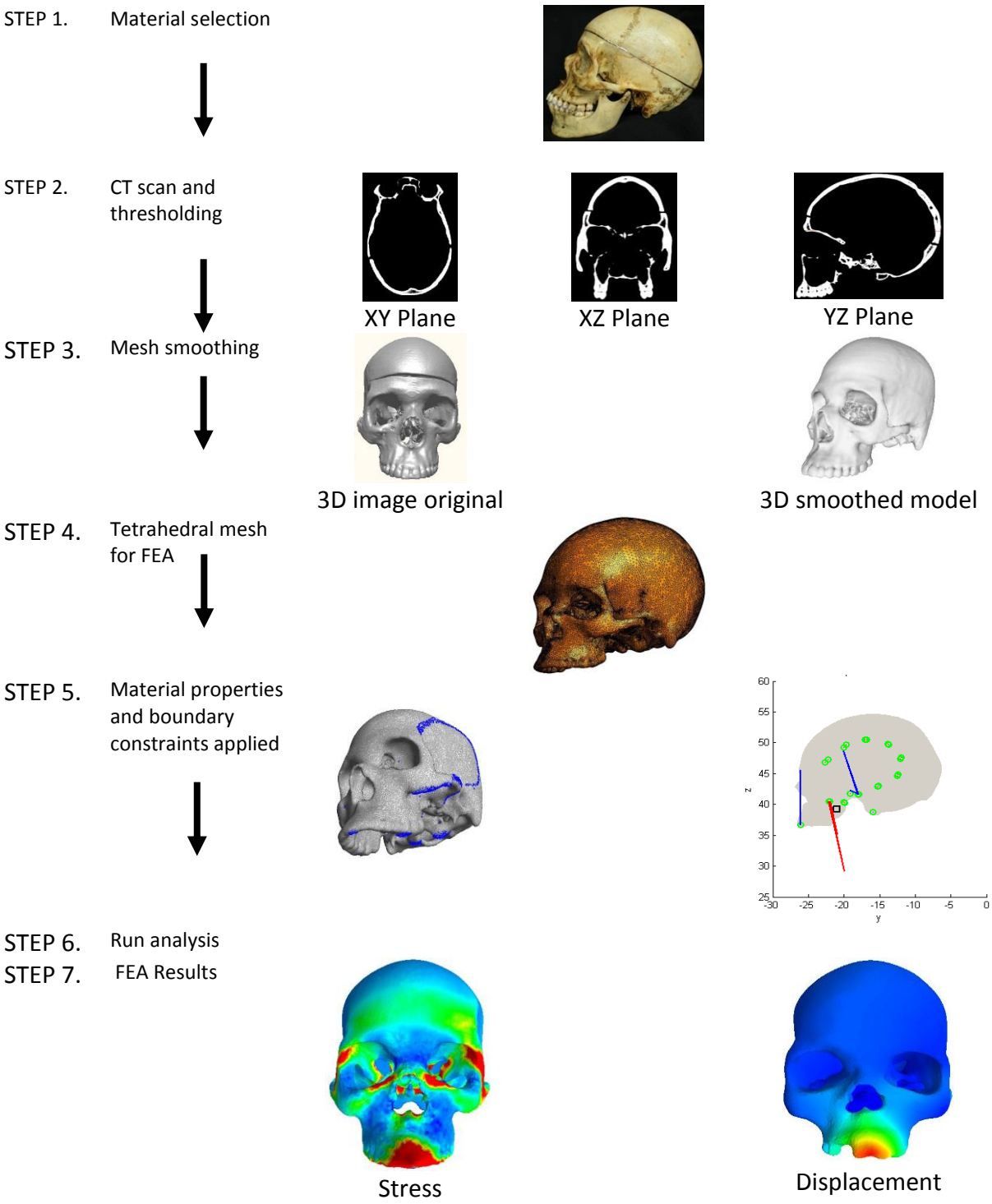

CHAPTER 3

MATERIALS AND METHODS

To study the transfer of the forces of mastication in two morphologically different facial forms two techniques were employed. Firstly, standard anthropometric measurements and morphological observations of the crania and teeth were used to assess the relationship between prognathism and the metric and morphological characteristics of the face and skull. These results were used to assist in interpreting the results of the finite element analysis. Secondly, the relatively new engineering technique to anthropology, the finite element method, was used to model the stress distribution due to bites at the left central incisor and left first molar of the maxilla, in an individual with a prognathic and orthognathic facial form. The incisors function in cutting and tearing food during mastication while the first molar is effectively suited for grinding and crushing food within the masticatory system (Spears and Macho, 1998; Bowers, 2004)

3.1 MATERIALS

The skeletal material of known age, sex, and ancestry for the project was obtained from the Pretoria Bone Collection (PBC) (L'Abbe´ *et al.*, 2005) housed within the Department of Anatomy, University of Pretoria and the Raymond Dart Collection (Dayal *et al.*, 2009) (Department of Anatomical Sciences, University of the Witwatersrand, Johannesburg). Skeletal material was examined both metrically and morphologically. Some factors influenced the choice of measurements for the study;

1) areas specific to muscle attachment of masticatory muscles 2) landmarks that can be consistently identified for repeatability of the study 3) measurements used to calculate molar crown area which is one factor that plays a role in determining the masticatory force an individual can produce.

The skeletal material used in this research was composed of individuals from the Gauteng area. However, the sample includes several black South African groups including Venda, "Bantu", Tsonga, Sotho, Xhosa, Ndebele and Zulu, for example. All groups combined were used to represent the South African black male population as a whole, exhibiting a range of projection of the mid-face. Only skulls of black males were included in the data set to eliminate the effects of variations introduced by using different sexes and ancestral groups.

Data were collected from 162 skeletons of known male adult individuals with an age range of 15 to 80 years (mean 39.3) and with sufficiently present dentition ante-mortem. Only those skeletons with at least 50% dentition were used in the study with extra care to look for presence of the first molars. The dental inventory was recorded because skulls with fewer molars will have a smaller occlusal area, and therefore, a smaller bite force. Individuals with decreased bite force have smaller muscles of mastication and attachments which may become evident in the collection of metric data.

A selection of Southern African skulls were chosen to give an adequate spread of prognathic and orthognathic individuals. The gnathic index was calculated using the measurement basion to prosthion relative to the basion to nasion distance (basion – prosthion/ basion- nasion) x 100 (De Villiers 1968). The purpose of this index is to

eliminate the effect of overall size differences between individuals and concentrate solely on degree of prognathism examined. The facial types fall into three categories: orthognathic facial forms are characterized by having a gnathic index of up to 97.9, mesognathic as 98- 102.9 and prognathic as 103 or higher (Knußman, 1988). The distribution of skulls used in this study and mean gnathic index values are recorded in Table 1.

3.2 ANTHROPOMETRIC ANALYSIS: MEASUREMENTS AND INDICES

The following previously documented or tested standard skeletal measurements, two new measurements, nine calculated indices and one area were recorded using the appropriate instruments and underwent statistical analysis (Table 2). Each measurement was taken on the left side to the nearest $\frac{1}{10}$ millimetre.

3.2.1 STANDARD MEASUREMENTS

1. Maximum cranial length- (g-op) the maximum distance from the most forward projecting point at the lower border of the frontal bone which lies above the nasal root (glabella) to the most posteriorly protruding point on the back of the brain case located on the occipital bone (opisthocranion) (De Villiers, 1968; Knußman, 1988). A spreading caliper was used to record this measurement.
2. Maximum cranial breadth- (eu-eu) the maximum width of the skull perpendicular to the most laterally positioned point on the side of the skull (euryon) (De Villiers, 1968; Knußman, 1988). A spreading caliper was used to record this measurement.

3. Bizygomatic breadth- (zy-zy) the direct distance between the most laterally positioned point on the zygomatic arches (zygion) (De Villiers, 1968; Knußman, 1988). A sliding caliper was used to record this measurement.
4. Basion – bregma height- (ba-b) the distance from the lowest point in the median plane on the external surface of the anterior margin of the foramen magnum (basion) to the point where the sagittal and coronal sutures meet (bregma) (De Villiers, 1968; Knußman, 1988). A spreading caliper was used to record this measurement.
5. Cranial base length- (ba-n) lowest point in the median plane on the external surface of the anterior margin of the foramen magnum (basion) to the midline point where the two nasal bones and the frontal bone intersect (nasion) (De Villiers, 1968; Knußman, 1988). A spreading caliper was used to record this measurement.
6. Basion – prosthion- (ba-pr) measurement from the lowest point in the median plane on the external surface of the anterior margin of the foramen magnum (basion) to the most anterior point on the process between the sockets of the upper central incisor teeth (prosthion) (De Villiers, 1968; Knußman, 1988). A spreading caliper was used to record this measurement.
7. Maxillo-alveolar breadth- (ecm-ecm) the maximum breadth across the alveolar borders of the maxilla measured on the lateral surfaces at the location of the second maxillary molars (ectomolare) (De Villiers, 1968). A sliding caliper was used to record this measurement.

8. Maxillo-alveolar length- the distance from the most anterior point on the process between the sockets of the upper central incisor teeth (prosthion) to the most posterior point of the palate (White, 2000). A spreading caliper was used to record this measurement.
9. Upper facial height-(n-pr) the direct distance from the midline point where the two nasal bones and the frontal bone intersect (nasion) to the most anterior point on the process between the sockets of the upper central incisor teeth (prosthion) (Knußman, 1988). A sliding caliper was used to record this measurement.
10. Minimum frontal breadth- (ft-ft) the direct distance between the points located generally forward and inward on the superior temporal line directly above the zygomatic process (frontotemporale) (De Villiers, 1968; Knußman, 1988). A sliding caliper was used to record this measurement.
11. Nasal height- the distance from the midline point where the two nasal bones and the frontal bone intersect (nasion) to the lowest point on the inferior margin of the nasal aperture on either side of the nasal spine (nariale) (De Villiers, 1968). A sliding caliper was used to record this measurement.
12. Nasal breadth- (al-al) the maximum breadth of the nasal aperture from the most laterally positioned points on the left and right sides (alare) (De Villiers, 1968). A sliding caliper was used to record this measurement.
13. Orbital breadth- (mf-ec) the measured distance from the medial border of the orbit at the point of intersection of the anterior lacrimal crest and the suture between the maxillary and frontal bones (maxillofrontale) and the lateral

border parallel to the upper and lower orbital margins (ectocanthion) (Knußman, 1988). A sliding caliper was used to record this measurement.

14. Orbital height- measured as the maximum orbital height, found perpendicular to orbital breadth (Knußman, 1988). A sliding caliper was used to record this measurement.
15. Interorbital breadth- (mf-mf) the direct distance between points on the medial borders of orbits where the anterior lacrimal crest meets the suture of the maxillary and frontal bones (maxillofrontale) (Knußman, 1988). A sliding caliper was used to record this measurement.
16. Mandibular body breadth- the maximum breadth measured in the region of the mental foramen perpendicular to the long axis of the mandibular body (Knußman, 1988). A sliding caliper was used to record this measurement.
17. Bigonial width- (go-go) the bigonial width is measured as the distance between left and right gonion of the mandible. The gonion is the point on the mandible where the inferior margin of the mandibular corpus and the posterior border of the mandibular ramus meet (De Villiers, 1968). A sliding caliper was used to record this measurement.
18. Minimum ramus breadth- the minimum distance between the anterior margin on the mandibular ramus and the line to the closest posterior point (De Villiers, 1968). A sliding caliper was used to record this measurement.
19. Maximum ramus breadth- the distance between the most anterior point on the mandibular ramus and line connecting the most posterior border of ascending

ramus (Moore-Jansen *et al.*, 1994). A sliding caliper was used to record this measurement.

20. Maximum ramus height- the direct distance from the highest point on the mandibular condyle to the point on the mandible where the inferior margin of the mandibular corpus and the posterior aspect of the ramus meet (gonion) (De Villiers, 1968). This measurement was taken using a mandibulometer with the mandible in position 1. Position 1: Where the mandible was in its standard horizontal plane. The rameal wing of the mandibulometer maintains contact with the left ramus at the condyle and the area above the angle, and with the right ramus at one or both of these regions of the mandible.
21. Mandibular projective length- the distance of the anterior margin of the chin from a centre point on a projected straight line placed along the posterior border of the two mandibular angles (De Villiers, 1968). This measurement was taken using a mandibulometer with the mandible in position 1.
22. Mandibular angle- the angle formed by the inferior border of the mandibular corpus and the posterior border of the ascending ramus (De Villiers, 1968). This measurement was taken using a mandibulometer with the mandible in position

3.2.2 NEW MEASUREMENTS

1. Zygomatic arch height- minimum distance vertically from the most inferior point on the margin of orbit to the inferior margin of zygomatic arch (Figure 13). A sliding caliper was used to record this measurement.
2. Temporal fossa height- measured as the height from the level of the porion which is the highest point on the superior margin of the external auditory

meatus, to the most superior point on the superior temporal line (Figure 13). The temporal fossa height measurement was taken while the skull was positioned in the Frankfurt plane. With the lateral side of the skull facing the observer one can eyeball a position so an imaginary plane passes through the porion and the lowest portion on the inferior margin of the orbit. The stationary arm of the sliding caliper helps to visualize this line. A sliding caliper was used to record this measurement.

3.2.3 DENTAL MEASUREMENTS

Measurements of central and lateral incisors, canines and first molars of both the maxilla and mandible on the left side were recorded. These teeth were chosen because they represent the dentition used for two very different functions of mastication. The anterior teeth are used for holding and biting where the posterior teeth, more specifically the first molars, are used in crushing and grinding food.

1. Mesio-distal crown diameter- (M-D) is the maximum length of the crown of the tooth in the mesio-distal direction at the midline perpendicular to the bucco-lingual crown width (Jacobson, 1982). A sliding caliper was used to record this measurement.
2. Bucco-lingual crown diameter- (B-L) maximum width of the crown of the tooth in the labial-lingual direction at the midline perpendicular to the mesio-distal crown length measurement (Jacobson, 1982). A sliding caliper was used to record this measurement.

3.2.4 INDICES/AREA

From the measurements taken as described above, the following indices and one area were calculated.

1. Cranial index- maximum cranial breadth/maximum cranial length x 100 (De Villiers, 1968).
2. Cranial height index- basion-bregma/ maximum cranial length x 100 (De Villiers, 1968).
3. Vertical index- basion-bregma/ maximum cranial breadth x 100 (De Villiers, 1968).
4. Frontoparietal index- minimum frontal breadth/ maximum cranial breadth x 100 (De Villiers, 1968).
5. Zygomaticofrontal index- minimum frontal breadth/ bizygomatic breadth x 100 (De Villiers, 1968).
6. Upper facial index- upper facial height/ bizygomatic breadth x 100 (De Villiers, 1968).
7. Gnathic index- basion – prosthion/ basion- nasion x 100 (De Villiers, 1968).
8. Oribital index- orbital height / orbital width x 100 (De Villiers, 1968).
9. Nasal index- nasal breadth / nasal height x 100 (De Villiers, 1968).
10. Molar crown area- (M-D x B-L) calculated from the product of the mesio-distal crown diameter and bucco-lingual crown diameter, the result gives an assessment of overall robustness of the tooth (Brace, 1967; Jacobson, 1982).

3.3 MORPHOLOGICAL ASSESSMENT

Table 3 gives descriptions of the morphological observations that were taken in a manner previously described in the literature. Four non-metric characteristics were observed and scored for their degree of expression for each skull in all groups.

1. Browridges- are located above the orbital margins on the frontal bone and extend laterally from the glabella. A browridge classified as one, lacking prominence, is typically the female form where a classification of five is very prominent and typically male.
2. Glabellar prominence- is the region of the frontal bone joining the two browridges superior to cranial landmark nasion. The degree of prominence classed as category one indicates very little expression and five as a very prominent glabellar region.
3. Mastoid process- one of the projecting processes of the temporal bone. It is a cone shaped projection located posterior and slightly inferior to the external auditory meatus. The mastoid process serves as muscle attachment for the sternocleidomastoid (sternomastoid) muscle which is used in rotation and flexion of the head. The mastoid's degree of development was observed and recorded. A score of one in mastoid development was very small and more typically female where a five was large and typically the male form.
4. Contour of dental arcade- the dental arcade shows three forms when observed in norma basalis. 1) horse-shoe shaped- varies from the U-shape where in the sides of the arcade converge slightly, often occurring around the second and third molars. 2) U-shaped- where the sides of the dental arcade are almost

parallel and the anterior region of the arcade has a smooth curvature. 3) divergent- the anterior region of the dental arcade appears slightly flattened in appearance unlike the horse-shoe and U-shaped expression. The sides of the arcade diverge posteriorly.

Morphological characteristics were scored on a scale of one to five, except for contour of the dental arcade. Figure 14 represents an estimated expression for grading browridges, where Figure 15 depicts the glabella region. The grading scheme for glabellar prominence and browridges was adapted from its original method recorded by De Villiers (1968) to give a grading scheme here from one to five. The mastoid processes in the male sample were also recorded and grades represented in Figure 16. Where previously De Villiers (1968) had graded the mastoid as small, medium or large here it was also graded on a scale of one to five. The dental arcade had three shapes in the South African black sample. A horse-shoe, U-shaped or divergent expression were classified and examples showed in Figure 17.

3.4 REPEATABILITY OF MEASUREMENTS

With data collection it is necessary to determine the reliability and repeatability of the measurements and observations collected. In order to do this the inter- and intra- observer agreement needed to be determined. Inter- and intra-observer agreement was assessed using the inter-/intra-class correlation coefficient (ICC) that can be determined from one-way analysis of variance (ANOVA). Inter-observer error was determined by randomly choosing 30 skulls that were previously measured and underwent a second evaluation of both morphological characteristics and measurements by another observer and values recorded and subjected to statistical

analysis to establish observer agreement. Intra-observer error was carried out by using the same 30 skulls, repeating and recording measurements and observations and then comparing results to the original data set recorded previously by the primary observer. The inter-and intra-observer agreement with respect to skull measurements allows us to determine the repeatability and accuracy of methodology used in this study.

The results of the correlation coefficient statistics follow previously accepted values. An ICC value of one is considered a perfect correlation where a value of 0.75 or higher is a high degree of correlation, a value of 0.5 to 0.74 indicates a moderate degree of correlation between measurements and anything below 0.49 is considered a low degree of correlation for observer agreement (Allan, 1982).

For the inter-observer and intra-observer error statistics for the examination of the chosen morphological characteristics of the skull the Cohen's kappa coefficient was calculated. The kappa value measures agreement between two observers or between multiple data sets collected by the same observer. A kappa value can range between zero and one. A kappa value of one says observations are in perfect agreement which is the ideal situation (Ferrante and Cameriere, 2009).

3.5 STATISTICAL ANALYSIS

The metric and morphological data were divided into three groups, based on their relative expression of prognathism. Group 1 (orthognathic) had a gnathic index of less than 97.9, group 2 (mesognathic) had an index of 98 – 102.9 and group 3 (prognathic) with an index of 103 or higher. Data collected for metric characteristics were used to calculate indices and areas. Both metric and morphological data were

subjected to statistical analysis. Descriptive statistics for the variables observed and for the data collected produced the means of cranial and tooth dimensions, indices and areas as well as the standard deviation (Strait, 1989). The descriptive statistics give a summary of the distribution of the data set used in this project.

A one-way ANOVA analysis of variance for cranial dimensions, tooth dimensions as well as indices and areas was run to determine if significant differences occurred between groups. The one-way analysis of variance tests the effect of one factor in response to a specific variable, in this case the cranial dimensions. The sum of squares which shows the measure of variation in the data set as well as the f-ratio was calculated. The f-ratio is the between groups mean square value divided by the within group mean square value (Cronk, 1999). The level of significance ($p \leq 0.05$, $p \leq 0.01$, $p \leq 0.001$) tells whether the f-ratio is greater than one for a specific variable. A value less than one for the f-ratio determines that the variation among the groups is not significant. The greater the calculated f-ratio for a specific cranial dimension the greater the level of significance between groups. Testing was done at the 0.05 level of significance.

The relationship between gnathic index and each of the various facial parameters, dental measurements, indices and areas needed to be determined. Statistics were performed to determine the Pearson correlation coefficients between the gnathic index and data collected. The Pearson correlation has a range of values from -1 to +1 where a value of -1 is a perfect negative correlation and a value of +1 is a perfect positive correlation. Coefficient of determination r^2 value indicates the goodness of fit of the regression line and was also recorded. R^2 values fall between 0%

and 100%. A value of zero for r^2 indicates that knowing the X variable does not help to determine a Y value, therefore, no correlation. A 100% r^2 indicates all values of the scatter plot fall exactly on the regression line and there is a 100% correlation between the two variables (Magee, 1990). In this case the X value is the cranial variable and the Y value is the gnathic index. The p-values were also recorded for the Pearson correlation statistics which determined whether the relationship was statistically significant.

Morphological data underwent statistical analysis to determine frequency and percent of distribution of expression for each morphological characteristic. Pearson Chi^2 statistic was carried out to compare observed and expected frequencies and to determine if there was a pattern of distribution (Cronk, 1999). A large Chi^2 value indicates that the distributions are different while a small Chi^2 value means distributions are similar. The p-value was given for each Pearson Chi^2 to determine if there was a level of significance to the distribution across the groups for each morphological characteristic.

3.6 FINITE ELEMENT ANALYSIS

The finite element portion of this study was done with the collaboration of other colleagues and departments. The Department of Mechanical and Aeronautical Engineering, University of Pretoria was instrumental in helping to perform the finite element analysis. The finite element model and analysis was generated and run with a studying engineer, Jaco Jansen Van Rensburg, under the direct supervision of Prof. Kok. Model development was carried out using skeletal material from the Pretoria Bone Collection, anatomical knowledge from the researcher on muscle insertion points

and knowledge of the finite element program on the part of the engineers. The finite element analysis was carried out at The Council for Scientific and Industrial Research (CSIR) in Pretoria, South Africa.

3.6.1 MATERIALS

For this part of the study, two skulls from the Pretoria Bone Collection were used (L'Abbe´ *et al.*, 2005). The selection of the two skulls was based on the gnathic index, as explained previously. A skull with a gnathic index of 106.9 was used to represent the prognathic facial form while a skull with gnathic index of 91.5 represented the orthognathic facial form. The skulls selected to be modeled were also chosen based on the fact that they had sufficient dentition antemortem. Any skull with significant tooth loss adapts to a decreased bite force, and therefore modeling higher forces in finite element analysis may produce unrealistic results.

3.6.2 METHODS

Computer tomography (CT) scans of the prognathic and orthognathic skulls were performed by Labuschagne and Partners at the Little Company of Mary Hospital, Pretoria, South Africa using a Siemens SOMATOM 16 medical CT scanner at 0.75 mm thickness. The prognathic skull file was a single stack of 629 slices, exported as DICOM files while the orthognathic skull was a single stack of 656 DICOM files.

3.6.2.1 THRESHOLDING

Using the stacks of CT scans and a computer aided design (CAD) program, a 3D surface mesh model was created. The program Amira® 5.1 (Visage Imaging, 2009) was used to perform the thresholding procedure where adjustments of the grey scale and attenuation of the CT scans was performed to highlight the bony morphology of the

two skulls and eliminate any unwanted material picked up by the scanner. A mesh model is a 3D shape represented by a finite number of geometric elements called finite elements. These elements are connected at their vertices by nodes. The exported DICOM files generated a three dimensional image of the structures enhanced during adjustment of the grey scale, creating an image of polygon file format (.ply).

The resultant skull covered by the specific number of finite elements is called a mesh (Figure 18). The current project used tetrahedral elements which consist of four triangular faces and contain four nodes (Figure 19). Four noded tetrahedral elements were used as a compromise between accurately representing skull geometry, the resultant stress patterns and the time necessary to run computational analysis. The final model for the prognathic skull consisted of 113 104 nodes and 401 455 elements where the orthognathic skull model consisted of 110 645 nodes and 397 354 elements.

The 3D model surface mesh was then edited looking for any imperfections, holes in the mesh or areas where triangles intersected or inconsistencies existed in the model by using the software VRMesh Studio (VirtualGrid, Seattle City, WA). The model was then smoothed by remeshing where triangles had sharp edges to avoid possible singularities and jumps in stress distribution. Smoothing of the mesh produces more accurate results when recording Von Mises stress (Camacho *et al.*, 1997; Boryor *et al.*, 2008). The volumetric finite element mesh model was created using TetGen freeware software (Numerical Mathematics and Scientific Computing, Berlin, Germany).

3.6.2.2 MATERIAL PROPERTIES

Pre-processing work on the skull models was carried out using PreView Finite Element Pre-Processing software (University of Utah, Musculoskeletal Research

Laboratories, Salt Lake City, Utah). The material properties of the bones being investigated needed to be attributed to the model. Only the material constants of Young's modulus and Poisson's ratio need to be provided when modeling properties of isotropic materials. Linear elastic isotropic material properties have been used previously throughout the literature when modeling bone (Yamada, 1970; Borchers and Reichart, 1983; Tanne *et al.*, 1988; Korioth *et al.,* 1992; Meijer *et al.,* 1993; Clelland *et al.,* 1995; Meijer *et al.,* 1996; Sertgoz and Guvener, 1996; Camacho *et al.*, 1997; Gross *et al.,* 2001; Ichim *et al.*, 2006; Reina *et al.*, 2007; Kupczik *et al.*, 2007; Provatidis *et al.*, 2008; Boryor *et al.*, 2008; Gröning *et al.*, 2009). Authors using linear isotropic properties to model bone, although it is anisotropic by nature, found it capable of producing patterns of stress comparable to those of realistic patterns (Tanne *et al.*, 1989a; Tanne *et al.*, 1989b; Tanne and Sakuda, 1991; Daegling and Hylander, 1998; Strait *et al.*, 2005; Ichim *et al.*, 2006; Provatidis *et al.*, 2008; Curtis *et al.*, 2008).

The Young's modulus used for this project was taken from the literature (Peterson and Dechow, 2003). Peterson and Dechow (2003) determined the various material properties in the bones of the human cranial vault, specifically areas of the parietal, frontal, occipital, temporal and zygomatic bones. Although their results found significant differences between bones and within bones themselves, in order to model linear elastic material properties an approximate average was taken of the Young's modulus of all bones and was used in the finite element analysis (E= 16 GPa). Poisson's ratio of 0.3 was used which has been used previously in other finite element models using bone (Tanne *et al.*, 1988; Ichim *et al.*, 2006; Provatidis *et al.*, 2007;

Kupczik *et al.*, 2007; Provatidis *et al.*, 2008; Boryor *et al.*, 2008; Boryor *et al.*, 2008; Gröning *et al.*, 2009).

3.6.2.3 BOUNDARY CONDITIONS

When modeling force vectors for muscles and indicating the direction of forces, a coordinate system in relation to the skull needs to be defined. The direction of the x,y and z axes are as follows: the x-axis represented the horizontal plane; the y-axis is orientated anterior-posteriorly in relation to the skull while the z-axis is superior-inferior to the skull.

The next step in creating the finite element model was to determine the boundary conditions and load magnitudes. A critical limit exists within bone where failure occurs. This project was not concerned with the critical limits which the bones could withstand, but the distribution of the stress itself throughout the skull. Forces exerted on the skull by the muscles that are primarily used in elevation of the jaw during mastication were modeled as external loads and it was assumed that muscle fibres themselves were attached directly to the bone.

Muscles were modeled by applying forces to the nodes in the region representing the site of muscle attachment (Sellers and Crompton, 2004; Ross *et al.*, 2005; Ichim *et al.*, 2006; Reina *et al.*, 2007; Kupczik *et al.*, 2007; Röhrle and Pullan, 2007).

3.6.2.4 FORCE VECTORS MAGNITUDE AND ORIENTATION

A vertical force was applied to the first molar and first incisor on the left side at nodes of the occlusal surface. The total force applied to the occlusal surface of the

molar and incisor was 657.2N and 410.6N respectively. The resultant magnitude of the forces for muscles and individual contributions are found in Tables 4 to 7.

In the case of the temporal muscle, forces were applied along the nodes representing the temporal lines of the lateral sides of the skull. The muscle was divided into seven segments and the geometric average nodal coordinate for each segment was determined (Figure 20). The direction of the force for each segment was taken as the direction from the average nodal coordinate to a point representing the coronoid process of the mandible.

Blanksma and van Eijden (1990) determined the activity of various regions of the temporalis muscle for a vertical bite force. The activity of the muscle segment together with the number of nodes in that segment was used to divide the total force across the defined areas of the temporalis using the weight factors. Because this temporal muscle was divided into seven sections running from anterior to posterior and Blanksma and van Eijden (1990) used a temporal muscle divided into six, the data were modified. For this temporalis section 6 an average value from the data used from Blanksma and van Eijden (1990) temporalis section's 5 and 6 was used. Section 7 of the temporalis was weighted as previously done for Blanksma and van Eijden's (1990) section six. Values of temporalis muscle forces used for each skull modeled are summarized in Tables 4 and 5 for molar and incisor bites respectively.

The nodes of the superficial masseter muscle were selected on the inferior anterior margin of the zygomatic arch. The force was divided evenly by the total number of nodes in the muscle origin area. The direction of the force was towards a point representative of the angle of the mandible. The deep masseter was modeled

with the direction of the muscle force orientated towards the site of insertion on the body of the mandible. The muscle force of the medial pterygoid was distributed evenly about the nodes of the pterygoid fossa of sphenoid bone and directed towards a point representing the insertion area on the medial side of the angle of the mandible.

3.6.2.5 BALANCING AND WORKING SIDES OF THE MUSCLES

Muscle action during the cycles of mastication vary for the working and balancing sides (Sellers and Crompton, 2004; Ross *et al.*, 2005; Reina *et al.*, 2007; Röhrle and Pullan, 2007). The working side is characterized as the same side of the dental arcade where the bite occurs. In this study the working side was always the left side of the skull. Forces on the working and balancing sides were scaled in the same way as described in the literature (Strait *et al.*, 2007). The balancing side forces for temporalis were calculated to be approximately 41% of the working side, 47% for superficial masseter, 36% for deep masseter and 20% for medial pterygoid. Muscle forces for balancing and working sides can be found in Tables 6 and 7 for molar bite and incisor bite, respectively.

3.6.2.6 REACTION FORCES AT ARTICULUR EMINENCE

The model was constrained in the region of the foramen magnum at the occipital condyles in all three degrees of freedom to prevent rigid body movement (Tanne *et al.*, 1988; Provatidis *et al.*, 2007; Provatidis *et al.*, 2008). General skeletal anatomy shows that the area of the foramen magnum articulates with the spinal column. The masticatory forces are an internally balanced system, therefore, forces at the tooth and articular eminence are required so that the occipital condyles do not incur any twist or rotational forces (force multiplied with lever arm).

For each skull the geometric average nodal coordinate where the muscle forces were applied to each model are defined. Reaction forces expected, along with known force values, were used to set up and solve a system of linear equations. There are seven unknowns, six in terms of the force values at the articular eminence in the x,y, z-axis and one at the tooth in the z-axis. A maximum of six unknowns can be solved for in three dimensional rigid body static analyses. Therefore, a seventh equation was assumed, where the force values in the x-axis for the articular eminences on the left and right sides are the same.

After solving the set of linear equations, a sensitivity analysis on the assumption of the seventh equation was performed. In modifying the range of the scale of Von Mises stress distribution it was observed that there are minor differences in the stress pattern at the articular eminence between the left and right sides. These differences were deemed negligible in terms of the scale used in the final analysis.

The forces resulting from the set of linear equations were applied as boundary conditions in the finite element model. Forces were applied to a set of nodes and not a single nodal coordinate as assumed in the static analysis. This, together with the fact that the skull is not a rigid body and does in fact slightly deform, produces some stress in the area of the condyles. These resultant stresses were orders of magnitude smaller than the stress patterns observed in that of the facial skeleton.

3.6.2.7 SCALING

In order to compare models, size needs to be controlled by scaling. Patterns of stress distribution using finite element analysis are more sensitive to model shapes than the change in material properties or muscle magnitude and loading (Dumont *et*

al., 2009). Normalizing the geometry needed to be done so that the differences in the stress distribution patterns were not due to the size of the geometry but attributed to the geometry itself. For the prognathic skull the cranial landmark basion was chosen as nodal coordinate (0,0,0). The orthognathic skull was scaled so that a line from the basion to nasion landmarks was the same size for both models. Muscle and resultant forces in the orthognathic model were scaled so bite forces were equal for both models.

3.7 ANALYSIS

The methodology and material properties were constant for generating both models for finite element analysis. Muscle force vectors and areas of attachment were determined by the bony morphology of each skull.

Several finite element analyses were run using FEBio Finite Elements for Biomechanics 1.1.7 (University of Utah, Musculoskeletal Research Laboratories, Salt Lake City, Utah), a list of which is provided below:

1. The resultant displacement which occurs during an incisal and molar bite force were run and scaled to show deformation in the craniofacial region.
2. Analysis was run for pressure for an incisor and molar bite force in both models.
3. All masticatory muscle forces (temporalis, deep and superficial masseter and medial pterygoid) were applied to the model as well as a vertical force on the occlusal surface of the left first maxillary molar and Von Mises stresses observed.

4. The forces of individual muscles at their origins were then modeled in order to see how they contribute to the overall stress in molar biting and Von Mises stresses observed.
5. All jaw elevator muscles were then modeled with an incisal bite force in the vertical direction for both models and Von Mises stresses observed.
6. Individual muscles were modeled again to see their contribution to the overall stress of an incisal bite force and Von Mises stresses observed.

PostView Finite Element Post Processing (University of Utah, Musculoskeletal Research Laboratories, Salt Lake City, Utah) was used to manipulate and visualize stress states and displacement plots for the results after the analyses were run.

Table 1. Group distribution and gnathic index values.

GROUP	N	Gnathic Index Mean	Std. Deviation	Minimum	Maximum
Orthognathic	52	96.1	1.6	91.5	97.9
Mesognathic	59	100.9	1.4	98.0	102.9
Prognathic	51	105.5	2.2	103.0	113.0
Total	162				

Table 2. List of measurements recorded for each skull.

Measurement	Landmarks
STANDARD MEASUREMENTS	
Maximum cranial length	glabella-opisthocranion
Maximum cranial breadth	euryon- euryon
Bizygomatic breadth	zygion-zygion
Basion – bregma height	basion-bregma
Cranial base length	basion-nasion
Basion – prosthion	basion –prosthion
Maxillo-alveolar breadth	ectomolare- ectomolare
Maxillo-alveolar length	
Upper facial height	nasion-prosthion
Minimum frontal breadth	frontotemporale- frontotemporale
Nasal height	
Nasal breadth	alare-alare
Orbital breadth	maxillofrontale-ectocanthion
Orbital height	
Interorbital breadth	maxillofrontale-maxillofrontale
Mandibular body breadth	
Bigonial width	gonion-gonion
Minimum ramus breadth	
Maximum ramus breadth	
Maximum ramus height	
Mandibular projective length	
Mandibular angle	
NEW MEASUREMENTS	
Zygomatic arch height	
Temporal fossa height	
DENTAL MEASUREMENTS	
Mesio-distal crown diameter	
Bucco-lingual crown diameter	
INDICES AND AREA	
Cranial index	
Cranial height index	
Vertical index	
Frontoparietal index	
Zygomaticofrontal index	
Upper facial index	
Gnathic index	
Orbital index	
Nasal index	
Molar crown area	

Table 3. List of standard morphological characteristics recorded for each skull.

Standard Morphological Characteristics Recorded		**Grading Scheme**
1	Browridges	Graded on their prominence classified from 1 to 5, zero being flat with lacking prominence (typical female form) and five being very prominent (typical male form) (De Villiers, 1968).
2	Glabellar prominence	Varying degrees of glabellar prominence classified in five classes ranging from 1 (flat- typical female form) to 5 (very prominent- typical male form) (De Villiers, 1968).
3	Mastoid process	Judged according to the degree of development graded from 1 (small- typical female form) to 5 (large-typical male form) (De Villiers, 1968).
4	Contour of dental arcade	Variation in shape graded as either in category of horseshoe shape (1), U- shape (2) or divergent (3) (De Villiers, 1968).

Table 4. Total muscle forces (N) for the sections of temporalis muscle for balancing and working sides at molar bite with unit vector coordinates (x,y,z).

		Working Side	Balancing Side
Prognathic Model			
Section	1	183.5	70.4
		(-0.5,0.14,-0.98)	(0.03,0.15,-0.98)
	2	73.4	36.7
		(-0.10,-0.14,-0.98)	(0.069,-0.14,-0.98)
	3	52.4	26.3
		(-0.13,-0.36,-0.92)	(0.11,-0.38,-0.91)
	4	62.3	23.0
		(-0.18,-0.58,-0.79)	(0.14,-0.58,-0.79)
	5	32.9	11.8
		(-0.19,-0.73,-0.64)	(0.15,-0.74,-0.65)
	6	15.8	6.9
		(-0.21,-0.82,-0.51)	(0.18,-0.83,-0.51)
	7	27.5	9.9
		(-0.23,-0.84,-0.47)	(0.24,-0.85,-0.46)
Orthognathic Model			
Section	1	167.6	68.1
		(-0.6,0.22,-0.97)	(0.94,0.15,-0.98)
	2	70.4	28.9
		(-0.10,-0.09,-0.99)	(0.10,-0.12,-0.98)
	3	65.1	23.2
		(-0.12,-0.32,-0.93)	(0.11,-0.34,-0.93)
	4	45.8	22.7
		(-0.16,-0.55,-0.81)	(0.13,-0.56,-0.81)
	5	30.4	13.6
		(-0.18,-0.72,-0.66)	(0.13,-0.72,-0.67)
	6	19.2	7.0
		(-0.23,-0.82,-0.52)	(0.16,-0.82,-0.54)
	7	26.2	10.1
		(-0.30,-0.80,-0.51)	(0.23,-0.81,-0.53)

Table 5. Total muscle forces (N) for the sections of temporalis muscle for balancing and working sides at incisor bite with unit vector coordinates (x,y,z).

		Working Side	Balancing Side
Prognathic Model			
Section	1	183.5	70.4
		(-0.05,0.14,-0.98)	(-0.23,-0.84,-0.47)
	2	73.4	36.7
		(-0.10,-0.14,-0.98)	(0.03,0.15,-0.98)
	3	52.4	26.3
		-0.10,-0.14,-0.98)	(0.06,-0.14,-0.98)
	4	62.3	23.0
		(-0.13,-0.36,-0.92)	(0.11,-0.38,-0.91)
	5	32.9	11.8
		(-0.18,-0.58,-0.79)	(0.14,-0.58,-0.79)
	6	15.8	6.9
		(-0.19,-0.73,-0.64)	(0.15,-0.74,-0.65)
	7	27.5	9.9
		(-0.21,-0.82,-0.51)	(0.18,-0.83,-0.51)
Orthognathic Model			
Section	1	170.1	69.2
		(-0.06,0.22,-0.97)	(0.09,0.15,-0.98)
	2	71.5	29.4
		(-0.10,-0.09,-0.99)	(0.10,-0.12,-0.98)
	3	66.1	23.5
		(-0.12,-0.32,-0.93)	(0.11,-0.34,-0.93)
	4	46.4	23.0
		(-0.16,-0.55,-0.81)	(0.13,-0.56,-0.81)
	5	30.9	13.8
		(-0.18,-0.72,-0.66)	(0.13,-0.72,-0.67)
	6	19.5	7.1
		(-0.23,-0.82,-0.52)	(0.16,-0.82,-0.54)
	7	26.6	10.3
		(-0.30,-0.80,-0.51)	(0.23,-0.81,-0.53)

Table 6. Total muscle forces (N) for muscle on working and balancing sides of molar bite for superficial and deep masseter and medial pterygoid with unit vector coordinates (x,y,z).

		Force (N)	Orientation unit vector x,y,z
Prognathic Model			
superficial masseter			
	Working side	229.7	(-0.09,0.22,-0.97)
	Balancing side	107.9	(0.09,0.22,-0.97)
deep masseter			
	Working side	100.0	(-0.36,-0.12,-0.91)
	Balancing side	36.0	(0.36,-0.12,-0.91)
medial pterygoid			
	Working side	250.6	(0.46,0.39,-0.78)
	Balancing side	50.1	(-0.46,0.39,-0.78)
Orthognathic Model			
superficial masseter			
	Working side	216.6	(-0.06,0.18,-0.97)
	Balancing side	101.7	(0.06,0.18,-0.97)
deep masseter			
	Working side	94.2	(-0.15,-0.18,-0.96)
	Balancing side	33.9	(0.15,-0.18,-0.96)
medial pterygoid			
	Working side	235.2	(0.65,0.12,-0.75)
	Balancing side	47.0	(-0.65,0.12,-0.75)

Table 7. Total muscle forces (N) for muscle on working and balancing sides of incisor bite for superficial and deep masseter and pterygoid with unit vector coordinates (x,y,z).

	Force (N)	Orientation unit vector x,y,z
Prognathic Model		
superficial masseter		
Working side	229.7	(-0.9,0.22,-0.97)
Balancing side	107.9	(0.09,0.22,-0.97)
deep masseter		
Working side	100.0	(-0.36,-0.12,-0.91)
Balancing side	36.0	(0.36,-0.12,-0.91)
medial pterygoid		
Working side	250.6	(0.46,0.39,-0.78)
Balancing side	50.1	(-0.46,0.39,-0.78)
Orthognathic Model		
superficial masseter		
Working side	219.9	(-0.06,0.18,-0.97)
Balancing side	103.2	(0.06,0.18,-0.97)
deep masseter		
Working side	95.6	(-0.15,-0.18,-0.96)
Balancing side	34.4	(0.15,-0.18,-0.96)
medial pterygoid		
Working side	238.7	(0.65,0.12,-0.75)
Balancing side	47.7	(-0.65,0.12,-0.75)

Figure 13. Lateral view of zygomatic arch height (A) and temporal fossa height (B) measurements.

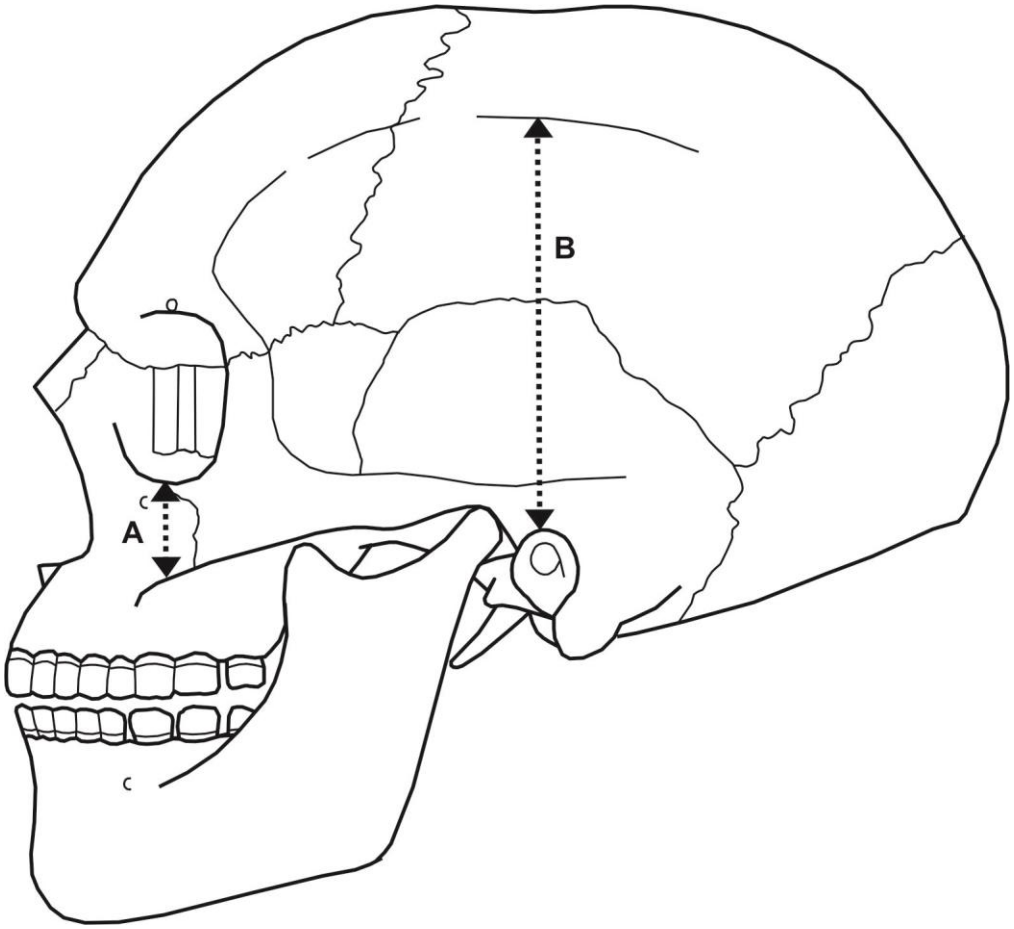

Figure 14. Grading scheme (1-5) of browridge detail. Browridge detail of one lacking prominence and grade five is most prominent.

browridge 1 browridge 2 browridge 3 browridge 4 browridge 5

Figure 15. Grading scheme from 1 (small) to 5 (large) for glabella region. Grade one is a flat glabella region and five is very prominent.

glabella 1 glabella 2 glabella 3 glabella 4 glabella 5

Figure 16. Grading scheme 1 (small) to 5 (large) for mastoid process expression. Grade one is smallest and more typical female form and five is large and the more male expression of the mastoid.

mastoid 1

mastoid 2

mastoid 3

Figure 16 (con't). Grading scheme 1 (small) to 5 (large) for mastoid process expression. Grade one is smallest and more typical female form and five is large and the more male expression of the mastoid.

mastoid 4

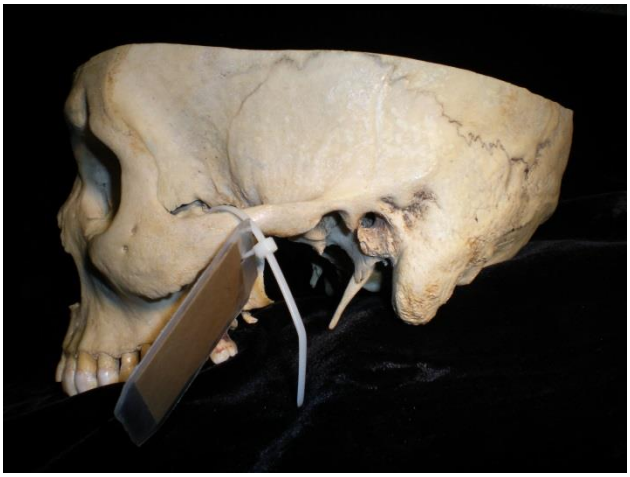

mastoid 5

Figure 17. Grading scheme (1-3) for dental arcade morphology.

dental arcade 1= horseshoe

dental arcade 2= U-shape

dental arcade 3= divergent

Figure 18. Mesh of prognathic skull finite element model.

Figure 19. Four nodded tetrahedral element used to create three dimensional volumetric mesh model of each skull.

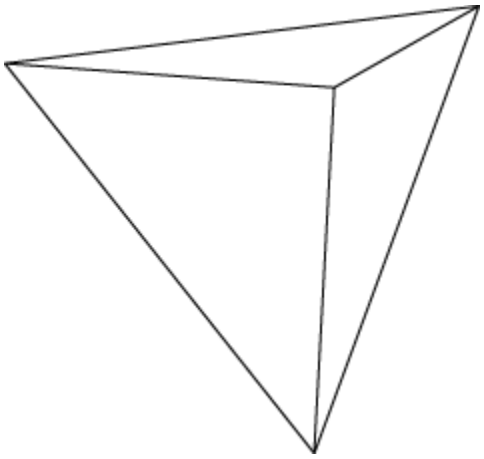

Figure 20. Temporal muscle sections, area of average nodal coordinate and muscle force direction.

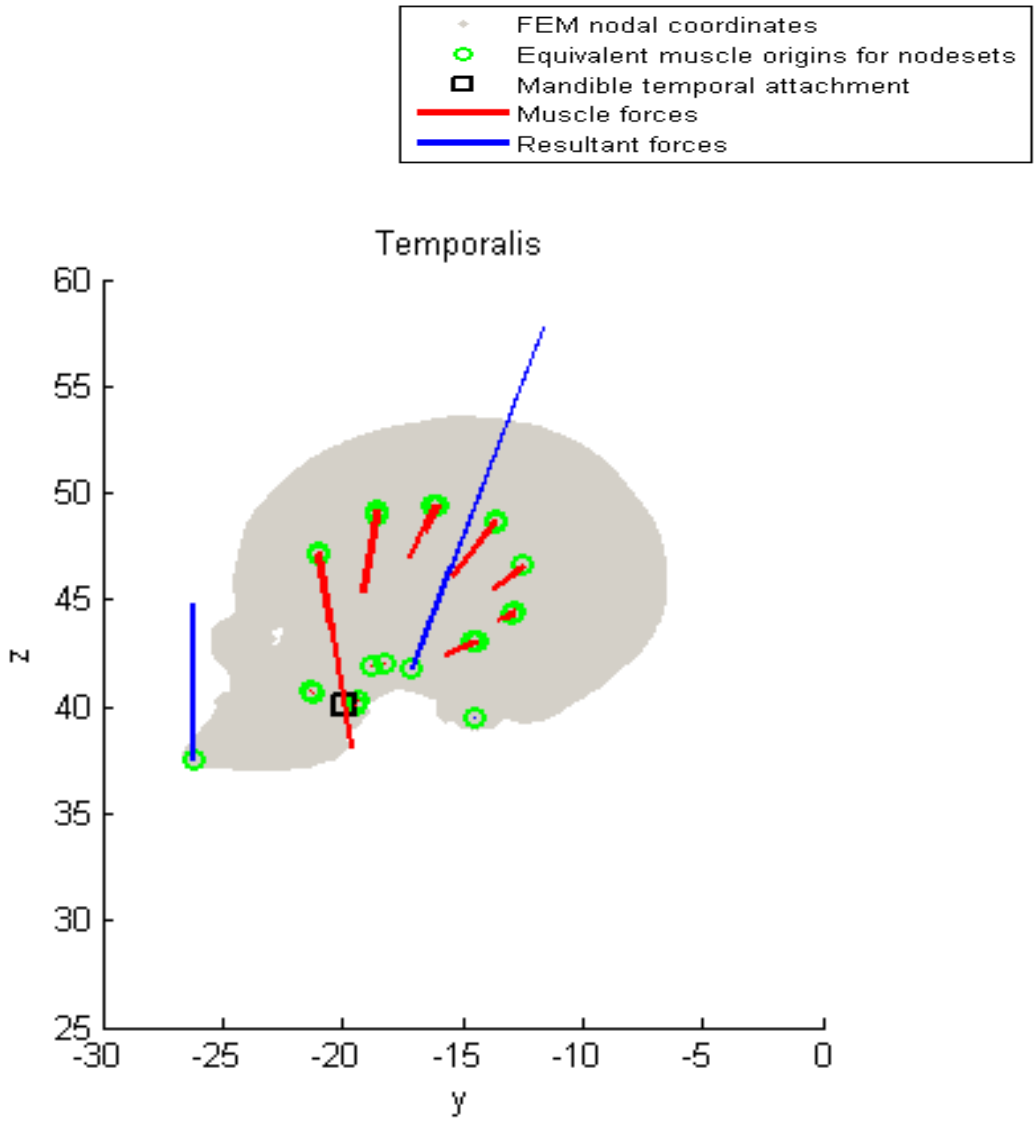

CHAPTER 4

RESULTS OF METRIC ANALYSIS

4.1 DESCRIPTIVE STATISTICS

Descriptive statistics which show the extent of the variation recorded within the sample for all cranial dimensions with their mean, minimum and maximum values are given in Table 8. The cranial length and basion-bregma measurement showed the highest variability within the sample while the mandibular body breadth recorded the lowest. Table 9 shows the descriptive statistics for tooth dimensions of the maxilla and mandible recorded for the first and second incisors, canines and first molars. The number of mesio-distal measurements per tooth varies because some of the dental measurements could not be taken if the tooth was missing ante-mortem or post-mortem, or in some cases the tooth was broken and could not be measured accurately. The number of teeth in the sample ranges from 81 to 152 per tooth type. The first molars were the only molars measured and understandably produced the largest mean values for bucco-lingual and mesio-distal measurements overall, in both the maxilla and mandible. The values recorded from this skeletal sample for dental measurements were in the range of values previously recorded for other South African black populations (Kieser, 1990).

The values for indices calculated from cranial measurements and molar crown areas from dental measurements are shown in Table 10. The mean gnathic index for all individuals was calculated to be 100.8. The greatest variability was found with the orbital index from this sample. The calculated areas recorded from the molar dental

measurements showed the mandibular molar mean area (120.64) was greater than that calculated for the maxillary molar mean area (117.85).

4.2 ONE-WAY ANOVA STATISTICS

One-way ANOVA analyses were run to determine if statistically significant differences existed between the orthognathic, mesognathic and prognathic groups for the various cranial dimensions (Table 11). The mean values of cranial length, cranial breadth, minimum frontal breadth, orbital breadth, orbital height, and bigonial width appear to get smaller as prognathism increases. These changes were however slight, with large standard deviations appearing in all three groups. Values of basion-prosthion, maximum alveolar length, mandibular body breadth, mandibular projective length and zygomatic arch height increase with the degree of prognathism. Nasal breadth and nasal height appeared not to be affected by the degree of prognathism within this sample, while the remaining dimensions also did not show any clear trends.

One-way ANOVA statistics for differences between groups showed that nine of the 24 measurements differed significantly between groups. Three cranial measurements were found to be significantly different between groups at $p \leq 0.001$ those being basion-nasion, basion-prosthion and maximum alveolar length (Table 11). Four measurements were found significantly different at $p \leq 0.01$, namely the basion-bregma and all three measurements of the ramus specifically the minimum ramus breadth, maximum ramus breadth and maximum ramus height. The measurements of interorbital breadth and mandibular projective length differed significantly between the three groups at $p \leq 0.05$.

Mean values for the group dental measurements are found in Table 12. Dental measurements showed that the maxillary first and second incisors in the mesio-distal direction and the molar in the bucco-lingual direction increased with the degree of

prognathism. The mesio-distal measurement of the mandibular first incisor also increased across groups with prognathism. For every measurement of the teeth there was an increase in size from the orthognathic to the mesognathic group, with some increases from mesognathic to prognathic group. The larger standard deviations found in the prognathic group showed that there is a general trend to increase the size of the dentition with increased prognathism.

Although there was a trend for the increase in both mesio-distal and bucco-lingual dental dimensions with the increase in prognathism, just five of the sixteen measurements were found significant. One-way ANOVA results for statistically significant differences between groups for tooth measurements showed the mesio-distal measurements of the maxillary canine ($p=0.012$) and mandibular canine ($p=0.0477$) were significant at $p\leq0.05$ (Table 12). The canine size in both the maxilla and mandible was clearly associated with the degree of prognathism. Only the bucco-lingual measurements of maxilla and not those of the mandible were found statistically significant between groups. The bucco-lingual measurements showed significant differences between the groups in the maxillary first incisor, canine and first molar at the $p\leq0.01$ level of significance.

Shape changes with the degree of prognathism can be observed by looking at the calculated cranial indices. Cranial vault shape is characterized by three indices, which are the cranial, cranial height and vertical indices. In looking at the mean values of the indices across the three groups, the trend toward a specific cranial shape is unclear. However, when comparing the orthognathic and prognathic groups directly, the trend for a lower, narrower cranium as prognathism increases becomes obvious.

Mean values of indices (Table 13) found to be largest in the orthognathic group were the cranial index (71.5), cranial height index (72.1), vertical index (100.9) and orbital index

(91.6). There is no trend in any of the indices with the change in the degree of prognathism, except for the upper facial index and the molar area of the maxilla which are the only two weakly significant.

The prognathic group found largest values for the frontoparietal index (74.1), zygomaticofrontal index (76.1) and upper facial index (53.6). Only the upper facial index ($p \leq 0.05$) was found significantly different between groups. Maxillary molar crown area was the only area significantly different between groups with $p=0.027$, therefore, the prognathic group has significantly larger maxillary molars over mesognathic and orthognathic individuals.

There was no clear relationship found between the degree of prognathism and cranial shape, nasal shape, orbital shape or the area of the mandibular first molar. Only the upper facial index and the area of the first molar of the maxilla were significantly associated with the degree of prognathism.

4.3 LINEAR REGRESSION STATISTICS

Bonferroni adjustments are sometimes used to compare multiple hypotheses (Perneger, 1998). The current project was not testing a specific hypothesis (e.g., proposing that a specific cranial dimension or morphology correlates with the gnathic index), instead the author was exploring if correlations exist between cranial, facial, dental dimensions or morphology with the degree of prognathism. Applying the Bonferroni adjustment to the data is more restrictive in determining the significance of the relationship with prognathism because it adjusts by reducing the p-value for significance (Moran, 2003).

The Bonferroni adjustment was applied to the Pearson correlation results found in Tables 14, 15 and 16. When calculated, the Bonferroni corrected level at which the correlation would be deemed significant was changed to $p \leq 0.002$, $p \leq 0.003$ and $p \leq 0.005$ for

the cranial dimensions, dental dimensions and indices respectively. When the Bonferroni adjustment was applied to the data all but one of the values previously determined as significant were now excluded. The only dimension that remained significantly correlated to the gnathic index was the maximum alveolar length ($p \leq 0.001$), as would obviously be expected. The fact that many of the statistically significant correlations were lost suggests that the correlation between the given feature and prognathism is relatively small as can been seen by the other morphometric results.

The problem with applying Bonferroni adjustment in this instance is that it statistically reduces the power to detect possible significant correlations when they actually exist, as was discussed previously by other authors (e.g., Perneger, 1998; Cabin and Mitchell 2000; Nakagawa 2004; García, 2004). In addition, as discussed by Moran (2003), significant results mean something is happening with the data. Since no specific hypothesis was being tested the results that showed significant correlations should not be over looked with regard to their relationship with the degree of prognathism. Consequently, 0.05 was used for the α-level to determine significance of the following results.

Linear regression statistics showing relationships between gnathic index (basion-prosthion/ basion-nasion x 100) and cranial measurements are found in Table 14, giving Pearson correlation coefficients (r) for each variable. The measurement, which was not a variable of the gnathic index, with the highest correlation was the maximum alveolar length ($r = 0.58$). This clearly indicates a relationship between the degree of prognathism and the maximum alveolar length where an increase in one gives rise to an increase in the other parameter.

The direction of the correlation (relationship) is as important as the value of the coefficient itself. The Pearson correlation is positive for maximum cranial breadth,

maximum alveolar breadth, maximum alveolar length, upper facial height, mandibular body breadth, minimum and maximum ramus breadth, maximum ramus height, mandibular projective length and the zygomatic arch height. This indicates that with an increase in prognathism there is a subsequent increase in these other cranial dimensions. The measurements for the ramus of the mandible are all positively correlated with prognathism where this may be a function of the muscle attachments for the increased jaw size. All remaining Pearson correlation values for cranial measurements were negative, indicating a decrease in the cranial dimension with an increase in prognathism.

Nine of the measured parameters were significantly correlated with the gnathic index. Those that were negatively correlated to the gnathic index were the orbital height ($p \leq 0.05$), orbital breadth ($p \leq 0.01$), basion-bregma height ($p \leq 0.01$), and the interorbital breadth ($p \leq 0.01$). These measurements tended to decrease as the gnathic index increased.

Three parameters were found to be positively correlated to the gnathic index and statistically significant. Mandibular body breadth was positively correlated to the gnathic index significant at $p \leq 0.05$. The minimum ramus breadth and the maximum alveolar length were also positively correlated with gnathic index and achieved a $p \leq 0.01$ and a $p \leq 0.001$ level of significance respectively.

Some of the linear regression statistics may show significant correlations for small relationships due to the large sample size. The r^2 coefficients are also found in Table 14 for each of the cranial dimensions. Except for the coefficient for maximum alveolar length (33.75), the values are very low. The low r^2 coefficient indicates that almost none of the variation seen with the individual cranial dimension can be explained by prognathism alone.

Scatter plots were generated only for the dimensions or values with a significant level of correlation with the gnathic index. Figure 21 shows a scatter plot of gnathic index

against basion-bregma height. The linear relationship shows a negative slope of the regression line. The r^2 coefficient used to determine goodness of fit for the line shows that only 5.17% of the variation in the gnathic index is explained by the relationship between gnathic index and basion-bregma height, an indication that most of the variation in the gnathic index is due to some other characteristic. A slight trend can be seen with the increase in basion-bregma height there is a decrease in the degree of prognathism, therefore the higher the skull, the lesser the prognathism.

The relationship of the maximum alveolar length with the gnathic index can be seen in Figure 22. The positive slope of the regression line and a 33.75% goodness of fit for the maximum alveolar length made this relationship much clearer. The relationship showed that with an increase in the maximum alveolar length also came an increase in the degree of prognathism, as expected.

Figures 23 through 26 show interorbital breadth, mandibular body breadth, minimum ramus breadth, and orbital breadth each plotted against the gnathic index. All figures showed scatter about the linear regression line but with a negative trend for interorbital and orbital breadth. In these two, the dimension value increases as the gnathic index decreases. Mandibular body and ramus breadth appear to be positively correlated with the gnathic index and with an increase in their value an expected increase in the gnathic index may be observed.

Orbital height is plotted in Figure 27 with a negative slope of the regression line. A trend toward an increase in orbital height with the decrease in gnathic index of this sample set can be observed. This indicates that more prognathic individuals tend to have lower orbits and vice versa.

All Pearson correlation coefficient statistics assessing the relationship between gnathic index and tooth measurements were positive (Table 15). This in general means that the more prognathic individuals will tend to have larger teeth. Significant correlations were found in the mesio-distal direction for the maxillary second incisor, canine and mandibular second incisor and first molar. Bucco-lingual measurements showed significant correlations for the maxillary first incisor, canine and first molar. The levels of significance are indicated in the table.

The Figures 28 through 34 show scatter plots representing the dental measurements that were significantly correlated with the gnathic index. For all the plots a positive relationship was observed, and with the increase in tooth dimension came a subsequent increase in prognathism. The mesio-distal measurements of the maxillary canine (Figure 29) and mandibular second incisor (Figure 33) had the largest slope of the regression line.

Gnathic index regression statistics with other cranial indices and molar areas are found in Table 16. Statistically significant correlations were found with two indices only. The only facial shape to be significantly correlated with the gnathic index was that of the upper facial region (upper facial index), significant at $p \leq 0.05$. The scatter plot for the upper facial index illustrates a random distribution of data points with a positive slope for the goodness of fit line (Figure 35). As the degree of prognathism increased across groups so did the upper facial index, indicating a longer and narrower face. This result can most probably be explained by the increased nasion-prosthion length that can be expected in individuals with more mid-facial projection. The maxillary molar area also showed a $p \leq 0.01$ level of significance ($p=0.0244$) when correlated with the increased prognathism. Figure 36 illustrates the positive relationship between maxillary molar area and the gnathic index.

This reiterates the trend as described before, namely that more prognathic individuals tend to have larger teeth.

The metric results in this chapter show results for all individuals. The values achieved for individual group statistics are included as an Appendix. Table A of the Appendix shows results for the relationship between gnathic index and a specific facial parameter, Table B the gnathic index and its relationship with dental measurements and Table C the relationship between the gnathic index and calculated indices. These tables show the full data set and also results for relationships between the orthognathic, mesognathic and prognathic groups.

In summary, significant differences were found in some craniofacial and dental dimensions and shapes between the orthognathic, mesognathic and prognathic groups. Measurements associated with the masticatory apparatus which were directly affected by the degree of prognathism between groups were the maximum alveolar length and minimum ramus breadth. These measurements were also found to be significantly correlated with the gnathic index through linear regression statistics. Both measurements reflect an increase in size which may be functionally determined by the masticatory system due to the increased prognathism.

The cranial and facial dimensions significantly different between groups were the basion-bregma height and the interorbital breadth, respectively. Both measurements were found significantly related to the gnathic index. This indicates that with increased prognathism a subsequent decreased skull height and interorbital breadth can be expected. This can possibly be ascribed to function in the more efficient distribution of muscle attachments used in mastication. Otherwise it may be recognized as a more efficient way to

accommodate for stress during mastication. This will be addressed in more detail in the discussion.

Maxillary dentition is influenced more by the degree of prognathism than the mandibular teeth. Five of the eight dental measurements of the maxillary teeth were significantly correlated with the gnathic index as compared to two of the eight in the mandible. The area of the first molar of the maxilla was also significantly correlated to the gnathic index where the area increased with the degree of prognathism. The mandibular first molar area of the mandible was not found significantly correlated with prognathism. This is to be expected, as the degree of prognathism is directly related to the amount of space available for the maxillary teeth.

A clear association was found between the upper facial index and prognathism. The upper facial index was found to be significantly different between groups by one-way ANOVA statistics and also significantly correlated with the gnathic index. This shows that the shape changes due to the degree of prognathism can be expected in the facial skeleton reflecting a medium to long narrow face as prognathism increases.

4.4 INTER/INTRA-CLASS CORRELATION STATISTICS

Inter- and intra-class correlation statistics were calculated in order to determine whether the measurements could be repeated with a high degree of accuracy. The interclass correlation coefficient was calculated for each of the 56 measurements taken on the skull. A high observer agreement for both the inter- and intra-observer data was found for measurements with very clear landmarks such as the basion-nasion and basion-bregma measurements, for example (Table 17) (Allan, 1982). Good to very good agreement was recorded for the remainder of the cranial and dental measurements in the data set, and is within expected values found in the literature.

Intraclass correlation values for cranial dimensions above 0.90 were obtained for all measurements except for the orbital breadth (0.871) and mandibular body breadth (0.872). Interclass correlation values below 90% agreement in cranial dimensions were that of the orbital breadth (0.801), mandibular body breadth (0.831), maximum ramus breadth (0.707), mandibular projective length (0.891) and temporal fossa height (0.858). These were thus more difficult to record reliably.

The measurements of zygomatic arch width and temporal fossa height were of special interest as these are not standard measurements. These measurements were created due to their location and regions of muscle attachment on the skull. The high values for both inter and intra-observer correlations indicate that these measurements can be reliably recorded and can be repeated between specimens and observers with a high degree of accuracy (Table 17).

Dental measurements achieved correlation values for repeatability equal to those found previously. Hillson *et al.* (2005) found an increased error with the mesio-distal diameter measurements and an increased error for the molars as compared to the incisors and canines. The current results achieved similar results to previously documented data (Table 17). Hillson *et al.* (2005) stated that molars are more difficult to measure accurately and repeatedly. Intra-observer error values ranged from 0.875 to 0.989, while inter-observer error ranged from 0.732 to 0.978.

Table 8. Descriptive statistics of cranial dimensions.

Variable (mm)	N	Mean	Minimum	Maximum	Std. Deviation
Max Cranial Lng	162	185.63	133.0	240.0	8.85
Max Cranial Br	161	131.69	117.0	144.0	5.11
Bizygomatic Br	161	129.01	113.1	142.1	5.56
Basion- Bregma	161	132.07	118.0	190.0	7.21
Basion-Nasion	162	101.02	92.0	112.0	4.29
Basion- Prosthion	162	101.78	88.0	116.0	5.45
Max Alveolar Br	162	63.87	50.2	73.8	3.68
Max Alveolar Lng	160	57.56	43.6	66.7	3.82
Upper Facial Ht	162	68.15	50.0	80.5	5.03
Min Frontal Br	162	97.08	82.2	111.4	4.68
Nasal Ht	162	49.21	39.9	57.2	3.18
Nasal Br	162	26.83	20.1	31.7	2.23
Orbital Br	162	36.93	31.7	42.1	2.17
Orbital Ht	162	33.46	27.3	38.7	2.22
Inter-orbital Br	161	28.19	21.0	33.6	2.53
Mandibular Body Br	162	12.19	7.10	15.8	1.46
Bigonial Wdt	162	95.11	82.1	113.5	5.77
Min Ramus Br	161	35.52	26.5	42.9	3.12
Max Ramus Br	161	41.23	33.4	47.9	3.09
Max Ramus Ht	162	57.61	45.0	68.0	5.18
Mandibular Projective Lng	162	81.90	69.0	93.5	4.89
Mandibular Angle	162	31.99	13.0	46.0	6.90
Zygomatic Arch Ht	162	19.98	15.5	26.2	2.30
Temporal Fossa Ht	161	79.99	62.4	109.1	6.28

Max Cranial Lng= Maximum Cranial Length; Max Cranial Br= Maximum Cranial Breadth; Bizygomatic Br= Bizygomatic Breadth; Max Alveolar Br= Maximum Alveolar Breadth; Max Alveolar Lng= Maximum Alveolar Length; Upper Facial Ht=Upper Facial Height; Min Frontal Br= Minimal Frontal Breadth; Nasal Ht= Nasal Height; Nasal Br= Nasal Breadth; Orbital Br= Orbital Breadth; Orbital Ht= Orbital height; Inter-orbital Br= Inter-orbital Breadth; Mandibular Body Br= Mandibular Body Breadth; Bigonial Wdt= Bigonial Width; Min Ramus Br= Minimum Ramus Breadth; Max Ramus Br= Maximum Ramus Breadth; Max Ramus Ht= Maximum Ramus Height; Mandibular Projective Lng = Mandibular Projective Length; Zygomatic Arch Ht= Zygomatic Arch height; Temporal Fossa Ht= Temporal Fossa Height.

Table 9. Descriptive statistics of tooth dimensions of the maxilla and mandible.

	N	Mean	Minimum	Maximum	Std. Deviation
MAXILLA					
mesio-distal					
I1	81	8.52	5.59	10.20	0.84
I2	102	6.95	4.88	8.93	0.63
CAN	134	7.74	6.40	8.71	0.47
M1	152	10.26	8.61	12.19	0.63
bucco-lingual					
I1	88	7.20	6.15	8.27	0.45
I2	103	6.71	5.50	8.61	0.53
CAN	137	8.69	5.98	10.47	0.68
M1	152	11.49	9.87	13.32	0.61
MANDIBLE					
mesio-distal					
I1	98	5.25	3.00	6.46	0.55
I2	107	5.96	4.24	8.42	0.63
CAN	133	7.15	5.70	8.37	0.49
M1	147	11.25	9.28	12.96	0.67
bucco-lingual					
I1	98	5.88	4.86	9.20	0.62
I2	113	6.29	5.34	7.41	0.45
CAN	141	7.96	6.78	9.70	0.53
M1	147	10.70	9.17	11.93	0.54

I1= first incisor; I2= second incisor; CAN= canine; M1= first molar

Table 10. Descriptive statistics of cranial indices and molar areas.

	N	Mean	Minimum	Maximum	Std. Deviation
Cranial Index	161	71.08	50.83	92.48	3.94
Cranial Height Index	161	71.29	55.83	101.06	4.58
Vertical Index	160	100.46	87.32	138.69	6.13
Frontoparietal Index	161	73.81	63.34	81.50	3.58
Zygomaticofrontal Index	161	75.32	64.09	86.34	3.40
Upper Facial Index	161	52.87	39.58	63.17	3.95
Gnathic Index	162	100.80	91.50	113.00	4.16
Orbital Index	162	90.76	75.68	108.17	6.74
Nasal Index	162	54.63	45.26	73.65	4.82
Maxilla Molar Area	152	117.85	95.25	146.88	10.99
Mandible Molar Area	147	120.64	89.55	152.66	11.82

Table 11. Group values one-way ANOVA for cranial dimensions.

Variable (mm)	Group						One-way ANOVA
	Orthognathic		Mesognathic		Prognathic		p Value
	Mean	SD	Mean	SD	Mean	SD	
Max Cranial Lng	186.33	10.95	185.50	8.96	185.08	6.06	0.7684
Max Cranial Br	132.12	4.46	131.50	5.52	131.48	5.25	0.7717
Bizygomatic Br	128.88	6.02	130.01	4.92	127.99	5.66	0.1609
Basion- Bregma	132.84	5.25	133.73	8.79	129.39	6.17	**0.0041**[b]
Basion-Nasion	100.88	4.62	102.55	3.86	99.37	3.82	**0.0004**[c]
Basion- Prosthion	97.02	4.17	103.35	4.18	104.69	4.78	**0.0001**[c]
Max Alveolar Br	63.06	4.05	64.38	3.57	64.10	3.30	0.1465
Max Alveolar Lng	54.26	3.22	58.44	2.94	59.81	3.03	**0.0001**[c]
Upper Facial Ht	67.51	4.75	68.79	4.77	68.03	5.57	0.3983
Min Frontal Br	97.55	4.39	97.48	4.78	96.15	4.79	0.2296
Nasal Ht	49.08	3.16	49.46	3.49	49.05	2.84	0.7491
Nasal Br	26.81	2.21	27.09	2.39	26.56	2.07	0.4586
Orbital Br	37.20	2.24	37.19	2.26	36.37	1.90	0.0770
Orbital Ht	33.99	2.37	33.25	2.13	33.18	2.12	0.1464
Inter-orbital Br	28.45	2.40	28.71	2.50	27.34	2.51	**0.0119**[a]
Mandibular Body Br	11.84	1.22	12.21	1.57	12.53	1.46	0.0577
Bigonial Wdt	95.77	5.76	95.13	5.35	94.41	6.25	0.4946
Min Ramus Br	34.39	2.89	36.30	3.16	35.75	3.01	**0.0045**[b]
Max Ramus Br	40.51	3.16	42.26	2.89	40.76	2.95	**0.0045**[b]
Max Ramus Ht	55.90	5.93	58.88	4.18	57.82	5.04	**0.0090**[b]
Mandibular Projective Lng	80.34	4.80	82.41	4.39	82.88	5.22	**0.0187**[a]
Mandibular Angle	32.45	6.76	31.20	6.85	32.45	7.15	0.5407
Zygomatic Arch Ht	19.43	2.16	20.23	2.37	20.24	2.28	0.1144
Temporal Fossa Ht	79.92	6.87	81.00	6.06	78.90	5.83	0.2160

[a] $p \leq 0.05$
[b] $p \leq 0.01$
[c] $p \leq 0.001$

Table 12. Group values of one-way ANOVA statistics for tooth dimensions of the maxilla and mandible. (I1= first incisor; I2= second incisor; CAN= canine; M1= first molar)

Variable (mm)	Group						One-way ANOVA
	Orthognathic		Mesognathic		Prognathic		p Value
	Mean	SD	Mean	SD	Mean	SD	
MAXILLA							
mesio-distal							
I1	8.33	0.88	8.60	0.73	8.66	0.87	0.3003
I2	6.79	0.56	6.95	0.64	7.10	0.65	0.1350
CAN	7.57	0.44	7.83	0.45	7.82	0.48	**0.0122**[a]
M1	10.17	0.61	10.31	0.62	10.30	0.64	0.4492
bucco-lingual							
I1	7.00	0.39	7.35	0.40	7.30	0.49	**0.0047**[b]
I2	6.60	0.47	6.78	0.47	6.75	0.62	0.3355
CAN	8.44	0.66	8.89	0.52	8.72	0.79	**0.0061**[b]
M1	11.22	0.62	11.57	0.50	11.65	0.63	**0.0012**[b]
MANDIBLE							
mesio-distal							
I1	5.17	0.56	5.24	0.65	5.32	0.44	0.5475
I2	5.77	0.54	6.07	0.61	6.05	0.68	0.0779
CAN	7.03	0.49	7.28	0.44	7.13	0.52	**0.0477**[a]
M1	11.09	0.69	11.32	0.62	11.31	0.68	0.1655
bucco-lingual							
I1	5.72	0.38	6.01	0.67	5.94	0.73	0.1446
I2	6.18	0.40	6.41	0.39	6.30	0.51	0.0966
CAN	7.88	0.57	8.05	0.46	7.96	0.56	0.3329
M1	10.61	0.51	10.82	0.53	10.64	0.55	0.0852

[a] $p \leq 0.05$
[b] $p \leq 0.01$
[c] $p \leq 0.001$

Table 13. Group values of one-way ANOVA for cranial indices and molar areas.

Variable (mm)	Groups						One-way ANOVA
	Orthognathic		Mesognathic		Prognathic		p Value
	Mean	SD	Mean	SD	Mean	SD	
Gnathic Index	96.15	1.50	100.78	1.86	105.48	2.19	**0.0001**[c]
Cranial Index	71.55	3.27	70.69	3.16	71.06	5.21	0.5161
Cranial Height Index	72.18	5.28	70.54	3.10	71.26	5.17	0.1770
Vertical Index	100.98	7.43	99.91	5.12	100.59	5.81	0.6522
Frontoparietal Index	73.25	3.99	73.97	3.29	74.18	3.47	0.3932
Zygomaticofrontal Index	74.88	3.61	74.98	3.44	76.15	3.03	0.1063
Upper Facial Index	51.79	4.11	53.10	3.89	53.67	3.69	**0.0473**[a]
Orbital Index	91.65	7.12	89.65	6.38	91.19	6.69	0.2581
Nasal Index	54.61	4.75	55.00	5.32	54.23	4.30	0.7011
Maxilla Molar Area	114.24	10.95	119.33	9.97	119.51	11.51	**0.0274**[a]
Mandible Molar Area	117.90	11.65	122.91	11.59	120.54	11.91	0.1107

[a]$p \leq 0.05$
[b]$p \leq 0.01$
[c]$p \leq 0.001$

Table 14. Relationship between gnathic index and facial parameter for full data set (all groups) is shown by the Pearson correlation coefficients (r) and the coefficients of determination (r^2).

Variable (x)	r	r^2 x 100%	p- Value
Max Cranial Lng	-0.0598	0.36	0.4495
Max Cranial Br	0.0017	0.00	0.9832
Bizygomatic Br	-0.0998	1.0	0.2079
Basion- Bregma	-0.2273	5.17	**0.0037**[b]
Basion-Nasion	-0.1908	3.64	**0.0150**[a]
Basion-Prosthion	0.6040	36.48	**0.0001**[c]
Max Alveolar Br	0.0905	0.82	0.2518
Max Alveolar Lng	0.5809	33.75	**0.0001**[c]
Upper Facial Ht	0.0118	0.01	0.8814
Min Frontal Br	-0.1240	1.54	0.1159
Nasal Ht	-0.0084	0.01	0.9153
Nasal Br	-0.0567	0.32	0.4733
Orbital Br	-0.2217	4.92	**0.0046**[b]
Orbital Ht	-0.1879	3.53	**0.0167**[a]
Inter-orbital Br	-0.2130	4.54	**0.0067**[b]
Mandibular Body Br	0.1989	3.95	**0.0112**[a]
Bigonial Wdt	-0.1148	1.32	0.1459
Min Ramus Br	0.2102	4.42	**0.0074**[b]
Max Ramus Br	0.0073	0.01	0.9270
Max Ramus Ht	0.0802	0.64	0.3103
Mandibular Projective Lng	0.2282	5.21	0.3451
Mandibular Angle	-0.0020	0.00	0.9795
Zygomatic Arch Ht	0.1067	1.14	0.1768
Temporal Fossa Ht	-0.1022	1.05	0.1969

[a] $p \leq 0.05$
[b] $p \leq 0.01$
[c] $p \leq 0.001$

Table 15. Relationship between gnathic index and dental measurements for full data set (all groups) is shown by the Pearson correlation coefficients (r) and the coefficients of determination (r^2).

Variable (x)	r	r^2 x 100%	p- Value
MAXILLA			
mesio-distal			
I1	0.1524	2.32	0.1744
I2	0.2328	5.42	**0.0185**[a]
CAN	0.2541	6.45	**0.0031**[b]
M1	0.0917	0.84	0.2613
bucco-lingual			
I1	0.2143	4.59	**0.0450**[a]
I2	0.1295	1.68	0.1924
CAN	0.1795	3.22	**0.0359**[a]
M1	0.2485	6.18	**0.0020**[b]
MANDIBLE			
mesio-distal			
I1	0.1788	3.20	0.0782
I2	0.275	7.59	**0.0041**[b]
CAN	0.1305	1.70	0.1344
M1	0.2088	4.36	**0.0112**[a]
bucco-lingual			
I1	0.1307	1.71	0.1996
I2	0.1662	2.76	0.0785
CAN	0.1306	1.71	0.1227
M1	0.0471	0.22	0.5708

[a] $p \leq 0.05$
[b] $p \leq 0.01$
[c] $p \leq 0.001$

Table 16. The relationship between the gnathic index and the cranial indices and molar areas is shown by the Pearson correlation coefficients (r) and the coefficients of determination (r^2).

Variable (x)	r	r^2 x 100%	p- Value
Cranial Index	-0.0526	0.28	0.5075
Cranial Height Index	-0.1306	1.71	0.0986
Vertical Index	-0.0769	0.59	0.3337
Frontoparietal Index	0.0264	0.07	0.7393
Zygomaticofrontal Index	0.1040	1.08	0.1890
Upper Facial Index	0.1673	2.80	**0.0339**[a]
Orbital Index	-0.0142	0.02	0.8572
Nasal Index	-0.0426	0.18	0.5902
Maxilla Molar Area	0.1825	3.33	**0.0244**[a]
Mandible Molar Area	0.1489	2.22	0.0719

[a]$p \leq 0.05$
[b]$p \leq 0.01$
[c]$p \leq 0.001$

Table 17. Inter and intra-observer agreement statistics for metric data.

Measurement (mm)	**Interclass Correlation Coefficient**	
	Intra-observer	**Inter-observer**
Max cranial length	0.918	0.922
Max cranial breadth	0.932	0.943
Bizygomatic breadth	0.988	0.976
Basion bregma	0.981	0.988
Basion nasion	0.982	0.982
Basion prosthion	0.989	0.974
Max alveolar breadth	0.925	0.951
Max alveolar length	0.949	0.944
Upper facial height	0.988	0.974
Min frontal breadth	0.985	0.978
Nasal height	0.943	0.939
Nasal breadth	0.953	0.924
Orbital breadth	0.871	0.801
Orbital height	0.910	0.925
Inter-orbital breadth	0.962	0.931
Mandibular body breadth	0.872	0.831
Bigonial breadth	0.995	0.990
Min ramus breadth	0.968	0.987
Max ramus breadth	0.954	0.707
Max ramus height	0.957	0.905
Mandibular projective length	0.945	0.891
Mandibular angle	0.970	0.901
Zygomatic arch width	0.920	0.972
Temporal fossa height	0.933	0.858
MAXILLA		
mesio-distal		
I1	0.977	0.978
I2	0.939	0.917
CAN	0.931	0.833
M1	0.861	0.732
bucco-lingual		
I1	0.922	0.855
I2	0.948	0.891
CAN	0.989	0.883
M1	0.936	0.905
MANDIBLE		
mesio-distal		
I1	0.914	0.920
I2	0.911	0.854
CAN	0.857	0.850
M1	0.916	0.893
bucco-lingual		
I1	0.906	0.836
I2	0.952	0.866
CAN	0.871	0.850
M1	0.941	0.946

Figure 21. Scatter plot of gnathic index vs. basion-bregma measurement of all individuals (r^2x 100= 5.17 %; r= -0.2273; p≤ 0.01).

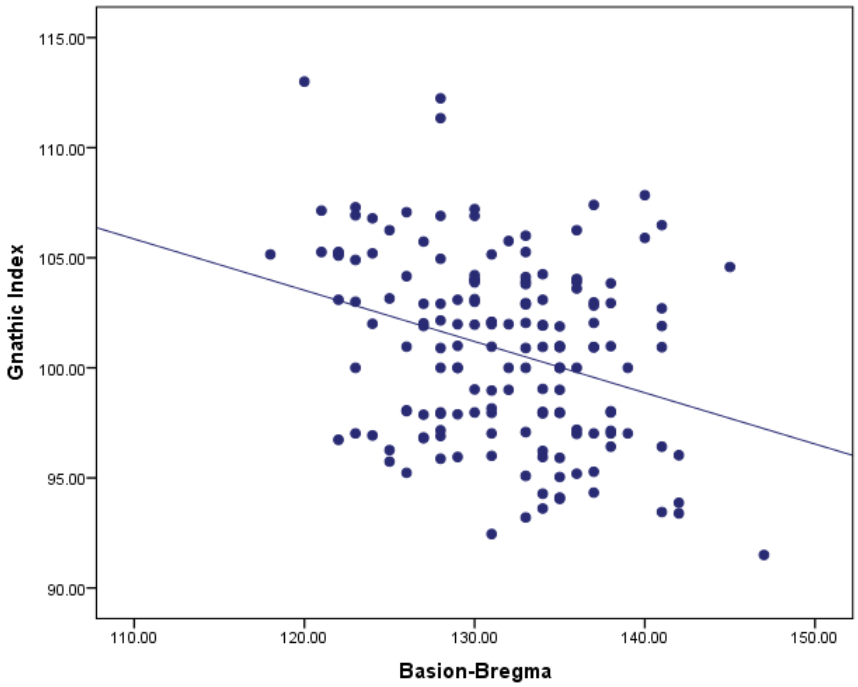

Figure 22. Scatter plot of gnathic index vs. maximum alveolar length of all individuals (r^2x 100=33.75%; r= 0.5809; p≤0.001).

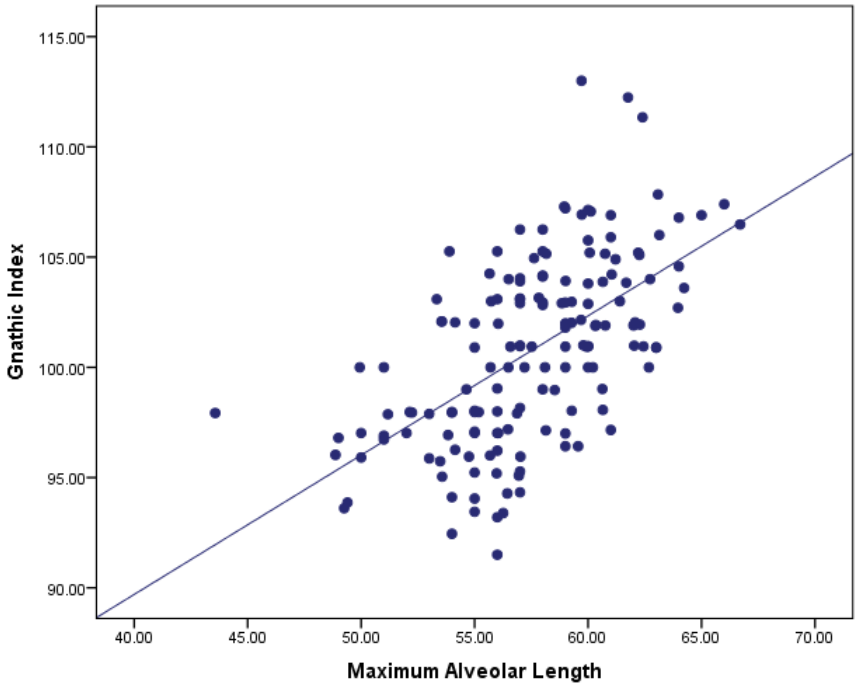

Figure 23. Scatter plot of gnathic index vs. interorbital breadth of all individuals (r^2x 100= 4.54%; r= -0.2130; p≤0.01).

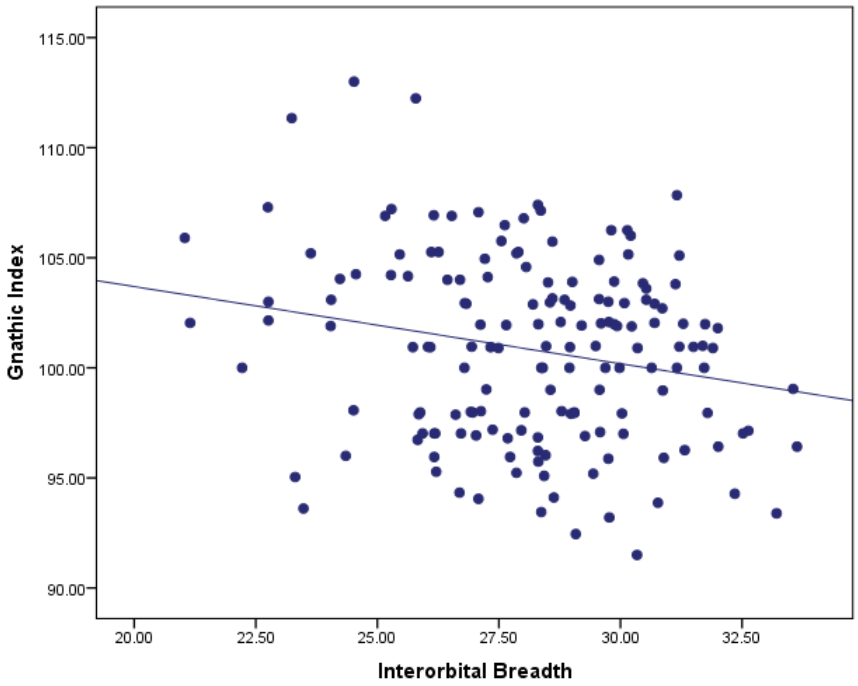

Figure 24. Scatter plot of gnathic index vs. mandibular body breadth of all individuals (r^2x 100= 3.95%; r= 0.1989; p≤0.05).

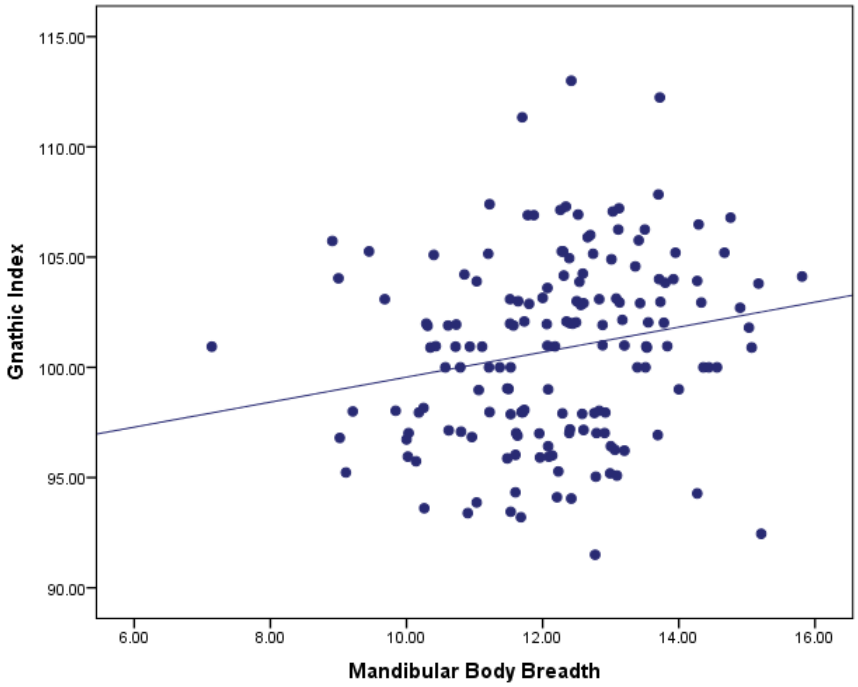

Figure 25. Scatter plot of gnathic index vs. minimum ramus breadth of all individuals (r^2x 100= 4.42%; r= 0.2102; p≤0.01).

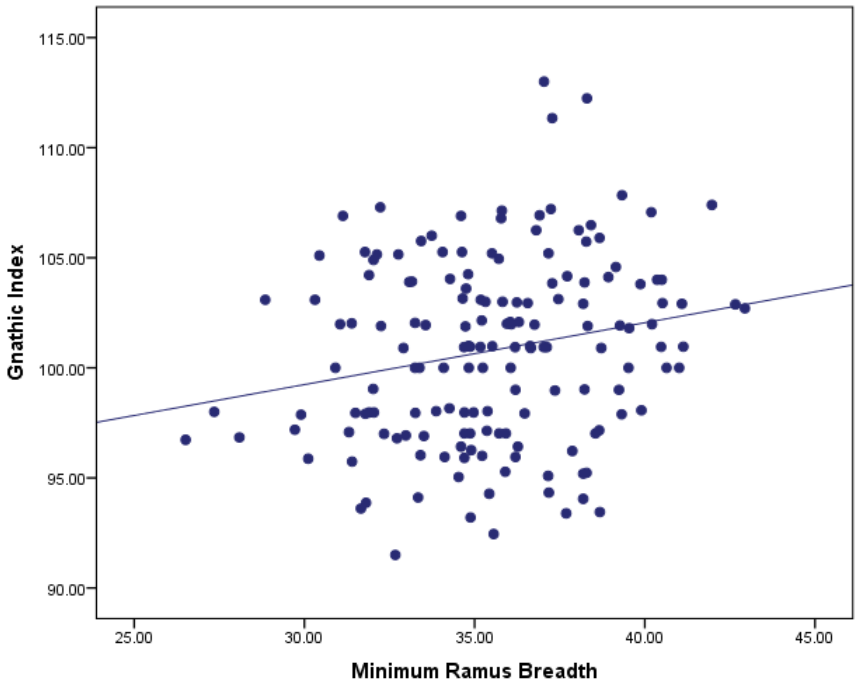

Figure 26. Scatter plot of gnathic index vs. orbital breadth of all individuals (r^2x 100= 4.92%; r= -0.2217; p≤0.01).

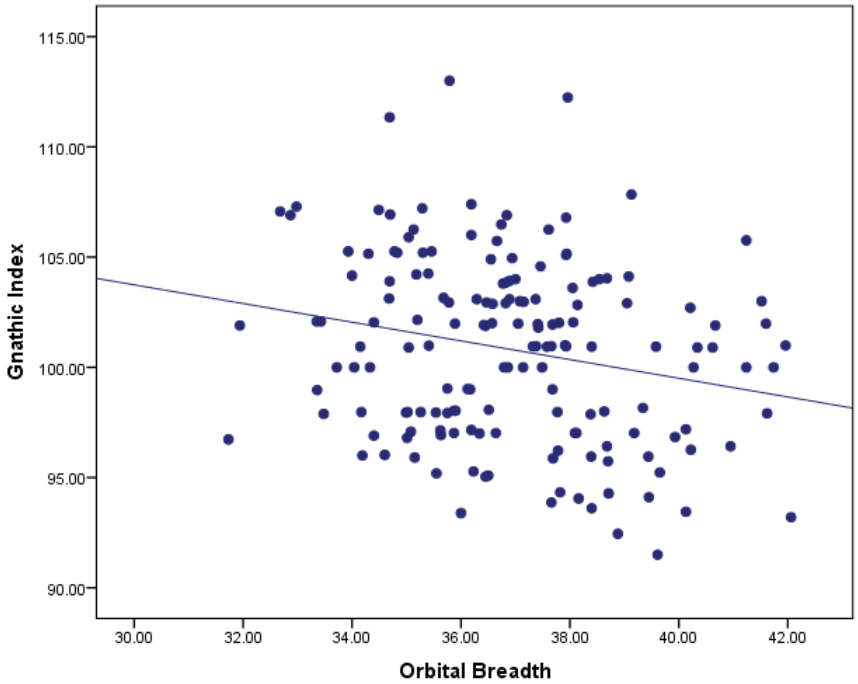

Figure 27. Scatter plot of gnathic index vs. orbital height of all individuals (r^2x 100= 3.53%; r= -0.1879; p≤0.05).

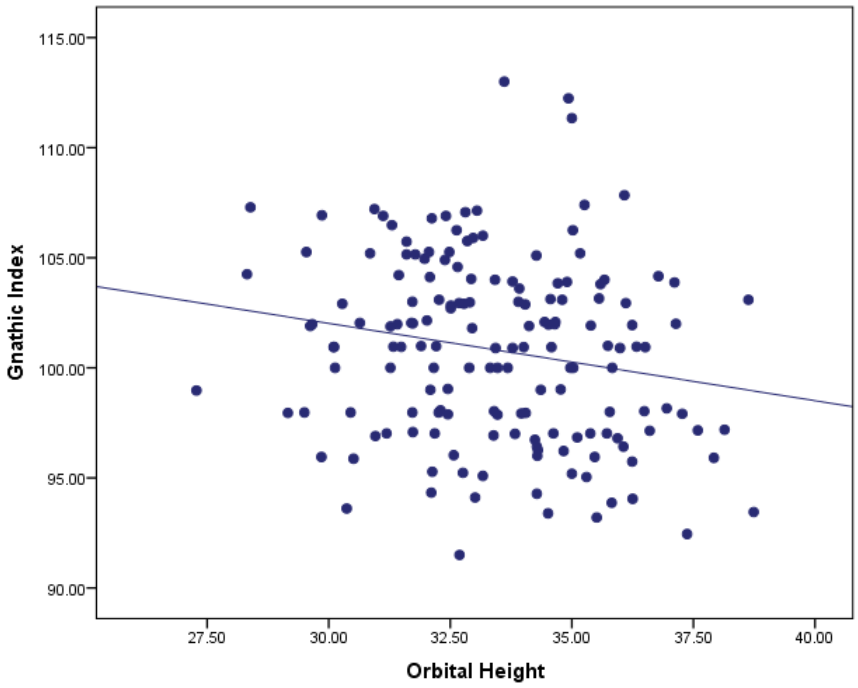

Figure 28. Scatter plot of gnathic index vs. mesio-distal measurement of the maxillary lateral incisor (r^2x 100= 5.42%; r= 02328; p≤0.05).

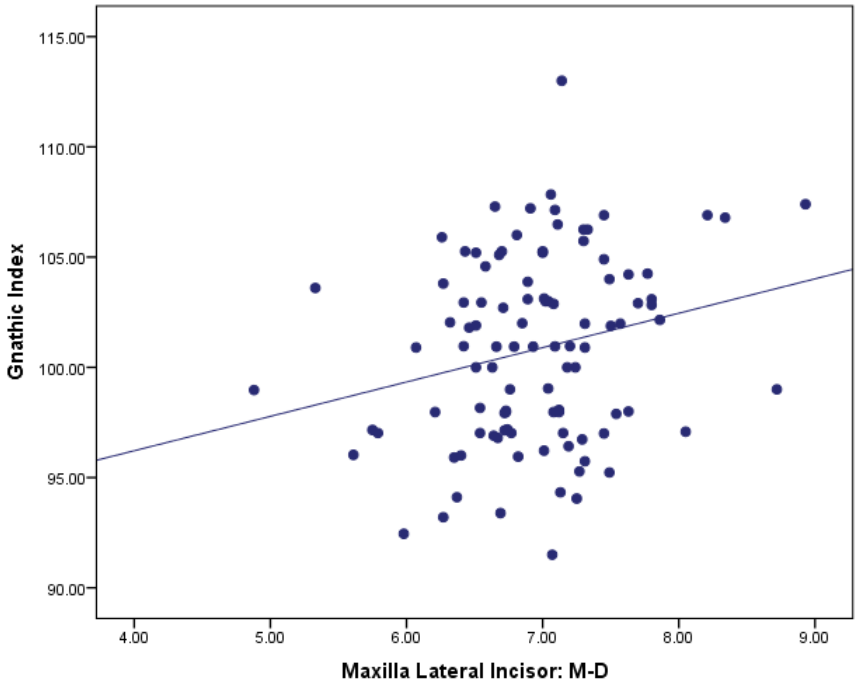

Figure 29. Scatter plot of gnathic index vs. mesio-distal measurement of maxilla canine (r^2x 100= 6.45%; r= 0.2541; p≤0.01).

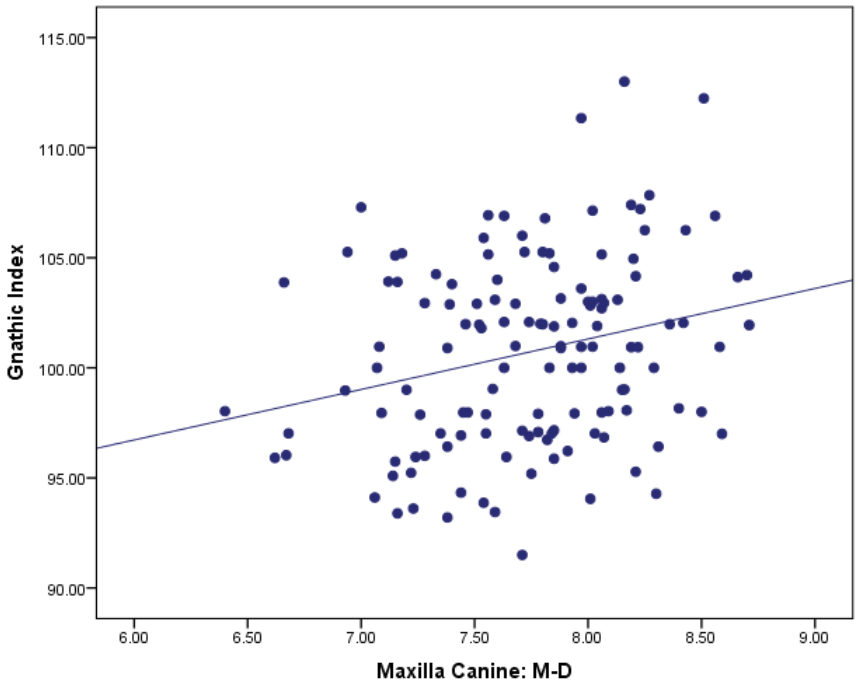

Figure 30. Scatter plot of gnathic index vs. bucco-lingual measurement of the maxilla first incisor of all individuals (r^2x 100= 4.59%; r= 0.2143; p≤ 0.05).

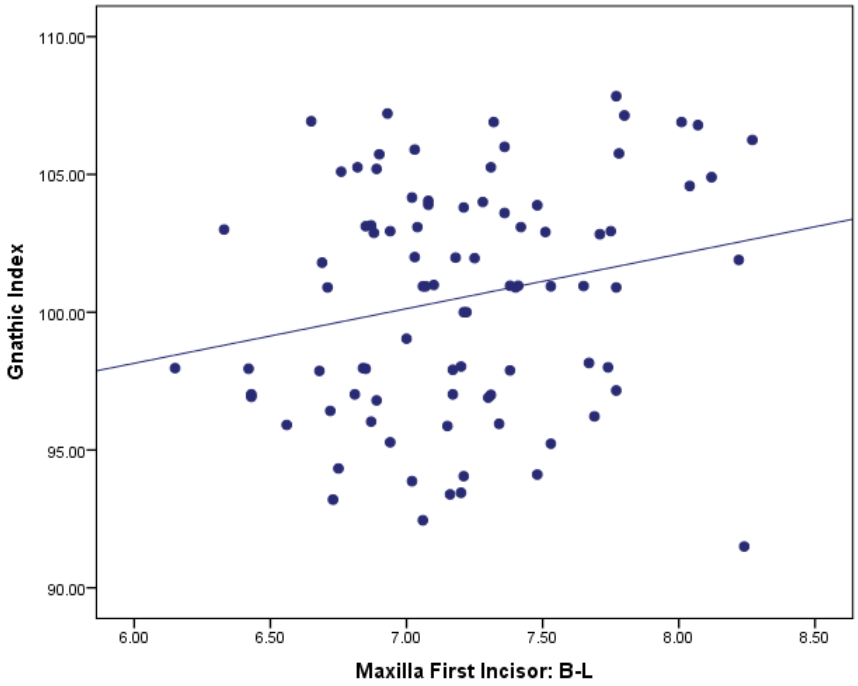

Figure 31. Scatter plot of gnathic index vs. bucco-lingual measurement of maxilla canine of all individuals (r^2x 100= 3.22%; r= 0.1795; p≤ 0.05).

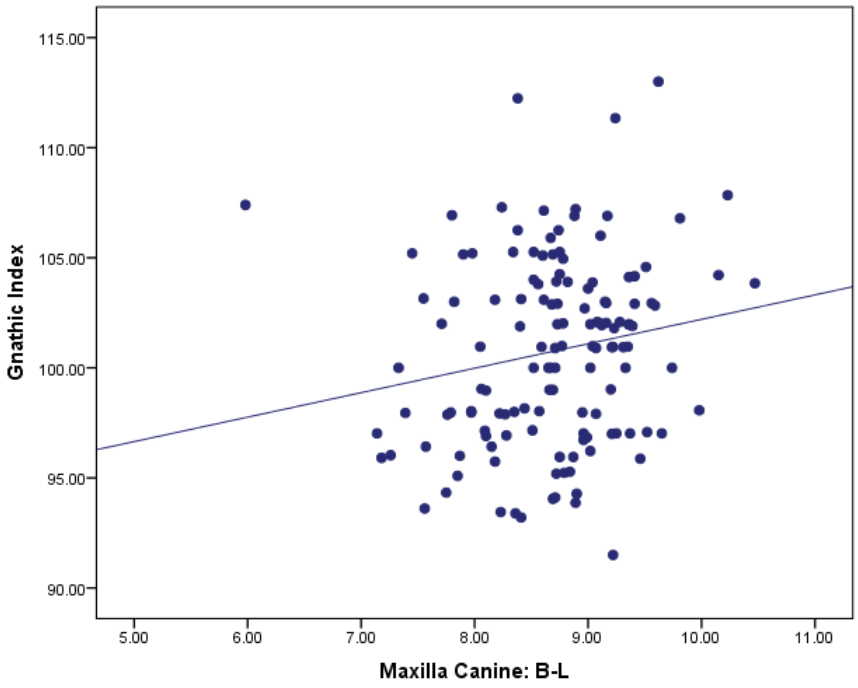

Figure 32. Scatter plot of gnathic index vs. bucco-lingual measurement of maxilla first molar of all individuals (r^2x 100= 6.18%; r= 0.2485; p≤ 0.01).

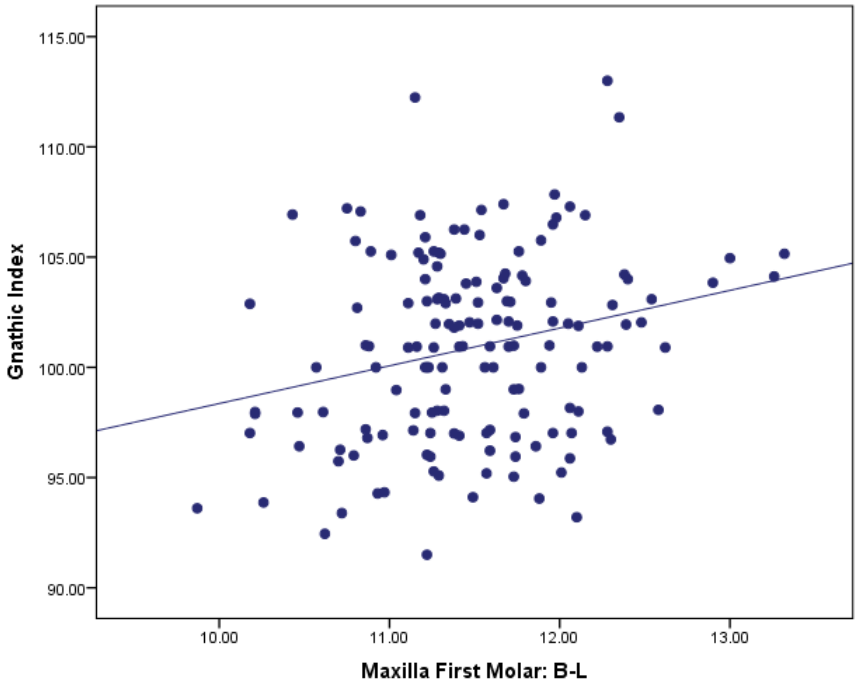

Figure 33. Scatter plot of gnathic index vs. mesio-distal measurement of mandibular second incisor (r^2x 100= 7.59%; r= 0.275; p≤0.01).

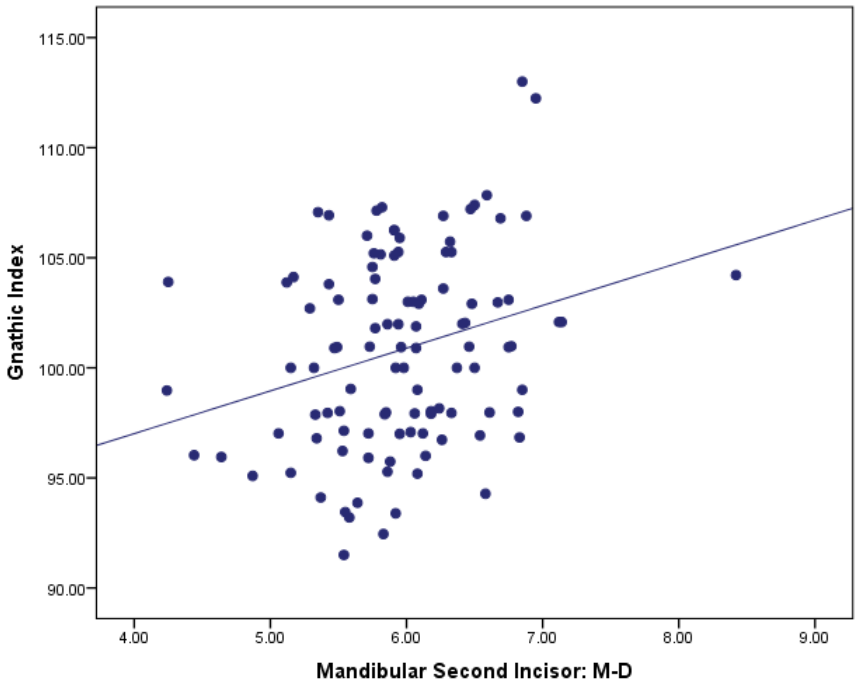

Figure 34. Scatter plot of gnathic index vs. mesio-distal measurement of mandible first molar of all individuals (r^2x 100= 4.36%; r= 0.2088; p≤ 0.05).

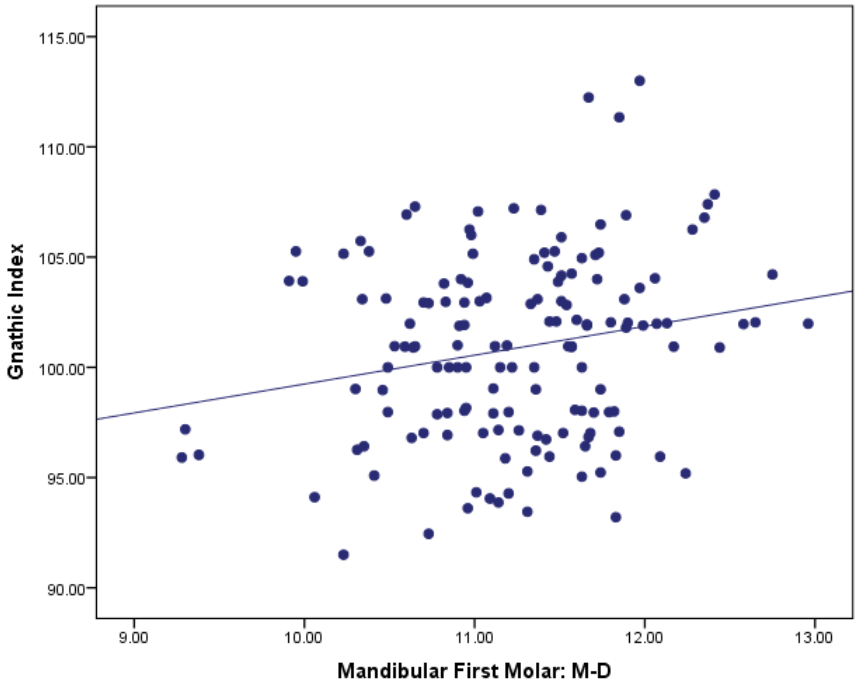

Figure 35. Scatter plot of gnathic index vs. upper facial index of all individuals (r^2x 100= 2.8%; r= 0.1673; p≤0.05).

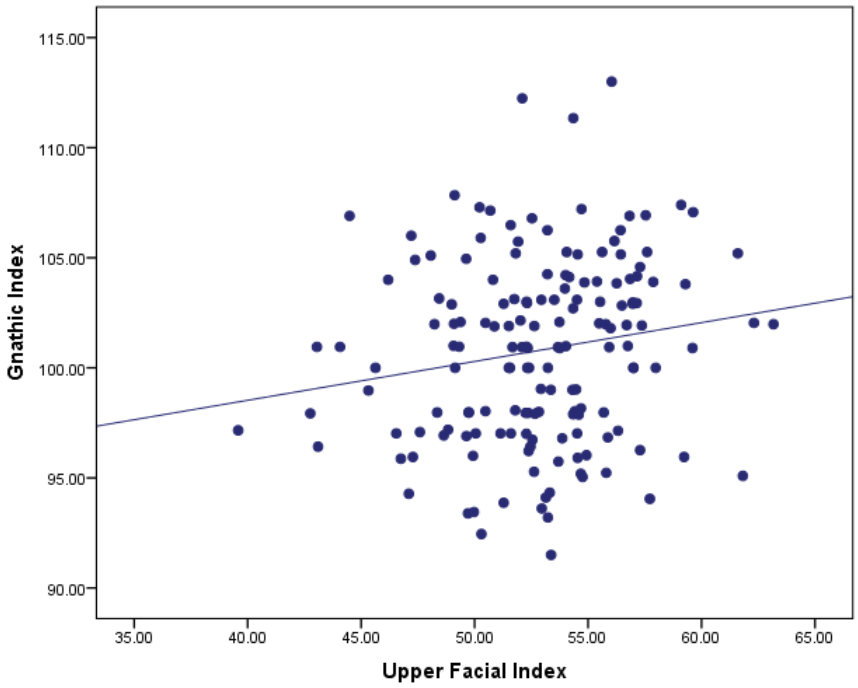

Figure 36. Scatter plot of gnathic index vs. maxilla molar area of all individuals (r^2x 100= 3.33%; r= 0.1825; p≤0.05).

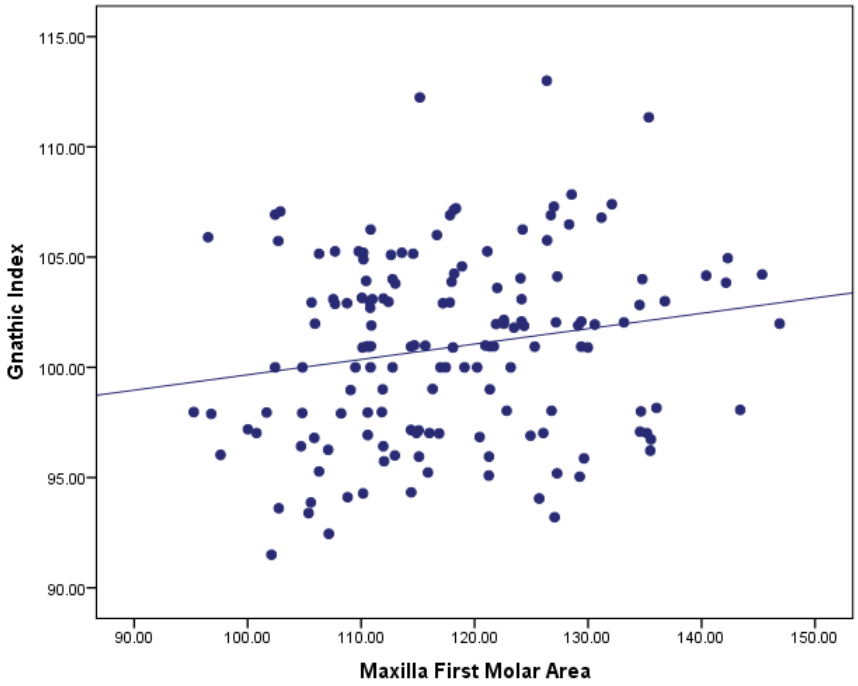

CHAPTER 5

RESULTS OF MORPHOLOGICAL ANALYSIS

A morphological examination of four cranial features was carried out on all skulls selected for data collection. The features of the browridge, glabella region, mastoid process and shape of the dental arcade were categorized as previously described in the literature (see Chapter 3: Section 3.3 Morphological Assessment). The morphological features selected for assessment were those in areas associated with muscle attachment and/or features which may function in the process of mastication. After the initial categorization of the morphological characteristics of all skulls, a random selection of 30 skulls were re-examined morphologically to assess the inter- and intra-observer error for each characteristic and ensure congruency between observers and repeatability of the study.

5.1 FREQUENCY DISTRIBUTION AND PEARSON CHI^2 ANALYSIS

5.1.1 BROWRIDGE EXPRESSION

The frequency distribution of browridge expression between the 5 categories indicated that 50% of the individuals evaluated had a browridge characterized as category 2, which is on the smaller end of the scale (Table 18). Nearly 57% of prognathic individuals, 42.2% of mesognathic and 52.9% of orthognathic individuals were classified into group 2, thus having relatively small browridges. Hardly any individuals had prominent browridges (categories 4 and 5) and no clear distribution pattern could be seen with regard to browridge expression in the different groups. This was confirmed by the Chi^2 test, which

was not significant (x^2= 7.56, p=0.47). Therefore there is no clear association between browridge size and the degree of prognathism.

5.1.2 GLABELLAR SIZE

The same pattern as was seen in browridges was found with glabella expression. Most individuals (72.2%) had relatively small glabellae (category 2), with very few (0.6%) having prominent glabellae (Table 19). Mesognathic and prognathic groups had a higher percentage in category 3 with 23.3% and 27.4% respectively versus the orthognathic group with 7.8%. Glabella expression did not vary significantly among the groups (x^2=12.51, p=0.130). Thus although not statistically significant, it seems as if more prognathic individuals have a tendency towards larger glabellae. In general, though, the whole group is fairly gracile in this regard.

5.1.3 MASTOID PROCESS EXPRESSION

Mastoid process expression among groups was determined and the results are shown in Table 20. Mastoid process expression appears to be more variable throughout the five categories of expression for each skull shape than the previously described morphological characteristics. In all three groups, most individuals had small or medium sized mastoids (orthognathic 71%, mesognathic 68%, prognathic 59%).

A larger mastoid process (category 4 and 5) was recorded in the highest frequency in the prognathic skulls with 29% of individuals ranked as a category 4 or 5 in mastoid expression. Orthognathic and mesognathic groups had fewer large mastoids with approximately 16% in orthognathic and 23% in mesognathic skulls.

The trend from these results is that the more prognathic the individual, the larger the mastoid process. Pearson Chi^2 statistic, however, was calculated to be 6.11 (p=0.635), indicating no significant difference among the three groups.

5.1.4 DENTAL ARCADE SHAPE

The dental arcade shape of an individual can be described as being characteristic of a horse shoe, U-shaped or divergent in its expression (Table 21). More than 72.2% of individuals were found to have the U-shaped (category 2) dental arcade. The second largest group was the divergent category with 19.1% of individuals having this expression. Most of the prognathic skulls (76.5%) had U-shaped dental arcades while 71.7% of mesognathic and 68.6% of orthognathic individuals also showed the U-shape (category 2) in dental arcade. No orthognathic individuals had a horseshoe shaped dental arcade expression but the other two cranial categories (mesognathic and prognathic) had expressions in all three categories of U-shaped, horseshoe and divergent.

The divergent dental arcade category showed higher numbers of orthognathic individuals at 31.4% as compared to 11.7% mesognathic and 15.7% prognathic. These results show a trend towards a divergent dental arcade in orthognathic individuals, however, as prognathism increases a U-shaped dental arcade may be expected. The Chi^2 statistic calculated for dental arcade shape was 15.19, and thus indicates significant differences between groups ($p \leq 0.01$). In conclusion, orthognathic people tend to have divergent shapes to create space for the dentition; whereas more prognathic individuals have U-shaped dental arcades.

5.2 INTER/INTRA CLASS CORRELATION STATISTICS

Intra- and inter-observer error calculation of the Cohen's kappa and percent agreement values are found in Table 22 for morphological characteristics. The kappa values fall in the category of good to very good agreement for intra-observer agreement for all morphological characteristics ranging from 0.62 to 0.81. Inter-observer error kappa values were lower at a range of 0.32 for browridge and 0.64 for mastoid expression.

The percent agreement for intra and inter-observer determinations had a high agreement for all characteristics except the inter-observer agreement for browridge expression. The glabella region had the highest agreement between observers (83.3%). The inter-observer error statistics show good agreement for both the morphological characteristics of dental arcade (76.7%) and mastoid process (73.3%). Browridge expression had the least agreement between observers at 53.3%. Inter-observer error can be expected to be lower as qualitative variables are often subject to interpretation by the observer and are influenced by the experience of the observers themselves (Adams and Byrd, 2002).

Table 18. The frequency distribution and percentage of browridge expression among groups. Browridge 1= lacking prominence through 5= most prominent.

	GROUP			
Browridge Category	Orthognathic	Mesognathic	Prognathic	TOTAL
1	3 (5.88%)	1 (1.67%)	2 (3.93%)	6 (3.70%)
2	27 (52.94%)	25 (41.67%)	29 (56.86%)	81 (50.00%)
3	15 (29.41%)	26 (43.30%)	16 (31.37%)	57 (35.17%)
4	5 (9.80%)	8 (13.33%)	4 (7.84%)	17 (10.49%)
5	1 (1.96%)	0 (0.00%)	0 (0.00%)	1 (0.62%)
TOTAL	51 (100%)	60 (100%)	51 (100%)	162 (100%)

Table 19. Percentage and frequency of glabella expression among groups. Glabella prominence 1= flat through 5= very prominent.

	GROUP			
Glabella Prominence	Orthognathic	Mesognathic	Prognathic	TOTAL
1	2 (3.92%)	2 (3.33%)	1 (1.96%)	5 (3.09%)
2	41 (80.39%)	41 (68.33%)	35 (68.63%)	117 (72.22%)
3	4 (7.84%)	14 (23.33%)	14 (27.45%)	32 (19.75%)
4	4 (7.84%)	3 (5.00%)	0 (0.00%)	7 (4.32%)
5	0 (0.00%)	0 (0.00%)	1 (1.96%)	1 (0.62%)
TOTAL	51 (100%)	60 (100%)	51 (100%)	162 (100%)

Table 20. Percentage and frequency of mastoid process expression among groups. Mastoid 1= smallest and more typically female form through 5= large and the more male expression.

	GROUP			
Mastoid Process	Orthognathic	Mesognathic	Prognathic	TOTAL
1	7 (13.73%)	5 (8.33%)	6 (11.76%)	18 (11.11%)
2	20 (39.22%)	26 (43.33%)	17 (33.33%)	63 (38.39%)
3	16 (31.73%)	15 (25.00%)	13 (25.49%)	44 (27.16%)
4	7 (13.73%)	8 (13.33%)	11 (21.57%)	26 (16.05%)
5	1 (1.96%)	6 (10.00%)	4 (7.84%)	11 (6.79%)
TOTAL	51 (100%)	60 (100%)	51 (100%)	162 (100%)

Table 21. Percentage and frequency of dental arcade expression among groups. The Chi^2 value of 15.19 was significant at p≤0.01 for distribution across the orthognathic, mesognathic and prognathic facial forms. Category 1= horseshoe; 2= U-shape; 3= divergent.

	GROUP			
Dental Arcade	Orthognathic	Mesognathic	Prognathic	TOTAL
1	0 (0.00%)	10 (16.67%)	4(7.84%)	14 (8.64%)
2	35 (68.63%)	43 (71.67%)	39 (76.47%)	117 (72.22%)
3	16 (31.37%)	7 (11.67%)	8 (15.69%)	31 (19.14%)
TOTAL	51 (100%)	60 (100%)	51 (100%)	162 (100%)

Table 22. Cohen's Kappa values for inter and intra-observer error of morphological characteristics along with percentage of agreement for inter- and intra-observer error while scoring morphological characteristics.

Morphological Characteristic	Intra-observer		Inter-observer	
	Kappa	% Agreement	Kappa	% Agreement
Browridge	0.7802	86.67	0.3269	53.33
Glabella	0.6273	86.67	0.5208	83.33
Mastoid	0.8160	86.67	0.6481	73.33
Dental Arcade	0.8000	90.00	0.6111	76.67

CHAPTER 6

RESULTS OF FINITE ELEMENT ANALYSIS

When using two individuals, where one represents the prognathic facial form and the other the orthognathic facial form, to simulate the stress due to the forces of mastication, modifications to the rendered three dimensional models needed to be made to insure accuracy and the ability to make direct comparisons between the two. Scaling was done for the finite element models in order to make the two models of equal size, thus causing any observed pattern differences in stress to be due to the geometry of the model and not because of differences in the size of the models.

In generating a bite at the first molar and central incisor, muscle forces varied between the two models. Average muscle forces for the orthognathic model were consistently less than those for the prognathic model when producing the same bite force at the molar (657.2 N) and the incisor (410.6 N). Values for muscle forces can be found in Chapter 3: Materials and Methods, Tables 4 through 7. In this study, the force on an incisor and molar bite were modeled directly across the entire occlusal surface of each tooth in each model; therefore, stress patterns should not be reflective of misdirected areas of stress as a result of a compromised occlusal surface.

In the first figure in the series of the finite element analyses (Figure 37), it can be seen in the orthognathic model that there is missing dentition on the right side of the dental arcade. During the selection of an orthognathic individual it was necessary to find an individual to model that was within the suitable range of the gnathic index

and also had sufficient dentition ante-mortem. The orthognathic model chosen had both of these parameters; however there was post-mortem dentition loss of the right lateral incisor and canine. This post-mortem loss of dentition does not influence the model or the resulting stress patterns, as accommodation of stress away from the bite force in the facial skeleton and vault was the primary focus and neither of the missing teeth were involved in the working side bite force.

6.1 DISPLACEMENT

The displacement results show how the skull was deformed while external forces caused by muscle contraction were applied. All analyses are scaled the same for comparative purposes while the units for displacement in Figures 37 through 44 are in centimetres.

6.1.2 DISPLACEMENT: MOLAR BITE

The total displacement for a molar bite in the orthognathic and prognathic facial form in the anterior view is found in Figure 37. The scale for total displacement in these figures starts at 0 (blue), indicating no displacement. As displacement increases the scale moves to the colour red; this is representative of the maximum displacement for each skull. The scale indicates that the largest total displacement for each skull was at least 0.02 mm. Any displacement values larger than the scale of the maximum displacement value will also be indicated as red.

From the anterior view of the displacement analysis (Figure 37), it can be seen that the area of displacement is smaller in the orthognathic facial form in the maxillary and facial regions. There is greater displacement on the balancing side in the prognathic skull over the orthognathic skull in the region of the maxilla and zygoma. Also, regions of the frontal bone experience more displacement in the prognathic

model over the same areas in the orthognathic facial form. The displacement in lateral view of a molar bite, as seen in Figure 38, shows an increase in the area and magnitude of displacement in most of the maxillary region of the prognathic facial form over the orthognathic form. The prognathic facial form also has greater displacement in the inferior orbit and along the temporal line. A larger area of the cranial vault is displaced than in the orthognathic facial form.

The maxilla has greater displacement in the balancing side of the prognathic facial form and by the scale the balancing side zygomatic arch has twice the displacement (~0.014 mm) in the prognathic over the orthognathic facial form (~0.006 mm) (Figure 39). The inferior view of a molar bite (Figure 40) shows that half of the dental arcade and maxilla region experiences maximum stress in the prognathic model, with the balancing side in the same regions also showing greater displacement than the orthognathic facial form. The area of attachment for the medial pterygoid muscle in both models shows little displacement during a molar bite (Figure 40).

6.1.3 DISPLACEMENT: INCISOR BITE

Loading with an incisor bite (Figure 41) shows areas of greater maximum displacement over a molar bite (Figure 37) for both facial forms. The orthognathic face has less displacement than the prognathic model in both molar and incisor bites. Displacement is found in the regions of the first incisor as expected, however, in the orthognathic model it is found below the nasal aperture. In the prognathic model, the displacement reaches areas up to the inferior orbital area lateral to the nasal aperture. Maximum displacement for the incisor is 0.03 mm and upward, but most noticeable in the frontal view of the prognathic model is the ~0.015 mm displacement in the frontal bone extending from the superior margin of the nasal aperture upward, covering most

of the frontal bone - more so superior to the balancing side orbit than the working side orbit. This same region in the orthognathic model during incisor bite appears to experience no displacement.

The displacement results, as viewed from the working side, are found in Figure 42. The greatest displacement is in the immediate region of the incisor, extending posteriorly on the dental arcade in the prognathic model. The displacement (~0.015 mm) in the vault can be seen in the prognathic skull model and is again minimal or absent in the orthognathic model. The majority of the displacement in the orthognathic facial form is concentrated in the facial region and area of muscle attachment on the zygomatic arch. The inferior margin of the working side orbit experiences more displacement in the prognathic over the orthognathic model in the same area.

The balancing side of the cranial vault and facial region undergoes more displacement in the prognathic versus the orthognathic facial form as viewed from the balancing side (Figure 43). The vault of the prognathic model shows some degree of displacement as far back as the area of the occipital protuberance. As a general statement, the balancing side of the prognathic model experiences more displacement than that of the same areas of the orthognathic model. From the basal view of the models as viewed through the foramen magnum, the increased vault displacement can again be seen in the prognathic model (Figure 44). The zygomatic arch on the working side of the prognathic has increased displacement over the orthognathic model, as does the balancing side. The maximum displacement (≥ 0.03 mm) can be found in a greater area of the dental arcade and palate of the prognathic model. The patterns appear similar, however, it varies in area and magnitude between the two models.

6.2 PRESSURE ANALYSIS

Figures 45 through 52 show the results of the volumetric component of the stress tensor, also called pressure (p), during a molar and incisor bite. The scale for the pressure results is the same for all figures (N/cm^2) - the sign convention is that positive values indicate compression while negative values indicate tension.

6.2.1 MOLAR BITE

Regions of compression are the same for the prognathic and orthognathic model, with increased area in the prognathic facial form (Figure 45). The areas of greater compression pressure are found in the medial and lateral orbital margins of the working side and in the lateral margins of the nasal aperture, although the area of compression is higher on the working opposed to the balancing side. The medial orbital margin in the prognathic model experiences compression, reaching almost to the medial margin of the right orbit spanning at least ¾ of the interorbital region. Compression can also be seen in the superior region of the maxilla on the working side in the area of infraorbital foramen and curvature where the zygoma and maxilla fuse at the suture.

In the frontal view of Figure 45, more tension is seen in the prognathic than the orthognathic model. Tension can be seen, although smaller in area than compression, in the lateral margins of the working and balancing side orbits in the prognathic model and also in the inferior orbital margin on the working side.

There appears to be very little if any pressure experienced in the cranial vault of either model as seen from the working side view in Figure 46. Pressure experienced by the molar bite appears to be restricted to the facial region and found in the form of both compression and tension. Compression at the bite point of the molar and

superior to that area is seen in both models, as can be expected. In the orthognathic face the compression area is directly in the area above the first molar, however, in the prognathic model the region of compression directly above the molar is more distant from the bite point. The zygomatic arch has a region of compression in the middle of the arch superiorly, although it is smaller in area in the orthognathic than prognathic model. The compression in the interorbital region in the prognathic model is clearly larger in area and magnitude as compared to the orthognathic facial form. The anterior and posterior regions of the zygomatic arch are undergoing tension in both models, with an additional region of tension in the inferior margin of the working side orbit in the prognathic facial form and seen only slightly in the orthognathic model.

Analysis of a molar bite, as viewed laterally in Figure 47, shows very little pressure being experienced on the balancing side for both models. Both models show points of tension in the area of the anterior and posterior margins of the zygomatic arch. This tension is most likely due to the attachment of the masseter muscle to the zygomatic arch, which experiences contraction while balancing the mandible during the molar bite.

Compression is experienced at both articular eminences (> 120 N/cm^2) (Figure 48). The figure shows there is more compression in the working side articular eminences than in the balancing side. Tension is present in the middle region of the zygomatic arch and in a few areas of the palate, likely indicating singularities found in the geometry of the palate itself.

6.2.2 INCISOR BITE

The distribution of compression and tension found in the prognathic and orthognathic models as a result of the pressure analysis for an incisor bite are found in

Figures 49 through 52. There are larger areas of maximum compression in the prognathic as compared to the orthognathic model (Figure 49). There are also notable decreased regions of compression in the interorbital area of the orthognathic model as compared to the prognathic model. The maxilla inferior and lateral to the nasal aperture undergoes the most compression, and it can be visualized by the pattern of how the compression travels superiorly into the interorbital region around the nasal aperture from the point of the bite force. The prognathic facial model has regions of tension around the lateral margin of the nasal aperture and inferior and lateral margins of the orbits.

In Figure 50 compression appears superior to the articular eminence on the temporal bone in both models, however, it is larger in area and magnitude in the prognathic model. This is likely due to compression experienced at the eminence traveling superiorly to the vault through the temporal bone. The incisor bite results in regions of tension in the frontal process of the zygoma at the curvature near the lateral margin of the orbit in both models (Figure 50). The prognathic skull model has larger areas of tension than the orthognathic model in the corresponding regions. Tension is found in both inferior margins of the working side orbit and the posterior/superior margin of the zygomatic arch at the area near the attachment to the temporal bone.

Maximum compression can be seen spanning the interorbital region from the working through to the balancing side in the medial margin of both balancing side orbits, with an increased area of maximum compression in the prognathic model (Figure 51). The anterior region of the maxilla on the balancing side of the prognathic model shows more compression over the orthognathic model. There is tension in both

models at the curvature of the zygomatic bone superior to the arch, however, it is larger in area and magnitude in the prognathic model. The posterior vertical margin of the maxilla in the prognathic model also experiences more tension than the orthognathic model. Tension is also seen in the inferior margin of the balancing side orbit of the prognathic model.

In the basal view of the two cranial models, found in Figure 52, maximum compression is experienced as expected at the point of the bite force at the first incisor. Compression at the articular eminence shows the same pattern and distribution of area in the prognathic and orthognathic models with the balancing side having an increase in maximum compression area in the orthognathic facial form. Tension is found in the middle of the zygomatic arch on both working and balancing sides; this is larger in area on the working side in both prognathic and orthognathic models. The attachment of the medial pterygoid muscle and regions of the dental arcade show similar patterns of tension with the prognathic model experiencing more tension.

When comparing each view of the volumetric component of stress between the molar and incisor results of the analysis in each case, the incisor results show an increase in both compression and tension along with their corresponding areas over the molar bite.

6.3 VON MISES STRESS ANALYSIS

Whereas the previous section indicated areas of positive and negative pressure which occurred in the craniofacial skeleton during muscle contraction, the Von Mises stress analysis indicates the magnitude of the deviatoric component of the stress

tensor. The Von Mises stress is independent of the pressure and is used often in failure analysis (Raghavan *et al.*, 2000; Chen *et al.*, 2005).

The maximum Von Mises stresses recorded for the full analysis was 14.7 MPa and 30.5 MPa for the prognathic model, for a molar and incisor bite force respectively. The maximum stresses for the orthognathic model for a molar and incisor bite force were 22.9 MPa and 41.8 MPa respectively. Although these values were recorded in the finite element analysis results, their magnitude is likely due to singularities occurring in the mesh model which is representative of the geometry of the skull. The internal and external geometry of the skull can be very detailed and intricate. Due to the detailed and fine bony geometry of the skull, a sudden change in geometry as in a styloid process or foramen, for example, can cause a spike in the stress analysis. This is called a singularity and is representative of a point of high stress and not representative of an entire region. In comparing the two facial forms it is more important to look at the patterns of distribution of stress than the exact numbers in N/cm^2 that the models incurred. The scale for the Von Mises results is in N/cm^2.

6.3.1 VON MISES FULL ANALYSIS: MOLAR BITE

When observing results for Von Mises stress, the prognathic facial form appears to have to withstand more stress than the orthognathic facial form during a molar bite (Figure 53). The cranial vault of both facial forms appears to have to withstand very little to no stress due to the forces of mastication being modeled. The frontal view shows the larger stress areas in the prognathic face in the area of the maxilla and medial and lateral margins of the working side orbit. The orbit on the balancing side also has more stress in the prognathic facial form, relative to the same regions in the orthognathic facial form. The inferior and lateral margins of the nasal

aperture also have an increase in stress on the working side as compared to the balancing sides in both skulls. The frontal area of the prognathic model experiences slightly more stress than the orthognathic model in the same region. A horizontal bar (region in green) of stress is present in the interorbital region of the prognathic model that is absent in the orthognathic model.

The lateral aspect of the two skulls shows the zygomatic arch experiencing high stresses at the posterior root. This is also true of the maxilla in the area directly above the first molar (Figure 54). The temporal lines of the prognathic facial form are slightly more stressed than that of the orthognathic facial form, while the nasal bone of the prognathic facial form has high stress over a greater region than the orthognathic facial form which has very little to none on the nasal bone. It was also interesting to note that the region directly at the first molar in the prognathic model has lower stress than the orthognathic facial form when viewed laterally. Where the orthognathic facial form has stress directed superiorly through the maxilla, the prognathic facial form accommodated the stress more in the facial region further away from the point of the bite force at the molar.

Von Mises stress distribution on the balancing side, lateral view, shows low levels as compared to the working side (Figure 55). The same regions as seen on the working side experience stress, however, in much lower levels and again less in the orthognathic facial form than that of the prognathic facial form. The zygomatic arch, posterior root of the arch, lateral margin of the orbit and the frontal regions showed low levels of stress on the balancing side in both facial forms.

Inferior views are similar for both skulls with a visible increase in stress for the prognathic skull at the area of the inferior and posterior margins of the zygomatic arch

(Figure 56). There appears to be maximum stress in the maxilla around the anterior root of the zygomatic arch and directly superior to the first molar in the orthognathic facial form. This same area viewed from the inferior aspect has a larger area in the prognathic facial form, however, it incurs a lower magnitude of stress throughout. Stress at the articular eminence is visible in both models with more areas of maximum Von Mises stress in the orthognathic model over the prognathic model as can be seen in the glenoid fossa of the orthognathic skull. The distribution of Von Mises stress between the balancing and working sides seems to be more uneven in the prognathic facial form where there is a region of higher stress and greater area in the working side articular eminence of the prognathic model over the balancing side.

6.3.2 VON MISES FULL ANALYSIS: INCISOR BITE

The incisal bite showed high levels of Von Mises stress distribution in the interorbital region and the lateral sides of the nasal sills, with greater magnitudes in the prognathic facial form (Figure 57). The stress of the prognathic face appears larger in the maxillary region and travels superiorly to the zygoma, almost equally, on working and balancing sides. The frontal bone of the prognathic form appears to have slightly more stress in this region than the orthognathic facial form.

The margins of the orbits in the prognathic skull experience higher stress values medially, laterally and inferiorly as compared to the orthognathic facial form. The balancing side stress in the lateral orbital margin of the orthognathic facial form is lower than in the prognathic facial form in the frontal view.

The posterior root of the zygomatic arch in the prognathic face has higher stress than the orthognathic facial form (Figure 58). The areas of the interorbital region can again be observed from this aspect, with the orthognathic facial form

having less stress than the prognathic facial form, especially in the area of the nasal bones.

Lower Von Mises stress can be seen on the balancing side over the working side of the two facial forms in Figure 59. The orthognathic model has less stress overall compared to the prognathic facial form where it experiences points of maximum stress at the medial and lateral orbital margins.

Inferiorly, the area of the incisors can be observed as having a larger region of high stress in the prognathic face and peaks in stress at the posterior areas of zygomatic arch are seen in both facial forms (Figure 60). The origin of the medial pterygoid muscle appears to be experiencing higher stress in the prognathic face than that of the orthognathic face which may be a result of the increased magnitude of muscle force in the prognathic facial form needed to produce the same bite force. The medial pterygoid muscle forces were recorded as 250.6 N in the prognathic model and 238.7 N in the orthognathic model for an incisor bite (Chapter 3: Materials and Methods, Table 7). The articular eminence of the orthognathic model shows larger differences in stress distribution between working and balancing sides with the stress on the working side being larger in area and magnitude and more directly in the glenoid fossa. The prognathic facial form also shows uneven Von Mises stress at the articular eminence with the highest area of stress being located more anteriorly in the area of the posterior root of the zygomatic arch.

6.4 MOLAR VS INCISOR BITE

The next series of figures (i.e., Figures 61-66) are those that have previously been shown, however, a single facial form is being looked at side by side to compare the Von Mises stress distribution while experiencing a molar or incisor bite. This

comparison allows direct interpretations on how the facial form, either prognathic or orthognathic, accommodates for masticatory stress for each type of bite force. The units for Von Mises stress remains the same at N/cm^2, where regions in blue show no stress and those in red are areas at or above the maximum on the figure's scale.

6.4.1 PROGNATHIC

The area of the orbits in the prognathic skull incurs more stress during an incisor bite over a molar bite as does the whole anterior region of the face (Figure 61). The lateral margins of the nasal aperture and nasal sills also have higher stress during a bite on the first incisor as compared to the first molar. The balancing and working sides differ more around the orbits in stress distribution and magnitude for the incisor bite.

The lateral view shows more stress in the area of the zygomatic arch at the posterior root during an incisor bite with almost equal maximum Von Mises stress in the lateral margins of the working side orbits (Figure 62). The area superior to the lateral orbital margin on the frontal bone has a region of higher stress in the molar bite than in the incisor bite for the prognathic facial form. The nasal bone region, as viewed laterally, shows a slightly larger area of maximum stress in the molar bite. However, in the incisor bite, although the area of maximum stress is smaller, almost the entire nasal bone to its most anterior tip is incurring stress as compared to the molar bite.

Inferiorly the stress at the articular eminence appears unevenly distributed but similar in both models (Figure 63). The anterior region of the palate is stressed more, and in a greater area, for an incisor bite than for a molar bite. The posterior region of the zygomatic arch has a larger region of stress in an incisor bite over the molar bite. If

decreased stress in the skull is an indicator of suitability (i.e., better adaptation), the prognathic facial form appears more suited to a molar bite on the dental arcade.

6.4.2 ORTHOGNATHIC

The facial region of the orthognathic skull appears to have less stress overall during molar than incisal biting, similar to the prognathic skull (Figure 64). The lateral orbital margin on the working side of both types of bite has a larger area of stress than the balancing side lateral orbital margin. The orthognathic facial form shows higher stress on the medial side of the working side orbit for an incisor bite and also stress on the medial side of the orbit on the balancing side. However, the molar bite shows a region of high stress on the medial side of the working side orbit with very little to no areas stressed on the balancing side. The interorbital region is more stressed during an incisor bite than a molar bite. The inferior margin of the orbit and zygoma has more stress in molar biting than in incisal biting.

Laterally the increased stress in the maxillary region can be observed in a molar bite force at the anterior root of the zygoma, superior to the bite point on the molar (Figure 65). Orbital margins on the working side appear to have similar stress for both types of bite. A moderate level of stress can be seen on the nasal bones with a small increase in stress on the medial orbital margin for both bites in the orthognathic form.

Figure 66 shows the inferior aspect of the two bites in an orthognathic facial form. Stress at the zygomatic process of the maxilla can be observed more so in a molar bite with similar stress patterns recorded in the zygomatic arch for both molar and incisal biting in the orthognathic facial form. The uneven distribution of stress at the articular eminence where the working sides' areas of stress are larger than those

of the balancing sides can be seen, however, the differences in size and magnitude of the working side over the balancing side are greater for the incisor bite force.

6.5 INDIVIDUAL MUSCLE CONTRIBUTION TO STRESS FOR A MOLAR BITE

The individual contribution of each of the muscles to the overall stress pattern was also assessed. Although the bony morphology of the skulls dictated that attachment sites varied, the analysis was scaled to produce the same bite force at the incisor and molar for both models. Higher stress in the area of the muscle origins may be due to a larger magnitude in force needed to produce a given bite force. It should also be noted that the scales for Figure 67 through Figure 88 vary in their maximum values for the different muscles that were modeled. Also note that the actual maximum stress value can be at the maximum of the scale or above. A range for the scale was determined during analysis to best show patterns in stress distribution for both skulls. Again with these comparisons the values for Von Mises stress are not as important as the patterns of stress. Varying patterns in stress throughout the facial skeleton between the prognathic and orthognathic facial forms were observed.

6.5.1 DEEP HEAD MASSETER

The comparison of Von Mises stress distribution in the prognathic and orthognathic facial forms from contribution of stress from contraction of the deep head of the masseter muscle for a molar bite is found in Figure 67. The muscle fibres of the deep head of the masseter muscle originate mostly from the posterior region of the zygomatic arch (Chapter 2: Literature Review, Figure 5), therefore, areas of muscle origin and insertion would be expected to have increased levels of stress as the force of contraction is acting directly on the bone in that region. Of interest to this study are

these areas, but more so regions of stress further away from muscle origins in the craniofacial skeleton.

The interorbital region of the working side of the prognathic facial form has a considerably larger area and higher magnitude of stress than that of the orthognathic facial form in the same region (Figure 67). The stress in the zygomatic arch reaches more anteriorly, encompassing larger regions of the zygoma inferior to the working side orbit in the prognathic facial form than that of the orthognathic face. The lateral margin of the orbit on the working side in the orthognathic face has a small area of higher stress, but is considerably less stressed throughout than that of the prognathic face.

The lateral side of the skulls shows the high stress in the zygomatic arch under deep masseter contraction and also in the region at the posterior point of origin (Figure 68). The prognathic face has high areas of stress in the anterior region of the zygomatic arch where the orthognathic model has less. The cranial vault seems void of any stress due to contraction of the deep head of the masseter muscle. The scale of the Von Mises stress between these models differs from the frontal and lateral views. A maximum value of 80 N/cm^2 is recorded for the frontal views of the deep masseter where the lateral sides have a scale of 0 - 350 N/cm^2. The areas of attachment on the zygomatic arch have approximately four times the stress of the facial region.

Inferiorly almost the entire working side zygomatic arch is experiencing stress with a larger pattern of maximum stress in the prognathic model (Figure 69). This same area of the orthognathic model is experiencing intermediate stress with a peak at the posterior root. This continuous observation of the high stress at the posterior root of the zygomatic arch can be a result of the arch having fixed ends. The deep

head of the masseter exerts slightly more force in the prognathic facial form than in the orthognathic model to achieve the bite force at the molar (Chapter 3: Materials and Methods, Table 6), however, it also exerts more stress on the zygomatic arch of the prognathic model than that of the orthognathic model.

In summary, the deep head of the masseter muscle can be said to contribute to increased Von Mises stress in the interorbital region and lateral orbital margins. The deep head of the masseter exerts less stress at the articular eminence and contributes to no stress in the vault of either facial form.

6.5.2 SUPERFICIAL HEAD MASSETER

The comparison between frontal views of the prognathic and orthognathic facial stress distribution during activity of the superficial head of the masseter is found in Figure 70. The superficial head of the masseter has its origin at the anterior 2/3 of the lower border of the zygomatic arch. The superficial portion of the masseter contributes to far more stress in the facial region than the deep head. The previous scale of peak stress of the deep head at 80 N/cm^2 is significantly less than that of the 250 N/cm^2 in the superficial masseter. Although the stress patterns appear the same, their magnitudes are very different. The maxillary region inferior to the zygomatic process and the lateral orbital margin of the working side experience more stress for the superficial than the deep head of the masseter. The superficial masseter contributes to stress in the interorbital region of both models with increased area in the prognathic skull and the same for the lateral orbital margins on the balancing side.

The lateral side of the skull in the orthognathic facial form experiences high stress in the anterior region of the zygomatic arch as well as the maxilla directly above the region of the bite force (Figure 71). The anterior region of the zygomatic arch is

the origin of the superficial head of the masseter (Chapter 2: Literature Review, Figure 5) and an increased stress in this area is to be expected. The prognathic face appears to have more stress in the region below the orbits, the complete frontal process of the zygoma and the medial wall of the orbit. Inferiorly the stress at the anterior region of the zygomatic arch can be observed in both models with a higher maximum value of Von Mises stress and area in the orthognathic facial form (Figure 72). The articular eminence of both models appears to have less stress while modeling the superficial masseter muscle.

Again the superficial masseter has to exert a little more force in the prognathic facial form on the working and balancing sides (229.7N, 107.9N) than the orthognathic model (216.6N, 101.7N) to achieve the same bite force at the first molar. The superficial masseter contraction leads to an increased stress in the anterior region of the zygomatic arch where it has its origins, but also in the anterior region of the zygoma and maxilla during a molar bite. The nasal bones of both models have increased stress relative to deep head of masseter contraction. There is little stress in the frontal region of the prognathic over the orthognathic facial form, with no stress in the cranial vault for either. The orthognathic model does not experience any stress in the frontal region or in the vault during superficial masseter contraction. Like the deep head of the masseter, the superficial head contributes to increased stress in the interorbital region, although it does not contribute to any stress in the vault of either form.

6.5.3 TEMPORALIS MUSCLE

The fan shaped temporalis muscle has origins farthest away from the facial skeleton on the lateral surface of the skull (Chapter 2: Literature Review, Figure 6).

Overall stress magnitude for the temporalis muscle is less than that of the superficial masseter in the facial region but more than the deep head of the masseter. Similar patterns are observed with the temporalis muscle as with the superficial masseter in the frontal view (Figure 73). The temporalis muscle causes more stress in the interorbital region with a distinct horizontal bar of stress (in green) between the two orbits of the prognathic facial form. There is a larger region of maximum stress on the medial margin of the working side orbit for the prognathic than that of the orthognathic facial form.

Differences in the stress distribution in the region of the temporal fossa are observed between the orthognathic and prognathic facial forms when viewed laterally (Figure 74). The prognathic face has larger areas of stress at the anterior temporal lines and the posterior root of the zygomatic arch. A larger part of the temporal fossa experiences stress in the prognathic model with temporalis contraction for a molar bite. Inferiorly the areas of high stress appear at the articular eminences and the first molar of both models with the zygomatic arch having more stress in the prognathic than the orthognathic facial form (Figure 75). The distribution at the articular eminences between the working and balancing side is observed in both models with more stress in the orthognathic facial form during temporal muscle contraction.

During its role in mastication for a bite at the first molar, the temporalis muscle contributes to low levels of stress in the frontal region of the prognathic facial form but not the orthognathic form. The temporalis muscle contributes to the most stress in the interorbital region, the temporal fossa and at the articular eminence. The temporalis muscle shows the greater regions of stress away from the origin of the

muscle and models indicate that a prognathic facial form experiences more stress under contraction than the orthognathic facial form for a molar bite.

6.5.4 MEDIAL PTERYGOID MUSCLE

The medial pterygoid has origins on the inferior side of the skull at the pterygoid fossa of the sphenoid bone. Although there are considerably smaller areas of stress attributed to the medial pterygoid muscles, they are at a much higher magnitude than those of the other masticatory muscles where the scale for the medial pterygoid is the largest ranging from 0 to 350 N/cm^2 (Figure 76). The prognathic model has higher stress than that of the orthognathic facial form in the region of the orbits on the working side margins. The distribution of stress seems to only vary in the region of the inferior nasal aperture of the maxilla for both models, with the prognathic model experiencing a larger area of stress with similar magnitude to the orthognathic model.

The inferior aspect of the skulls shows a concentrated area of stress at 350 N/cm^2 or above in the area of origin of the muscle (Figure 77). Articular eminence stress differences between the models are observed and appear larger in the orthognathic model due to medial pterygoid muscle contraction during mastication. The balancing side of the orthognathic model has a larger area and higher magnitude of stress at the articular eminence than the working side, which was not previously seen in other analyses.

In summary, the medial pterygoid has the highest magnitude during contraction of all masticatory muscles modeled (Chapter 3: Material and Methods, Table 6). The medial pterygoid contraction causes an increase in stress in the region of the nasal sills and laterally extending into the maxilla. During contraction of the medial pterygoid there is increased stress at the articular eminence but no stress in the vault

of either model as seen in the other muscles modeled under a molar bite. Overall the orthognathic model appears to have less stress during medial pterygoid contraction for a molar bite.

6.6 INDIVIDUAL MUSCLE CONTRIBUTION OF STRESS TO AN INCISOR BITE

Each individual muscle contraction for an incisor bite was modeled. Overall stress was higher for both facial forms in all muscles for an incisor bite over a molar bite.

6.6.1 DEEP HEAD MASSETER

The deep head of the masseter exerts more stress on the lateral margin of the orbit in both balancing and working sides of the prognathic facial form as compared to the orthognathic facial form (Figure 78). The interorbital region of the prognathic face experiences higher stress levels than the orthognathic facial form, which incurs little in comparison. The anterior region of the maxilla in both skulls incurs some stress throughout, radiating outward from the point of bite force at the incisor.

The lateral aspect of the skull shows a larger area of maximum stress in the prognathic facial form in the zygomatic arch (Figure 79). Highest points of stress in the orthognathic skull are in the area of the posterior zygomatic arch root. The lateral orbital margin in the prognathic model experiences more stress than in the orthognathic model. The inferior aspect of both skulls can be seen in Figure 80. The deep head of the masseter contributes stress to the posterior region of the zygomatic arch in greater magnitude and area for the prognathic facial form. There is low stress at the articular eminence for deep head contraction which is less in the orthognathic model, although the distribution of stress between the balancing and working sides is more uneven for the orthognathic model.

The deep head of the masseter during contraction for an incisor bite causes the most noticeable stress in the interorbital region, with much greater area in the prognathic facial form and inferior to the nasal sills. The deep head does not contribute to stress in the vault of either facial form and it appears that overall the orthognathic model experiences less stress during a bite at the first incisor.

6.6.2 SUPERFICIAL HEAD MASSETER

In comparing the Von Mises stress distribution for the deep head and the superficial head of the masseter the patterns of stress and area are similar. The superficial masseter muscle shows larger areas with higher stress than that seen with the deep head of the masseter for corresponding regions (Figure 81). In the region inferior and lateral to the nasal aperture of both facial forms, the areas of stress are larger and higher in magnitude. The interorbital region experiences more stress in the prognathic face than the orthognathic face. The lateral margin of the working side orbit has high regions of stress in both forms, with the greatest area in the prognathic facial form. This high stress distribution in the lateral margin of the orbit can be seen from the lateral view of the skull in Figure 82. The frontal bone superior to the orbit of the working side has a slight increase in the area of stress in the prognathic facial form over the orthognathic face in the same region. Similar patterns in stress distribution for the superficial head of masseter contraction for both models can be seen inferiorly, with the prognathic skull having more stress in corresponding regions (Figure 83). The orthognathic skull has high stress in the working side articular eminence relative to the balancing side, where the prognathic model has higher stress but more evenly distributed.

For the superficial masseter muscle, during contraction there is an increase in stress throughout the facial skeleton. The frontal region of the prognathic model is stressed where the orthognathic model is not stressed in the same areas. The cranial vault does not experience stress under superficial masseter contraction. To summarize the reaction in the facial skeleton, it appears that the Von Mises stress distribution radiates vertically away from the bite force at the incisor and travels superiorly around the nasal aperture up through the interorbital region and lateral orbital margins of both facial forms. However, the prognathic facial form experiences more stress and it appears more evenly distributed between the balancing and working sides. The superficial head contraction contributes little stress at the articular eminence. Neither the superficial nor deep head of the masseter contribute to stress in the vault. The orthognathic model again, as seen previously with other muscles, has to accommodate for less stress than the prognathic model during superficial masseter contraction.

6.6.3 TEMPORALIS MUSCLE

The contribution of the temporalis muscle contraction to stress distribution in the facial region for an incisor bite is found in Figure 84. The area of the alveolar bone in the maxilla and the region inferior to the nasal aperture experience the most stress, which appears to be similar for both forms. Again the prognathic skull experiences high stress in the interorbital region and high stress on both medial margins of the orbits extending to the nasal bones. A slight increase in stress in the area of the frontal bone at the forehead can be seen in the prognathic skull over the orthognathic skull.

The lateral aspect of the skull shows a well-defined temporal line in both facial forms (Figure 85). The overall stress distribution is greatest for the prognathic skull with larger areas for peak stress at the anterior temporal lines and the posterior root

of the zygomatic arch. The temporal fossa for both models has stress throughout the region but it is considerably larger in the prognathic facial form and decreased in the posterior region of the fossa in the orthognathic facial form.

The high stress level at the articular eminences is observed from the inferior view (Figure 86). The decreased moment arm of the maxilla in the orthognathic facial form may cause increased stress on both articular eminences under a constant load. The high values and uneven distribution can indicate that the contribution of the temporalis muscle for an incisor bite causes greater reaction forces and subsequent stress at the temporomandibular joint.

The temporalis muscle contributes to increases in stress in the interorbital region in both facial forms, with an increased region of stress in the frontal bone of the prognathic facial form. Temporalis contraction contributes to an increase in stress at the articular eminence over the masseter muscle contraction during an incisor bite. There is higher stress at the articular eminence in the orthognathic facial form, specifically in the balancing side eminence over the prognathic facial form, however, in other areas, the orthognathic model appears less stressed than the prognathic model under temporalis muscle contraction for an incisor bite.

6.6.4 MEDIAL PTERYGOID MUSCLE

The contributions from the medial pterygoid are only shown in anterior (Figure 87) and inferior views (Figure 88). The medial pterygoid contributes to the highest stresses where it has attachment at the base of the skull but the resultant stress from the muscle force is accommodated for in areas of the facial skeleton (Figure 88). The area of the nasal sills has the highest magnitude of stress, but they are larger in area for the prognathic facial form. The maxillary region of the prognathic skull has an

increased area of stress superior to the bite force over the orthognathic model, however, this may be expected as due to the morphology of the region it also has a larger maxilla due to increased prognathism.

Inferiorly the peaks in stress may be attributed to singularities in the mesh and the fossa area of muscle origin (Figure 88). The area of the articular eminence experiences more stress in the orthognathic facial form for medial pterygoid contraction which varies between the balancing and working sides as seen in previous analyses. However, in contrast to other muscle contraction results the increased stress for the medial pterygoid muscle contraction was found in the articular eminence of the balancing side at the region of the temporomandibular joint instead of the working side eminence. The pattern in the prognathic model appeared evenly stressed in the same areas.

Although the medial pterygoid again has the highest magnitude of contraction as compared to the other muscles, in distribution it contributes to smaller areas of stress in the facial skeleton. The medial pterygoid can be considered a contributor to stress in the region of the nasal sills both inferior and lateral to the nasal aperture. The medial pterygoid contraction does not contribute to Von Mises stress occurring in the vault of either facial form. Medial pterygoid contraction does not contribute to a large magnitude of stress at the articular eminence, however, the uneven distribution with increased stress in the balancing side eminence in the orthognathic model is noted. Overall, in the facial skeleton and vault the orthognathic model experiences less stress due to the medial pterygoid contraction during a bite on the first incisor.

Figure 37. Total displacement for a molar bite in a prognathic (left) and orthognathic (right) facial form: full analysis, anterior view.

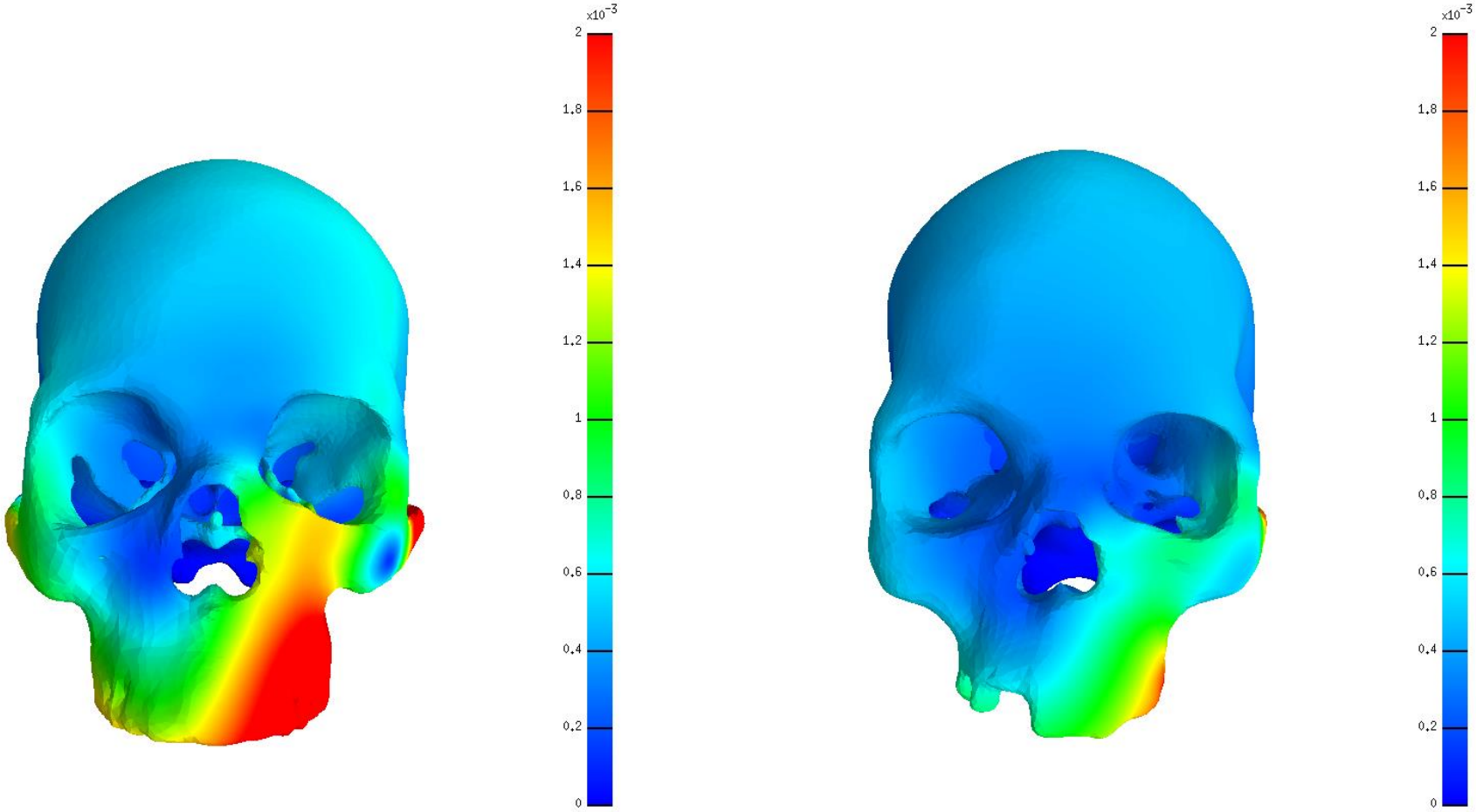

Figure 38. Total displacement for a molar bite in a prognathic (left) and orthognathic (right) facial form: full analysis, lateral view.

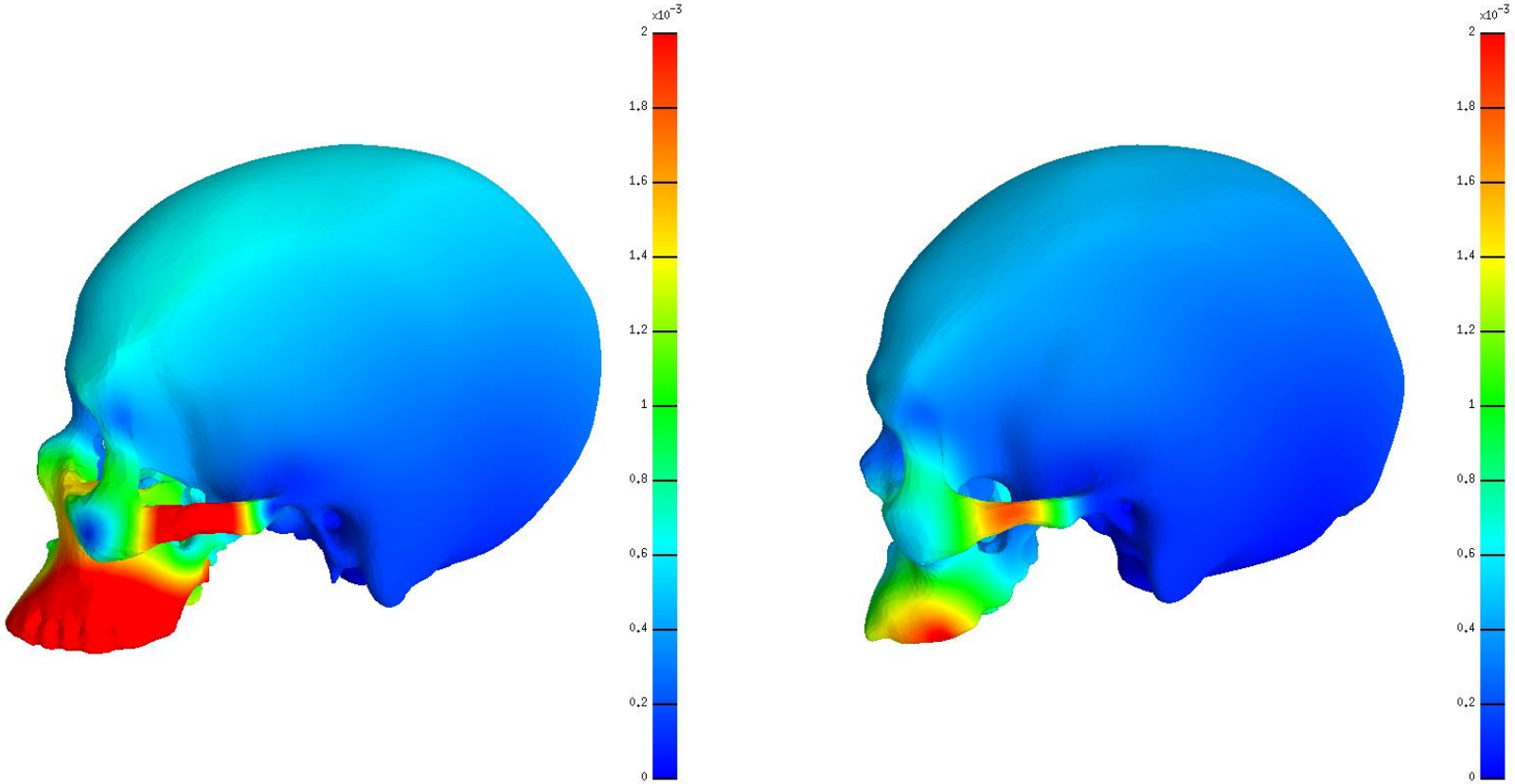

Figure 39. Total displacement for a molar bite in a prognathic (left) and orthognathic (right) facial form: full analysis, lateral view of balancing side.

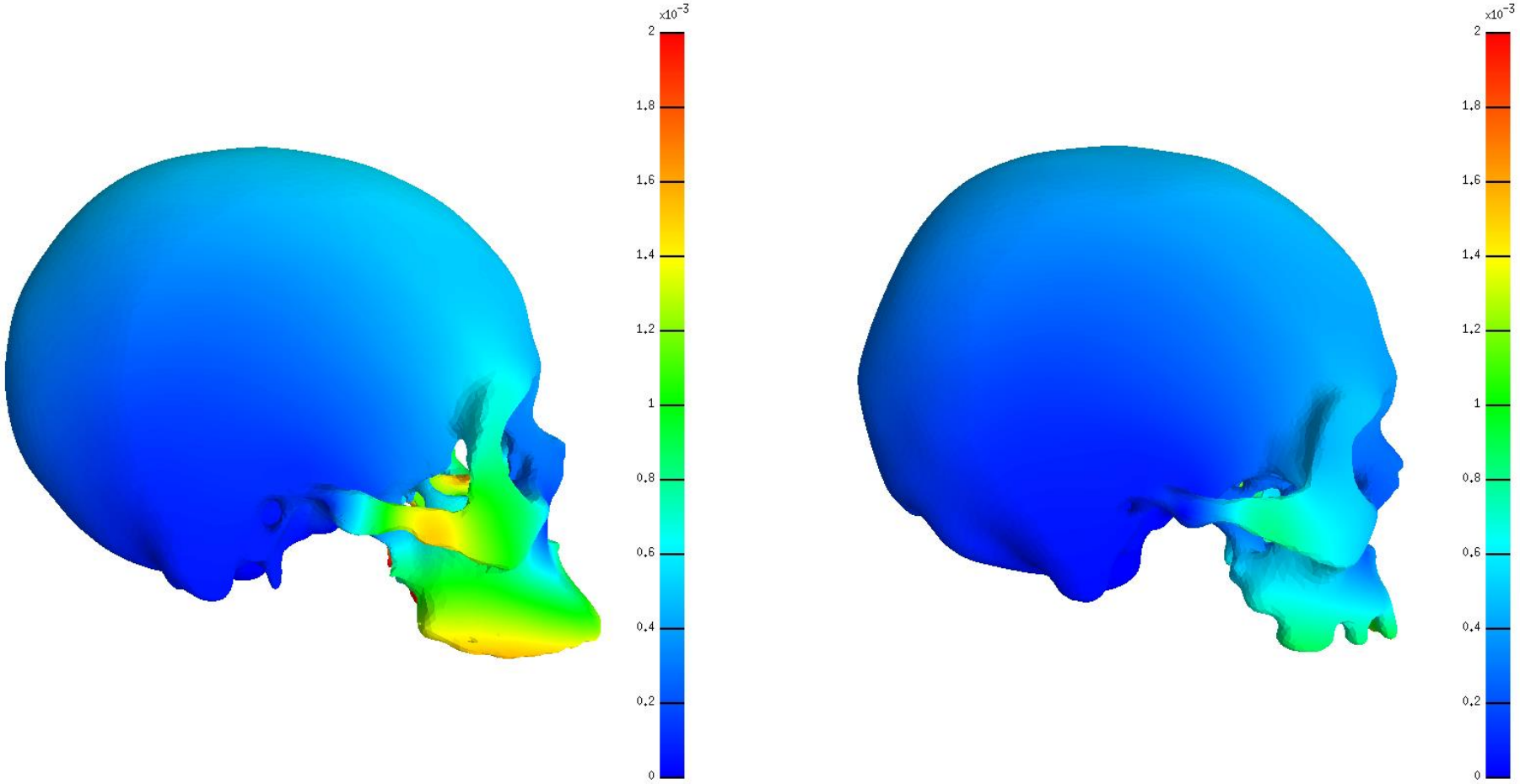

Figure 40. Total displacement for a molar bite in a prognathic (left) and orthognathic (right) facial form: full analysis, inferior view.

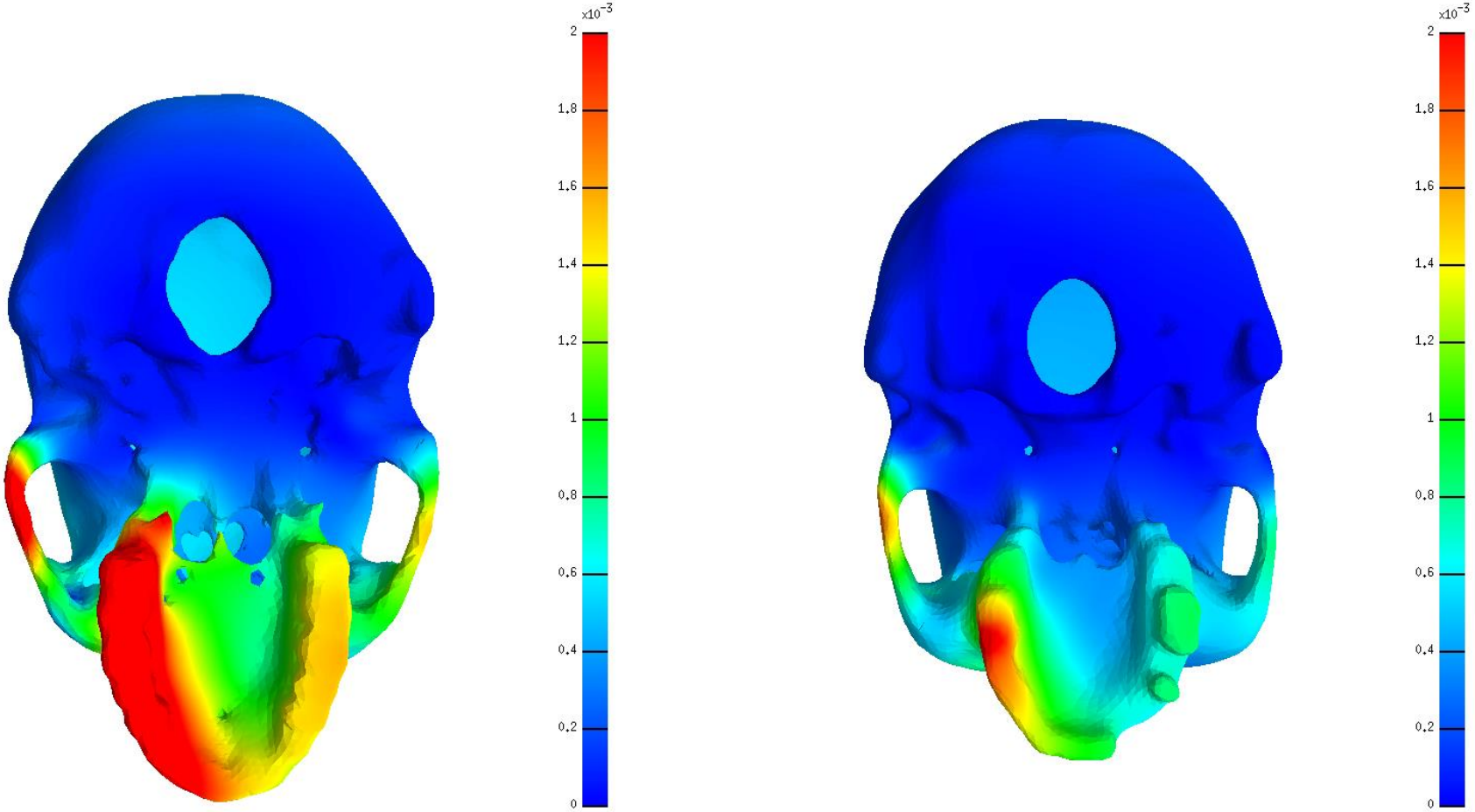

Figure 41. Total displacement for an incisor bite in a prognathic (left) and orthognathic (right) facial form: full analysis, anterior view.

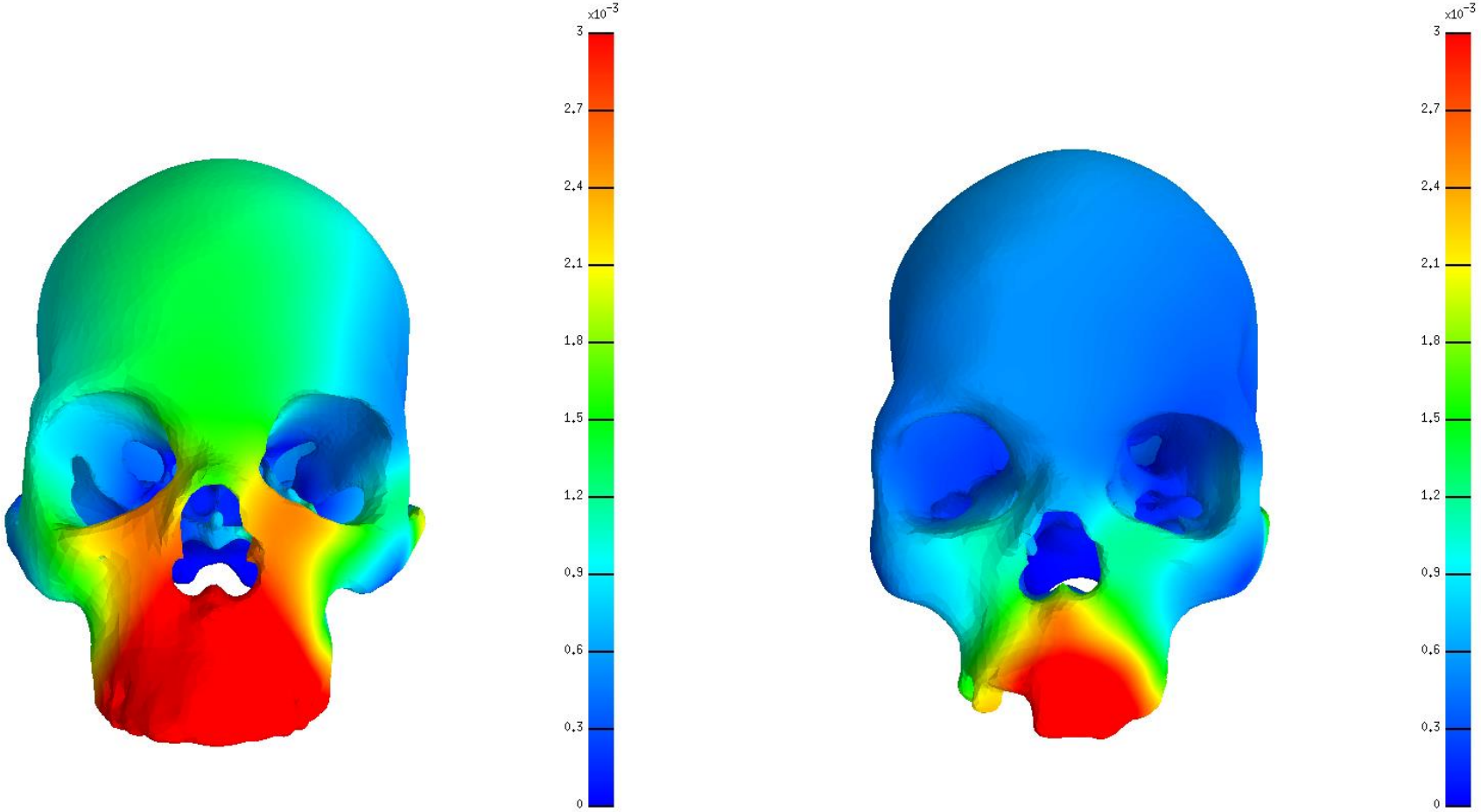

Figure 42. Total displacement for an incisor bite in a prognathic (left) and orthognathic (right) facial form: full analysis, lateral view.

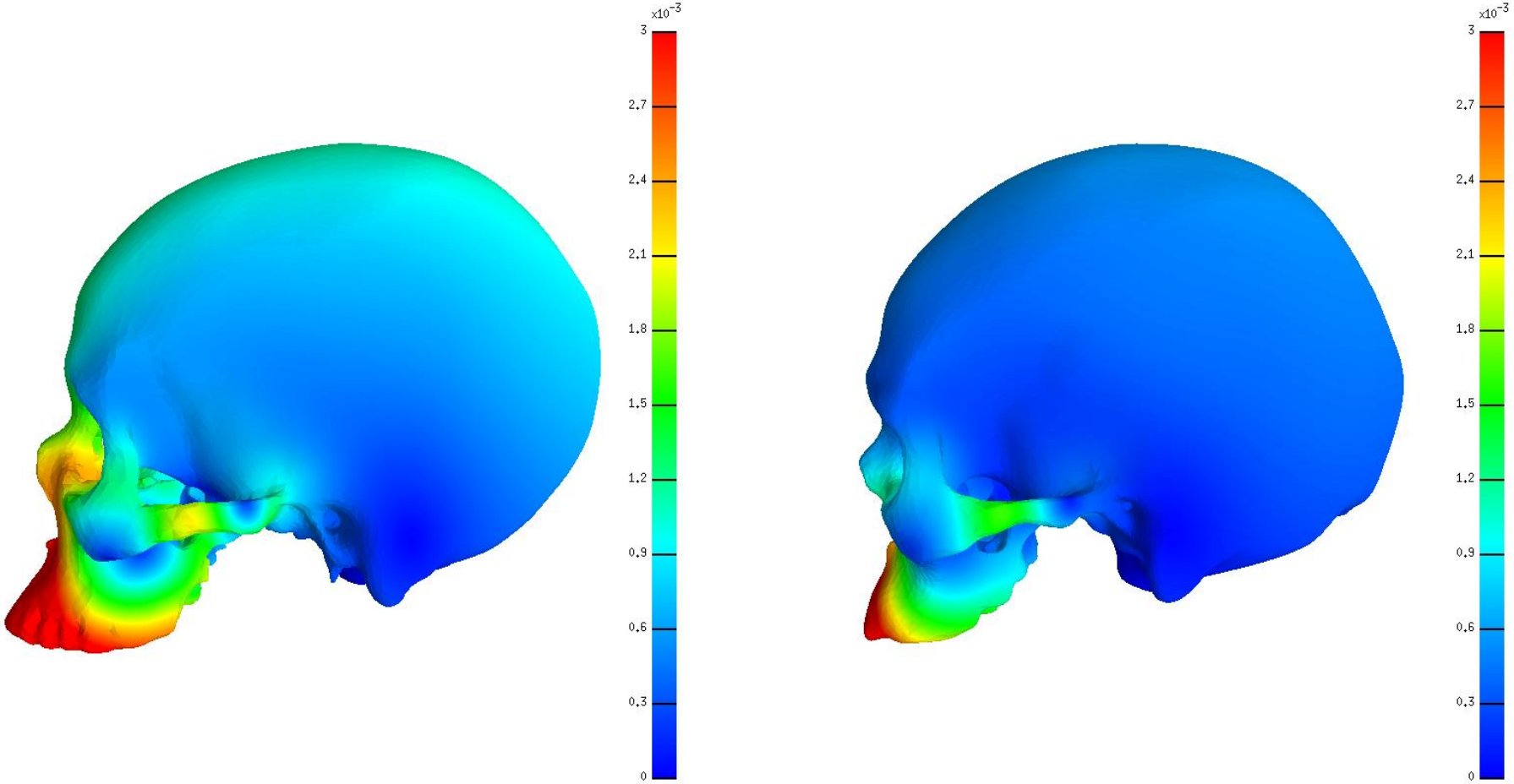

Figure 43. Total displacement for an incisor bite in a prognathic (left) and orthognathic (right) facial form: full analysis, lateral view of balancing side.

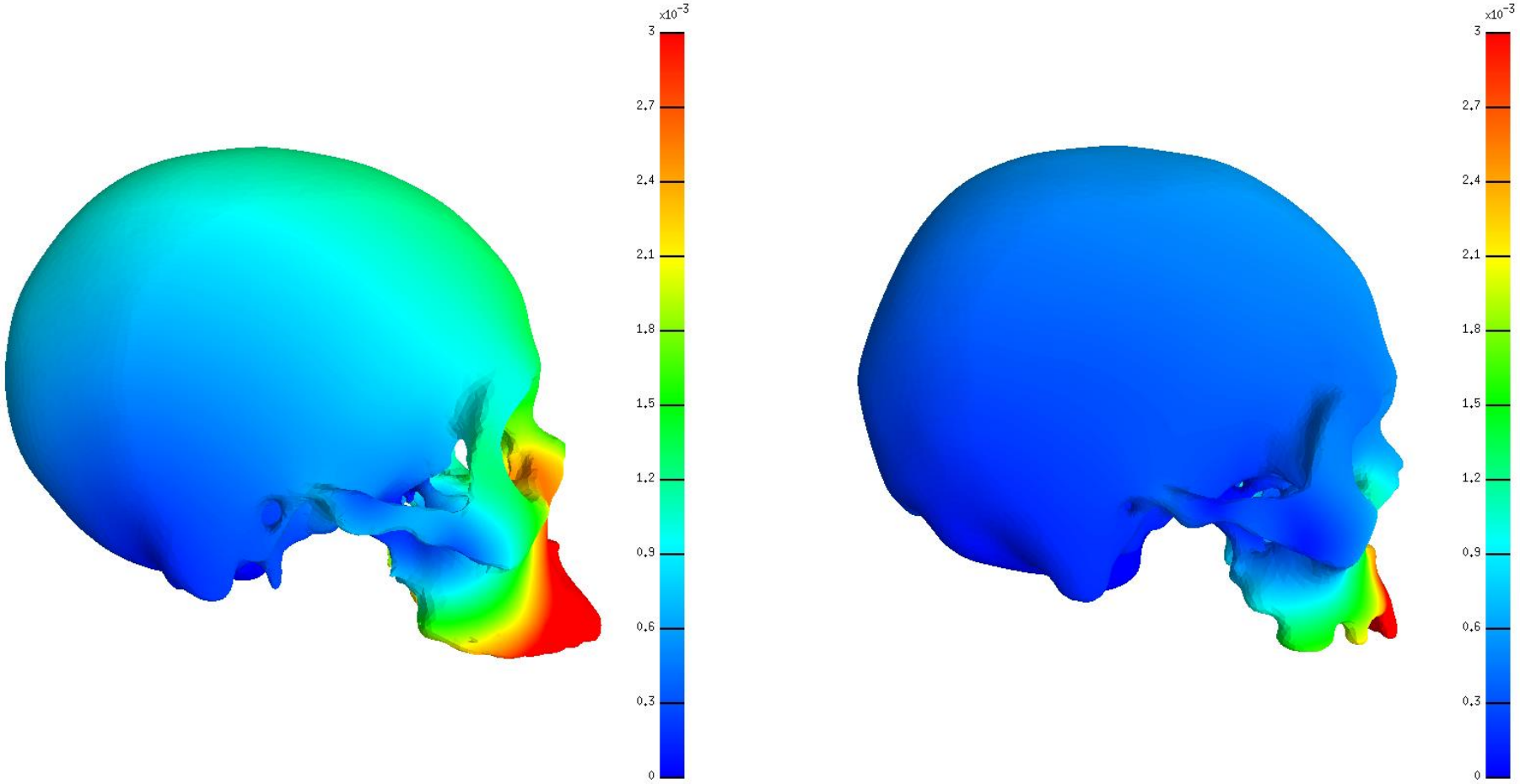

Figure 44. Total displacement for an incisor bite in a prognathic (left) and orthognathic (right) facial form: full analysis, inferior view.

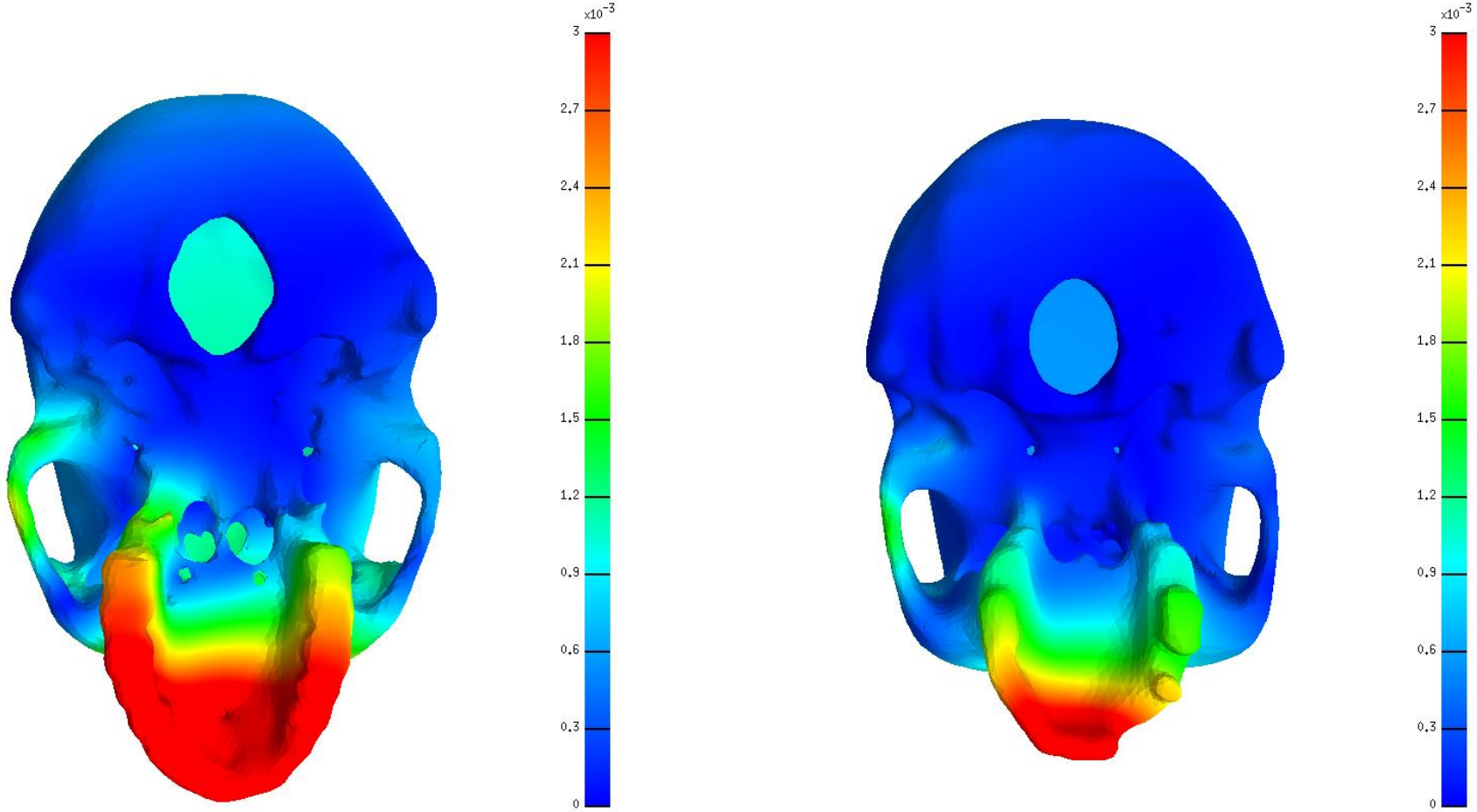

Figure 45. Pressure results for a molar bite in a prognathic (left) and orthognathic (right) facial form: full analysis, anterior view. Positive regions of the scale (red) indicate compression where negative regions (blue) are regions of tension.

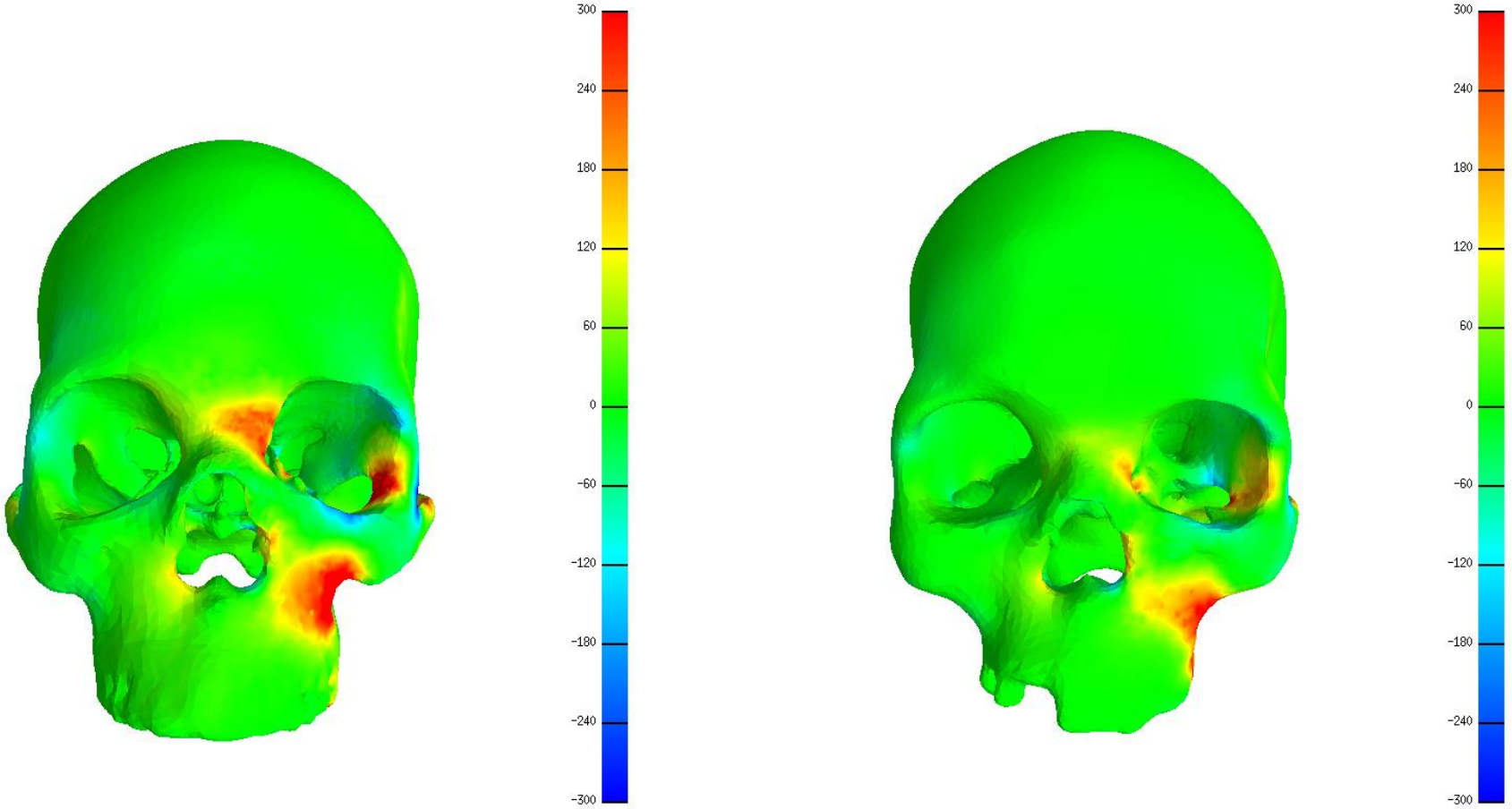

Figure 46. Pressure results for a molar bite in a prognathic (left) and orthognathic (right) facial form: full analysis, lateral view. Positive regions of the scale (red) indicate compression where negative regions (blue) are regions of tension.

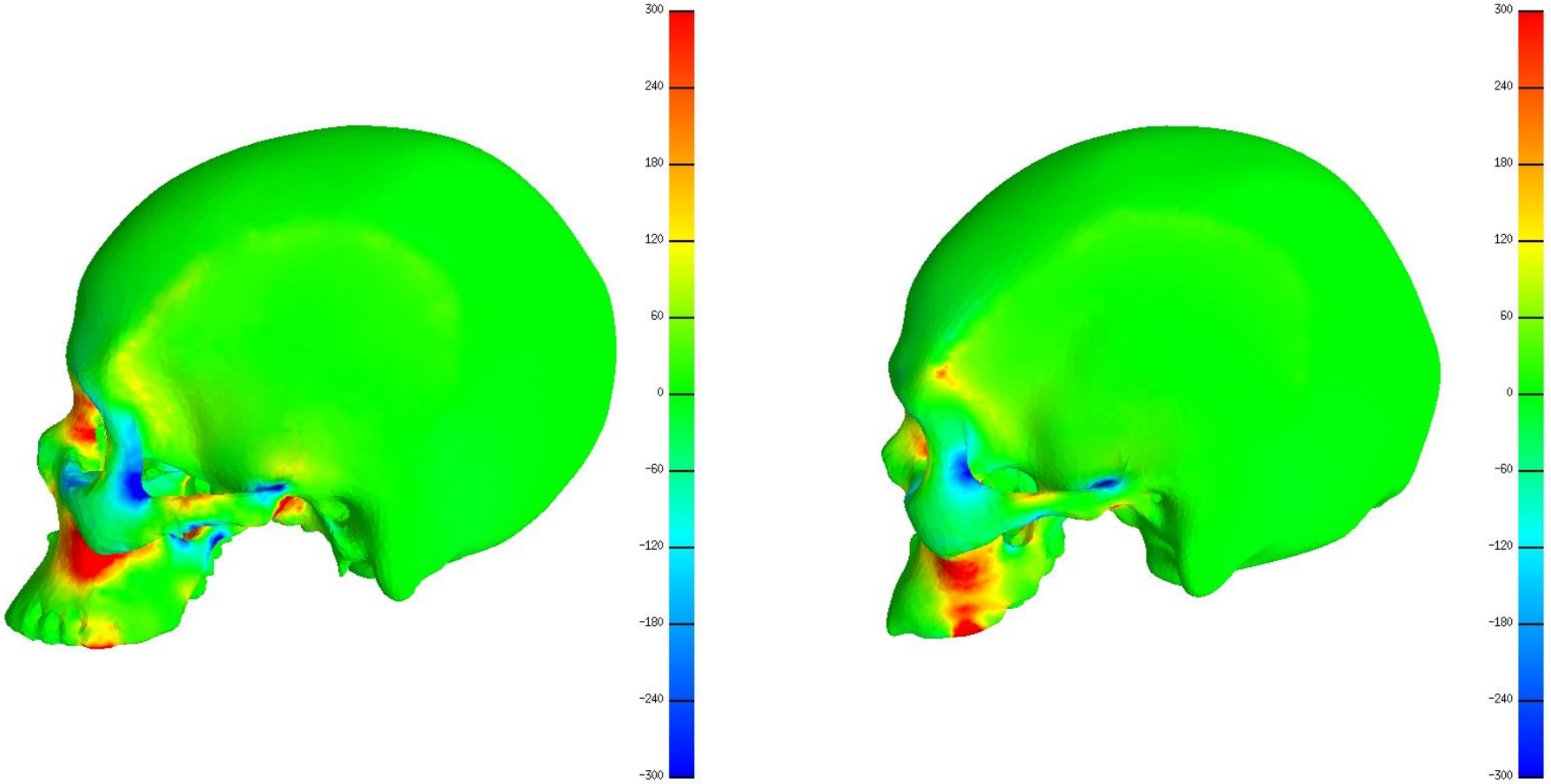

Figure 47. Pressure results for a molar bite in a prognathic (left) and orthognathic (right) facial form: full analysis, lateral view balancing side. Positive regions of the scale (red) indicate compression where negative regions (blue) are regions of tension.

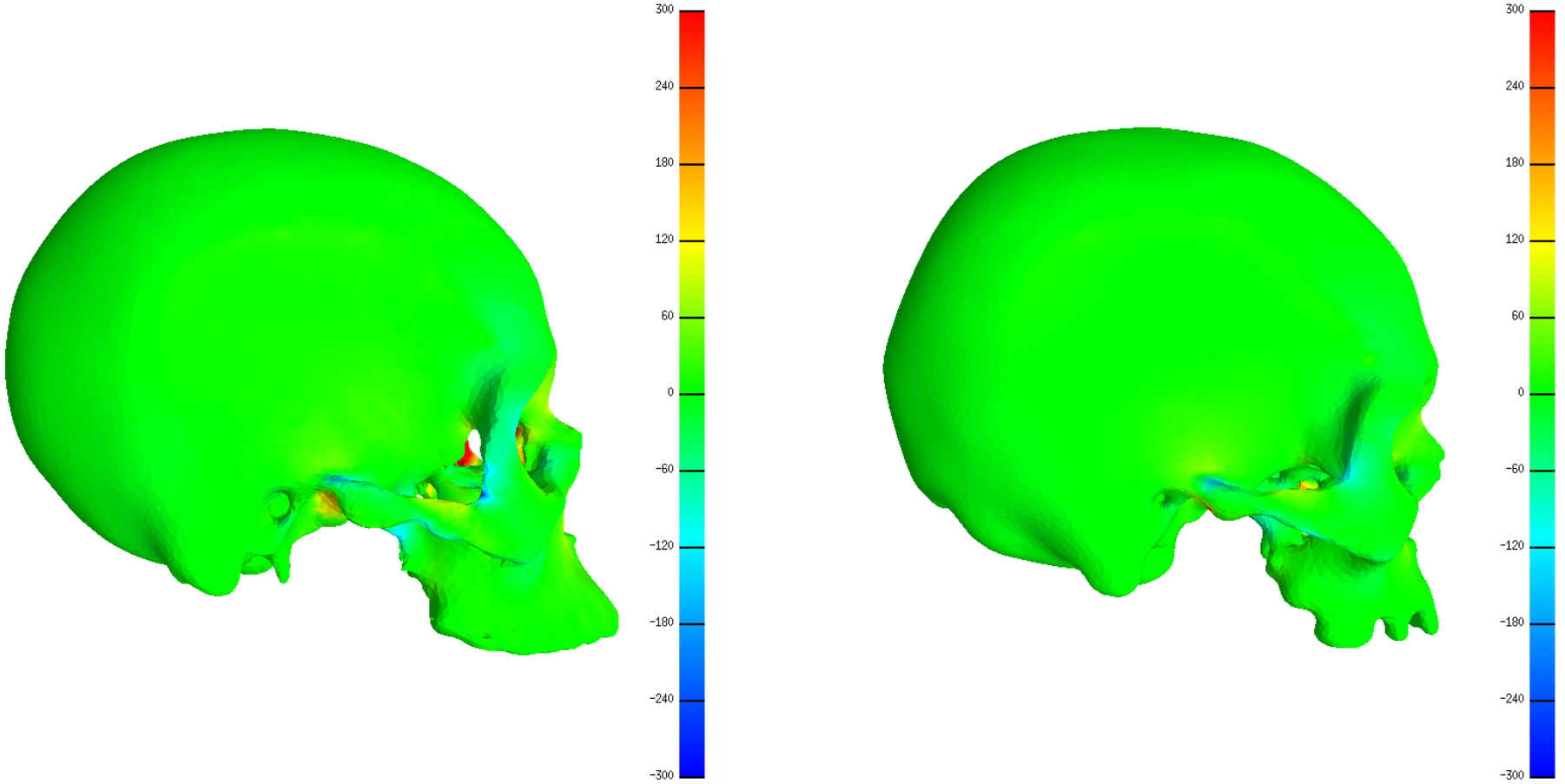

Figure 48. Pressure results for a molar bite in a prognathic (left) and orthognathic (right) facial form: full analysis, inferior view. Positive regions of the scale (red) indicate compression where negative regions (blue) are regions of tension.

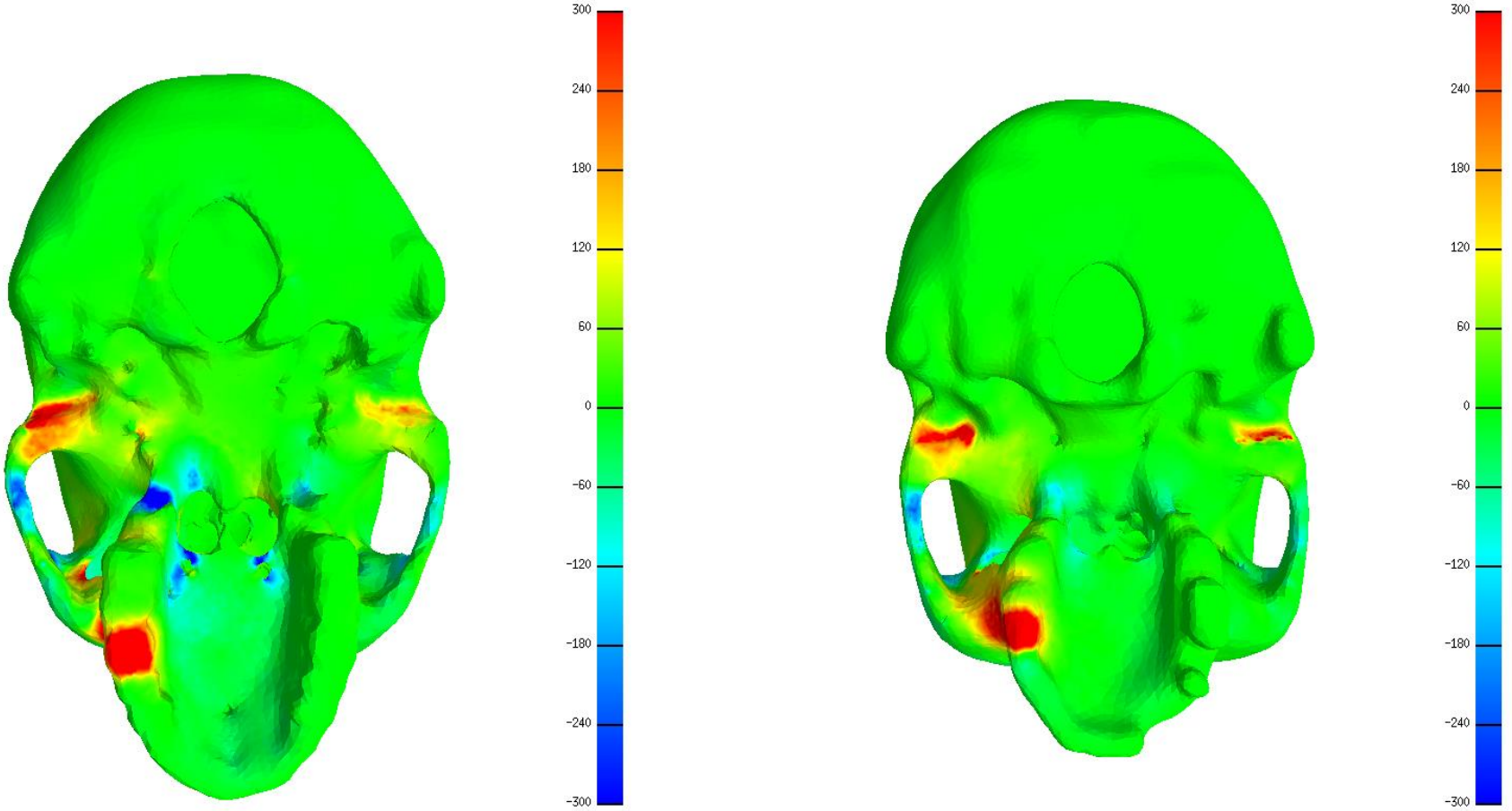

Figure 49. Pressure results for an incisor bite in a prognathic (left) and orthognathic (right) facial form: full analysis, anterior view. Positive regions of the scale (red) indicate compression where negative regions (blue) are regions of tension.

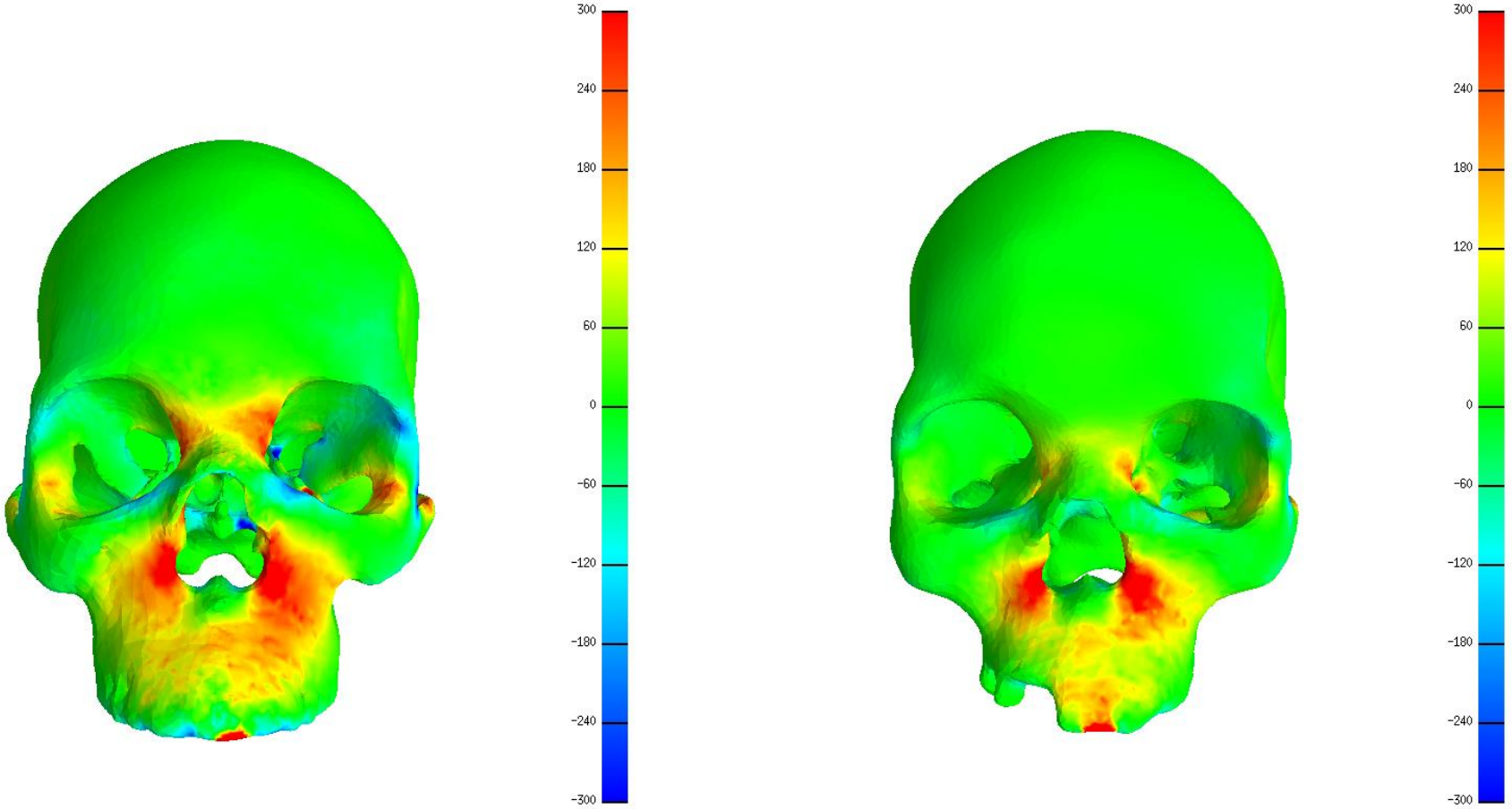

Figure 50. Pressure results for an incisor bite in a prognathic (left) and orthognathic (right) facial form: full analysis, lateral side. Positive regions of the scale (red) indicate compression where negative regions (blue) are regions of tension.

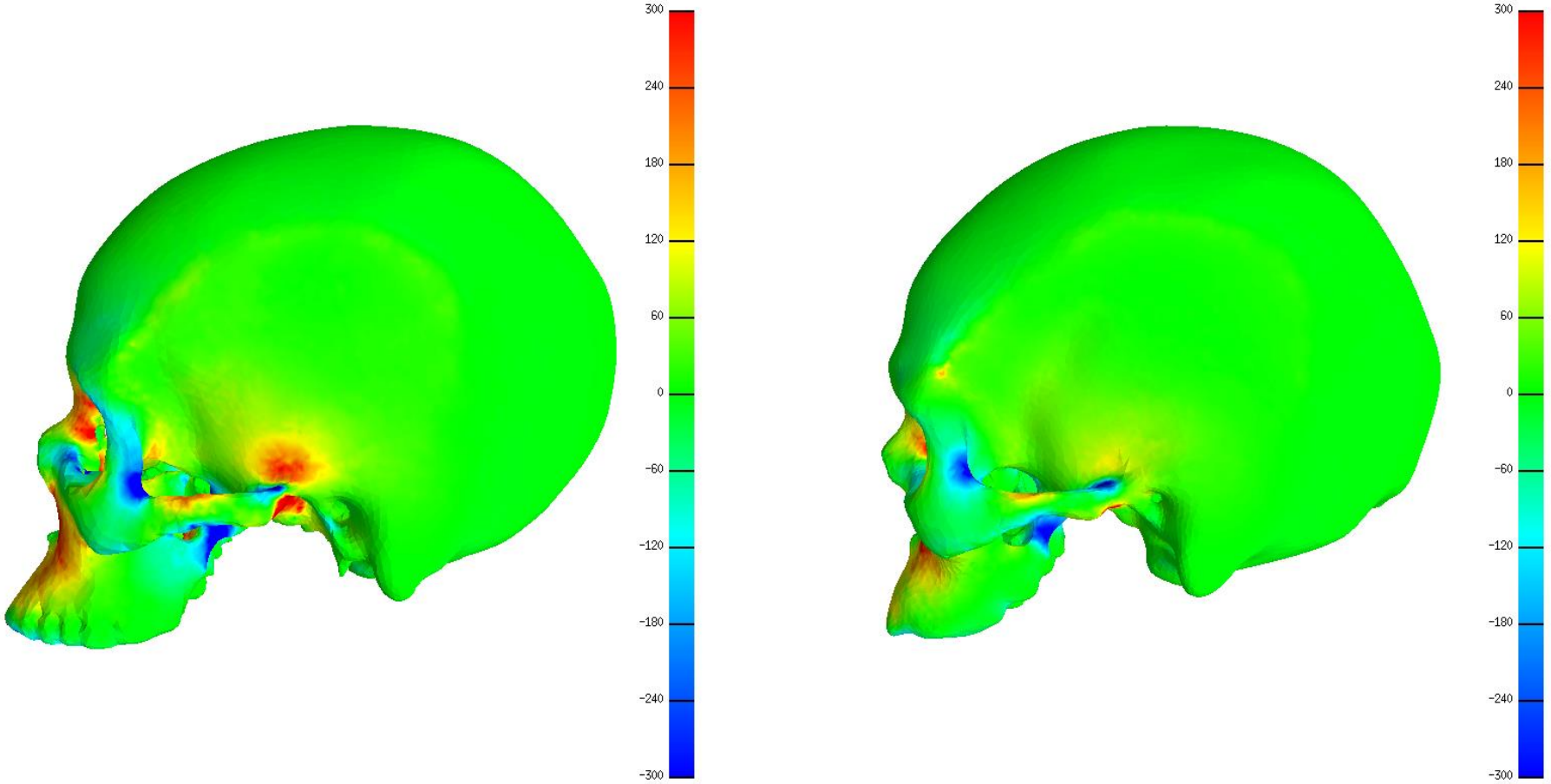

Figure 51. Pressure results for an incisor bite in a prognathic (left) and orthognathic (right) facial form: full analysis, lateral view balancing side. Positive regions of the scale (red) indicate compression where negative regions (blue) are regions of tension.

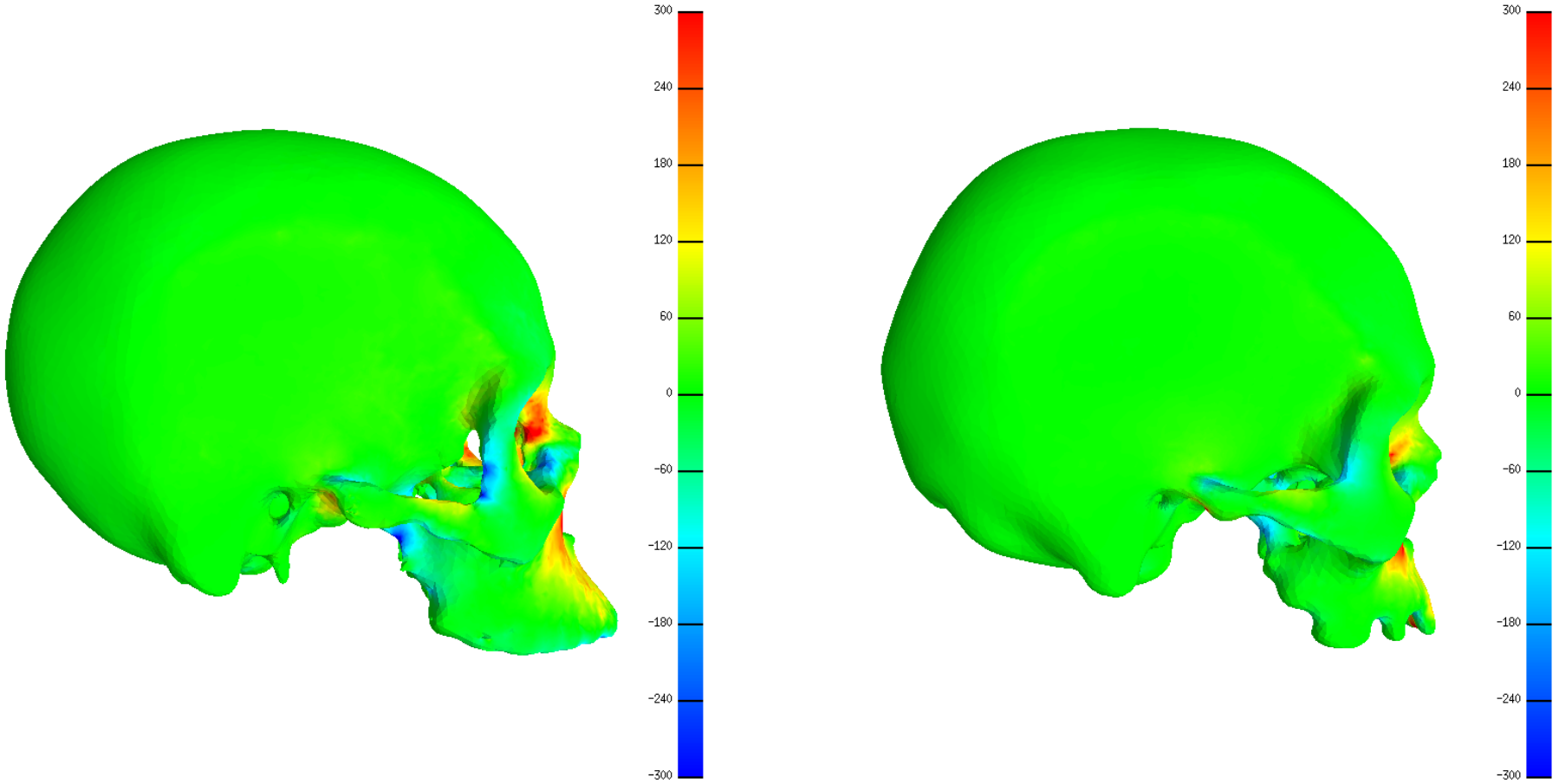

Figure 52. Pressure results for an incisor bite in a prognathic (left) and orthognathic (right) facial form: full analysis, inferior view. Positive regions of the scale (red) indicate compression where negative regions (blue) are regions of tension.

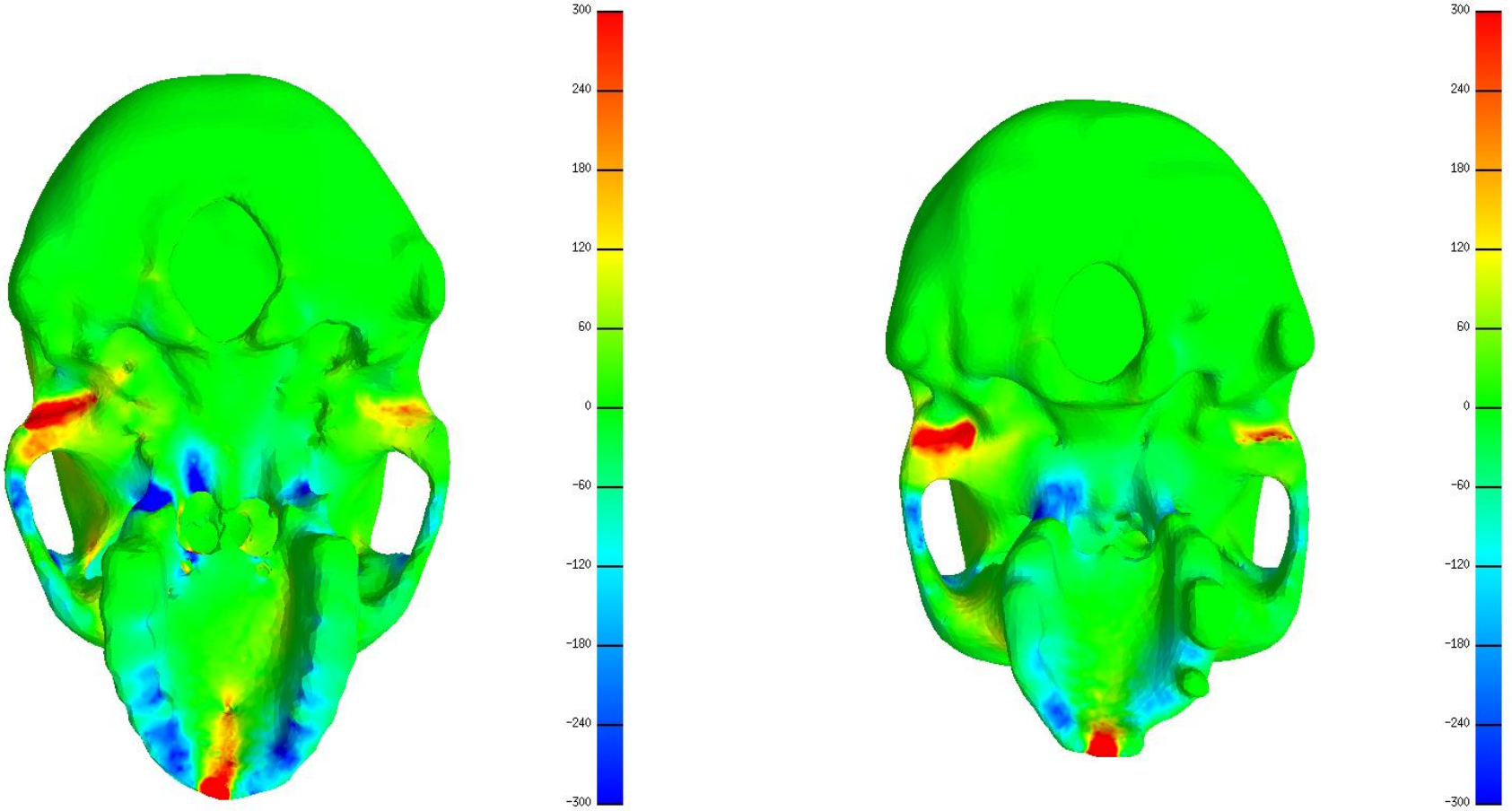

Figure 53. Von Mises stress distribution for a molar bite comparing prognathic (left) and orthognathic (right) facial form: full analysis, anterior view. The scale for the Von Mises results is in N/cm^2. Red indicates areas of high stress (a combination of tension, compression and shear) and blue indicates areas of low stress.

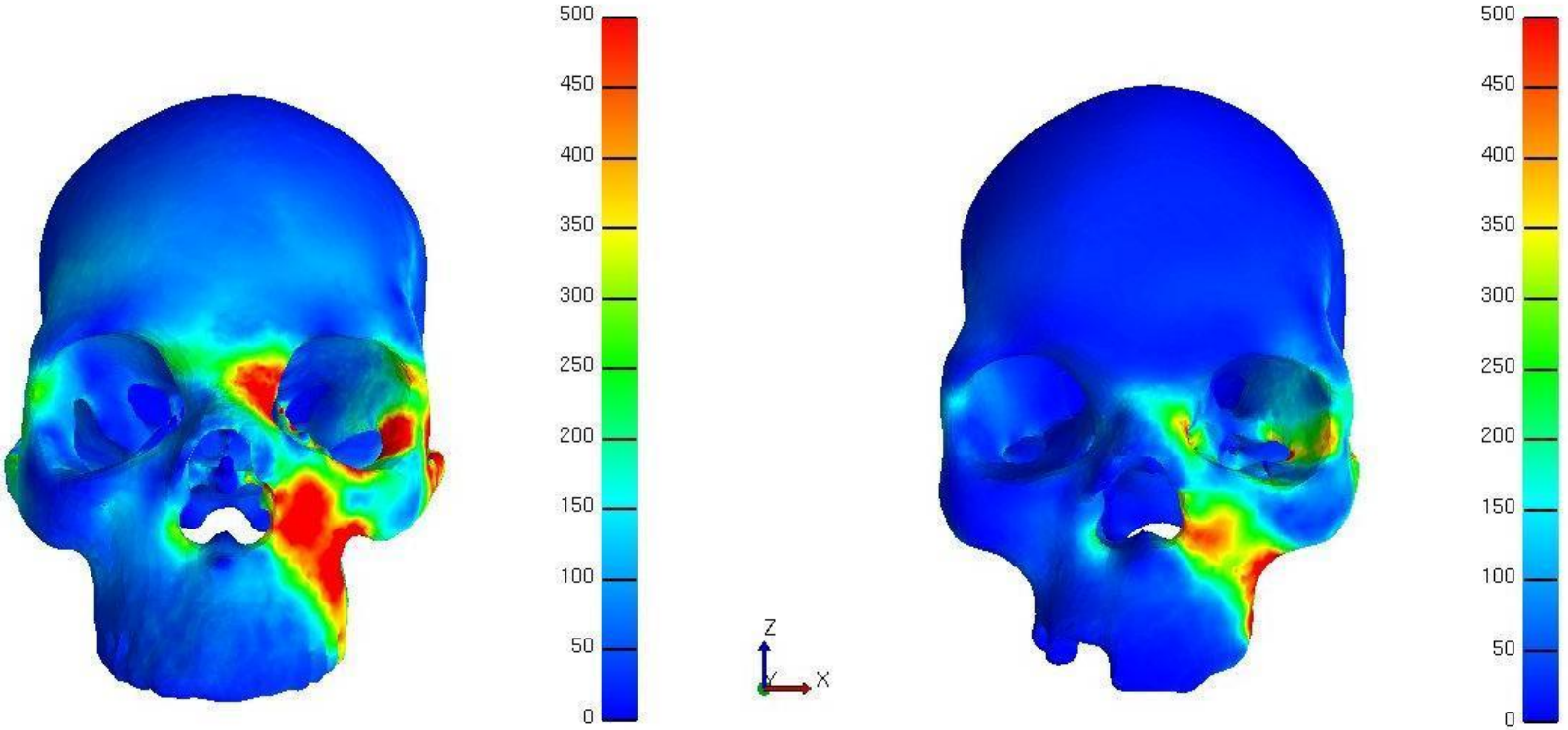

Figure 54. Von Mises stress distribution for a molar bite comparing prognathic (left) and orthognathic (right) facial form: full analysis, lateral view. The scale for the Von Mises results is in N/cm^2. Red indicates areas of high stress (a combination of tension, compression and shear) and blue indicates areas of low stress.

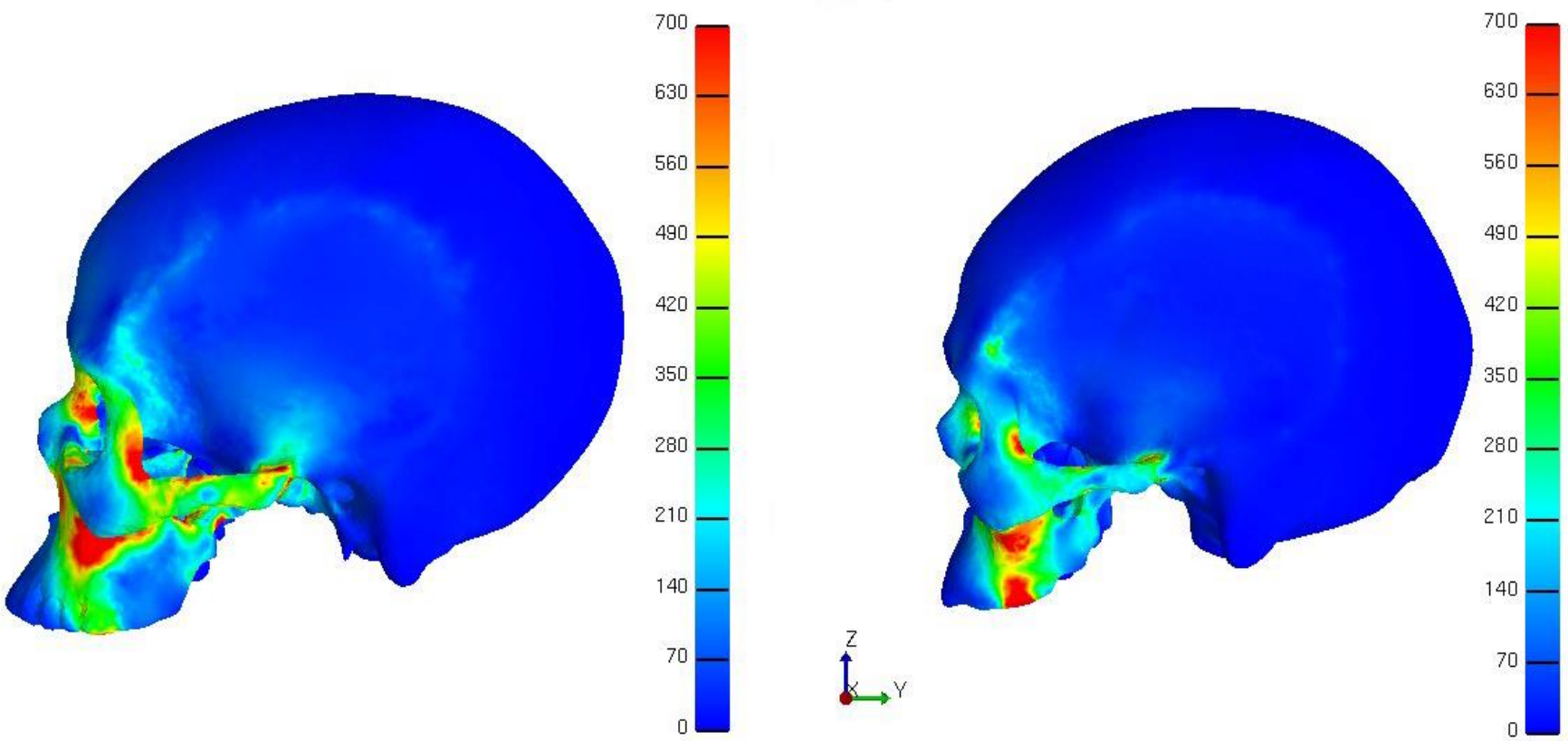

Figure 55. Von Mises stress distribution for a molar bite comparing prognathic (left) and orthognathic (right) facial form: full analysis, lateral view balancing side. The scale for the Von Mises results is in N/cm^2. Red indicates areas of high stress (a combination of tension, compression and shear) and blue indicates areas of low stress.

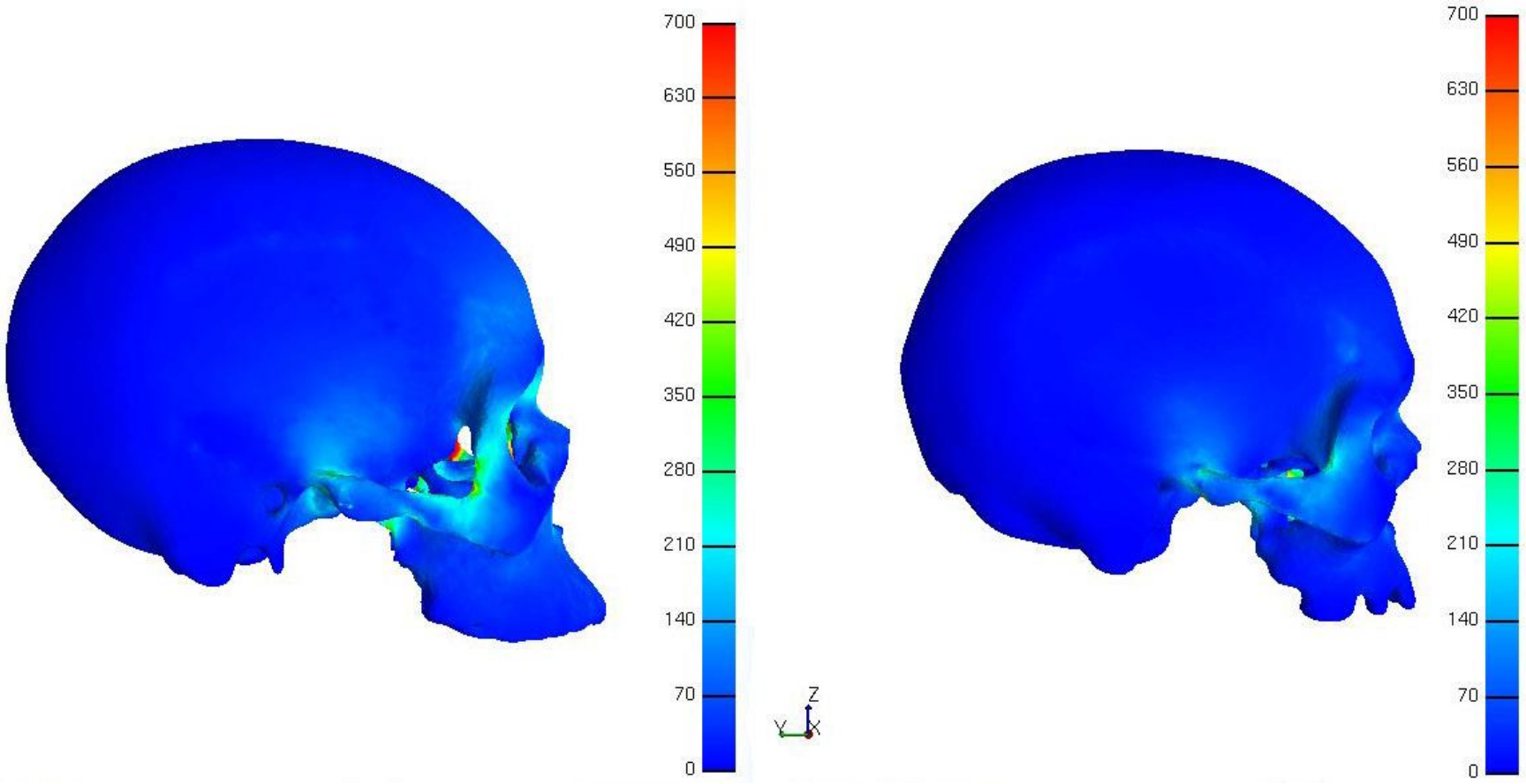

Figure 56. Von Mises stress distribution for a molar bite comparing prognathic (left) and orthognathic (right) facial form: full analysis, inferior view. The scale for the Von Mises results is in N/cm^2. Red indicates areas of high stress (a combination of tension, compression and shear) and blue indicates areas of low stress.

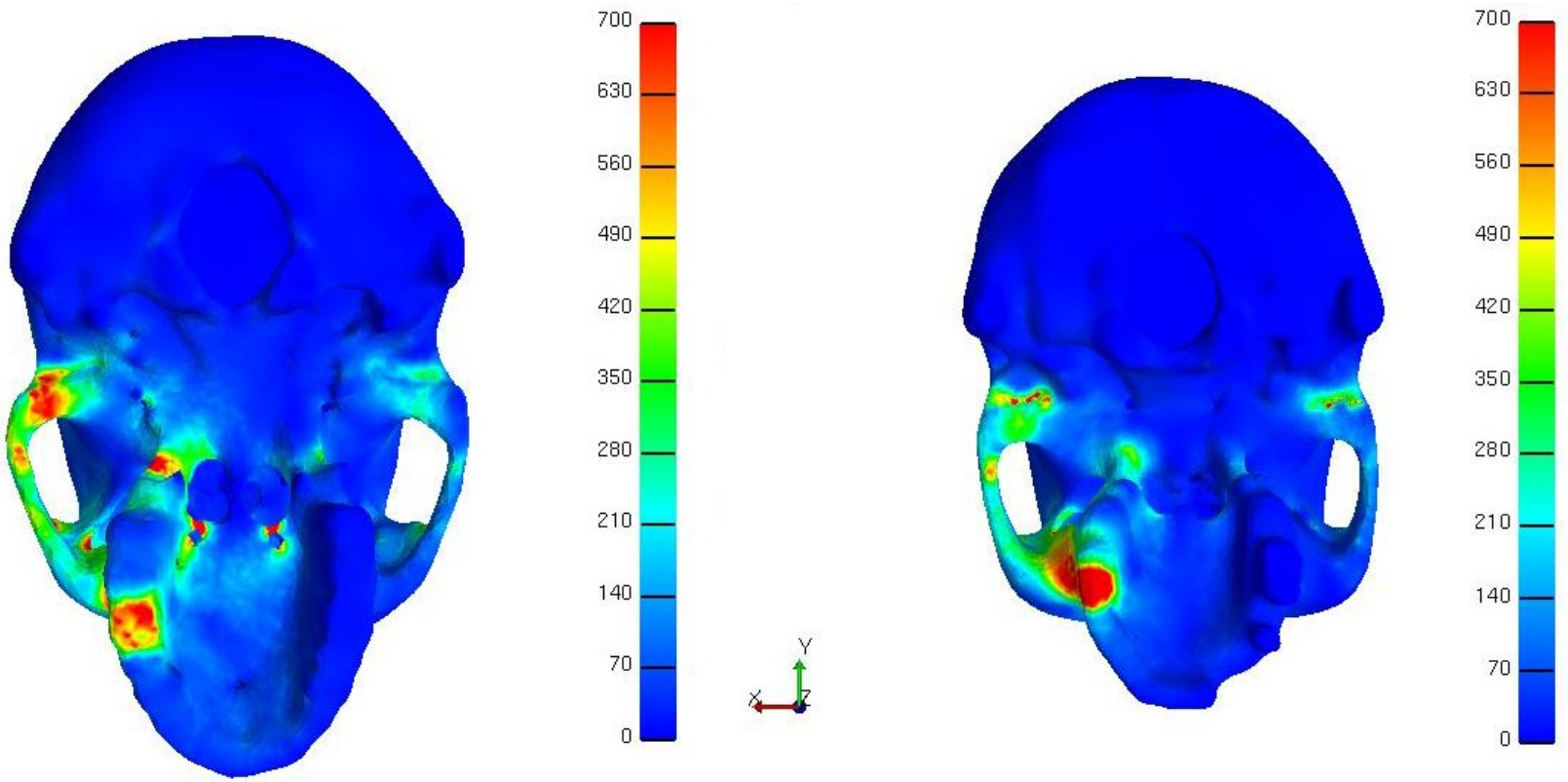

Figure 57. Von Mises stress distribution for an incisor bite comparing prognathic (left) and orthognathic (right) facial form: full analysis, anterior view. The scale for the Von Mises results is in N/cm^2. Red indicates areas of high stress (a combination of tension, compression and shear) and blue indicates areas of low stress.

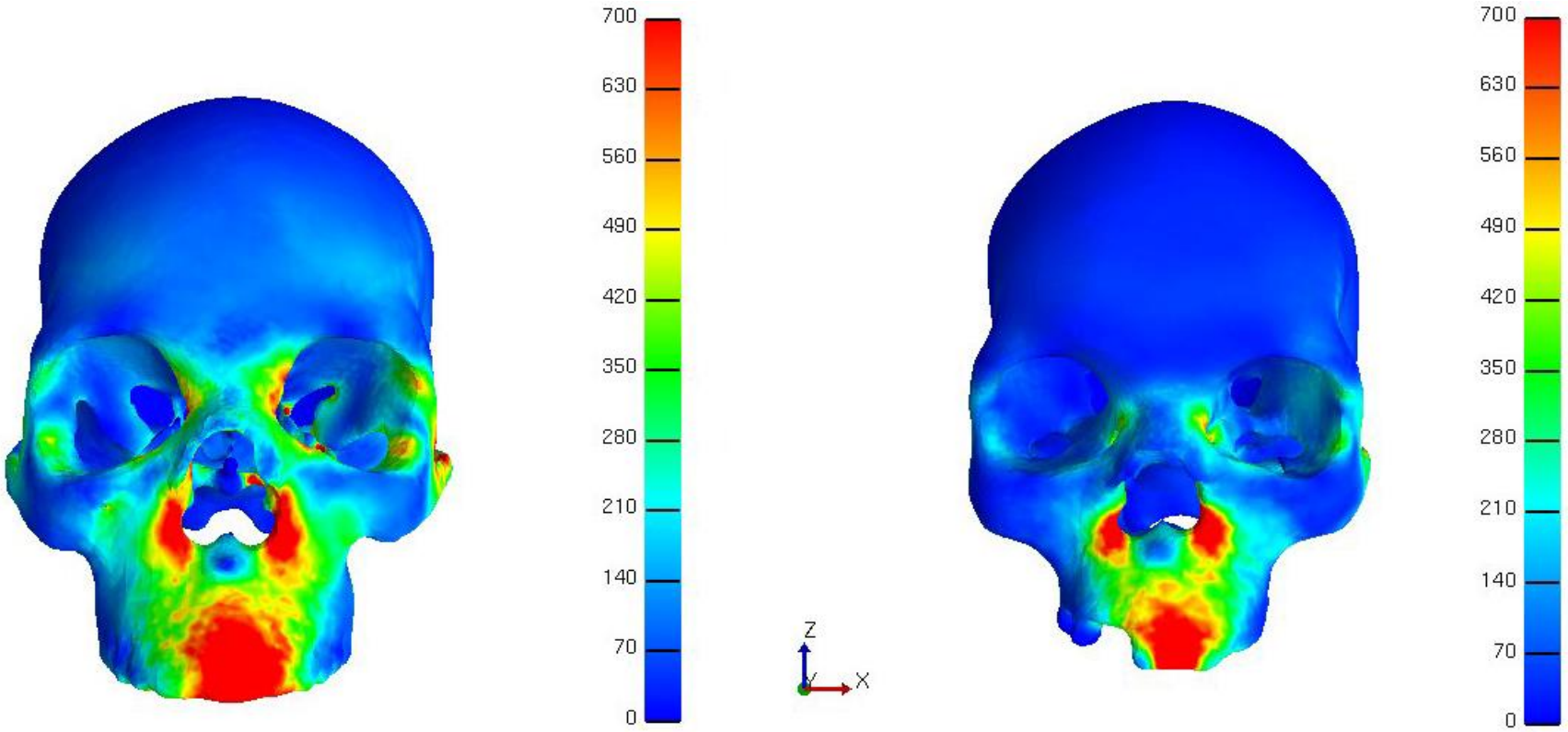

Figure 58. Von Mises stress distribution for an incisor bite comparing prognathic (left) and orthognathic (right) facial form: full analysis, lateral view. The scale for the Von Mises results is in N/cm^2. Red indicates areas of high stress (a combination of tension, compression and shear) and blue indicates areas of low stress.

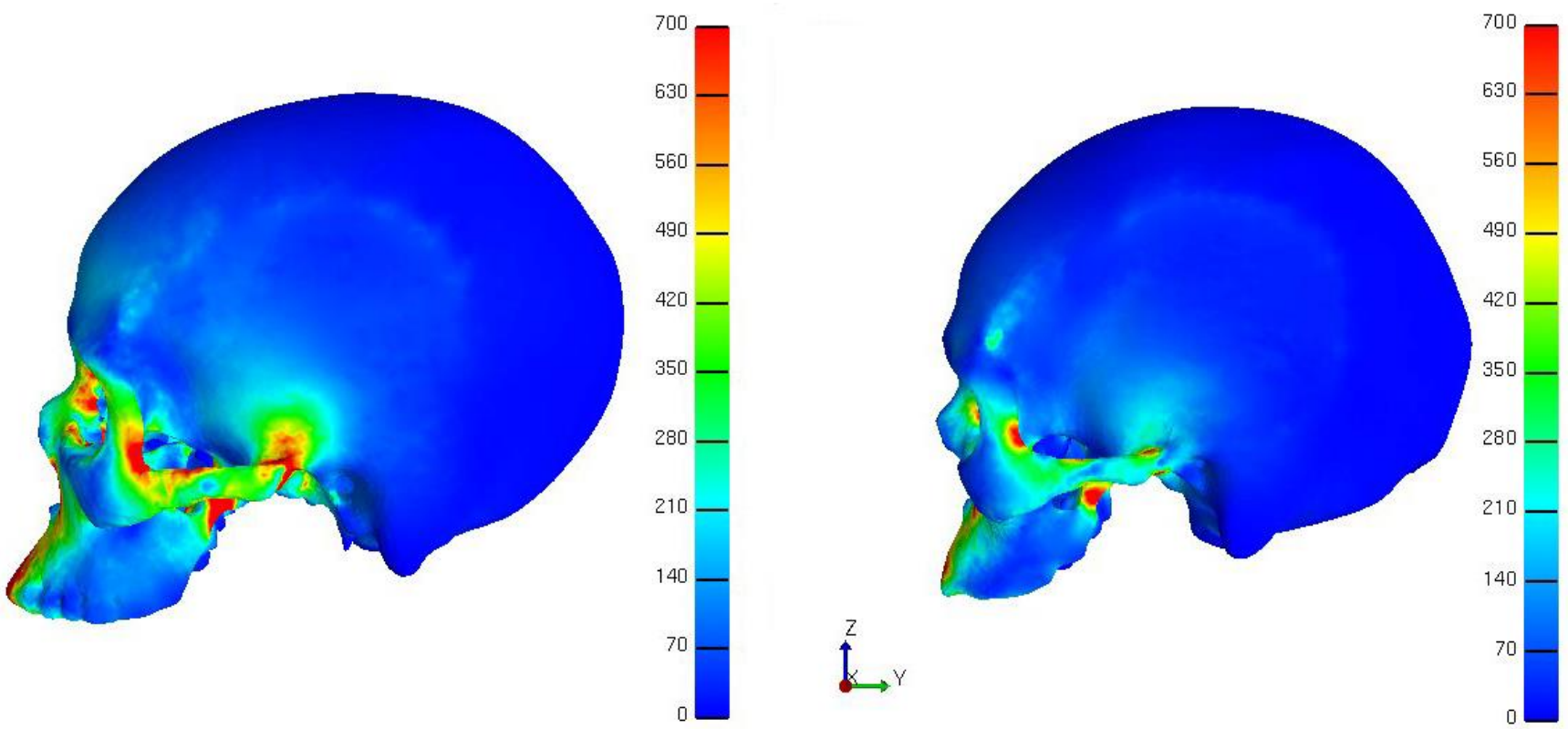

Figure 59. Von Mises stress distribution for an incisor bite comparing prognathic (left) and orthognathic (right) facial form: full analysis, lateral view balancing side. The scale for the Von Mises results is in N/cm^2. Red indicates areas of high stress (a combination of tension, compression and shear) and blue indicates areas of low stress.

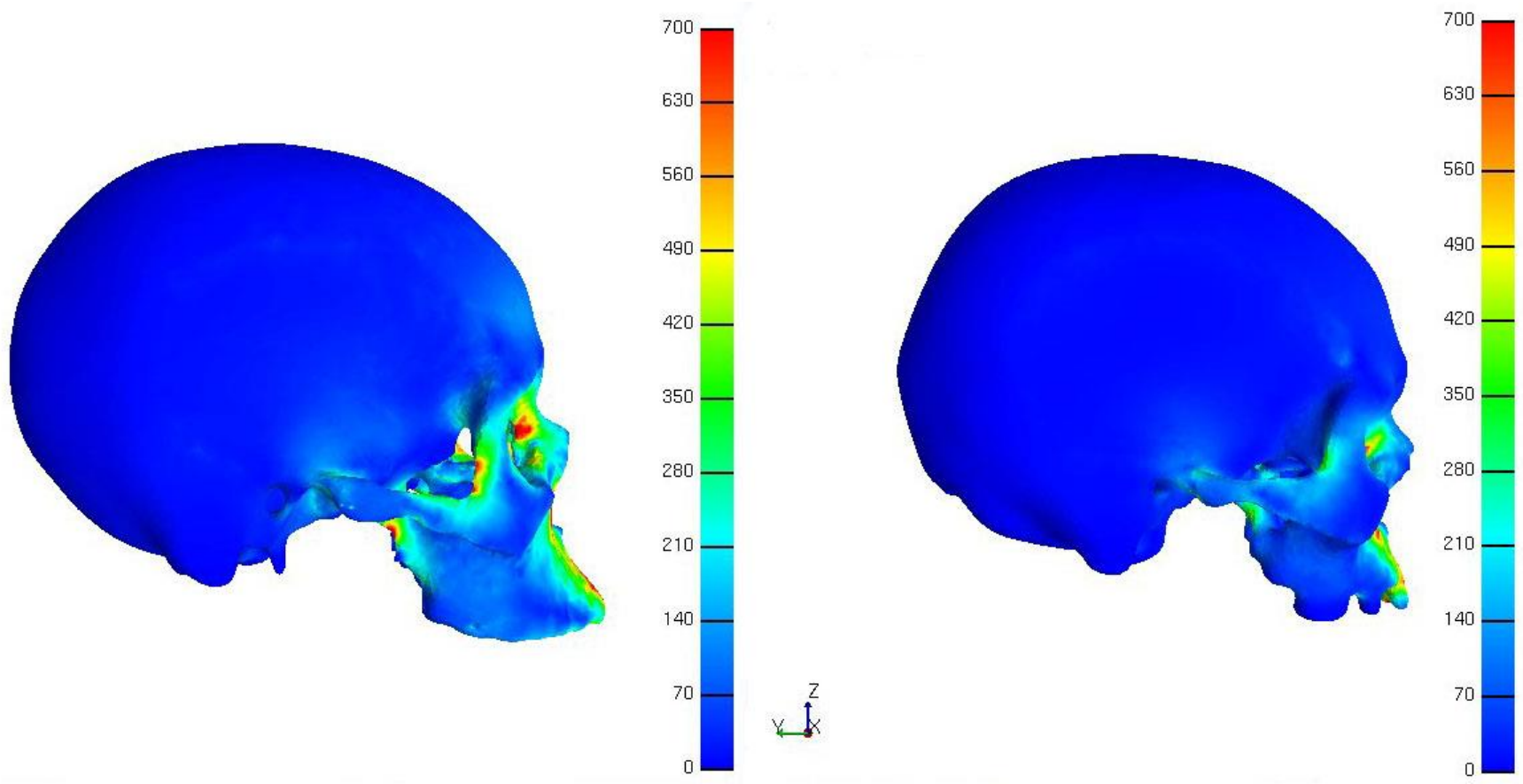

Figure 60. Von Mises stress distribution for an incisor bite comparing prognathic (left) and orthognathic (right) facial form: full analysis, inferior view. The scale for the Von Mises results is in N/cm^2. Red indicates areas of high stress (a combination of tension, compression and shear) and blue indicates areas of low stress.

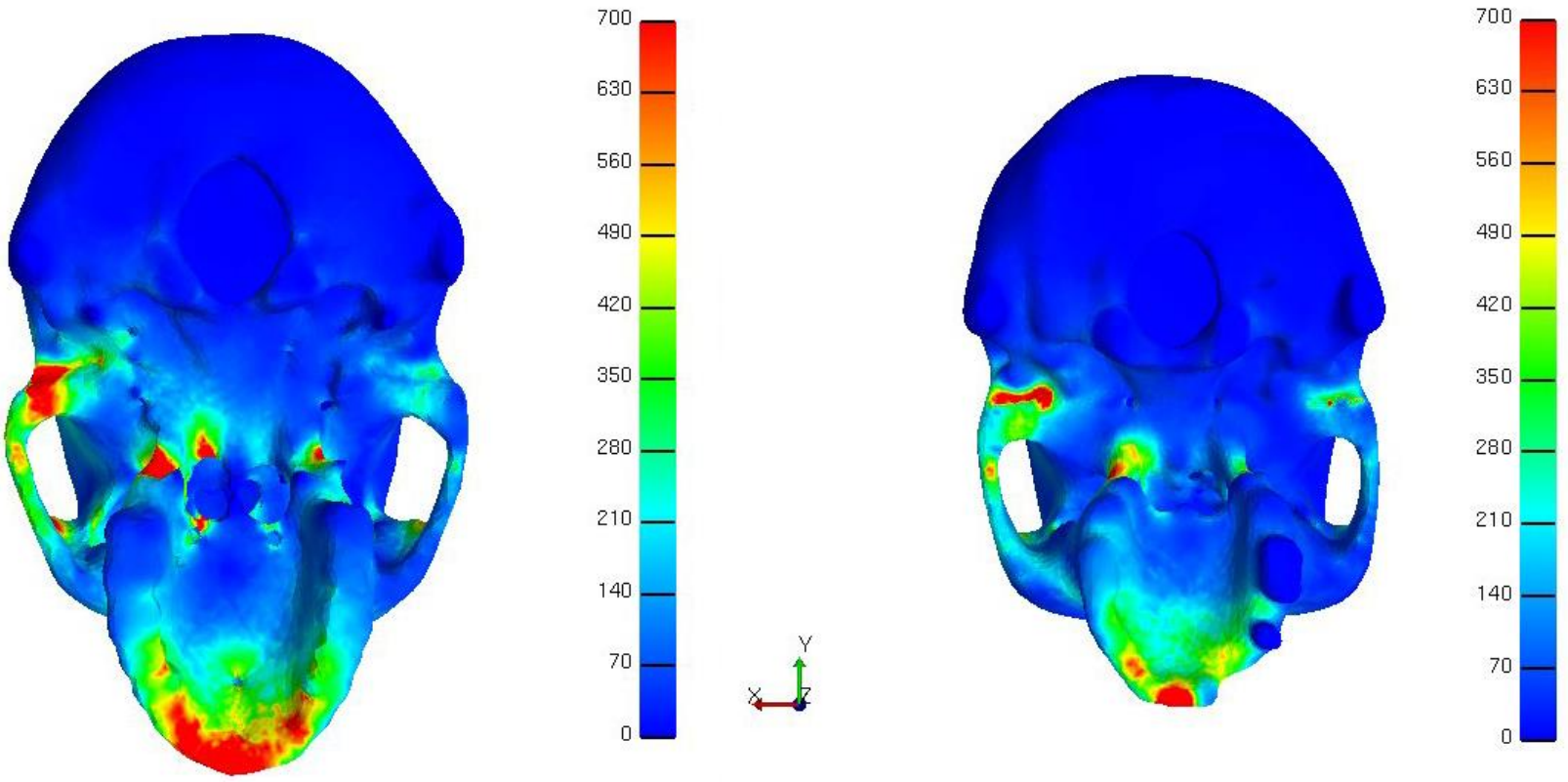

Figure 61. Von Mises stress distribution comparing molar (left) vs. incisor (right) bite in the prognathic facial form, frontal view. The scale for the Von Mises results is in N/cm^2. Red indicates areas of high stress (a combination of tension, compression and shear) and blue indicates areas of low stress.

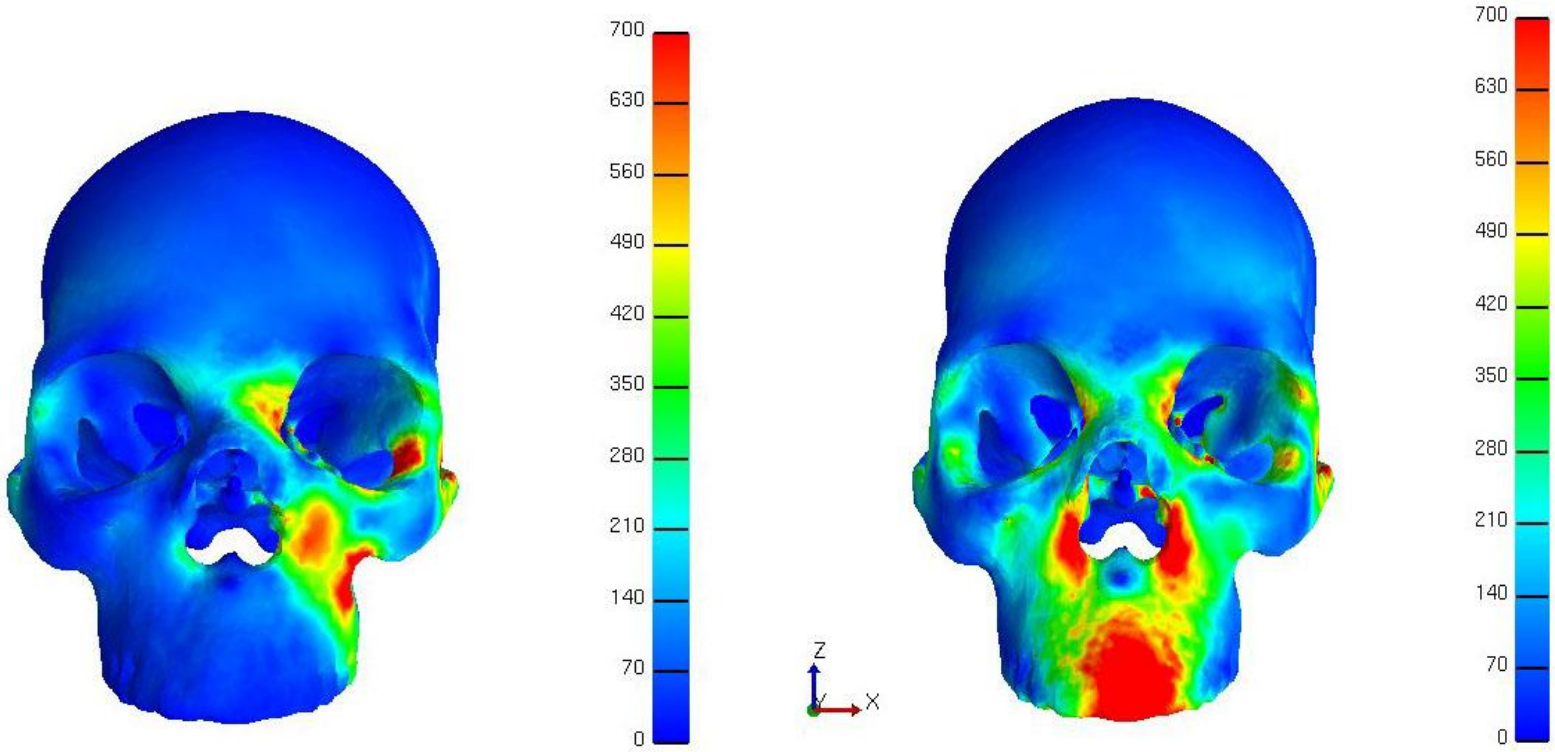

Figure 62. Von Mises stress distribution comparing molar (left) vs. incisor (right) bite in the prognathic facial form, lateral view. The scale for the Von Mises results is in N/cm^2. Red indicates areas of high stress (a combination of tension, compression and shear) and blue indicates areas of low stress.

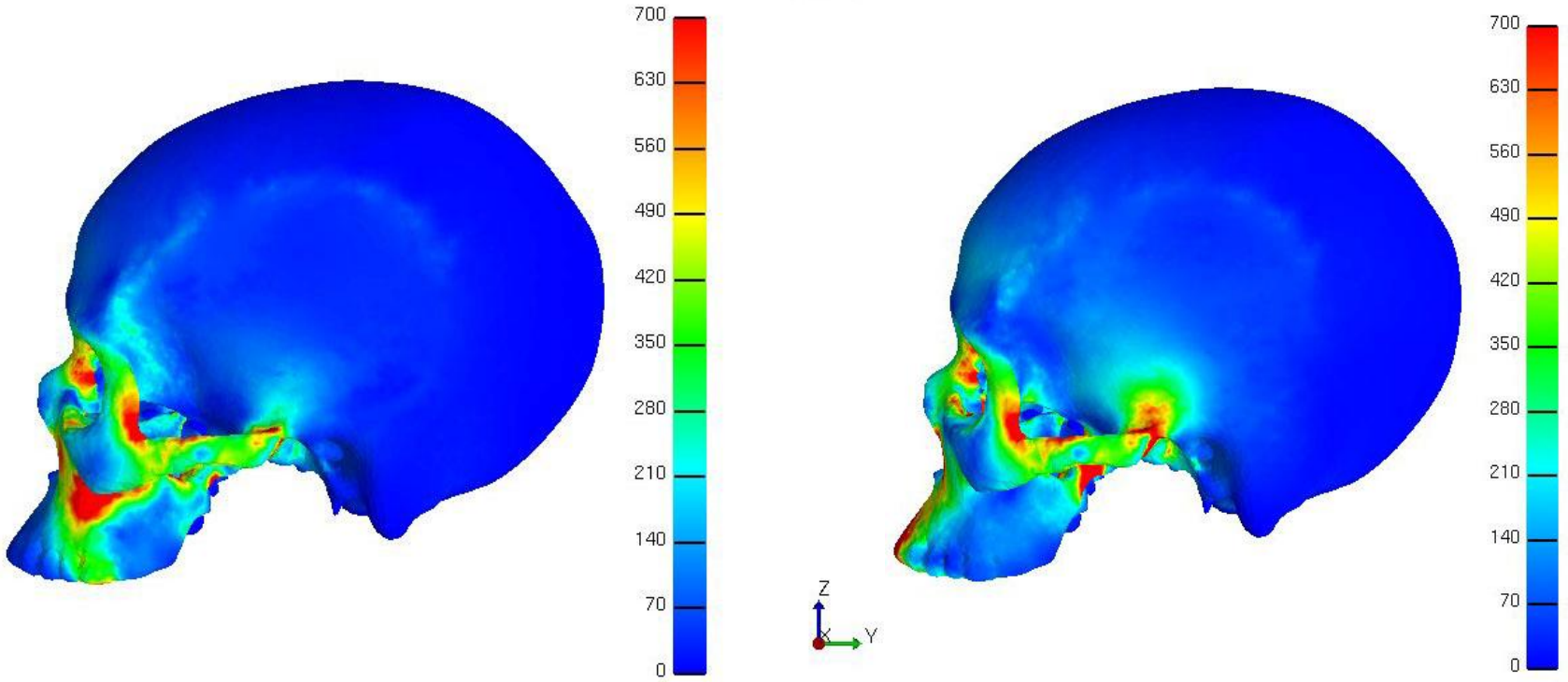

Figure 63. Von Mises stress distribution comparing molar (left) vs. incisor (right) bite in the prognathic facial form, inferior view. The scale for the Von Mises results is in N/cm^2. Red indicates areas of high stress (a combination of tension, compression and shear) and blue indicates areas of low stress.

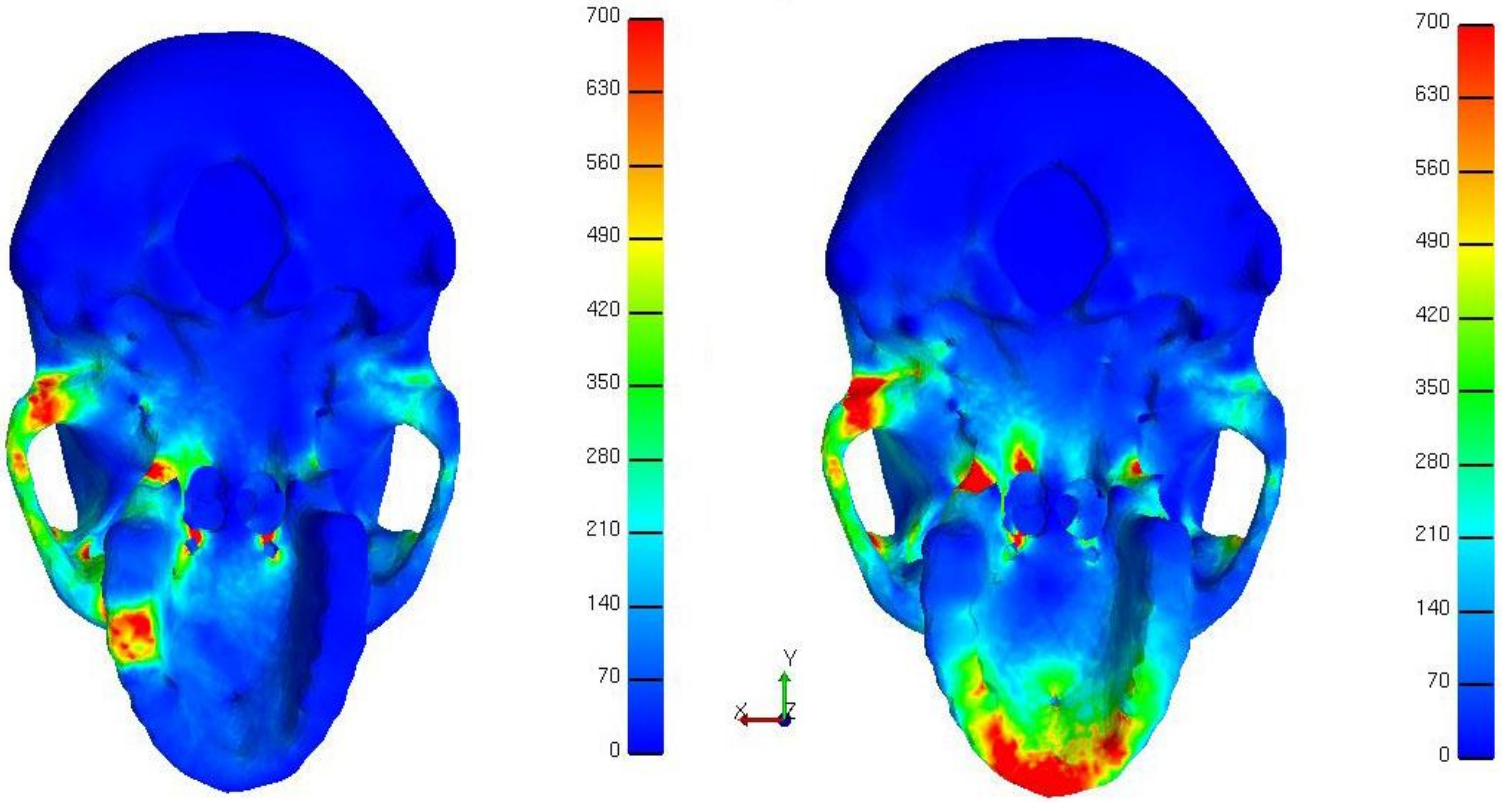

Figure 64. Von Mises stress distribution molar (left) vs. incisor (right) bite in orthognathic facial form, frontal view. The scale for the Von Mises results is in N/cm^2. Red indicates areas of high stress (a combination of tension, compression and shear) and blue indicates areas of low stress.

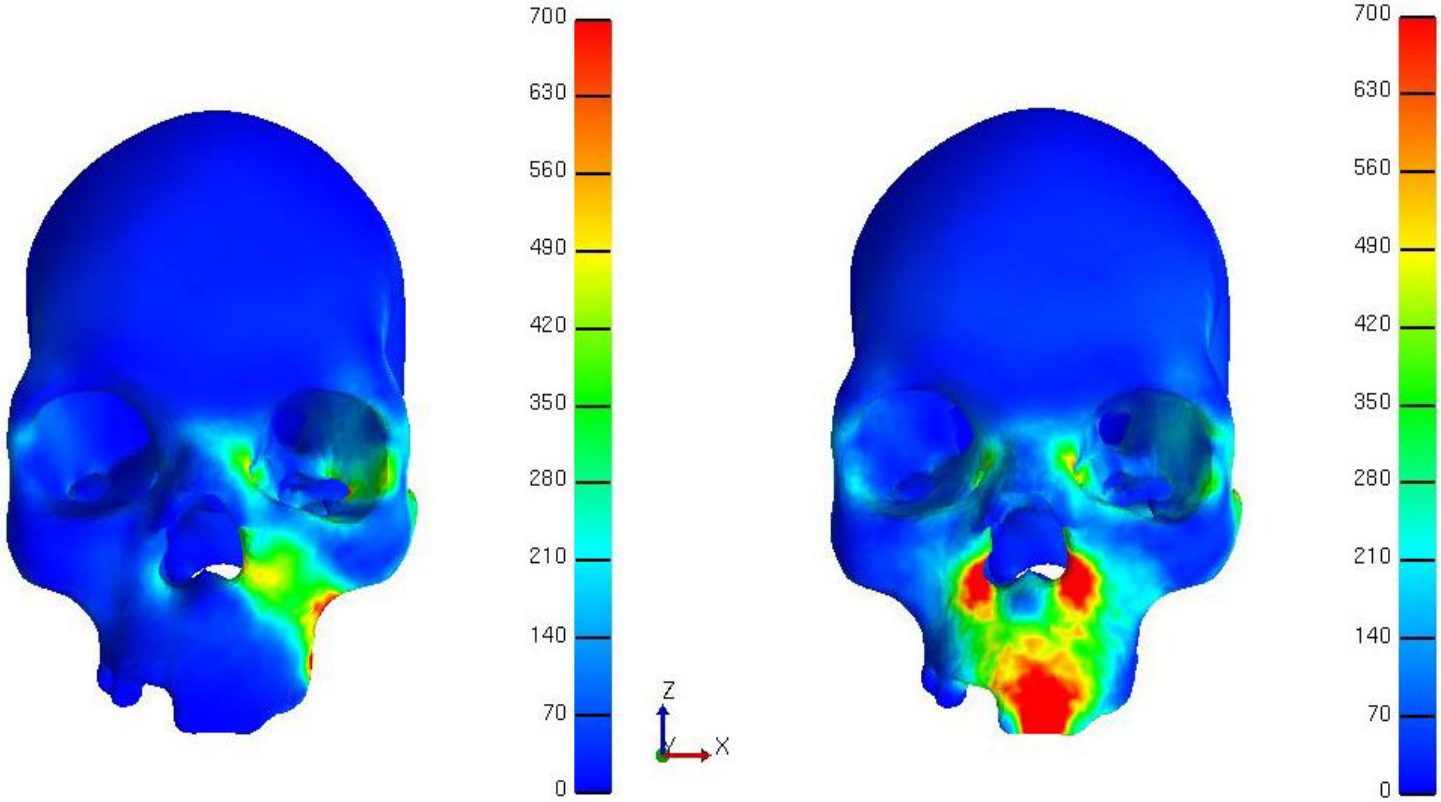

Figure 65. Von Mises stress distribution molar (left) vs. incisor (right) bite in orthognathic facial form, lateral view. The scale for the Von Mises results is in N/cm^2. Red indicates areas of high stress (a combination of tension, compression and shear) and blue indicates areas of low stress.

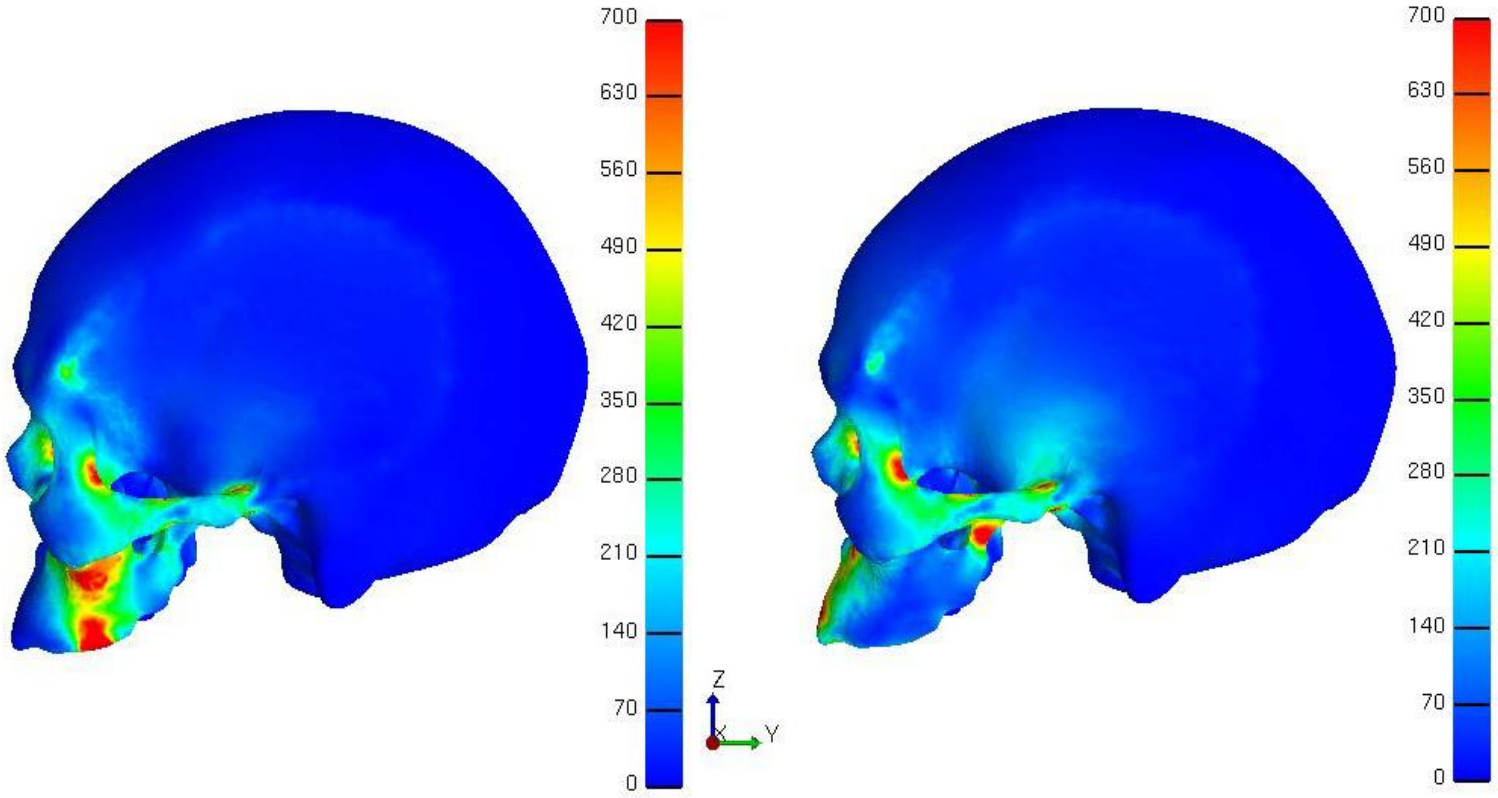

Figure 66. Von Mises stress distribution molar (left) vs. incisor (right) bite in orthognathic facial form, inferior view. The scale for the Von Mises results is in N/cm^2. Red indicates areas of high stress (a combination of tension, compression and shear) and blue indicates areas of low stress.

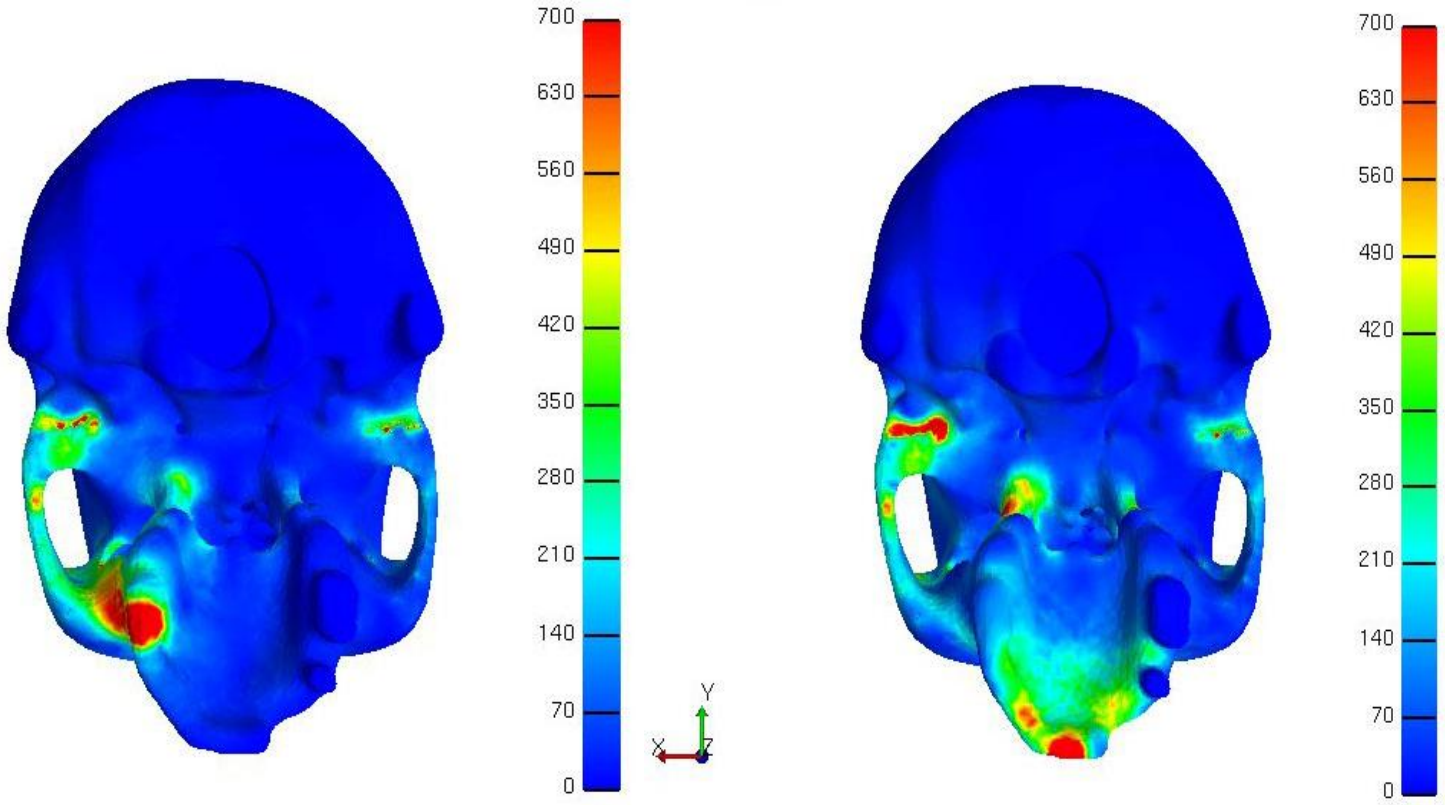

Figure 67. Von Mises stress distribution for a molar bite comparing prognathic (left) and orthognathic (right) facial form and the contribution of stress from the deep head of masseter muscle, anterior view. The scale for the Von Mises results is in N/cm^2. Red indicates areas of high stress (a combination of tension, compression and shear) and blue indicates areas of low stress.

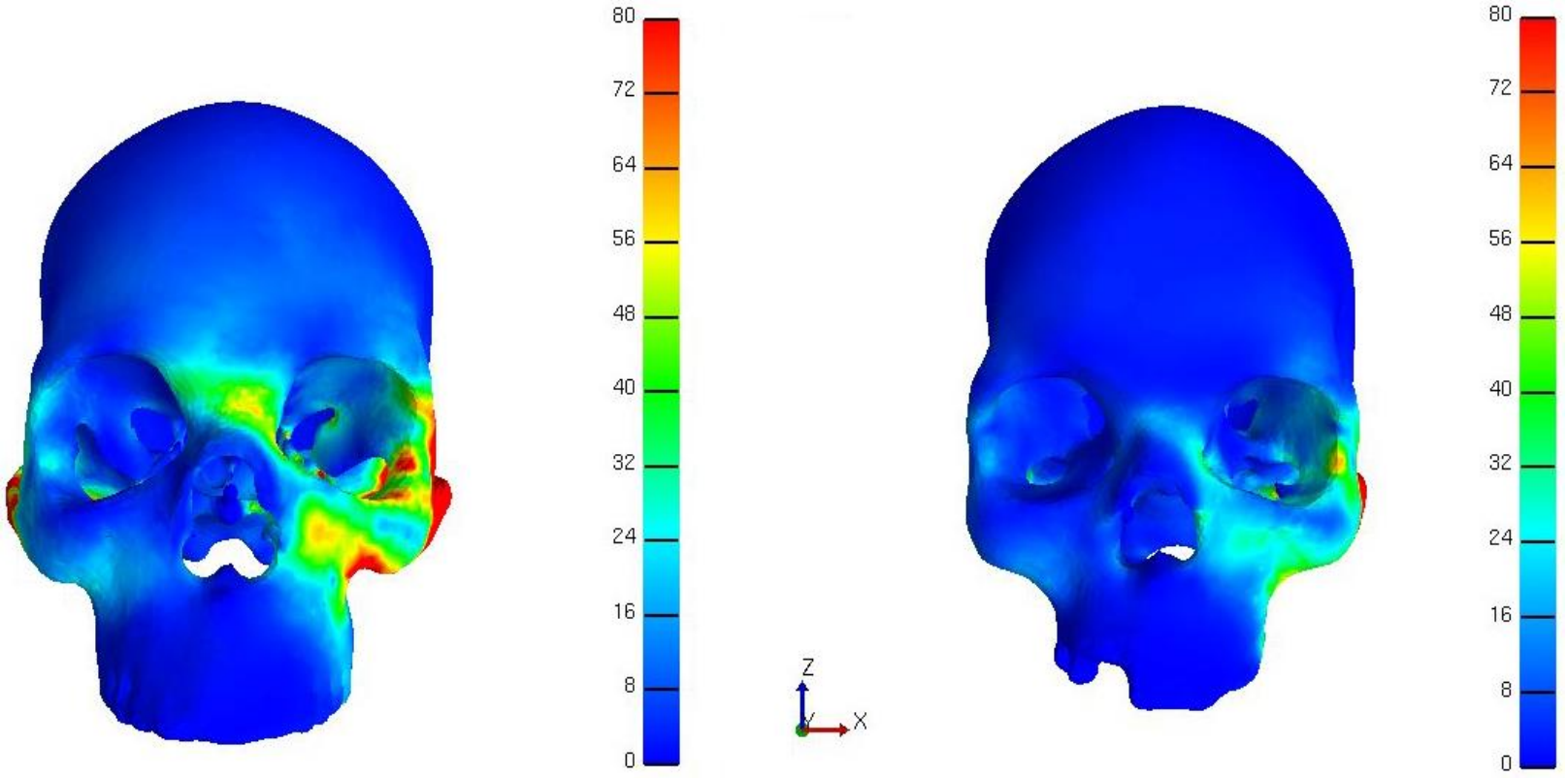

Figure 68. Von Mises stress distribution for a molar bite comparing prognathic (left) and orthognathic (right) facial form and the contribution of stress from the deep head of masseter muscle, lateral view. The scale for the Von Mises results is in N/cm^2. Red indicates areas of high stress (a combination of tension, compression and shear) and blue indicates areas of low stress.

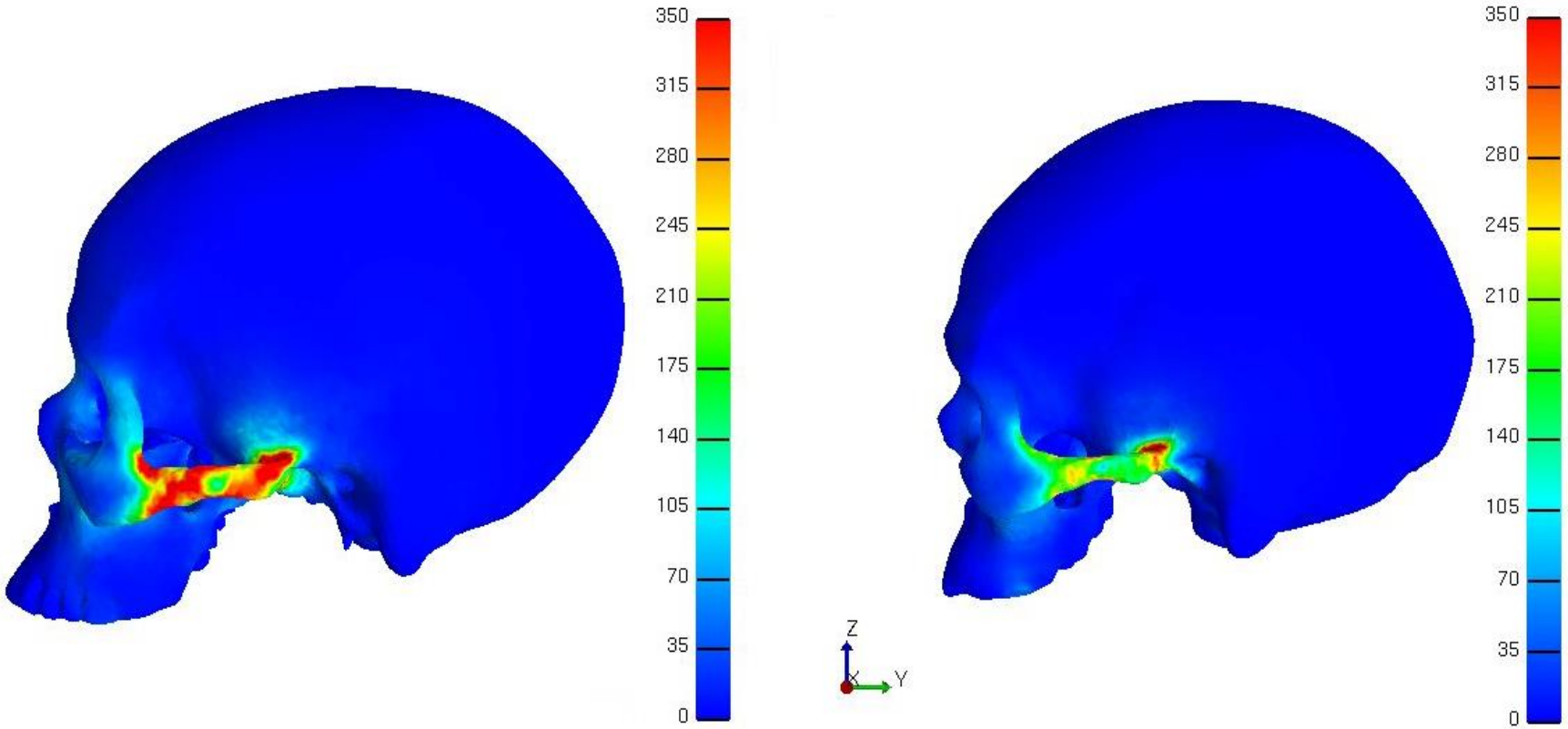

Figure 69. Von Mises stress distribution for a molar bite comparing prognathic (left) and orthognathic (right) facial form and the contribution of stress from the deep head of masseter muscle, inferior view. The scale for the Von Mises results is in N/cm^2. Red indicates areas of high stress (a combination of tension, compression and shear) and blue indicates areas of low stress.

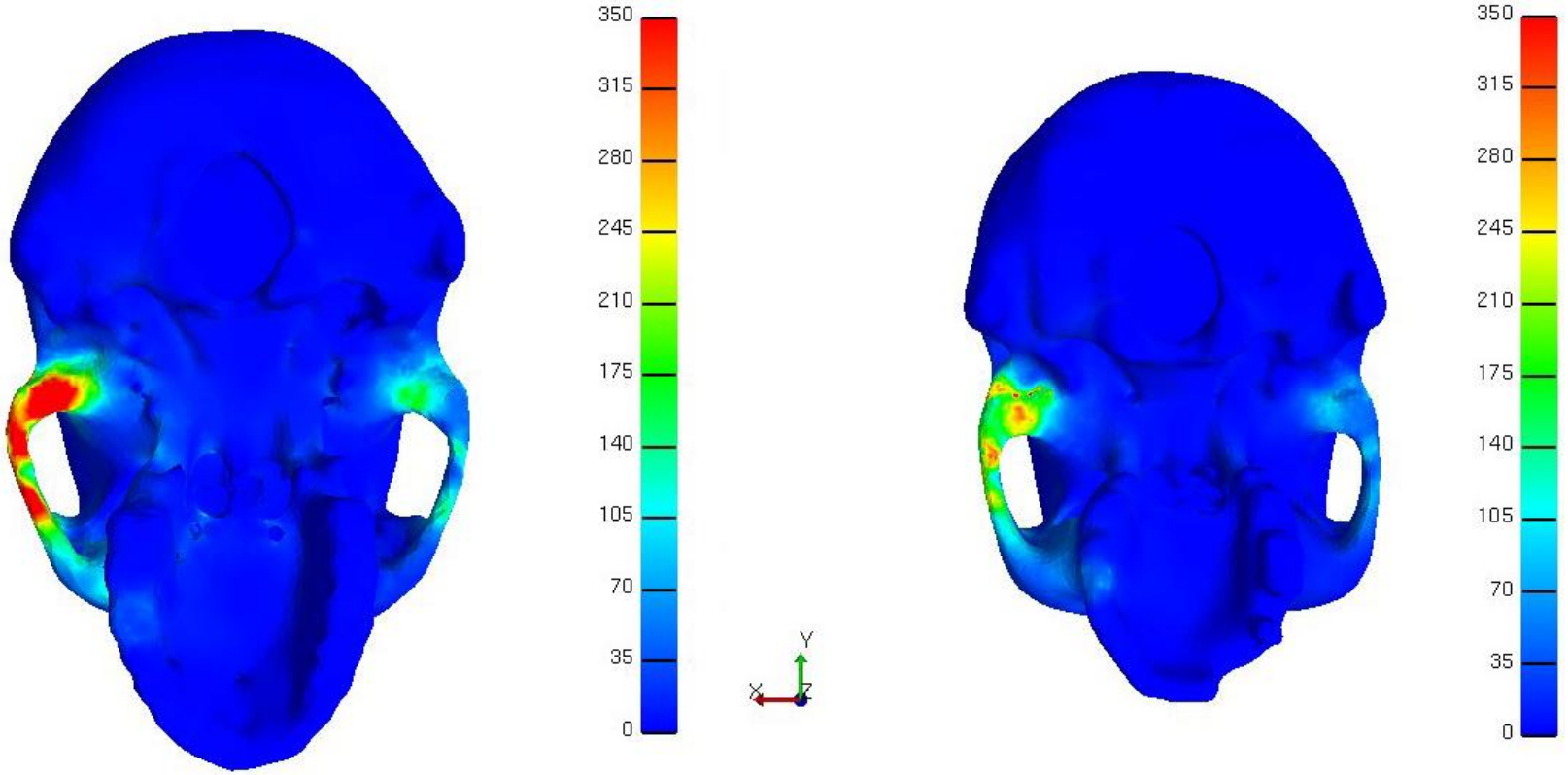

Figure 70. Von Mises stress distribution for a molar bite comparing prognathic (left) and orthognathic (right) facial form and the contribution of stress from the superficial head of masseter muscle, anterior view. The scale for the Von Mises results is in N/cm^2. Red indicates areas of high stress (a combination of tension, compression and shear) and blue indicates areas of low stress.

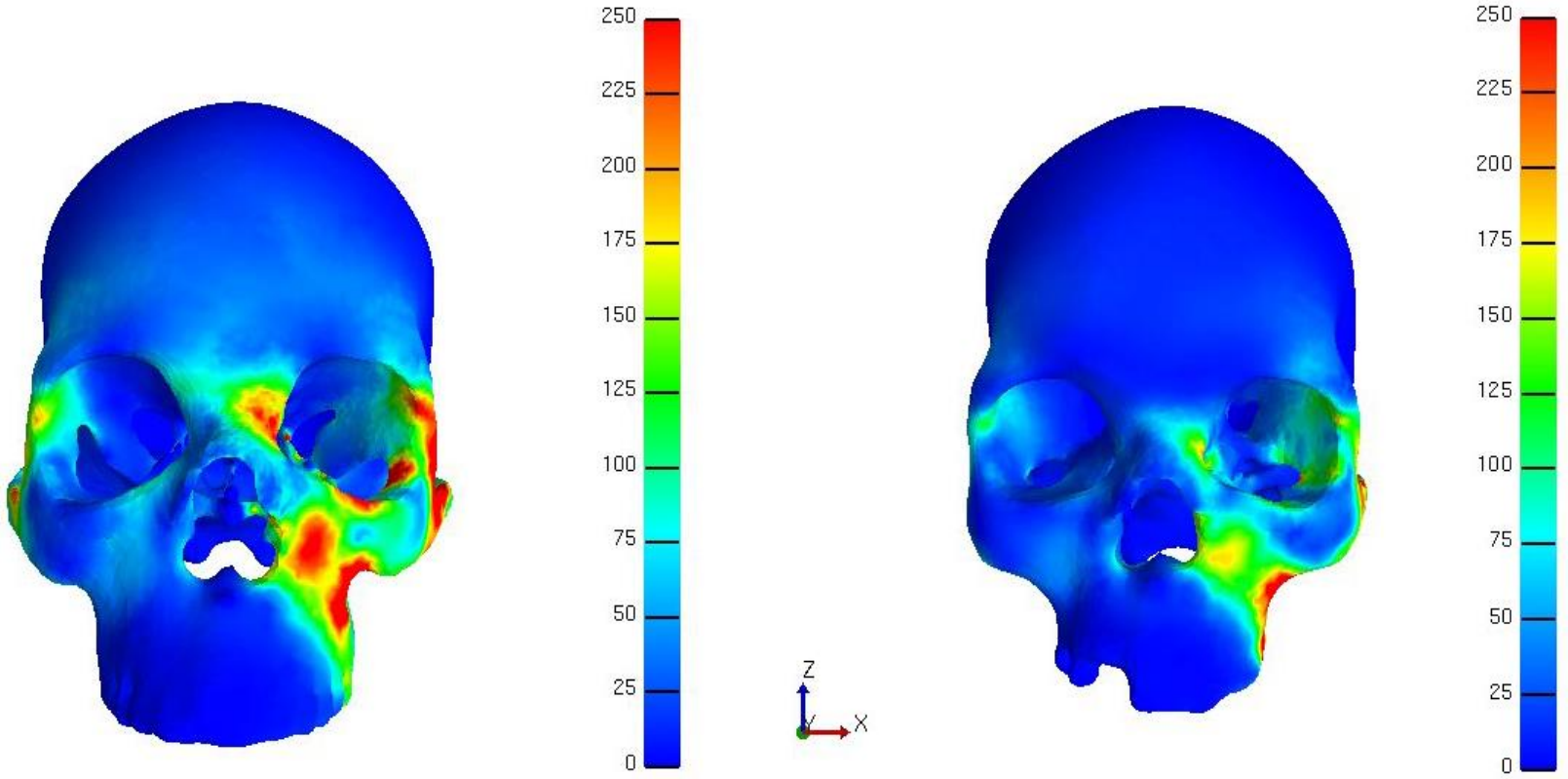

Figure 71. Von Mises stress distribution for a molar bite comparing prognathic (left) and orthognathic (right) facial form and the contribution of stress from the superficial head of masseter muscle, lateral view. The scale for the Von Mises results is in N/cm^2. Red indicates areas of high stress (a combination of tension, compression and shear) and blue indicates areas of low stress.

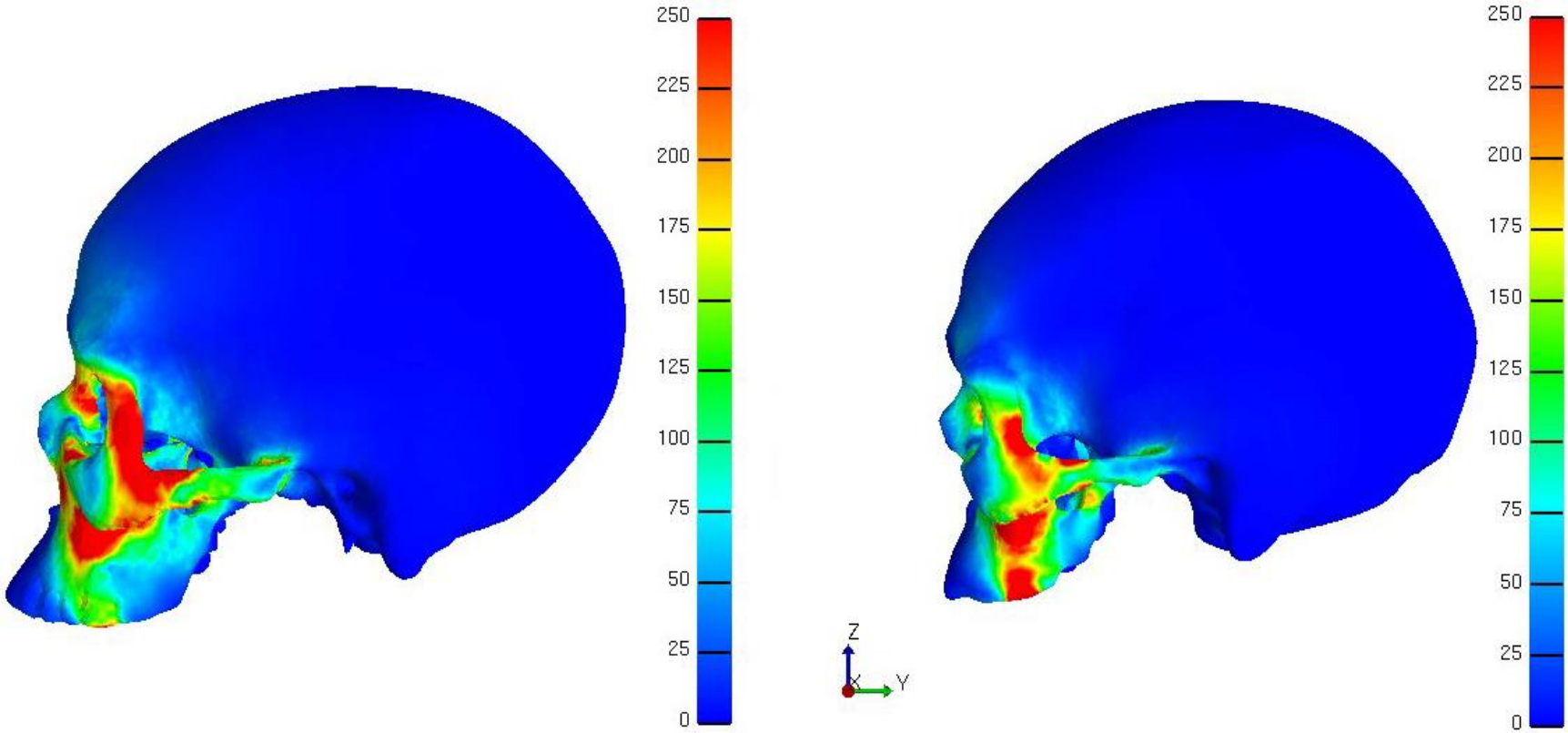

Figure 72. Von Mises stress distribution for a molar bite comparing prognathic (left) and orthognathic (right) facial form and the contribution of stress from the superficial head of masseter muscle, inferior view. The scale for the Von Mises results is in N/cm^2. Red indicates areas of high stress (a combination of tension, compression and shear) and blue indicates areas of low stress.

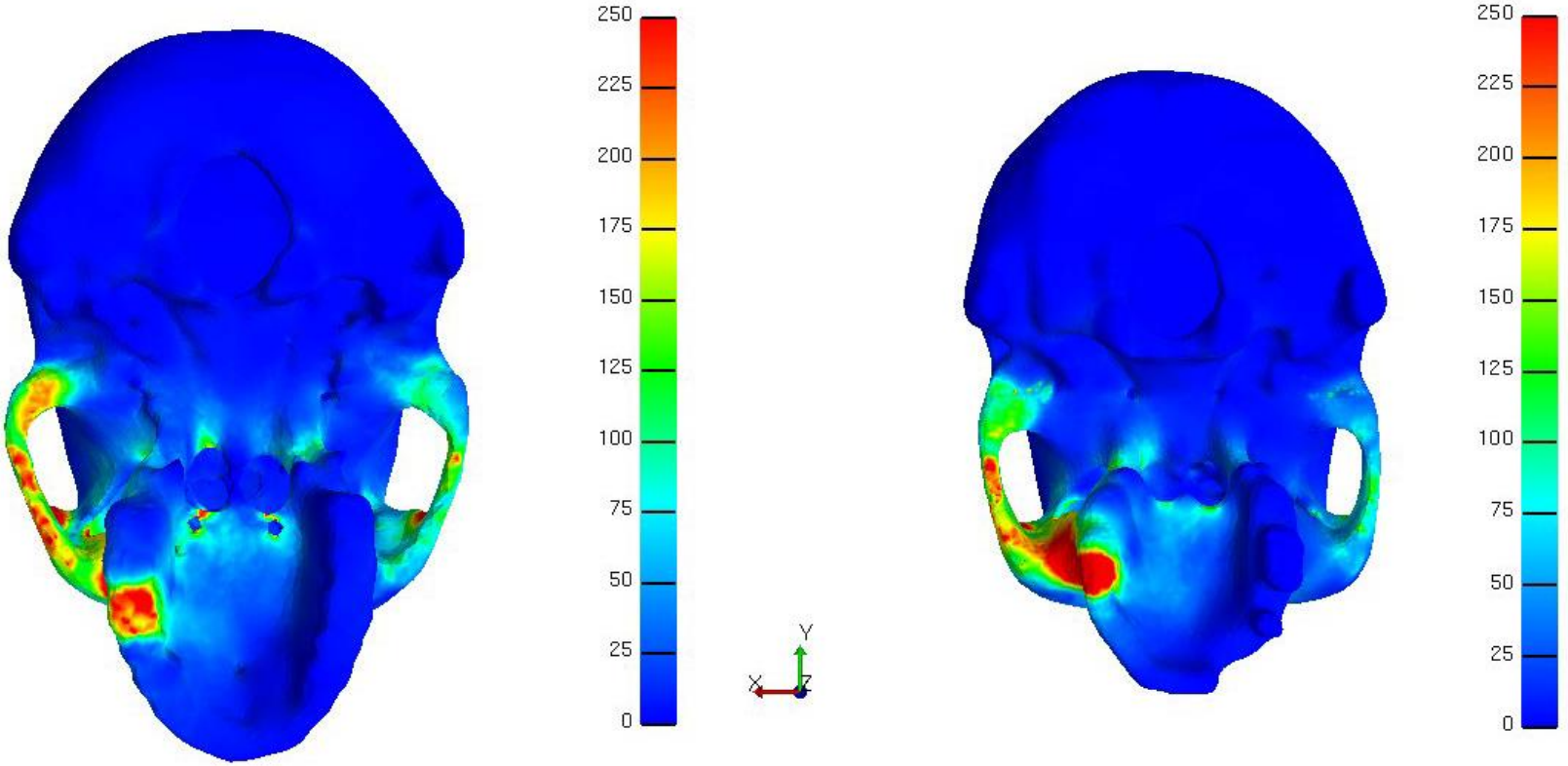

Figure 73. Von Mises stress distribution for a molar bite comparing prognathic (left) and orthognathic (right) facial form and the contribution of stress from the temporalis muscle, anterior view. The scale for the Von Mises results is in N/cm^2. Red indicates areas of high stress (a combination of tension, compression and shear) and blue indicates areas of low stress.

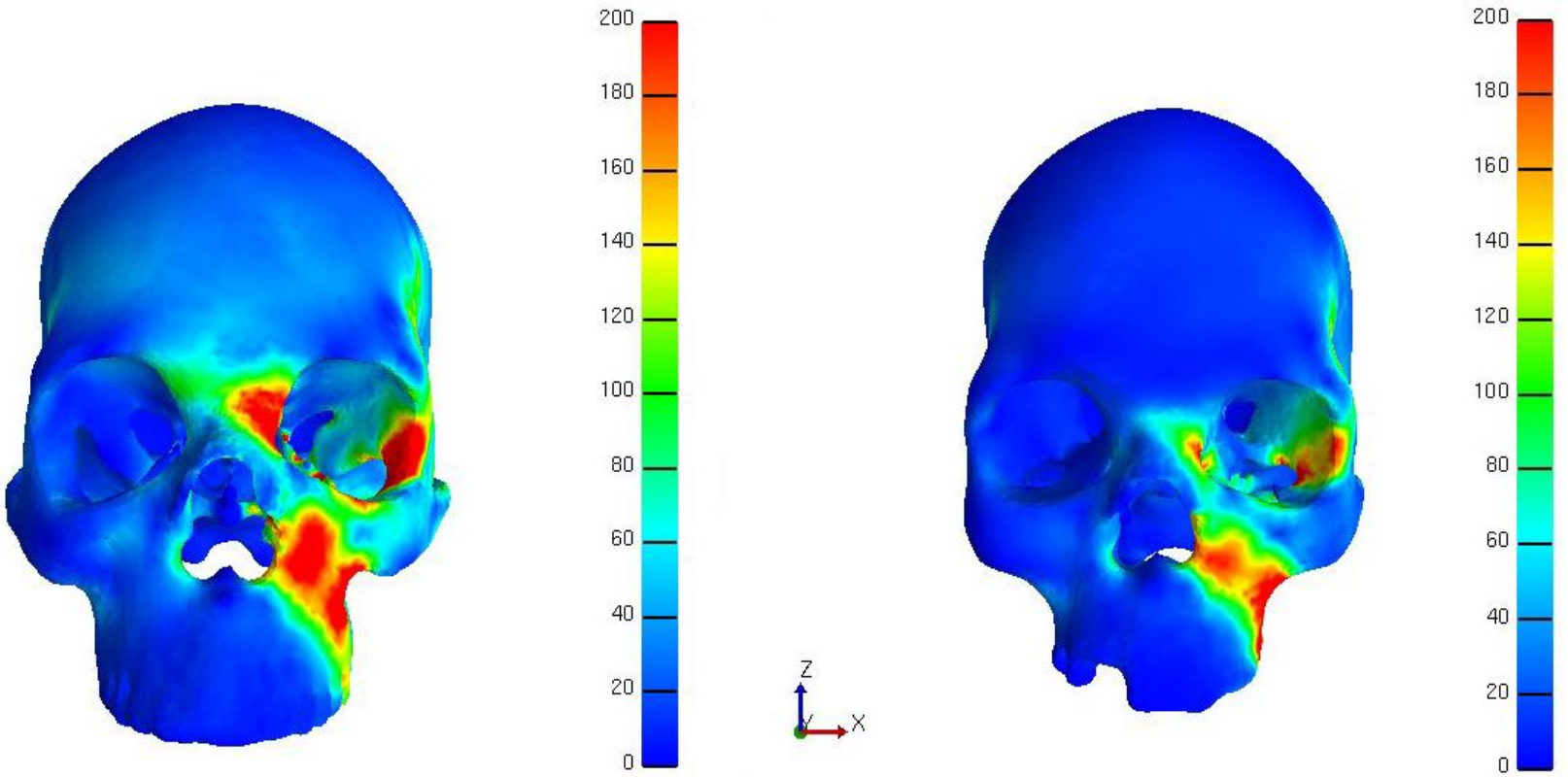

Figure 74. Von Mises stress distribution for a molar bite comparing prognathic (left) and orthognathic (right) facial form and the contribution of stress from the temporalis muscle, lateral view. The scale for the Von Mises results is in N/cm^2. Red indicates areas of high stress (a combination of tension, compression and shear) and blue indicates areas of low stress.

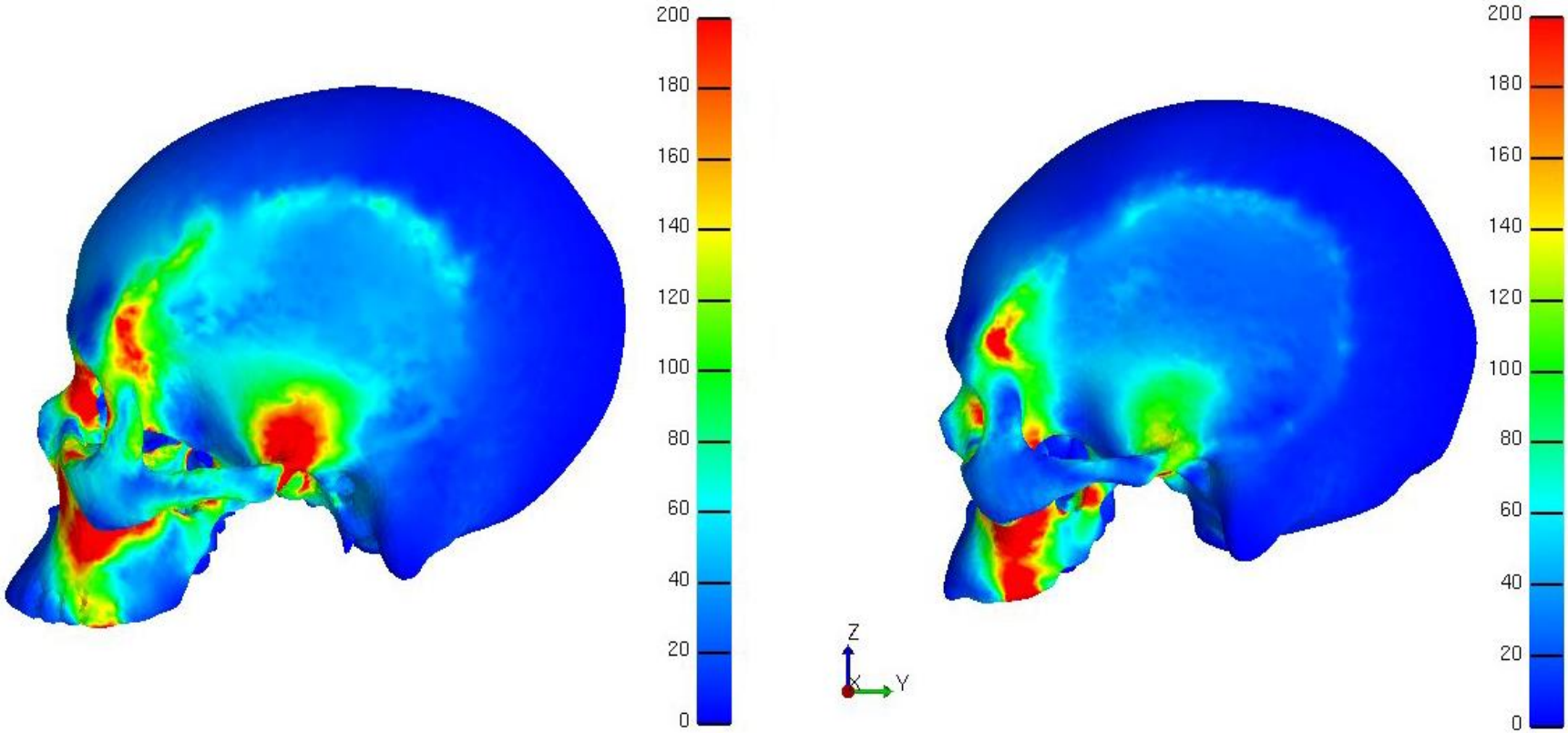

Figure 75. Von Mises stress distribution for a molar bite comparing prognathic (left) and orthognathic (right) facial form and the contribution of stress from the temporalis muscle, inferior view. The scale for the Von Mises results is in N/cm^2. Red indicates areas of high stress (a combination of tension, compression and shear) and blue indicates areas of low stress.

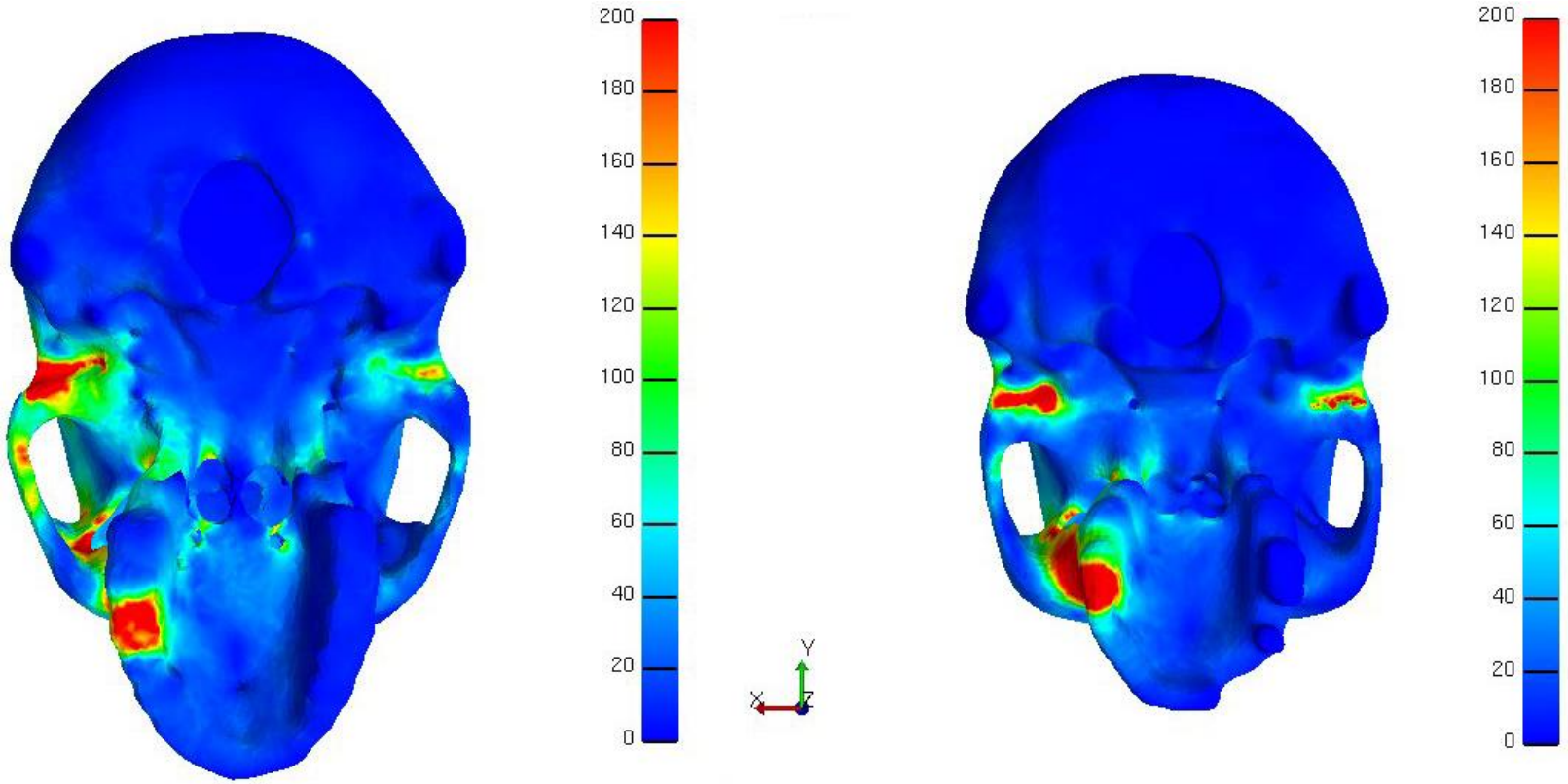

Figure 76. Von Mises stress distribution for a molar bite comparing prognathic (left) and orthognathic (right) facial form and the contribution of stress from the medial pterygoid muscle, anterior view. The scale for the Von Mises results is in N/cm^2. Red indicates areas of high stress (a combination of tension, compression and shear) and blue indicates areas of low stress.

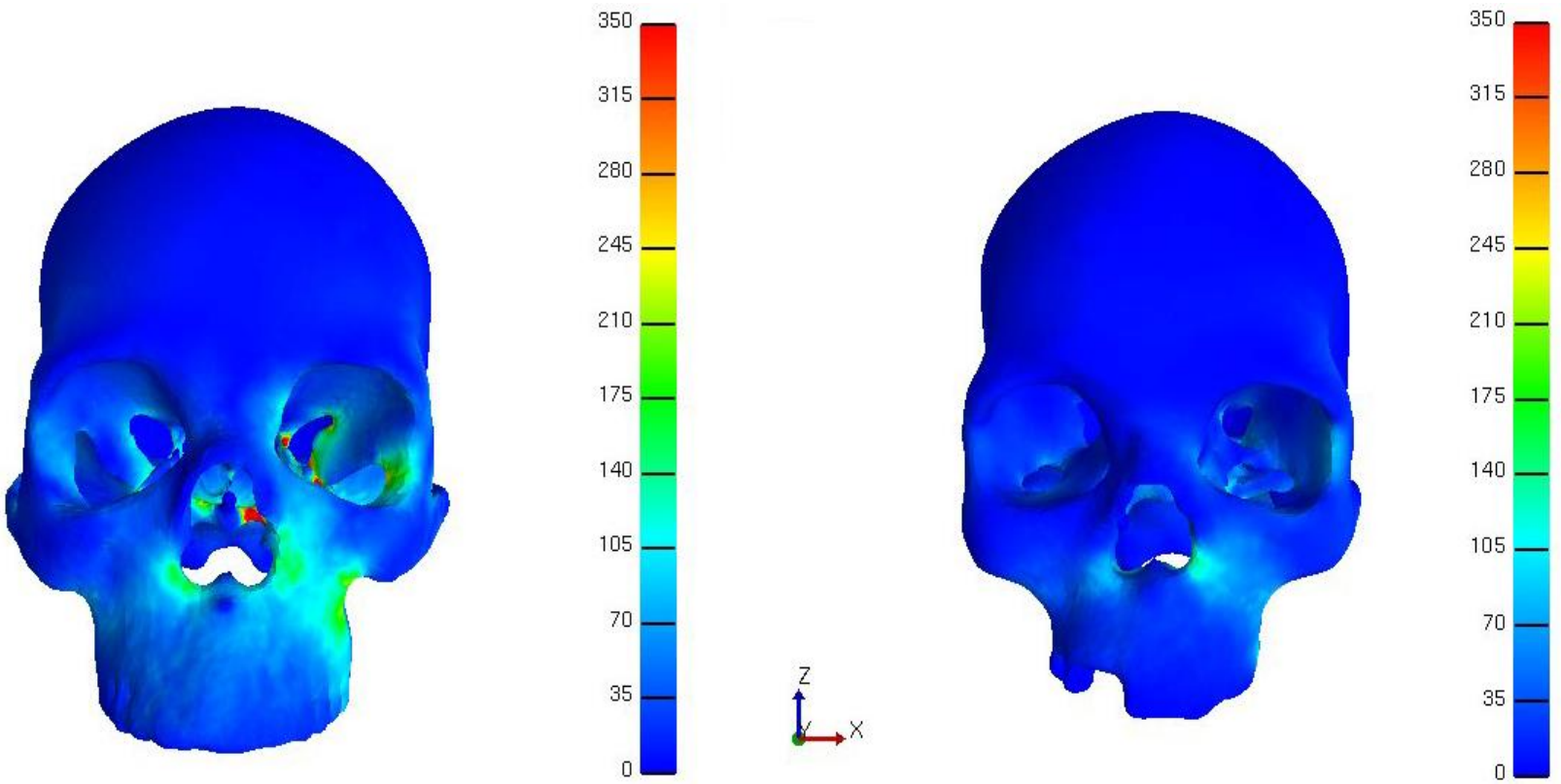

Figure 77. Von Mises stress distribution for a molar bite comparing prognathic (left) and orthognathic (right) facial form and the contribution of stress from the medial pterygoid muscle, inferior view. The scale for the Von Mises results is in N/cm^2. Red indicates areas of high stress (a combination of tension, compression and shear) and blue indicates areas of low stress.

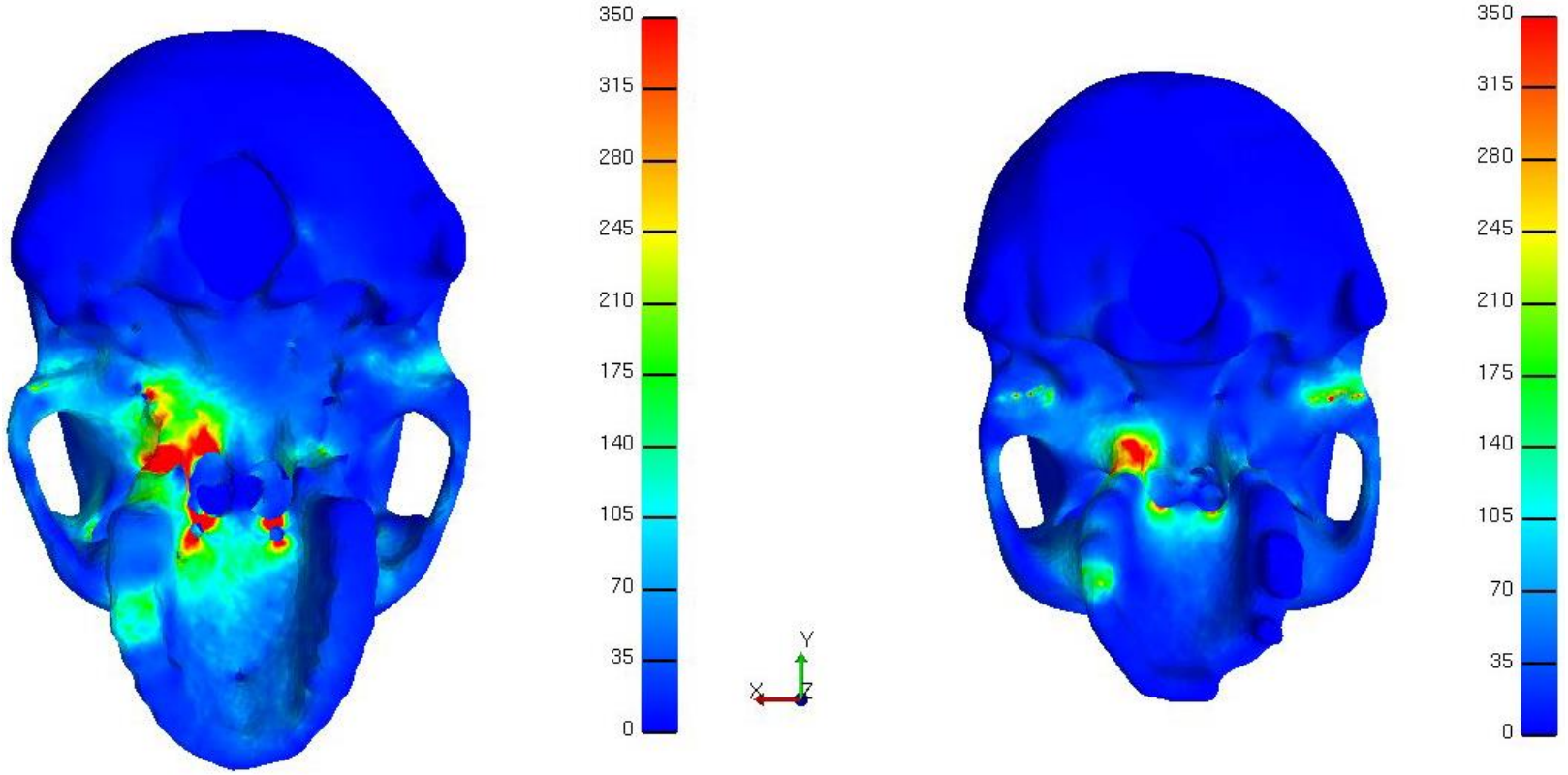

Figure 78. Von Mises stress distribution for an incisor bite comparing prognathic (left) and orthognathic (right) facial form and the contribution of stress from the deep head of the masseter muscle, anterior view. The scale for the Von Mises results is in N/cm^2. Red indicates areas of high stress (a combination of tension, compression and shear) and blue indicates areas of low stress.

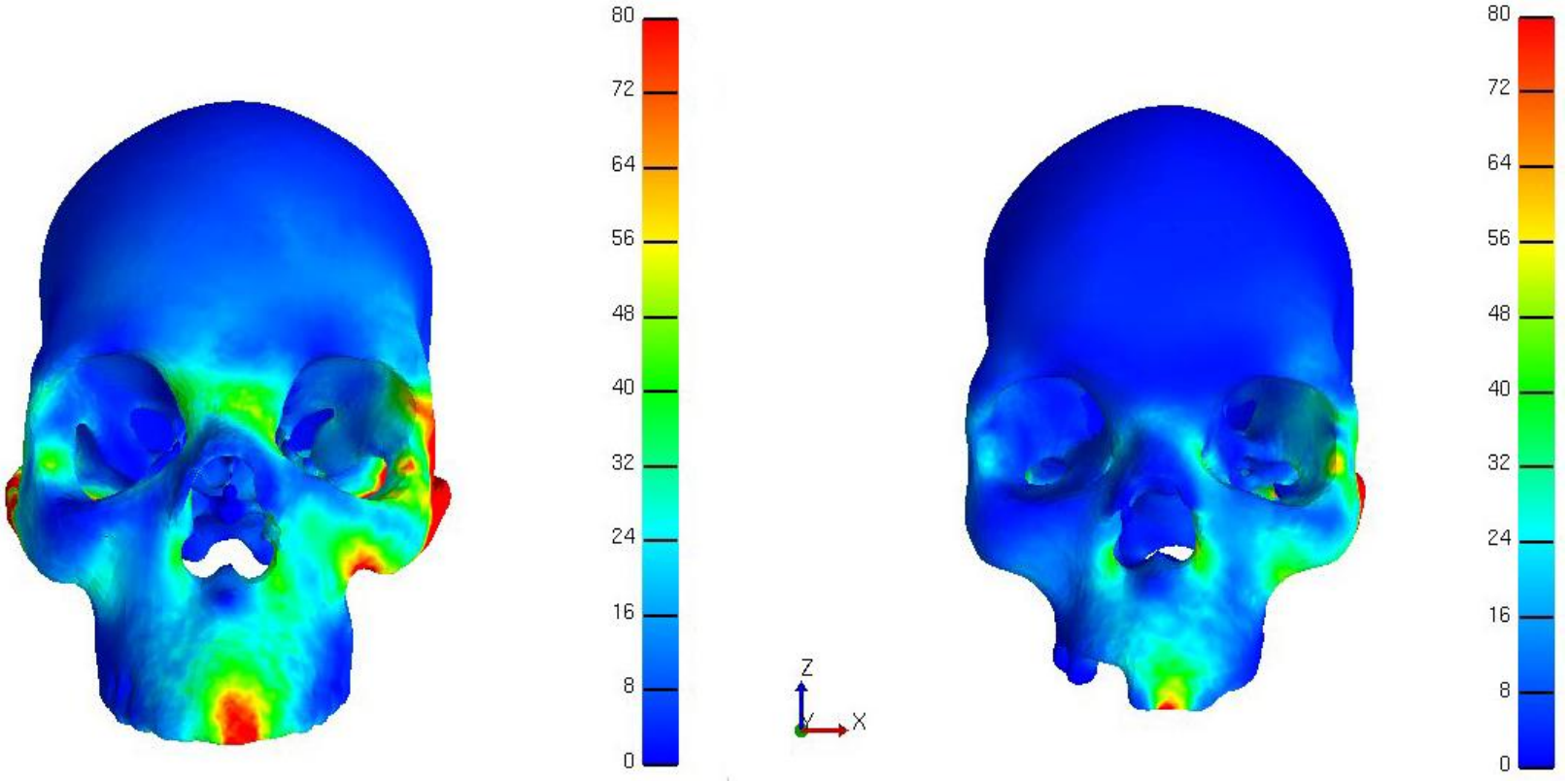

Figure 79. Von Mises stress distribution for an incisor bite comparing prognathic (left) and orthognathic (right) facial form and the contribution of stress from the deep head of the masseter muscle, lateral view. The scale for the Von Mises results is in N/cm^2. Red indicates areas of high stress (a combination of tension, compression and shear) and blue indicates areas of low stress.

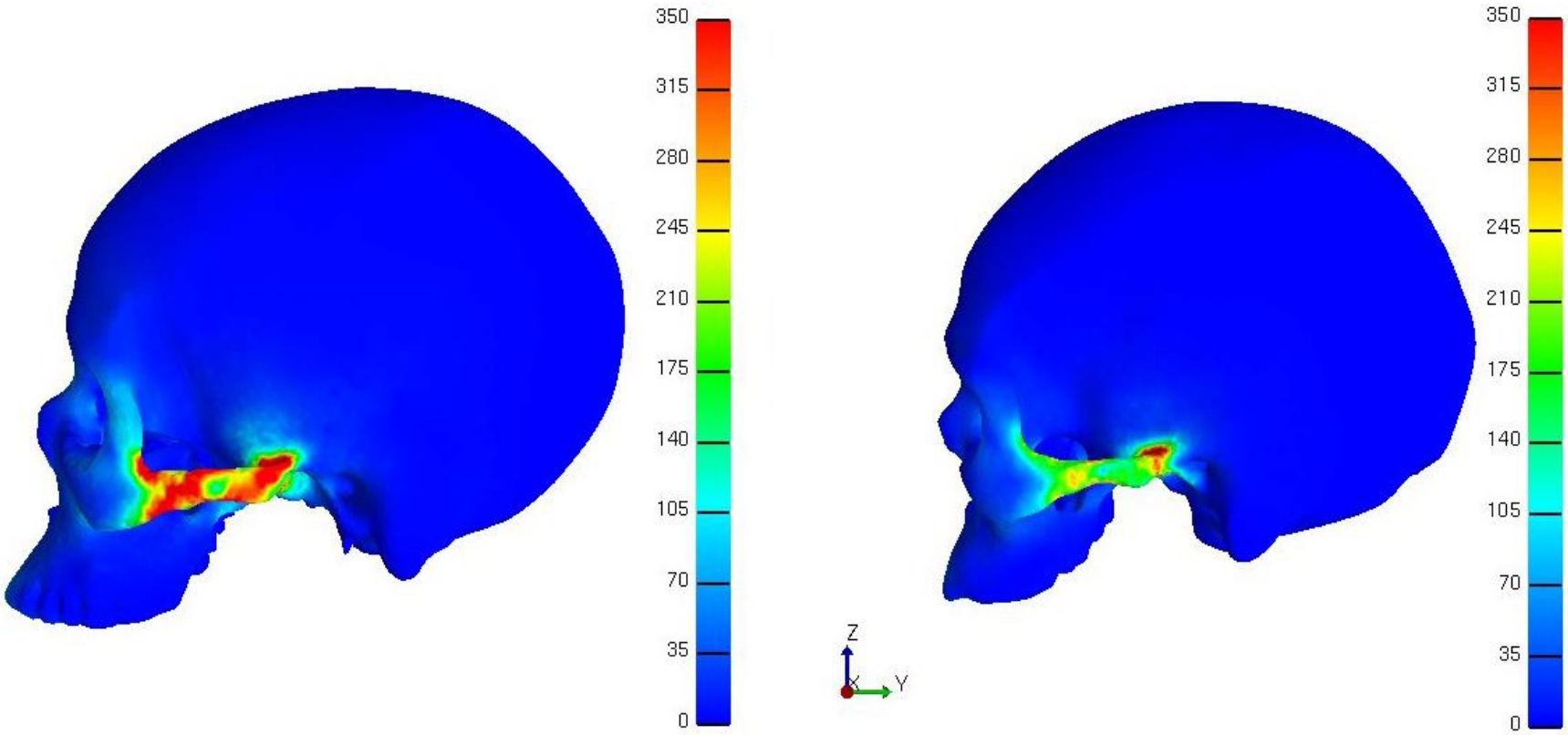

Figure 80. Von Mises stress distribution for an incisor bite comparing prognathic (left) and orthognathic (right) facial form and the contribution of stress from the deep head of the masseter muscle, inferior view. The scale for the Von Mises results is in N/cm^2. Red indicates areas of high stress (a combination of tension, compression and shear) and blue indicates areas of low stress.

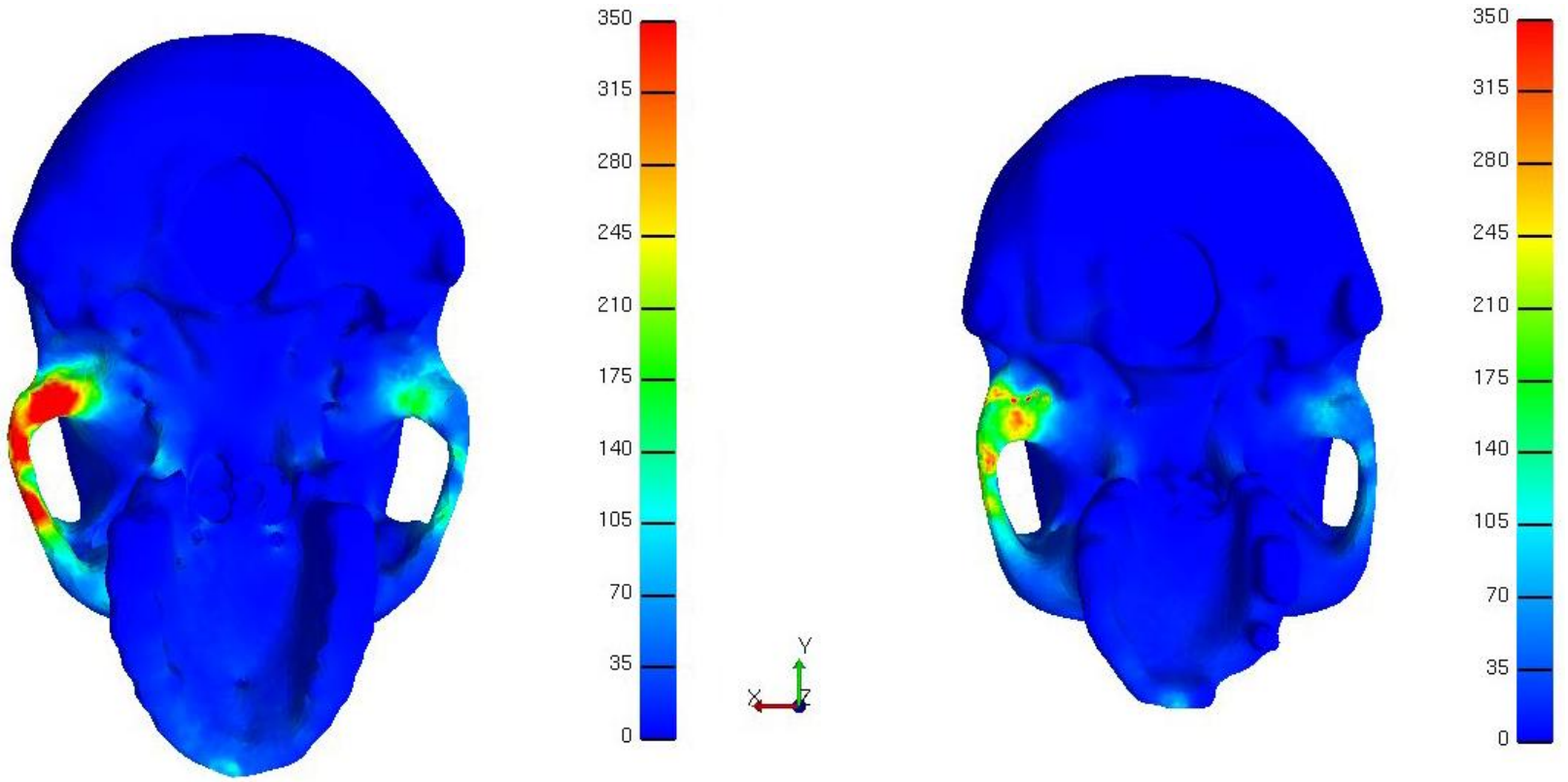

Figure 81. Von Mises stress distribution for an incisor bite comparing prognathic (left) and orthognathic (right) facial form and the contribution of stress from the superficial head of the masseter muscle, anterior view. The scale for the Von Mises results is in N/cm^2. Red indicates areas of high stress (a combination of tension, compression and shear) and blue indicates areas of low stress.

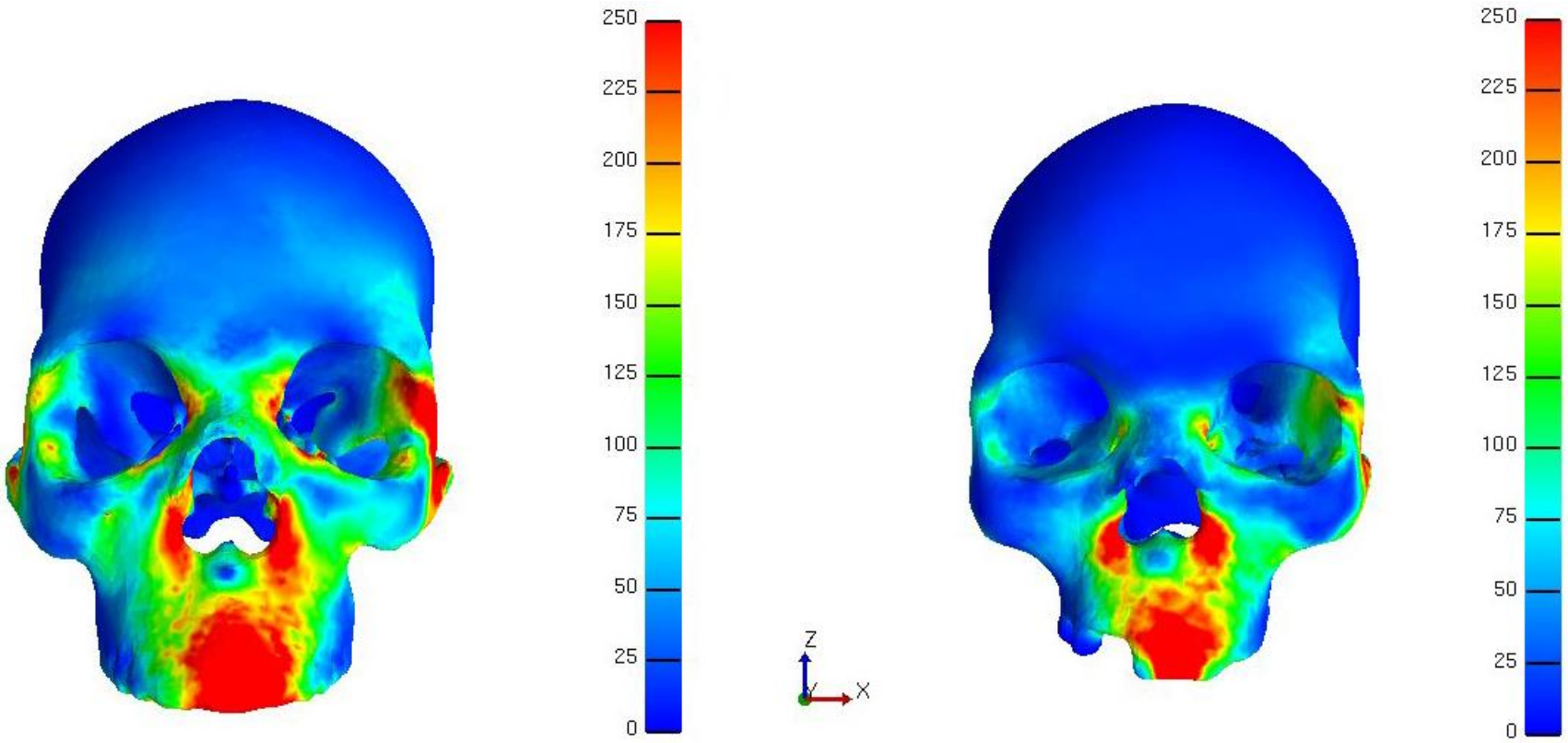

Figure 82. Von Mises stress distribution for an incisor bite comparing prognathic (left) and orthognathic (right) facial form and the contribution of stress from the superficial head of the masseter muscle, lateral view. The scale for the Von Mises results is in N/cm^2. Red indicates areas of high stress (a combination of tension, compression and shear) and blue indicates areas of low stress.

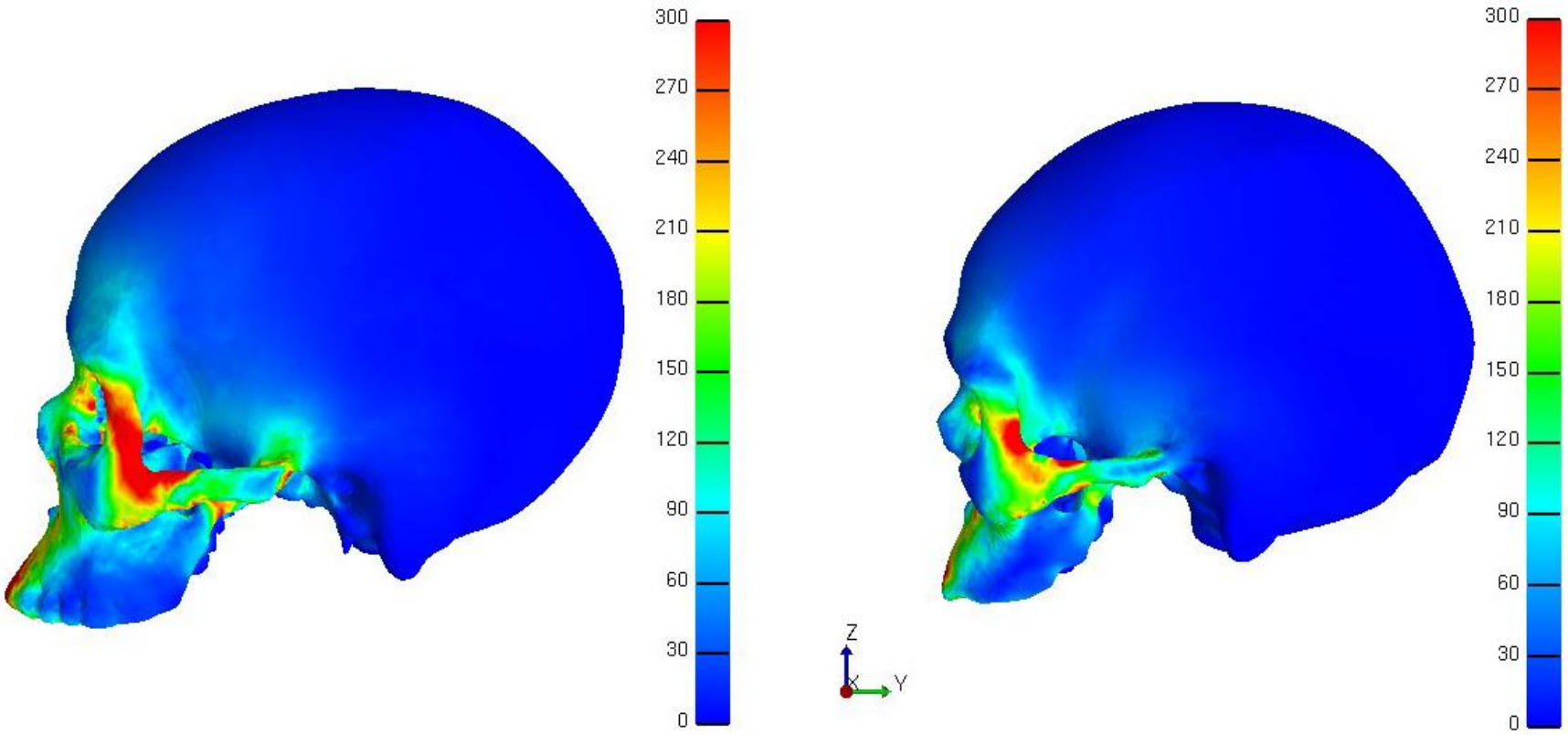

Figure 83. Von Mises stress distribution for an incisor bite comparing prognathic (left) and orthognathic (right) facial form and the contribution of stress from the superficial head of the masseter muscle, inferior view. The scale for the Von Mises results is in N/cm^2. Red indicates areas of high stress (a combination of tension, compression and shear) and blue indicates areas of low stress.

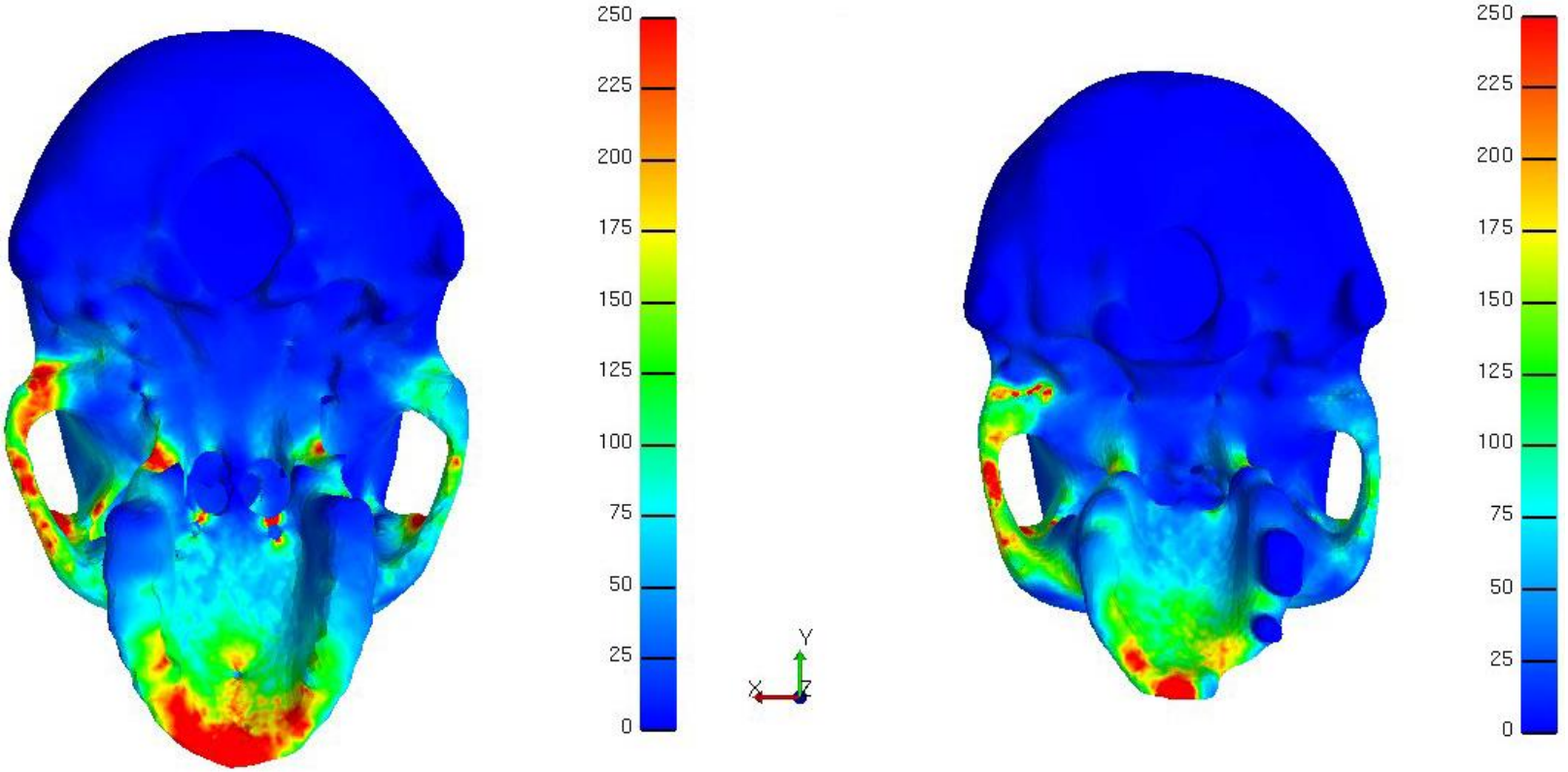

Figure 84. Von Mises stress distribution for an incisor bite comparing prognathic (left) and orthognathic (right) facial form and the contribution of stress from the temporalis muscle, anterior view. The scale for the Von Mises results is in N/cm^2. Red indicates areas of high stress (a combination of tension, compression and shear) and blue indicates areas of low stress.

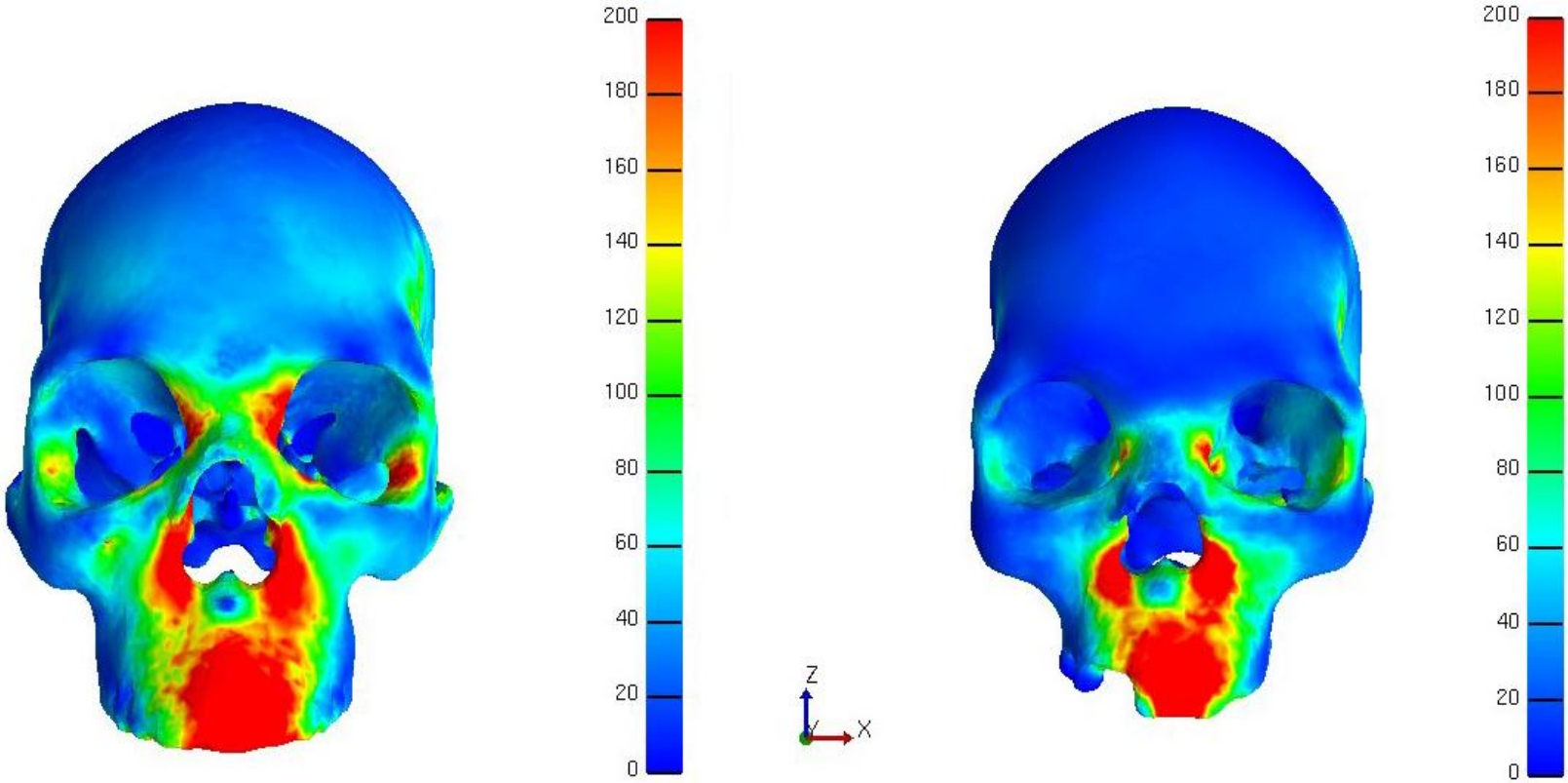

Figure 85. Von Mises stress distribution for an incisor bite comparing prognathic (left) and orthognathic (right) facial form and the contribution of stress from temporalis muscle, lateral view. The scale for the Von Mises results is in N/cm^2. Red indicates areas of high stress (a combination of tension, compression and shear) and blue indicates areas of low stress.

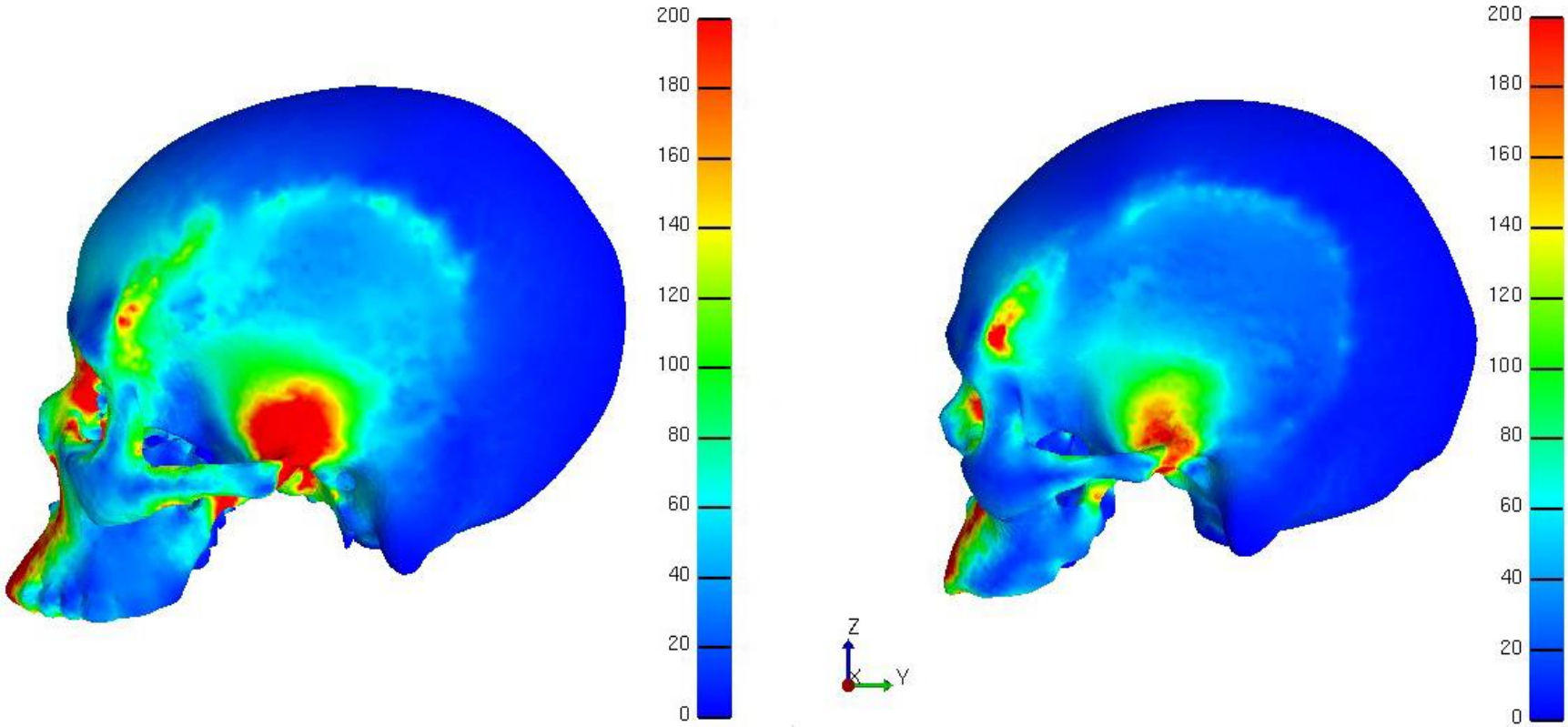

Figure 86. Von Mises stress distribution for an incisor bite comparing prognathic (left) and orthognathic (right) facial form and the contribution of stress from temporalis muscle, inferior view. The scale for the Von Mises results is in N/cm^2. Red indicates areas of high stress (a combination of tension, compression and shear) and blue indicates areas of low stress.

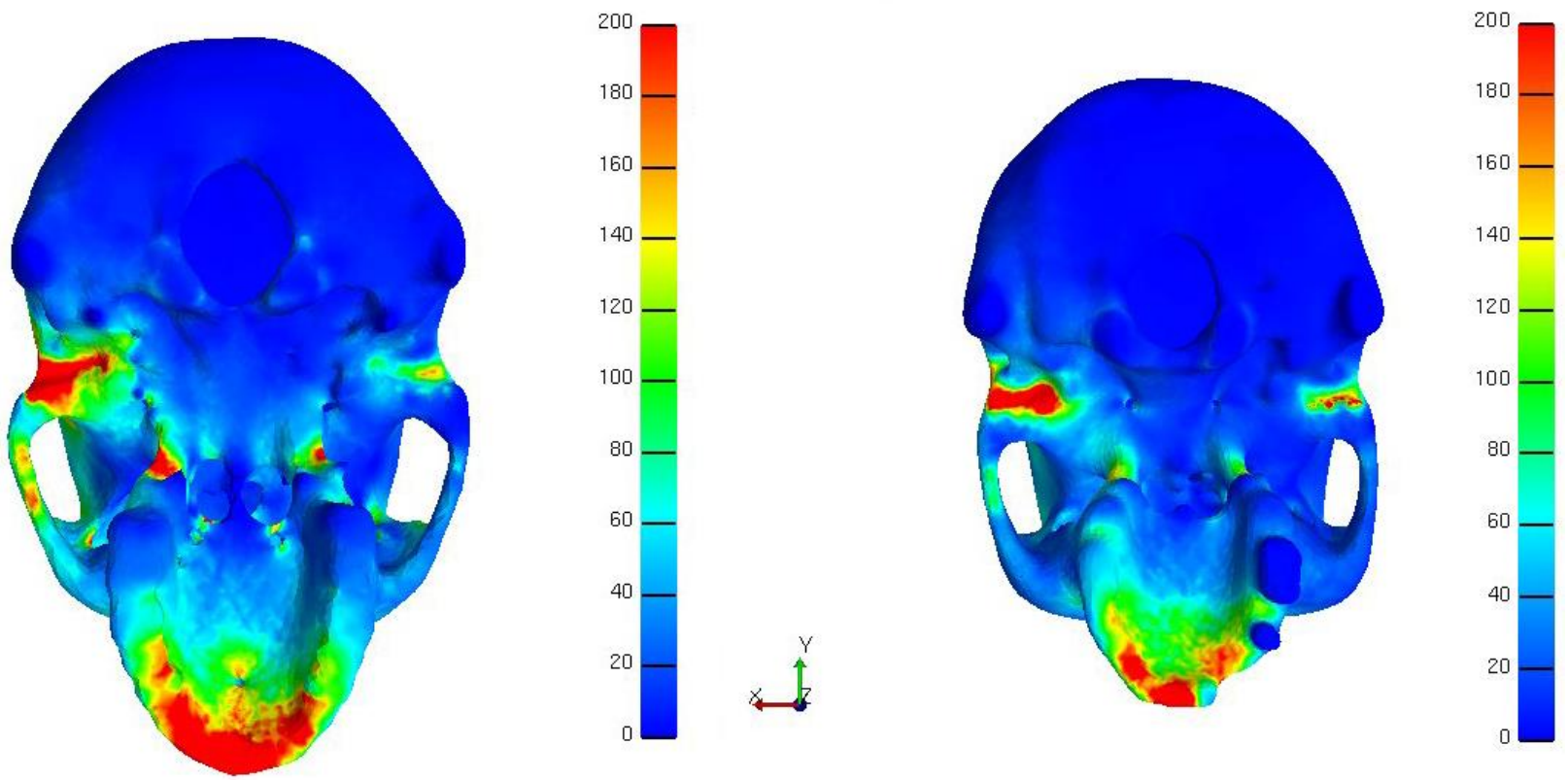

Figure 87. Von Mises stress distribution for an incisor bite comparing prognathic (left) and orthognathic (right) facial form and the contribution of stress from the medial pterygoid muscle, anterior view. The scale for the Von Mises results is in N/cm^2. Red indicates areas of high stress (a combination of tension, compression and shear) and blue indicates areas of low stress.

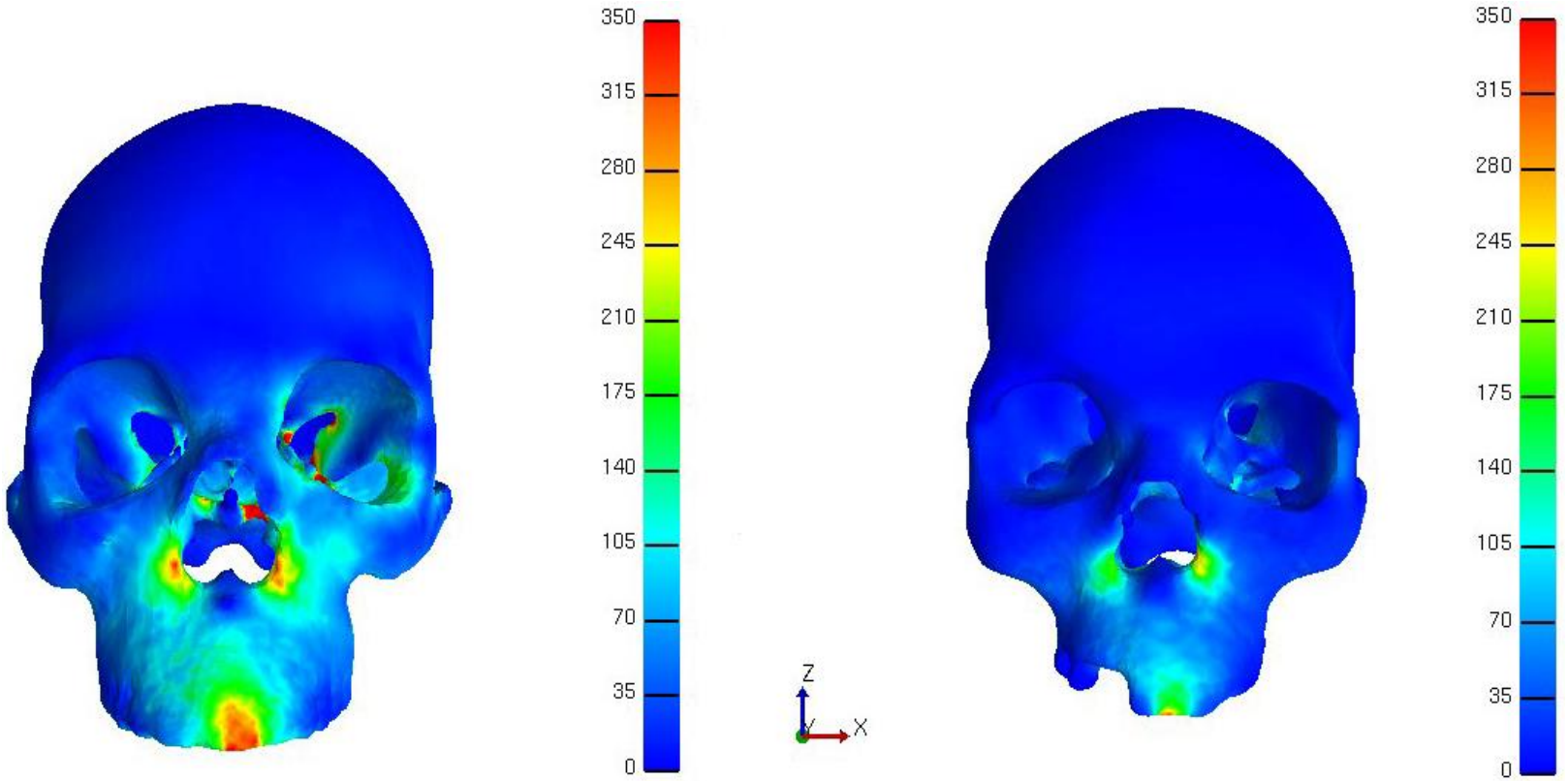

Figure 88. Von Mises stress distribution for an incisor bite comparing prognathic (left) and orthognathic (right) facial form and the contribution of stress from the medial pterygoid muscle, inferior view. The scale for the Von Mises results is in N/cm^2. Red indicates areas of high stress (a combination of tension, compression and shear) and blue indicates areas of low stress.

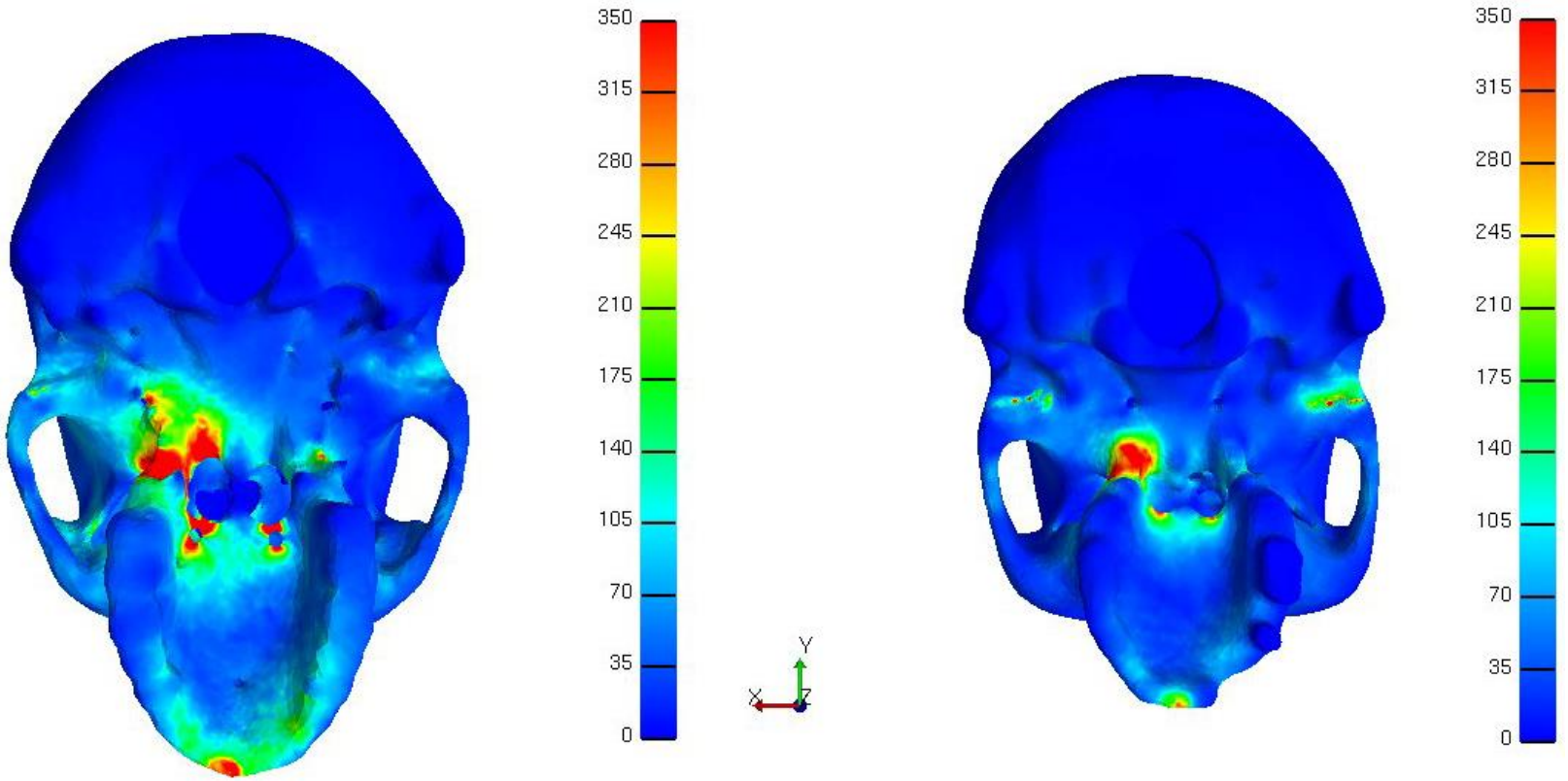

CHAPTER 7

DISCUSSION

7.1 INTRODUCTION

Anthropologists and paleoanthropologists have used skeletal material to help understand evolutionary relationships between various morphological aspects related to the craniofacial form. Amongst other things, research has evaluated the morphology and design of bone in terms of functional demands imposed upon the skeleton by biomechanical needs. However, these relationships and the factors that shape them are complex and not easily understood, both at the macroscopic and cellular level.

The basic building block of bone is the layered and varied arrangement of the collagen fibrils (Weiner and Wagner, 1998; Weiner *et al.*, 1999). Cortical and cancellous bone also varies between their structural make up within bones (Rho *et al.*, 1998). However, all structural components of bone are capable of becoming functionally adapted to a repetitive biomechanical loading history and, therefore, each bone becomes functionally adapted to their specific environment in both architecture and design (Wolff, 1892; Smith and Suggs, 1976; Frost, 2003; Cobb and O'Higgins, 2004; Ruff *et al.*, 2006).

For example, the more recent orthognathic craniofacial form may be a function of many factors that influence its expression, such as diet, brain size, development of language and bipedalism (Du Brul, 1977; Pearson and Lieberman, 2004). It is abundantly clear that a relationship exists between the morphology of bones of the skeleton and its biomechanical function. Bone adapts over time to its loading history. In response to this relationship, bone development is directly related to the mechanical stress it regularly endures (Pearson and

Lieberman, 2004). The idea that bone is functionally representative of its loading history has been commonly referred to as *Wolff's Law* (Wolff, 1892). In interpreting Wolff's Law, differences in morphology observed in the skeleton can be indicators of adaptation carried out by bone to accommodate for a past and current loading history.

Bone is developed such that it can resist deformation under mechanical loading. An increase in bone strength can be a result of adding mass, a change in geometry to redistribute stress or by altering the microstructure of the bone (Pearson and Lieberman, 2004). Understanding bone adaptive abilities to mechanical stress is crucial to interpreting the morphological variations found in bone that have evolved over time.

Bone tends to maintain an optimal strain environment, where there is maximum function with minimal bone mass. An increase in activity increases strains, and, in turn, initiates bone deposition by osteoblastic activity. An increase in bone density decreases strain again, maintaining the optimal strain environment. The opposite holds true for a decrease in activity; a decrease in the strain found in bone initiates osteoclast activity, which carries out bone resorption. This resorption of bone increases strain levels in a specific area and, again, maintains optimal strain environment (Hylander and Johnson, 1997). Adults exhibit very little or no response to changes in loading, however, adolescent activity contributes heavily to the development of the expression of adult bone morphology (Pearson and Lieberman, 2004).

Mechanical loading is important in determining variations in bone morphology when comparing individuals (Ruff *et al.*, 2006). Several factors can influence the degree of variation in bone morphology, such as age, genetic makeup and mechanical effects. Age of bone, which was not addressed in this study, is a factor in development and in

morphological changes seen in bone over an individual's lifetime (Kerley, 1965; Pfeiffer, 1980; Green *et al.,* 2011). Genes can influence bone in several ways and can dictate bone size and shape, or determine body weight and muscle mass, which affects underlying bony architecture. Genes can also determine bone response to mechanical loading (Ruff *et al.*, 2006). The differences between hominid species in craniofacial form can thus be attributed to differences in genetic makeup, extrinsic factors and environmental determinants.

Variations in skeletal morphology have evolved over time (Athreya, 2009; Freidline *et al.*, 2012). Several craniofacial forms and varying degrees in the expression of morphological characteristics have been recorded throughout primate and hominid evolutionary time line. One of the most marked features is the decrease in size of the facial skeleton (Stringer, 2002; Lieberman *et al.*, 2002; Trinkaus, 2003). Factors involved in the evolution of the reduction in the human facial skeleton are a decrease in canine tooth size and functional adaptations to a less rough diet (Cobb, 2008). As was seen in earlier hominids, rough diet, larger dentition and muscle-attachment demands were met with an increase in prognathism (Clement, 2012). It can be expected that changes in the craniofacial form to a characteristic, like decreased dentition, would similarly evolve to a selective pressure like a change in diet.

The masticatory system is adapted towards a specific diet. This has clearly been illustrated throughout human evolution. *Australopithecus* had increased posterior dentition and decreased anterior dentition, and muscles moved in relation to this dental arcade to be more efficient—adaptations resulting from a diet that required higher masticatory system demands (Strait *et al.,* 2008; Cobb, 2008). The maxilla of *A. africanus* had canine buttresses, which ran forward and downward like columns spreading below the glabella on the sides of

the nasal opening and ending at the canine sockets (Du Brul, 1977). *A. africanus* also had buttressing in the zygomatic region that slanted downward and forward from the lateral margins of the orbits to reach the level of about the second molar sockets. *A. biosei* showed immense zygomatic buttressing with great bony plates positioned forward to the premolar level. *A. biosei* had a massive zygomatic arch that was thickened medio-laterally and deep, top to bottom (Du Brul, 1977). Although little is known about the diet of earlier hominids, much of the changes in the masticatory apparatus have previously been attributed to adaptation to a specific diet. The specific diet resulted in the architectural changes in buttressing and the morphology to accommodate an increase in strain from masticatory muscle contraction.

The anterior dental loading and paramasticatory activities of Neandertal resulted in increased mechanical stress and necessitated reinforcement from the musculoskeletal system to accommodate for additional stress (Demes, 1987; Antón, 1990; Couture, 1993; Spencer and Demes, 1993; Antón 1994; O'Connor *et al*., 2005; Clement *et al.*, 2012). Therefore, the decrease in dental loading from changes in diet should initiate the same accommodating response in the craniofacial skeleton with a reduction in robusticity, size and architecture.

The diet of early *Homo* ancestors and modern humans has been investigated extensively (Kay, 1985; Picq, 1990; Larsen, 1995; Teaford and Ungar, 2000; Ungar and Teaford, 2001; Teaford *et al.*, 2002; Unger, 2004; Palubeckaite *et al.*, 2006; Esclassan *et al.*, 2009). *Australopithecus afarensis* was sufficiently equipped with large molars to accommodate its hard diet of seeds and nuts (Unger, 2004). Early *Homo*, with larger incisors, thinner enamel and reduced molars indicated that there was a decreased demand

mechanically on the masticatory system because of the diet change and the introduction of meat (Unger, 2006; Unger *et al.*, 2006). The anterior dentition now begins to function as a tool for slicing and tearing.

As diets changed, from hunter-gatherer to agriculture based, so did wear patterns on the dental arcade of the two groups. For example, hunter-gatherer diet wear patterns on the first molar were even and worn flat, while agriculturist diet wear patterns were oblique and uneven (Smith, 1984). With tools use (over teeth), reduction in diet toughness and subsequent teeth grinding, wear patterns changed accordingly.

Dental wear patterns from occlusal stress have been characterized as attrition, erosion and abrasion, with these patterns changing in human populations over time (d'Incau *et al*., 2012). Differentiation in wear patterns occurs from habitual forces on occlusal surfaces of teeth from masticatory muscles action. These forces, along with variations in wear patterns, caused by increased dental attrition, eruption/loss and pathology, may occur throughout an individual's life.

Overall, the trend from the *Australopithecine* morphology with prominent, mid-facial protrusion towards an orthognathic facial expression is a pronounced part of modern *Homo sapien* evolution (Spencer and Demes, 1993). Facial features of early *Homo* show a trend toward a more gracile orthognathic facial morphology. The presence of an elongated vertical facial dimensions is the beginning of orthognathic expression. Early *Homo* still housed broad, square anterior palates, relatively wide and square shaped piriform apertures, projecting browridge morphology, depressed internal nasal sills, posteriorly set zygomatic arches and larger infraorbital areas, than seen in its predecessors (O'Connor *et al.,* 2005).

Chapter 7
DISCUSSION

Moving through the timeline of hominid evolution, the appearance of *Homo habilis* approximately two million years ago marks the beginning of the greatest reduction in facial morphology and the trend towards an increase in brain size. *H. habilis* had an increased brain size over *Australopithecus*, however, it still represents the smallest brain size within the *Homo* fossil record. With the smallest brain size, *H. habilis* also had the largest teeth, huge vertically orientated zygomatics and pronounced prognathism. *H. habilis* also initiated tool use and fire for cooking (Wolpoff, 1996; Park, 1996). *H. erectus* also used tools, cooked food and had an increase in brain size with a subsequent reduction in other facial features, such as post canine teeth, smaller zygomatics and vertical shortening of the face, while retaining a large jaw, molars and pronounced prognathism and browridge expression (Wolpoff, 1996; Park, 1996).

Evidence of a forward projecting nose, like in modern humans, can be seen in of *H. erectus*. Archaic *Homo sapiens* is thought to be the step between modern humans and *H. erectus* (Wood, 2006). With an increase in brain size, migratory activity, more efficient use of tools and cooking, this species showed a larger brain size, accompanied by a steeper forehead. The further reduction in the facial skeleton took place with the decrease in molar size and browridges. When what is considered modern humans of today first appeared thousands of years ago, a further reduction of the facial skeleton was noticeable with the more gracile appearance, less pronounced browridges, a decrease in the size of the dentition, zygomatics and a reduction in sub-nasal prognathism (Comas, 1960; Wolpoff, 1996; Park, 1996; Bastir *et al.*, 2008; Kaifu *et al.*, 2011; Freidline *et al.*, 2012).

Modern human development has had several hypotheses applied; for example, the development of modern humans from one ancestor in Africa or the multi-regional

evolutionary approach. Regardless of hypothesis, several factors, such as climate, gene flow and mechanical adaptation must be taken into account when trying to explain craniofacial features difference (Hanihara, 1996).

Where mechanical adaptation is involved and change in facial morphology occurs, there must come a change in buttressing to accommodate strain from masticatory muscle contractions. In this study, an attempt was made to look at stress distribution difference due to masticatory forces in the two distinct craniofacial forms—orthognathic and prognathic—and observe differences in these patterns. Metric and morphological analyses were carried out and statistical analysis performed to determine not only differences in size and morphology with the degree of prognathism, but also determine correlations between the various craniofacial features (e.g., if prognathism is necessarily associated with well-developed browridges). A skull representative of an orthognathic individual and one representing a prognathic individual were modeled three dimensionally and underwent finite element analysis to assess the effect of prognathism on masticatory stress distribution in the craniofacial skeleton. Metric and morphological results were then used to aid in interpreting the finite element analysis results.

Geometric morphometric methods have been used as a tool in osteological and forensic anthropological research to analyze variation in bone morphology to differentiate between sexes and ancestral groups, and elucidate aspects of function. For example, it has been used to assess sex differences in the sub-adult mandible (Franklin *et al.,* 2007), pelvis (Gonzalez, 2009), scapula (Schultma *et al.,* 2010), and humerus (Vance, 2013) and also to differentiate ancestral groups from the nasal aperture (McDowell *et al.,* 2012).

The digitizing and landmarking for the purposes of undergoing geometric morphometric analysis was beyond the scope of this project. For the current research the time and resources were focused on the finite element analysis, and to help interpret the finite element results the morphometric data were recorded and analyzed concurrently. A future avenue of research may be to use geometric morphometrics to further help highlight and clarify shape changes which may occur in response to the biomechanical stress of mastication.

Below, more attention will be given to the specific areas that varied between the two models from the finite element results. In addition, the metric and morphological data collected with their statistical analysis can help in interpreting the finite element results. Furthermore, the degree of prognathism and its effect on cranial shape, size and the stress distribution during mastication will be considered.

7.2 PROGNATHISM AND SIZE

7.2.1 DIMENSIONS POSITIVELY CORRELATED WITH THE GNATHIC INDEX

Metric analysis of skulls in the orthognathic, mesognathic and prognathic groups allowed observations to be made regarding craniofacial size and shape relative to the degree of prognathism. Dimensions that increased across groups with the degree of prognathism were basion-prosthion length (as expected, p=0001); maximum alveolar length (p=0001); mandibular body breadth; mandibular projective length (p=0.02) and zygomatic arch height. Dimensions positively and significantly correlated with the gnathic index were maximum alveolar length (p=0.0001); mandibular body breadth (p=0.01) and minimum ramus breadth (p=0.007). Mandibular projective length (p=0.34) and zygomatic arch height (p=0.17) were positively correlated to the gnathic index but were not statistically significant.

Maximum alveolar length increases with the degree of prognathism, as expected because this length is highly correlated to the overall projection of the mid-face region. Palate length and maxilla protrusion have previously been found to have a relationship in primates (Smith and Josell, 1984). In humans, the increase in dentition size with the increase in prognathism could produce a longer palate length. This would also hold true for mandibular projective length, where, by definition, projection of the mandible forms part of the protrusion of the mid-facial area.

7.2.2 DIMENSIONS NEGATIVELY CORRELATED WITH THE GNATHIC INDEX

Basion-bregma height had the largest value in the mesognathic group and the smallest in the prognathic group and was statistically significant across the orthognathic, mesognathic and prognathic groups (p=0.004). It was determined that Basion-bregma (p=0.003); orbital breadth (p=0.004); orbital height (p=0.02) and interorbital breadth (p=0.006) were all significantly negatively correlated with the gnathic index. This relationship shows that the more prognathic individuals tend to have decreased skull height. Decreased height and long narrow skull is the dolichocranial shape previously found in those with African ancestry (De Villiers, 1968; Howells, 1972, 1989, 1995, 1996). With the orbital dimensions negatively correlated with prognathism, a shorter narrow orbital shape will be observed.

Orbital dimensions have previously been correlated with the degree of prognathism in other populations (e.g., Australia, East Asia, Japanese and Northern Africa) (Calcagno, 1986; Calcagno and Gibson, 1988; Brown, 1992; Brown and Maeda 2004). These authors found, as was the case in this study, that a trend toward orthognathism was met with an

increase in orbital height and a decrease in orbital breadth (Calcagno, 1986; Calcagno and Gibson, 1988; Brown, 1992).

Brown and Maeda (2004) examined a Japanese and an Australian Aboriginal sample. As is consistent with findings from the current study, a decrease in the gnathic index had an increased orbital height. As a population becomes more orthognathic, facial flattening allows for increased orbit height. The statistically significant correlation between orbital height and prognathism should not be disregarded. The decrease in orbital height found in the prognathic model may result in the increase in Von Mises stress in the margins of the orbits because of the depressed size of the orbits. This increase in stress may have also attributed to size change in orbits where the orthognathic model records less stress in these areas. The increase in orbital height may also take place because of the change in facial height from prognathism to orthognathism. Orbital height is correlated with prognathism, but this may be a result of multiple changes occurring in the facial skeleton with change in morphology and architecture and biomechanical functionality.

Other cranial dimensions, which have a trend to decrease in size across the orthognathic, mesognathic and prognathic groups (therefore, largest mean values in orthognathic facial form), were maximum cranial length and breadth, minimum frontal breadth, orbital breadth and height and bigonial width. However, of these measurements, none were found to be significantly different in their mean values of the groups and may, therefore, reflect a determination more by genetic influences than degree of prognathism.

Natural selection is thought to have acted on Neandertal craniofacial morphology for both a northern climate and adaptations to high mechanical stress (Weaver *et al.*, 2007; Holton *et al.*, 2011). Neandertal high masticatory mechanical stress, caused by specific

anterior dental loading, attributed to distinct facial morphology, but also genetic drift may also have played a role in facial skeleton development (Weaver *et al.*, 2007; Clement *et al.*, 2012). It is interesting that with the increased prognathism of Neandertal, the interorbital breadth recorded from a fossil sample by Weaver *et al.*, (2007), and data recorded from this research sample from a modern human, was the same at 28.1 mm. This being said, interorbital breadth is still used to accommodate for high masticatory loads or to more efficiently accommodate for masticatory loading stress incurred from a modern diet. In conclusion, the size of interorbital breadth for the current sample may function to decrease stress in that region during masticatory muscle contraction, as the craniofacial form becomes more orthognathic in the group sampled.

When investigating the relationship between prognathism and craniofacial skeleton size, it was found that of the 24 measurements taken, seven were significantly correlated with the gnathic index. In general, there does not seem to be a significant correlation with size (mm) and prognathism directly. In individuals with African ancestry, one may expect to have some characteristics with increased size related to prognathism (e.g., basion-prosthion length, maximum alveolar length) as a part of the underlying architecture of the facial skeleton. This relationship, however, may not necessarily be one of function. This is reflected in the results from the metric analyses that were used to interpret observations from the finite element analysis showing displacement, pressure and Von Mises stress distribution in the facial skeleton in the two craniofacial forms.

7.2.3 PROGNATHISM AND SIZE OF THE DENTITION

A diet for that is both coarse and difficult to break down needs a masticatory system of larger dentition and masticatory musculature. These modifications provide a higher bite

force and greater surface area, which facilitates individual success. With increased processing of food, for example, as well as cooking or tenderizing meat, demands on the masticatory system have decreased substantially over the last few hundred thousand years. Diet changes mean reduced need for a large occlusal area, resulting in fewer and smaller teeth.

Some dimensions of dentition were correlated with degree of facial projection. The mesio-distal dental measurements that increased across orthognathic, mesognathic and prognathic groups were that of the maxillary first and second incisors and the mandibular first incisor. The current research also reveals that the mesio-distal measurement of the second incisor and canine in the maxilla and second incisor and first molar in the mandible were significantly correlated with the gnathic index. These observations are in agreement with previous findings where an increase in the alveolar length and forward projection of the palate and mandible that is capable of housing larger teeth.

Larger anterior dentition was advantageous to prognathic Neandertals, where larger dentition better equipped them to hold objects in their anterior teeth for manipulation and to be used as tools (Brace, 1978). Selective forces like this use of tools allowed for the trend in deceased anterior dentition with hominid development. Brace (1979), suggests the modern facial configuration is an intermediate point in facial evolution because of previous selective pressures, like using anterior dentition as tools and the past and present preprocessing of the diet before mastication.

The canine mesio-distal measurement was found here to be significantly positively correlated to the gnathic index ($p=0.003$). These results are consistent with previous research (Jungers, 1978; Simpson *et al.*, 1991; Alba *et al.,* 2001). Dentition size has been

found to be correlated with the degree of prognathism; this shows that with an increase in teeth size, there is the expression of increased facial projection (Carlson and Van Gerven 1977; Brace 1979; Brace *et al.*, 1987; Simpson *et al.*, 1991; Alba *et al*., 2001; Cobb, 2008).

There was a positive correlation with the gnathic index and the mesio-distal length of the first molar in the mandible (p=0.01). With increased prognathism there was an increased mesio-distal length and subsequent occlusal surface area, however, occlusal area was not found significantly correlated with the gnathic index in this sample. Demes and Creel (1988) found that an increased bite force accompanied an increased molar crown area. Producing an increased bite force at the first molar has previously been found to be significantly correlated with a face having a narrow dental arch, a forward maxilla and mandible, as found in prognathic individuals (Hannam and Wood, 1989).

Late trends in hominid evolution with orthognathism were decrease in bite force, dentition and occlusal area. Tooth size reduction was about 1% per two thousand years until the end of the late Pleistocene; subsequently, reduction was twice that at 1% per one thousand years. This trend reflected changes in selective forces at that time (Brace *et al.*, 1987).

In summary, more of the measurements of maxilla dentition were positively significantly correlated with degree of prognathism. Measurements in both the mesio-distal and bucco-lingual direction in the anterior dentition of the maxilla became larger with prognathism, while only bucco-lingual dimension of the first molar was affected by facial projection. Current results indicate that maxilla dentition in both dimensions is more affected by the degree of facial projection than that of mandible dentition.

7.2.4 DIMENSIONS NOT CORRELATED WITH PROGNATHISM

Fifteen dimensions were found not to be statistically correlated with the gnathic index. The two measurements of the vault, maximum cranial length and breadth were not correlated with the degree of prognathism. These results indicate that the degree of facial projection alone does not influence cranial shape. The association between mid-facial projection and specific cranial shapes for determining ancestry may be rooted in genetics and population variation but not specifically to prognathism.

Facial skeleton dimensions that were not influenced by prognathism were bizygomatic breadth, maximum alveolar breadth, upper facial height and minimum frontal breadth. Facial dimensions of bizygomatic breadth, upper facial height and minimum frontal breadth are not located directly in the region of sub-nasal projection. Although upper facial height includes maxilla, its increased projection with more prognathic individuals is alone not enough to influence this facial dimension. The maximum alveolar breadth taking the maximum breadth of the dental arcade is not correlated with the degree of prognathism but may be more directly influenced by dentition size housed in the alveolar bone of the maxilla.

Neither the nasal height nor breadth is affect directly by the degree of prognathism. Therefore, nasal shape is not influenced by the sub-nasal projection. The association with prognathism and nasal shape via the nasal index when determining ancestry may be explained by genetics, climate adaptation but not an association between the morphology of the face in these regions.

In the mandibular dentition six of the eight measurements were not correlated with the gnathic index. Seven dimensions of the mandible were recorded and, of these, five were not influenced by prognathism: bigonial width, maximum ramus breadth and height,

mandibular projective length and mandibular angle. In general, the individual dimensions of the mandible are not influenced by the degree of prognathism. The mandible makes up a substantial part of the sub-nasal region and interacts directly with the maxilla at the occlusal surface of the teeth and with the vault at the condyles. Therefore, mandible size may be more influenced by intrinsic factors, such as the masticatory muscle attachments, dentition or the biomechanical loading history in order to maintain the masticatory apparatus.

Maxilla dentition was more influenced by prognathism than mandible dentition. Three measurements of the maxillary dentition were not influenced by prognathism: mesio-distal measurement of the first incisor and molar and the bucco-lingual measurement of the second incisor. Since dentition has interaction with the external environment because of diet it would be reasonable that the change in diet may be the selective pressure to influence the size of the dentition, as previously discussed. However, the degree of prognathism does not influence the mesio-distal measurement of the first incisor and molar despite the increase in alveolar length capable of housing larger dentition. In this study prognathism was not found to influence the mesio-distal measurements of the first incisor and molar.

Two new measurements were taken because of their relationship with the muscles of mastication and an association with the masticatory apparatus: zygomatic arch height and temporal fossa height. Neither measurement was influenced by the degree of prognathism. Temporal fossa height has a direct relationship with the associated muscle origin of the temporalis muscle. As muscle influences bone in response to a loading history, the muscle is likely more apt to influence fossa height than prognathism. The zygomatic arch height taken at the anterior region of the zygomatic arch is not influenced directly by sub-

nasal prognathism; therefore, it may have other factors, for example, genetics or be coupled with other morphological changes within the facial skeleton and not just prognathism.

7.2.5 SHAPE AND ROBUSTICITY

The difference in indices and, therefore, shape that occurred from the orthognathic, mesognathic to the prognathic group was in the frontoparietal, zygomaticofrontal and the upper facial index. These three indices increased in value with the degree of prognathism. The zygomaticofrontal index was in the range indicating an oval shaped face can be observed in the individuals sampled but was not significant between groups. Only the upper facial index was found to be significantly different between the three facial groups ($p=0.04$). Indicating that with an increase in prognathism the facial skeleton can be described as narrow or long faced. Also, the upper facial index was the only index significantly correlated with the gnathic index ($p=0.03$). The frontoparietal index (relating the least frontal breadth of the skull to the maximum cranial breadth) showed a slight increase across groups with largest mean value in the prognathic group, indicating that with prognathism the forehead became relatively broader.

Degree of robusticity and the relationship with the craniofacial skeleton has been previously investigated (Lieberman, 1996; Lahr and Wright, 1996; Petersen, 2000). In the current project, four morphological characteristics were considered for observation, and their relationship to prognathism assessed, namely browridge expression, glabellar prominence, mastoid expression and dental arcade shape. The expression of morphological characteristics (i.e., browridge, glabella prominence) can reflect robusticity.

The glabellar prominence, browridge expression, and frontal bone characteristics, like the frontoparietal index, were selected as morphological characteristics of the facial

skeleton to be observed because of the debate found in the literature with regard to their ability to accommodate stress from the forces of mastication (Endo, 1970; Oyen *et al.*, 1979; Russell, 1985; Hilloowala and Trent, 1988; Picq and Hylander, 1989; Hylander *et al.*, 1991a; Athreya, 2009).

Results of this study demonstrated that the morphological characteristics of browridge expression, glabellar prominence and mastoid process size between orthognathic, mesognathic and prognathic groups were not distributed in a significant pattern. These observations in the craniofacial morphology indicate that there is no specific relationship between the expression of browridge, glabella or mastoid shape and the degree of prognathism.

The broader forehead, as represented by the frontoparietal index, of the prognathic group lends to a larger surface area to accommodate stress. The prognathic model must accommodate for more stress in the frontal region during both molar and incisor bite. If the browridge, glabella and broader forehead, calculated from the frontoparietal index are coupled together, the three characteristics can function to accommodate more stress and might be an accommodating function of the frontal bone architecture. The three characteristics are found in the region of the frontal bar of buttressing in the craniofacial skeleton. However, glabella and browridge expression as a reflection of robusticity were not significantly distributed to correlate with prognathism. Browridge robusticity has been found to be significantly sexually dimorphic in modern populations and might attest to the genetic origins of this characteristic more than a functional association with facial projection (Shearer *et al.*, 2012).

It might be said that within the skeletal sample used here the degree of robusticity found within the skull does not play a structural role in mastication. It may be postulated that increased robusticity in earlier hominids was in response to larger dentition and tougher diet and larger musculature of the masticatory apparatus. Degree of robusticity in the craniofacial skeleton at the browridges may have had its origins from multiple elements, such as soft tissue attachment, vertical orientation of the face, facial size, palate length, orbital orientation and the decrease in the cranial base (Weidenreich, 1941; Ravosa, 1991a, 1991b; Lieberman, 1998, 2000, 2011).

As morphological characteristics have been shown not to vary with prognathism, the implied use of the browridge and the glabellar robusticity as accommodators of stress of masticatory forces does not hold true. These characteristics seem to not play a major role in the masticatory apparatus function in this sample. Muscle attachment sites are complex areas of bone, which can reflect the muscle activity of an individual (Zumwalt, 2005). The robusticity is a morphological characteristic and is related to the degree of development and associated with muscle attachment sites (Weiss, 2003; Niinimäki, 2011). If there is less demand on the masticatory apparatus from diet, a subsequent decrease in the masticatory musculature and therefore a decrease in robusticity may result. The robusticity of the facial skeleton may reflect its ability to produce force and not its ability to withstand the stress of mastication (O'Connor *et al.*, 2005). The masticatory apparatus must still function under repetitive loading. This being said, cortical bone composition of the frontal bone may be the underlying architecture that has the ability to accommodate for the stress, but robusticity is a more variable characteristic, which also has genetic and regional influences.

Bernal and colleagues (2006) examined the robusticity in two populations within South America. One population was hunter-gatherers (a diet of harder foods) and the other of farmers (softer foods). The browridge area was a morphological characteristic investigated, and the degree of robusticity recorded through morphometric analysis. Bernal *et al.,* (2006) found no correlation with size and robusticity in the craniofacial skeleton and attributed differences to sexual dimorphism in the population and not due to biomechanical stress. Crania sampled showed similar levels of robusticity and was not correlated to the toughness of the diet; therefore, robusticity was not biomechanically influenced. Bernal *et al.,* (2006) also suggested that the physiological adaptations to climate and endocrine behaviours might play a larger role in population robusticity. Bernal *et al.* (2006) found that higher latitudes populations had the most robust craniofacial morphologies. These other influences may partially explain the lack of robust browridges and correlation with prognathism and biomechanical function seen in the South African males.

The relationship with the minimal frontal breadth to the bizygomatic breadth was determined from the zygomaticofrontal index. The calculated value of the zygomaticofrontal index was largest in the prognathic group, positively correlated—but not significantly correlated—with the gnathic index. This makes the shape of the face in prognathic individuals appear broader and rounder due to the more robust zygomae associated with increased prognathism (Freidline *et al.*, 2012). Neither the frontoparietal nor zygomaticofrontal index was found to be significantly correlated with prognathism; therefore, the subsequent shape change cannot be solely attributed to the degree of prognathism in an individual.

The upper facial index, relating the upper facial height to bizygomatic breadth increased with the degree of prognathism. The upper facial index was significant between groups at p=0.04 and positively and statistically correlated with the gnathic index (p= 0.03). The facial morphology of individuals sampled was in the mesene range. (The mesene face is described as round in appearance.) The forward projection of the maxilla in prognathic individuals increases the nasion-prosthion distance of the upper facial height. With the increase in the gnathic index an increase in the upper facial index also occurred.

Two indices of interest that were not significantly correlated across groups or with the degree of prognathism were the cranial and nasal indices. Krogman and İşcan (1986) mentioned that the cranial shape characteristic of people with African ancestry, like the South African population sampled here, was that of a long, narrow head (dolichocephaly). The lack of relationship between overall cranial shape and degree of prognathism suggests that head shape may be related to factors other than prognathism, such as genetic differences or climatic adaptation, as has been previously discussed by Beals and Smith (1983). With admixture of populations and differences in cranial shape between these groups, the head shape in populations will continue to change.

Nasal shape can be characterized by its index. With an increase in the value of the nasal index an individual will have a relatively broader nose. Individuals of African ancestry are often described as having both a higher gnathic index and broader nasal shape (De Villiers, 1968; Holton and Francisus, 2008). This research did not find a significant correlation in the nasal index across groups (p=0.7) or with the gnathic index (p=0.6). Glanville (1969) found no significant relationship with the degree of prognathism and nasal breadth as the current research also found (p=0.4). Nasal shape has been previously attributed to climatic

adaptation by other authors (Coon, 1962; Trinkaus, 1983; Dean, 1988; Francisus and Trinkaus, 1988; Yokley, 2006).

Holton and Francisus (2008) looked at factors affecting nasal shape, one of which being the intercanine breadth. The authors suggested that intercanine breadth was affected by the maxilla having to house larger anterior dentition—this in turn caused a spreading in nasal aperture, making it wider. Holton and Francisus (2008) indicated that prognathism accounted for more variation in nasal shape than the intercanine breadth did, but other factors such, as genetic makeup of the population, should also be considered when looking at nasal shape. Therefore, nasal index differences seen in global populations are most likely due to genetic variation and not related directly to prognathism or more specifically the effects of mastication.

The findings of the current research support a relationship between dentition and nasal shape as previously found by Glanville (1969) and Holton and Francisus (2008). The relationship between nasal shape and prognathism is not supported with this research. Nasal shape in the current research shows no relationship to degree of prognathism, but the metric data does show an increase in the size of the anterior dentition with the degree of prognathism; therefore, nasal shape may be partially a function of large dentition and indirectly influenced by mastication due to tooth size.

With regard to the forces of mastication and the morphological characteristics of prognathism and nasal shape, it seems less likely the two are functionally correlated. When looking at the region of nasomaxillary vertical buttress in the facial skeleton, the prognathic model has more stress than the orthognathic during both molar and incisor bite. This can be seen from Von Mises stress distribution of the finite element results. Also, stress exists

around the nasal aperture during an incisor bite over a molar bite. If the facial skeleton is functionally adapted to accommodate stress, it would appear the prognathic facial form would functionally adapt to have a narrower nasal aperture to allow it to potentially incur less stress during the forces of mastication. It can also be surmised that with the incisors being used for paramasticatory activities it would also hold true that early hominids would also become functionally adapted to incur less stress in the facial skeleton. Consequently, with extrinsic factors such as climate, texture of diet and masticatory activities, it seems unlikely the reverse occurred, where nasal shape influenced degree of prognathism. So, if having a broader shaped nose is less efficient, so to speak, when it comes to mastication, then nasal shape does not seem to be changed due to selective pressure surrounding mastication. Multiple aspects of cranial facial growth, climate and genetic influences likely function to determine nasal shape and the variability in the mechanical stress of mastication is a less likely factor.

Dental arcade varies in accordance with facial form, as has been shown in primate and hominid evolution (Osborn, 1996). Current research identified that the narrow 'U' shaped dental arcade, where the left and right sides of the posterior dentition appear to be almost parallel to one another in position, was found among more prognathic individuals (76.5%). The prognathic group did have more individuals with a U-shape dental arcade than the orthognathic group, as previous research has determined (De Villiers, 1968; Osborn, 1996). A divergent shape with shorter sides is characteristic of orthognathic individuals, where it was assessed to be found in 31.4% of individuals.

The dental arcade shape was the only morphological characteristic investigated to show a significant pattern of distribution across groups. The Pearson Chi^2 was significant at

p≤0.01 for distribution across the orthognathic, mesognathic and prognathic facial forms for dental arcade shape. The orthognathic group observed fewer horseshoe shaped and more divergent dental arcades than expected, while the mesognathic group had more horseshoe shaped dental arcades than expected. The higher frequency of U-shaped dental arcades differs from previous research, also conducted on a South African black population. De Villiers (1968) found that the divergent U-shape was the most frequent expression of palate shape. However, it was also stated that the population sampled showed only a slight degree of total facial prognathism (DeVilliers, 1968). Prognathism has an effect on the dental arcade shape where an increase in the palate length and maxillary projection is able to accommodate larger dentition and exhibit the characteristic U-shape of the dental arcade. It appears that with decreased prognathism, a more divergent dental arcade can be expected, as was presented in this research.

7.3 PROGNATHISM AND STRESS DISTRIBUTION AS REVEALED BY FINITE ELEMENT ANALYSIS

The current body of work, through the use of the finite element analysis, demonstrates differences in patterns of displacement, pressure and Von Mises stresses between the prognathic and orthognathic facial form. The prognathic facial form had a greater displacement for both a molar and incisor bite. Pressure results show greater magnitude and area of positive pressure (compression) and negative pressure (tension) in the prognathic facial form over the orthognathic facial form. For Von Mises stress distribution, the orthognathic facial form consistently experiences a lower magnitude and area in Von Mises stress for both incisor and molar biting over the prognathic model.

The use of the finite element method helps in understanding the functional significance of the shape of an object, and also how it responds under external loading (Ross, 2005; Strait *et al.,* 2008). An advantage of the finite element model is that it allows researchers the ability to model behaviour of material that would normally be inaccessible or ethically unavailable, like that of the human skull. The finite element analysis has the ability to demonstrate how objects with complex internal and external geometries, like the human skull, resist loads (Wang *et al.,* 2006).

The results of the finite element analysis can be interpreted in many ways, and conclusions on how the stress distribution changes with morphology will be addressed by area of the craniofacial skeleton. Results of this study demonstrated that the accommodation of stress in the craniofacial region differed between the prognathic and orthognathic model. In designing this study, both models were attributed linear elastic isotropic homogenous material properties. Previous research modeling human bone has found this method adequate to represent stress and displacement of the skull in a realistic manner (Tanne *et al.*, 1989a; Tanne *et al.*, 1989b; Tanne and Sakuda, 1991; Daegling and Hylander, 1998; Strait *et al.*, 2005; Ichim *et al.*, 2006; Provatidis *et al.*, 2008; Curtis *et al.*, 2008; Strait *et al.*, 2009). Areas of the facial skeleton, which had differences in the stress magnitude or area between the two facial forms, were the frontal bone in the supraorbital region, the interorbital region, lateral and medial margins of the orbit and the lateral margins of the nasal aperture on the maxilla, articular eminence and the zygomatic arch.

7.3.1 VAULT STRESS

Cortical bone from the cranial vault is subject to mechanical stress from the muscles used in mastication (Peterson and Dechow, 2003). It has previously been reported that the

vault endures very low strain compared to the mandible during mastication (Endo, 1966; Endo, 1970; Hylander, 1987). Low strains suggest that a low threshold of strain is necessary for mechanical maintenance and that mechanical loading is less important in the vault than in other parts of the craniofacial skeleton (Hylander and Johnson, 1997). The results of this analysis are in agreement with these suggestions. Stresses found in the cranial vault did not vary greatly between the orthognathic and prognathic facial forms. The finite element analysis results showed very little stress in the vault region in general. The only areas of the vault which showed Von Mises stress, more specifically tensile stress, was in the frontal bone superior to the orbits in the prognathic facial form, but this was minimal. The orthognathic facial form has a value of close to zero in this region for Von Mises stress. The slight increase in stress in the frontal bone region may be a function of the bone accommodating for small amounts of masticatory stress in the prognathic facial form, however, the levels are very low.

7.3.2 NASAL APERTURE STRESS

Glanville (1969) investigated a group of Europeans and found that the nasal index significantly correlated with orbital and upper facial indices but not with cranial indices. Glanville found that increased prognathism was associated with an increasingly short, broad nose (Glanville,1969). Glanville (1969) also mentions the association between intercanine breadth and nasal breadth, suggesting the developed root of the canine tooth reaches far into the maxilla, and the forces incurred by the anterior loading of the teeth (specifically the canine) during biting and tearing was accompanied for by the boney buttressing on either side of nasal opening.

As previously mentioned, the nasal shape has been dictated by the adaptation to cold conditions by the extension of the pyriform aperture away from the base of the skull (Rak, 1986). A larger nasal opening stretched the rest of the face forward along with it. Using finite element analysis, Strait *et al.* (2009) investigated the role that feeding mechanics played in the evolution of craniofacial morphology. Columns of bone on either side of the nasal aperture were shown in strain analysis for a premolar bite. *A. africanus* craniofacial region was shown to experience more stress as compared to the *M. fascicularis* model; therefore, *A. africanus* craniofacial morphology is being influenced more by biomechanical stress induced by the forces of mastication. Strain observed along the nasal margins in *A. africanus* meant that bone in this area was biomechanically adapted to successfully accommodate stress during mastication. An increase in stress at the anterior pillars means a change in this buttressing would be detrimental to feeding behaviours of *A. africanus*.

However, as representatives of a group, but expressing a difference in the degree of prognathism, the region surrounding the nasal aperture between models in this study showed variation in Von Mises stress results. Differences in Von Mises stress occurred even though nose dimensions did not differ. This pattern may be attributed to the degree of prognathism and the presence of buttressing in the region of the anterior maxilla lateral to the nasal margins. As seen here, a wider nasal aperture forces the distribution of stress around the curvature of the nose and around the lateral margins to transfer stress up into the interorbital region.

Gross *et al.* (2001) modeled the skull of a modern male of European ancestry. Although their model used much fewer nodes (1800 as compared to the 110 645 nodes

used in the orthognathic modeled here) a general pattern of Von Mises stress under masticatory loads could be observed. Gross *et al.,* (2001) observed an increase in stress in the facial region of the model under compressive loads at the first incisor and second molar. Stress dissipated in the facial skeleton, traveled upward from the loading sight around the nasal aperture to the interorbital region. The zygomatic arch also accommodated for high levels of Von Mises stress as was seen in the current research. Similarly the authors attributed high stress in the zygomatic arch to masseter muscle origins. From the finite element analysis carried out by Gross *et al.,* (2001), a general pattern of stress is observed and is directed by the geometry of the model, which is much less refined than the two models in the current research.

In looking at the nasal aperture, differences in nasal breadth are very slight between the two individuals that were modeled in the finite element analysis, however, the stress distribution pattern in this region does differ. The pattern in stress between the two models may be a direct reflection of facial skeleton accommodation for changes in morphology associated with prognathism. Although the patterns are the same in relative shape for both models, the prognathic has a greater area of stress between the tooth that is loaded and the nasal aperture.

7.3.3 SUPRAORBITAL REGION STRESS

The role of the supraorbital region has been debated as to its functional use in accommodating for the stress of large masticatory loads. Well-developed browridges are thought to accommodate for stress for an increased bite force in primates and are more associated with anterior tooth loading (Hylander *et al.,* 1991b). Hylander *et al.* (1991b) found that overall stress in the supraorbital region was not larger in more prognathic non-

human catarrhines, and that no clear connection between browridge expression and masticatory stress in these primates existed. They concluded that, in this, case browridge expression was related to brain position.

Dechow *et al.* (1993) found that the magnitude of stress in the browridge region of humans is low compared to other areas of the facial skeleton. The current research also established that there are lower levels of stress in the frontal region than the rest of the craniofacial skeleton. Dechow *et al.* (1993) measured the material properties in human craniofacial bone specifically within the supraorbital region and the mandible and found that these areas differed in their elastic properties. This was thought to be because of differences in function of the two areas, and the fact that the mandible accommodated for a higher magnitude of stress, more similarly found in the femur than the supraorbital region.

Strait *et al.* (2009), also while using finite element analysis on the skulls of *A. africanus* and *M. fascicularis,* found low levels of Von Mises stress in the browridge area of both models. As it is shown here, and is consistent with current research, mastication and forces experienced while chewing do not have a direct influence on the browridge morphology or its degree of expression.

7.3.4 ZYGOMATIC ARCH STRESS

Load bearing bones have more strength than is needed to keep typical mechanical loads from causing harm, and the zygomatic arch is considered a cranium load bearing bone (Frost, 2003). Peterson and Dechow (2003) investigated the material properties in human crania. These authors found that the zygoma experiences greater levels of strain than the adjacent temporal and frontal bone due to its masseter muscle origins. The authors also found that it has a large maximum stiffness value to withstand the forces under contraction

(Peterson and Dechow, 2003). Muscle bearing sites, like that of the zygomatic arch, adapt to local strain environments caused by forces incurred during muscle contraction like that of masticatory muscles (Rubin *et al.,* 1990; Bertram *et al.,* 1991; Peterson and Dechow, 2003). Under normal circumstances bone development and remodeling maintains a degree of deposition and resorption directly related to the mechanical environment of the skeletal tissue.

Reaction of the zygomatic arch to the contraction of masticatory muscles has been investigated in several facial forms. An investigation into the zygomatic arch of macaques found increased strains in the anterior region and decreased strain posteriorly (Hylander and Johnson, 1997). The zygomatic arch has fixed ends, with the origin of the masseter muscle attachment along the anterior inferior portion (White, 2000). Hylander and Johnson (1997) found that there was three times more strain anteriorly than posteriorly in the zygomatic arch and that dimensions and architecture differed from anterior to posterior. The anterior region of the zygomatic arch is comprised of nearly solid cortical bone, whereas the posterior region has more trabecular bone with a thin layer of cortical bone surrounding it. Decreased strains recorded in the posterior region corresponded with the regions previously found to have a subsequent decrease in mass.

Kupczik *et al.* (2007) investigated the zygomatic arch of *Macaca fascicularus.* In this case, the zygomatico-temporal suture was modeled while using linear isotropic homogenous material properties with a bite force on the first and second molars. Results again showed an increase in the bone strain at the anterior region of zygomatic arch and a decrease in strain posteriorly as previously reported. Also, a high strain was recorded at the base of the zygomatic arch root at the temporal bone (Kupczik *et al.*, 2007).

The results of this study demonstrate, through displacement analysis, that the zygomatic arch of the prognathic facial form in humans is inferiorly displaced more than in the orthognathic facial form during both an incisor and molar bite. Tensile stress is high in both the anterior and posterior regions of the zygomatic arch, but decreases in the middle region for both models. The zygomatic arch of the prognathic facial form incurs more stress than the orthognathic facial form. Zygomatic arch stress can be a function of increased muscle force having to be exerted by the prognathic model because of the increase in the length of the lever arm.

The size of the area of stress at the zygomatic arch varies between the two models. As a load bearing bone and one with direct attachment of the masseter muscle, the zygomatic arch appears as though it incurs high magnitudes of stress. Increased anterior zygomatic arch stress has been previously recorded in macaques by Hylander and Johnson (1997), which is consistent with the current study. Hylander and Johnson (1997) described actions of the zygomatic arch, as it was being twisted about the long axis. This twisting was due to the direct attachment of the masseter muscle; therefore, the zygomatic arch experiences higher stress levels in the anterior region than the posterior. Similar results were observed on the arch itself for Von Mises analyses during a molar bite, an incisor bite and when the superficial head of the masseter was modeled.

7.3.5 STRESS OF THE INTERORBITAL REGION

Previous research modeling bone has found that the interorbital region incurs higher stress than other regions of the craniofacial skeleton when external forces are loaded (Hylander *et al.*, 1991b). Hylander *et al.* (1991b) recorded that bending in the frontal plane occurs in the area of the interorbital region of the *Macaca fascicularis*. These authors

recorded that the interorbital region experiences the most intense bending stress during incision or anterior tooth loading. Bending of this area is thought to be due to the bite force pushing upward from the dental arcade and the masseter and temporalis muscles pulling downward (Hylander *et al.,* 1991b). Peterson and Dechow (2003) found that the site of the glabella region on the frontal bone had a direction of maximum stiffness parallel to the browridge.

The interorbital region of macacas has recorded lower strain levels than in other regions of the primate face (Hylander and Johnson, 1997). The lower levels of stress recorded in the interorbital region maybe a direct reflection of the bone composition in that area, since Hylander and Johnson (1997) also noted that this area is made up of a thick, dense layer of cortical bone. However, with its function to accommodate mechanical strain, there is a heritably factor involved, as well in the interorbital regions architecture in *Macaca fascicularis*.

The results of the finite element analyses showed that stress distribution in the interorbital region was different between the two facial forms. The interorbital region incurs more stress in the prognathic facial form over the orthognathic facial form. Incisor biting causes more stress at the interorbital region than molar biting. The pressure analysis shows a section in the interorbital region running horizontally between the orbits that are experiencing more compression stress in the prognathic model.

Additional evidence from the current study showed that the interorbital breadth between the two facial forms was significantly different between the groups ($p \leq 0.05$) and correlated to the degree of prognathism ($p \leq 0.01$). When an individual is more orthognathic, the interorbital breadth distance tends to be increased. These results are supported from

Von Mises stress distribution in the frontal views, where the orthognathic facial form has less stress in area and magnitude in the interorbital region. The interorbital area is functioning to decrease stress in this facial form with increased cortical bone forming a boney pillar between the orbits. The decreased stress in the interorbital region occurs with the increased distance between the orbits in the orthognathic facial form, and could possibly be due to the change in cortical bone thickness functioning to withstand masticatory stress resulting in the orthognathic cranial facial form being more functionally adapted to accommodate for masticatory stress in this region.

Interorbital breadth has previously been used to help distinguish ancestry within a South African sample, but was found to be highly variable (L'Abbé *et al*., 2011). Hefner (2009) found that the morphological expression of the interorbital region (narrow, intermediate, wide) from a North American sample was wide in those of African ancestry and intermediate to narrow in those of European ancestry. In the current study, the significant correlation of a wide interorbital breadth with orthognathism seems to contradict Hefner's (2009) work where those of European ancestry would be more orthognathic but have a more narrow interorbital breadth.

In the current study, the significant correlation of orthognathism and larger interorbital breadth was derived from a sample of 162 individuals and supported by the modeling of an individual orthognathic skull from that sample. The increased interorbital breath may have variability in genetic origins but it also might be rooted in the multiple changes in the craniofacial skeleton to a more orthognathic facial form. Within a South African sample with high variability in the interorbital width this feature might be one of the many facial characteristics, which modifies slightly (yet with a degree of significance) in

accommodating for the variation in prognathism in this population. However, if interorbital width has its origins in ancestry, maybe a slight increase in the facial feature can be correlated with orthognathism in this population specifically. The increase in interorbital width does function to accommodate masticatory stress and the orthognathic model has less stress in this region over the prognathic model.

Grant (1972) mentioned that there are various buttresses of the face to prevent bone of the craniofacial region from being displaced upwards. One of these bony buttresses is in the region of the nasal part of the frontal bone in the interorbital region (Grant, 1972). The rigid frame models developed by Endo (1966) indicated that the face is made up of a series of straight uniform pillars with the same cross sectional area. One of these pillars is said to be vertically orientated in the interorbital region. In the area of the interorbital pillar during anterior biting this area is subjected to compressive forces. While loading posterior teeth, the interorbital region experienced both laterally directed bending and compressive forces.

The skeletal architecture of the face has been developed to accommodate the mechanical loading of mastication. The stress transmitted to the skull is directed and accommodated for by a series of vertical and horizontal buttresses in the face and vault (Rowe and Killey, 1955; Stanley, 1995; Berryman and Symes 1998). As the origin of force is on the occlusal surface of the tooth, the stress throughout the skeleton travels away from the point of compression and is directed by the path of least resistance in the craniofacial skeleton and by muscle insertion points. Stanley (1995) states that the zygomaticomaxillary buttress must accommodate for the greatest amount of force incurred from occlusal loading.

Chapter 7
DISCUSSION

Le Fort fractures are characterized as those that appear in specific patterns indicative of weak points in the facial skeleton (LeFort, 1972; Rogers and Allan, 2012). The stress pattern for a molar bite for the prognathic model appears to follow the route as described in the Le Fort fracture pattern II and III. The path of stress runs along the zygomaxillary suture and shows a horizontal region of stress through the lateral margins of both orbits and the intraorbital region as seen from the anterior and lateral views. Also, the anterior zygomaticotemporal sutural region of the anterior zygomatic arch is affected, as seen in the lateral view, mimicking the Le Fort III. The incisor bite has the same horizontal stress in the orbits and intraorbital region as the molar bite and characteristic of Le Fort III. In the alveolar region stress appears to be localized in the buttress of the hard palate of the maxillary/alveolar bone subnasally and does not clearly follow the classic Le Fort I fracture pattern as the entire region is accommodating for high stress especially in the incisor bite of both models. However, for both models during a molar and incisor bite the bone lateral to the nasal aperture records high Von Mises stress because the stress is directed by the buttressing of the alveolar ridges and the nasofrontal process of the maxilla. The Von Mises stress patterns occur along the weaker points of the facial skeleton. Therefore stress patterns due to mastication follow the Le Fort fracture patterns as seen in trauma. It is also important to note that the observed patterns from the finite element analysis which support the Le Fort fracture patterns gives credibility to the accuracy of the model creation and imposed constraints.

The current research also indicates differences in the compressive stress a molar has compared to an incisor bite. When looking at the pressure results in Figure 46 (molar) and in Figure 50 (incisor), during the molar bite, the interorbital area experiences less compressive

forces than when the incisor bite is modeled. Molar compression is localized to the working side of the interorbital region, where the incisor bite shows compression horizontally across the interorbital region. When individual muscles were modeled, the superficial head of the masseter and the temporalis muscle generated the highest Von Mises stress levels in the interorbital region, creating an even lateral region of stress that ran between the orbits. The increased length of the temporalis muscle because of the dolichocranial shape, coupled with the necessary increased muscle force needed for the prognathic model to produce the bite force may account for this stress pattern. Both muscles created high stress in the interorbital area, but the prognathic facial form incurred a larger region of Von Mises stress over the orthognathic facial form, showing the orthognathic facial form is more suited to accommodate stress in this region.

7.3.6 STRESS AT THE ARTICULAR EMINENCE

Working and balancing reaction force at the temporomandibular joint for incisor biting has been previously observed in Pleistocene hominids and recent humans (O'Connor *et al.,* 2005). Neandertal had a more equal distribution of reaction forces between the working and balancing side at the articular eminence than was recorded in modern humans. The reason that the articular eminence forces were more evenly distributed between the two condyles in Neandertal than in modern humans is due to the fact that Neandertals had a wider intercondylar distance. The wide intercondylar distance is related to the wide cranial base of Neandertal, and this distance proved advantageous under masticatory stress (O'Connor *et al.,* 2005).

Forces at the articular eminence for this study were modeled in the finite element analysis as reaction forces of the muscles on the working and balancing sides. In the skulls

modeled, the working side incurred a greater magnitude in force than the balancing side. The resultant stress from simulated mastication at the articular eminence also reflected this phenomenon. The prognathic model had a greater difference in stress between the working and balancing sides over the orthognathic model. In the basal view of the models, patterns of compressive stress appear to be more equal in area and magnitude for the orthognathic model than in the prognathic model for both incisor and molar bite, which is consistent with previous research (Hylander, 1975, 1977; O'Connor *et al.,* 2005). From this current study, being orthognathic seems to be more advantageous than prognathic when looking at a more even distribution of stress at the articular eminence, however, the orthognathic has a larger area and degree of stress in the balancing sides over prognathic.

In the inferior view (Figure 76) the temporalis muscle during a molar bite appears to cause larger differences in Von Mises stress distribution at the articular eminence for the prognathic facial form than that found in the orthognathic facial form. It might be said that the increased cranial length in the prognathic model and subsequent increased length of the temporalis muscle both in the anterior and posterior portions causes a decrease in stability at the condyle. The orthognathic model, however, has more stress in the balancing side articular eminence with a more even distribution in the articular eminence. This recorded increase in stress in both condyles can represent a greater stability during articulation with the mandible and, therefore, a decrease in temporomandibular disorders with this facial form.

Contraction of the medial pterygoid muscle during a molar and incisor bite (Figure 78 and 89) showed that Von Mises stress increased in area and magnitude in the balancing side at the articular eminence of the orthognathic model. The prognathic facial model recorded

relatively even stress for a molar bite at the articular eminence. These results indicate that an increase in prognathism may be helpful in equalizing both balancing and working's side forces of the medial pterygoid muscle. However, from a clinical perspective, if the malocclusion of an individual results in the medial pterygoid muscle being used as the dominant muscle for the cycles of mastication or if the medial pterygoid is the dominant muscle for an individual for mastication, then this could result in chronic stress at the articular eminence. If the overall area of the articular eminence incurs more chronic stress, this may indicate a reason for a higher incidence of temporomandibular joint disorders.

Temporomandibular joint disorders have been described in the literature with symptoms such as pain in the masticatory muscles, limited movement and joint discomfort (De Boever and Carlsson, 1994; Ostermann *et al*., 1999). The etiology of temporomandibular joint disorders is multifactorial and may not be attributed to a single cause, in most cases, but the masticatory muscles and occlusion of the individual are key factors (Solberg *et al*., 1986; Wadhwa *et al*., 1993; Nie *et al*., 2010; Badel *et al*., 2012).

It can safely be stated that the origins of temporomandibular joint disorder are rooted in the biomechanics of the masticatory system (Singh and Detamore, 2009). However, the results shown in the current study indicate less stability for the prognathic individual, and this can lead to an increase in temporomandibular joint disorders. The implications for this study with regard to maxillo-facial surgery is that with an understanding that prognathic individuals are more susceptible to temporomandibular joint disorders, any alterations to the craniofacial architecture may further aggravate this condition. More specifically, if surgery directly affects the origins or attachment sites for specific masticatory muscles there could be further repercussions. For example, if masticatory muscle

contraction force of the medial pterygoid or temporalis is increased to accommodate the masticatory system function, an already unbalanced stress at the articular eminence may be further intensified and increase temporomandibular joint pain or discomfort.

7.4 CONSTRAINTS OF METHODOLOGY

The methodology in creating the two digitized 3D models of the crania for the finite element analysis was taken from previous studies (Tanne *et al.*, 1988; Motoyoshi *et al.*, 2002; Mota *et al.*, 2003; Provatidis *et al.*, 2007; Röhrle and Pullan, 2007) . Although the creation of each model was the same, the individual geometry not related to prognathism can play a role in the results. Such factors as the modeling of the muscles between the skulls may affect the stress distribution results. Even though muscles were modeled the same way, the origins of the muscles differed within each individual skull in their attachment location and area. Because of this, the number of nodes selected on each model can vary. For example, one skull may have 200 nodes representing the superficial masseter muscle on the zygomatic arch and the other might have 250 nodes. The skull with the higher number of nodes will have the force of the muscle distributed over a larger number of nodes. The specific areas of muscle attachment in a muscle, like the temporalis, which is located higher on the lateral sides of the skull in the orthognathic skull than in that of the prognathic skull, may play a role in differences in stress distribution as well. As much as the intricate details may be different between the skulls, it was the aim of this study to observe patterns of stress in the craniofacial skeleton away from the direct insertion points and the point of compressive bite force on the occlusal surface of each tooth. If more than the two skulls were modeled it would still reflect the individual geometry of that skull. The patterns of distribution will be different when analysis is run reflecting the architecture. However, the

overall regions, patterns and magnitude observed due to muscle contraction forces in the Von Mises analysis would be similar.

Differences in force production may contribute to differences in the stress analysis between the two models. Vertical force of the bite on the incisor and molar was held constant, but individual muscle forces varied between the two models where the orthognathic skull produced less muscle force to achieve incisor and molar bites than the prognathic model.

Determining the specific magnitude of force to be used for individual masticatory muscles was difficult. Problems occurred in determining force values because previous research in some cases did not look at a specific muscle, the force data for the species was not available or muscle origins were previously defined differently. For example, in the case of the temporalis muscle, data from the literature were modified to suit the current models. As was previously discussed, (Chapter 3: Materials and Methods, Section 3.6.2.4) because the temporalis muscle was divided into seven sections in this study, running from anterior to posterior, and Blanksma and van Eijden (1990) used a temporal muscle divided into six, the data were modified. For the temporalis section 6 here, an average value from the data used from Blanksma and van Eijden (1990) temporalis section's 5 and 6 was used. Section 7 of the temporalis was weighted as previously done for Blanksma and van Eijden's (1990) section six. This change in modeling the temporalis muscle may have altered the outcome of the results, however, it follows a realistically simulated method previously used by Blanksma and van Eijden's (1990). As muscle contraction forces will also vary by individual, the models prove to be sufficient to depict stress patterns under masticatory loading.

One factor that was accounted for was the difference in skull size; as a consequence, everything was adjusted to the same scale, so the overall size did not have an effect on the stress distribution results, just the geometries. Several aspects in differences in geometry besides prognathism may also have an effect on stress distribution, as the models represent individuals. An option to overcome this might have been to use the same model and vary the degree of prognathism, however, using the same model and only varying the degree of prognathism would not be realistic. As it is understood from the current research other craniofacial dimensions are also affected by prognathism, and these would not have been accounted for if a single skull was modified and the finite element analysis run.

The decision to model forces of mastication through the forces of muscle insertions points and as compressive forces at the incisor and molar creates a more accurate result. The alternative of simply pulling the face forward would create less accurate results than seen here because of the bone varying its response to areas of compression and tension forces.

Another possible constraint of the methodology used in the current research may be in the assignment of material properties. Previous studies (Tanne *et al.*, 1989a; Tanne *et al.*, 1989b; Tanne and Sakuda, 1991; Daegling and Hylander, 1998; Strait *et al.*, 2005; Ichim *et al.*, 2006; Provatidis *et al.*, 2008; Curtis *et al.*, 2008; Savoldelli *et al.*, 2012; Merdji *et al.*, 2013) have found linear elastic homogenous properties to achieve realistic results instead of using anisotropic properties. It stands to reason that the more accurate the model created, the more accurate the responses to external forces that can be achieved (Cattaneo *et al.*, 2003; Koolstra, 2003; Richmond *et al.*, 2005; Strait *et al.*, 2005; Ross, 2005; Wang *et al.*, 2006; Liao *et al.*, 2007). The finite element method allows researchers to get insight into the

biomechanical responses to masticatory stress where in vitro studies would be impossible. As the technology and programs involved with running a finite element analysis become more available to researchers, a more accurate model can be generated and analyses run. Increasing the accuracy of the models would be done by including the heterogeneous material properties of craniofacial and vault bones. This increased accuracy of the models would be advantageous to clinicians. A specific finite element analysis could be run on a patient-by-patient basis using anisotropic material properties and reflecting their specific cranial geometry. Various types of implant and orthodontic surgery would benefit by understanding bone response before the procedures were carried out. It is the power of the finite element analysis to predict bone response to loads, which makes it an asset to the field of medicine. The modeling of heterogeneous material properties for the skull and dentition was beyond the scope of this project.

7.5 SUMMARY

When modeling a biological tissue like bone, it must be understood that, although the 3D model is representative of the geometry of the skull, the geometry and the material properties of the bone are influenced by many factors. The morphology of the skulls can be affected functionally and, therefore, be remodeled in response to a mechanical loading history. Also, morphological features and geometry are influenced by genetics, forces selected against for evolutionary purposes and the constant physiological process of remodeling over time (Voo *et al.,* 1996).

The results of the finite element analysis can be interpreted in many ways. If the two facial forms are taken as a time line, with the prognathic facial form changing over time to a more orthognathic expression, a number of points can be made about the change in

patterns observed. If changes take place over time to make the craniofacial regions adapted to be more mechanically efficient, they should undergo less stress. Areas of high stress in the prognathic facial form should be presented as areas of lower stress in the orthognathic facial form. This is what was observed between the 3D models. The greatest reduction in size and robusticity of the craniofacial skeleton followed the change in the diet of early hominids. It can be seen here that the process of accommodating for masticatory stress to become more biomechanically efficient continues in modern humans. The process of bone remodeling is likely to be influenced more as modern human populations become more heterogeneous and genetically influenced patterns of morphology arise in the craniofacial skeleton.

Notable patterns of high stress occur in the areas of the interorbital region, the lateral margins of the orbits on both working and balancing sides and at the lateral margins of the nasal aperture for both an incisor and molar bite in the prognathic facial form. All these areas have a reduction in stress when results of the finite element analysis are observed for the orthognathic facial form. A reduction in stress can be indicative of a system more efficiently suited to mastication of softer foods. Over time, these areas of high stress have become functionally adapted to incur lower levels of stress.

Overall these results suggest that the shape of the cranial vault has little to do with the accommodation of mechanical stress due to the forces of mastication. Morphological changes in the vault is most likely a function of genetic differences between populations, or due to geographic and climatic differences (Steele and Bramblett, 1988; Bass, 1995; Gill, 1998; Byers, 2002; Roseman and Weaver, 2004). The stress distribution patterns also correlated with the metric results with regard to vault length and breadth and the degree of

prognathism. Stress, vault shape and prognathism do not appear to have a direct association.

Nasal shape does not seem to be functionally related to dealing with the forces of mastication, however, the difference in shape of the maxillary region due to prognathism causes the skull to experience different stress patterns surrounding the nasal opening. A correlation between the degree of prognathism and nasal shape was not supported with this research. Nasal shape does not appear to have a function in masticatory apparatus, besides creating an area in the maxillary region to direct stress around the aperture.

The size of areas of the craniofacial skeleton, vault, dentition or mandible does not have a direct correlation with the function of mastication. Areas of stress observed and the size recorded in specific areas thought to be biomechanically influenced cannot be explained solely by masticatory factors. For both models, areas of high Von Mises stress for a molar bite was in the interorbital region, maxilla, working side of the nasal aperture, lateral margin of the working side orbit, the anterior superior region of the zygomatic arch and the posterior root of the zygomatic arch. Areas of high Von Mises stress summarized for an incisor bite were in the interorbital region, lateral sides of the nasal aperture, lateral margin of the working side orbit, working side anterior regions of the zygomatic arch and the posterior root.

Morphological characteristics graded on degree of robusticity did not correlate to size, prognathism or Von Mises stress distribution, however, both the prognathic and orthognathic are more efficient during masticatory forces on the first molar. These results indicate that as a skeletal biologist, attributing change in the skeleton just for

accommodating masticatory forces would be incorrect. A multifactorial approach to bone remodeling or morphological changes should be the common practice.

7.6 FUTURE DIRECTIONS

The availability of the finite element method to anthropologists and researchers in biomechanics has proved to be a useful tool in predicting stress patterns in the skeleton. As material properties of specific bones and regions of bones become available, models will become more accurate representations of the intricate geometry found in the human skeleton.

The current research is a starting point from which to build the knowledge of masticatory forces in modern human populations. As ancestry and sex differences were accounted for here, future research should do the same to run new masticatory stress analysis within genetically different populations. Genetically different population would still need to integrate the variations in morphology with the biomechanical needs of the masticatory apparatus. In accomplishing this stress analysis would result in different patterns of Von Mises stress and shed insight on how the facial skeleton accommodates for masticatory stress with variations in architecture. Direct comparisons could then be made to draw conclusions on the more efficient morphology for mastication and possible areas correlating to pathologies within the masticatory apparatus. The results should then be compared to stress patterns seen in the two crania modeled in the current research. Changes in patterns would then need to be attributed to biomechanical influences and other intrinsic or extrinsic factors. Interpreting the patterns of stress researchers should always take into account a multifactorial approach.

Future research directions that have arisen as a result of this work should be focused in the area of the articular eminence. Stress distribution at the articular eminence and how it varies from balancing to working sides in the masticatory apparatus needs further understanding with regard to muscle involvement and the craniofacial forms of orthognathism, prognathism and retrognathism. Here the decreased stability at the articular eminence was observed in the prognathic model over the orthognathic model. Future research needs to compare the stress at the articular eminence of a retrognathic model. Results from such research can add further knowledge to the debate of temporomandibular disorders.

CHAPTER 8

CONCLUSIONS

- Considerable debate exists as to the evolutionary mechanisms that initiated a reduction in mid-facial projection and dentition in modern humans. As part of the masticatory apparatus, a change in diet from harder to softer foods and consequently the mechanical loading of the jaws could possibly have influenced these regions of the facial skeleton. This region of the face formed the focus of this study.
- Due to the need of the facial skeleton to accommodate strain from the actions of mastication, prognathic and orthognathic facial forms produce different compression and tension stresses. In this study, the observed differences that may be attributed to sex and ancestry were accounted for by using only black South African males so differences could be directly related to mastication and prognathism in this population.
- Results from this study suggest that the orthognathic facial form is biomechanically more adapted to accommodate masticatory stress. The orthognathic group shows a larger inter-orbital dimension with a subsequent decrease in stress in that area. The evolutionary trend toward a more orthognathic facial form in modern humans may have biomechanical origins.

- A trend was noted for a number of cranial dimensions to increase or decrease with prognathism. Shape changes were also associated with the degree of prognathism found in the upper facial index, maxillary molar crown area and the dental arcade shape. Cranial dimensions significantly correlated with the gnathic index were the basion - bregma height, maximum alveolar length, orbital breadth, orbital height, inter-orbital breadth, mandibular body breadth, and minimum ramus breadth. The null hypothesis that no relationship would exist between the degree of prognathism and cranial characteristics was rejected and therefore it was concluded that a relationship does exists with cranial dimensions and morphology and the degree of prognathism.
- Mechanical loading greatly influenced different regions of the facial skeleton during mastication and varied with morphological patterns. Therefore, when changes to the masticatory apparatus arise from clinical involvement, patterns of stress should be further investigated to possibly avoid or predict failure in the underlying architecture.
- When masticatory muscles were modeled individually, temporalis and medial pterygoid muscles accounted for the greatest amount of uneven stress distribution between the working and balancing side articular eminences. Future research needs to examine masticatory stress in the area of the articular eminence in other cranial facial forms as a means to provide insight into the origins of temporomandibular disorders.

- The application of finite element analysis to orthodontic surgery would be valuable to assess how patients respond to changes in loading of the facial skeleton and/or the masticatory apparatus.
- Future projects may involve generating a model of white adult males loaded with the same external loads for comparison to both the prognathic and orthognathic model used in this study. Although the degree of prognathism was investigated and ancestry accounted for, it is predicted that the white male patterns of Von Mises stress would be different from the orthognathic model of African ancestry.
- There are characteristics of the black African male craniofacial form that are related to the degree of prognathism. However, modification in an individual characteristic cannot solely be attributed to prognathism. As changes occurred to produce a more orthognathic facial profile this also shaped a more biomechanically efficient craniofacial form to accommodate for masticatory stress. These results support Wolff's Law where a change in function, which can be seen by the differences in Von Mises stress patterns between the two models, is met with a change in shape while maintaining a masticatory system that efficiently, and without failure, accommodates for the stress experienced by bone during mastication.

REFERENCES

Abbie AA. 1947. Head form and Human Evolution. Journal of Anatomy 81:233-258.

Adams BJ and Byrd JE. 2002. Inter-observer error Variation of Selected Postcranial Measurements. Journal of Forensic Sciences 47:1193-1202.

Adams DC, Rohlf FJ and Slice DE. 2004. Geometric morphometrics: ten years of progress following the 'revolution'. Italian Journal of Zoology, 71(1), 5-16.

Agarwal SC and Grynpas MD. 1996. Bone Quantity and Quality in Past Populations. The Anatomical Record 246:426-432.

Alba DM, Moyà-Solà S, Köhler M (2001) Canine reduction in the Miocene hominoid *Oreopithecus bambolii*: behavioural and evolutionary implications. *J Hum Evol* 40, 1–16.

Allan JC. 1982. About Correlation. In: Learning about Statistics. Johannesburg, South Africa: Macmillan South Africa (PTY) Ltd. p 122-140.

Amira® 5.1 User's Guide, Visage Imaging, 2009. Available at http://www.amira.com/documentation/manuals-and-release-notes.html

Anderson DJ, Matthews B (eds). 1976. *Mastication*. Bristol: John Wright.

Antón SC. 1990. Neandertals and the anterior dental loading hypothesis: a biomechanical evaluation of bite force production. Kroeber Anthropol. Soc. Paper. 71e72, 67e76.

Antón SC. 1994. Biomechanical and other perspectives on the Neandertal face. In: Corruccini, R.S., Ciochon, R.L. (Eds.), Integrative Paths to the Past. Prentice Hall, Englewood Cliffs, pp. 677e695.

Antón SC. 1996. Tendon-associated bone features of the masticatory system in Neandertals. Journal of Human Evolution 31:391-408.

Ashman RB, Cowin SC, Van Buskirk WC, and Rice JC. 1984. A Continuous Wave Technique for the Measurement of the Elastic Properties of Cortical bone. Journal of Biomechanics 17:349-361.

Athreya S. 2009. A comparative study of frontal bone morphology among Pleistocene hominin fossil groups. Journal of Human Evolution 57 (6): 786–804.

Baab KL, Freidline SE, Wang SL, Hanson T. 2010. Relationship of Cranial Robusticity to Cranial Form, Geography and Climate in *Homo sapiens*. American Journal of Physical Anthropology 141:97-115.

References

Badel T, Marotti M, Pavicin IS, Basić-Kes V. 2012. Temporomandibular disorders and occlusion.Acta Clin Croat. Sept, 51(3):419-24.

Bass WH. 1995. Human Osteology: a laboratory and field manual. Columbia: Missouri Archaeological Society.

Bastir M and Rosas A. 2006. Correlated variation between the lateral basicranium and the face: a geometric morphometric study in different human groups. *Archives of Oral Biology*, *51*(9), 814-824.

Bastir M, Rosas A, Lieberman DE, O'Higgins P. 2008. Middle cranial fossa anatomy and the origins of modern humans. Anatomical Record 291 (2):130-140.

Beals KB., Smith CL., Dodd, SM. 1983. Climate and the evolution of brachycephalization. Am. J. Phys. Anthropol. 62, 425–437.

Benjamin M, Toumi H, Ralphs JR, Bydder G, Best TM, Milz S. 2006. Where tendons and ligaments meet bone: attachment sites ('entheses') in relation to exercise and/or mechanical load. Journal of Anatomy 208:471-490.

Bernal, V., S. I. Perez, and P. N. Gonzalez. 2006. Variation and causal factors of craniofacial robusticity in Patagonian hunter-gatherers from the late Holocene. Am. J. Hum. Biol. 18:748-765.

Berryman HE, Symes SA. 1998. "Recognizing gunshot and blunt cranial trauma through fracture interpretation." *Forensic osteology: advances in the identification of human remains. Springfield: Charles C. Thomas*. pp 333-352.

Bertram, JEA, Swartz SM. 1991. The 'Law of Bone Transformation': A Case of Crying Wolff?. *Biological Reviews* 66.3: 245-273.

Birkby WH. 1966. An evaluation of race and sex identification from cranial measurements. American Journal of Physical Anthropology 24:21-28.

Björk A. 1950. Some Biological Aspects of Prognathism and Occlusion of the Teeth. Acta Odontologica Scandinavica 9:3-27.

Blanksma NG, van Eijden TMGJ. 1990. Electromyographic Heterogeneity in Human Temporalis Muscle. Journal of Dental Research 69:1686-1690.

Blanksma NG, van Eijden TMGJ, van Ruijven LJ, Weijs WA. 1997. Electromyographic Heterogeneity in the Human Temporalis and Masseter Muscles during Dynamic Tasks Guided by Visual Feedback. Journal Dental Research 76:542-551.

Borchers L, Reichart P. 1983. Three dimensional stress distribution around a dental implant at different stages of interface development. Journal of Dental Research, 62, 155.

Boryor A, Geiger M, Hohmann A, Wunderlich A, Sander C, Sander FM, Sander FG. 2008. Stress distribution and displacement analysis during an intermaxillary disjunction- A three-dimensional FEM study of a human skull. Journal of Biomechanics 41:376-382.

Bowers CM. 2004. Forensic Dental Evidence: An Investigators Handbook. San Diego: Elsevier Academic Press.

Brace CL. 1967. Environment, Tooth Form, and Size in the Pleistocene. Journal of Dental Research 46:809-816.

Brace CL. 1979. Krapina, "Classic" Neanderthals, and the evolution of the European face. J. Hum. Evol. 8:527-550.

Brace CL, Rosenberg KR, Hunt KD. 1987. Gradual Change in Human Tooth Size in the Late Pleistocene and Post-Pleistocene. Evolution 41:705-720.

Brkic H, Milicevis M, Petrovecki M. 2006. Age estimation methods using anthropological parameters on human teeth- (A0736). Forensic Science International 162:13-16.

Brodie AG. 1953. Late growth changes in the human face. Angle Orthodontist 23:146-157.

Brooks S, Brooks RH, France D. 1990. Alveolar prognathism contour, an aspect of racial identification. In: Gill GW and Rhine S, editors. Skeletal Attributions of Race Methods for Forensic Anthropology. Albuquerque, New Mexico: Maxwell Museum of Anthropology. p 41-46.

Brown P. (1992) Recent human evolution in East Asia and Australasia. Philosophical Transactions of the Royal Society of London, Series B 337: 235-242.

Brown P, Maeda T. 2004. Post-Pleistocene diachronic change in East Asian facial skeletons: the size, shape and volume of the orbits. Anthropological Science 112:29-40.

Bruner E, Manzi G. 2007. Landmark-Based Shape Analysis of the Archaic homo Calvarium from Ceprano (Italy). American Journal of Physical Anthropology 132:355-366.

Byers SN. 2002. Introduction to forensic anthropology. Boston: Allyn and Bacon.

Cabin RJ, Mitchell RJ. 2000. To Bonferroni or Not to Bonferroni: When and How Are the Questions. Bulletin of the Ecological Society of America. 81(3): 246-248.

Calcagno JM. (1986) Dental reduction in post-Pleistocene Nubia.American Journal of Physical Anthropology, 70: 349-363.

Calcagno JM., Gibson KR. (1988) Human dental reduction: natural selection or the probable mutation effect. American Journal of Physical Anthropology, 77: 505-517.

Camacho DLA, Hopper RH, Lin GM, Myers BS. 1997. An Improved Method for Finite

Element Mesh Generation of Geometrically Complex Structures with Application to the Skullbase. Journal of Biomechanics 30:1067-1070.

Carlson, D. S., & Van Gerven, D. P. (1977). Masticatory function and post-Pleistocene evolution in Nubia. *American Journal of Physical Anthropology*, *46*(3), 495-506.

Cattaneo PM, Dalstra M, Melsen B. 2003. The transfer of occlusal forces through the maxillary molars: A finite element study. American Journal of Orthodontics and Dentofacial Orthopedics 123:367-373.

Chandrupatla TR , Belegundu AD. 2002. Introduction to Finite Elements in Engineering. Upper Saddle River, NJ: Prentice-Hall Inc.

Chatvanitkul C, Lertchirakarn V. 2010. Stress Distribution with Different Restorations in Teeth with Curved Roots: A Finite Element Analysis Study. Journal of Endodontics 36:115-118.

Chen CS, Chen WJ, Cheng CK, Jao SHE, Chueh SC, Wang CC. 2005. Failure analysis of broken pedicle screws on spinal instrumentation. *Medical engineering & physics*, *27*(6), 487-496.

Chu C-S, Lin M-S, Huang H-M, Lee M-C. 1994. Finite element analysis of cerebral contusion. Journal of Biomechanics 27:187-194.

Clarke B. 2008. Normal Bone Anatomy and Physiology. Clin J Am Soc Nephrol 3: S131–S139.

Clement AF, Hillson SW, Aiello LC. 2012. Tooth wear, Neanderthal facial morphology and the anterior dental loading hypothesis. Journal of Human Evolution 62:367-376.

Clelland NL., Lee JK, Binbent OC, Brantley A. 1995. A three dimensional finite element stress analysis of angled abutments for an implant placed in the anterior maxilla. Journal of Prosthodontics, 4, 95.

Cobb SN, O'Higgins P. 2004. Hominids Do Not Share A Common Postnatal Facial Ontogenetic Shape Trajectory. Journal of Experimental Zoology 302B:302-321.

Cobb SN. 2008. The facial skeleton of the Chimpanzee-human last common ancestor. Journal of Anatomy 212:469-485.

Collard M, Wood B. 2001. Homoplasy and the early hominid masticatory system: inferences from analyses and extant hominoids and papionins. Journal of Human Evolution 41:167-194.

Comas J. 1960. Manual of Physical Anthropology. Springfield, Illinois: Charles C. Thomas.

Coon CS. 1962. The Origin of Races. New York: Alfred A. Knopf.

Couture C. 1993. Changements de position du massif facial et de l'articulation temporomandibulaire dans la lignée Néandertalienne. Organisation crâniomaxillo-faciale des néandertaliennes. C. R. Acad. Sci. II. 316, 1627e1633.

Cowin SC. 1989. Bone Mechanics. Boca Raton: CRC Press.

Cronk BC. 1999. How to use SPSS: A Step-By-Step Guide to Analysis and Interpretation. Los Angeles, CA: Pyrczak Piblishing.

Cullinane DM, Einhorn TA. 2002. Biomechanics of Bone. In: Bilezikian JP, Raisz LG, Rodan GA, editors. Principles of Bone Biology. San Diego: Academic Press.

Curran BK. 1990. The application of measures of mid-facial projection for racial classification. In: Gill GW and Rhine S, editors. Skeletal Attributions of Race Methods for Forensic Anthropology. Albuquerque, New Mexico: Maxwell Museum of Anthropology. p 55-57.

Curtis N, Kupczik K, O'Higgins P, Moazen M, Fagan M. 2008. Predicting Skull Loading: Applying Multibody Dynamics Analysis to a Macaque Skull. The Anatomical Record 291:491-501.

Curtis N, Kupczik K, O'Higgins P, Moazen M, Fagan M. 2008. Predicting Skull Loading: Applying Multibody Dynamics Analysis to a Macaque Skull. The Anatomical Record 291:491-501.

Daegling DJ, Hotzman JL. 2003. Functional Significance of Cortical Bone Distribution in Anthropoid Mandibles: An In Vitro Assessment of Bone Strain Under Combined Loads. American Journal of Physical Anthropology 122:38-50.

Daegling DJ, Hylander WL. 1998. Biomechanics of torsion in the human mandible. American Journal of Physical Anthropology 105:73-87.

Daegling DJ, Hylander WL. 2000. Experimental observation, theoretical models, and biomechanical inference in the study of mandibular form. American Journal of Physical Anthropology 112:541-551.

Daegling DJ. 2007. Relationship of bone utilization and biomechanical competence in hominid mandibles. Archives of Oral Biology 52:51-63.

Dayal MR, Kegley AD, Strkalj G, Bidmos MA, Kuykendall KL. 2009. The history and composition of the Raymond A. Dart Collection of Human Skeletons at the University of the Witwatersrand, Johannesburg, South Africa. American Journal of Physical Anthropology 140:324-335.

Dean MC. 1988. Another look at the nose and the functional significance of the face and nasal mucous membrane for cooling the brain in fossil hominids. Human Evolution 17:715-718.

De Boever JA, Carlsson GE. 1994. Etiology and differential diagnosis. In Temporomandibular Joint and Masticatory Muscle Disorders. Zarb, G.A., Carlsson, G.E., Sessle, B.E., Mohl, N.D. (Eds.). pp. 171-187. Munksgaard-Mosby, Copenhagen.

Dechow PC, Nail GA, Schwartz-Dabney CL, and Ashman RB. 1993. Elastic Properties of Human Supraorbital and Mandibular Bone. American Journal of Physical Anthropology 90:291-306.

De Greef S, Williems G. 2005. Three-dimensional Cranio-Facial Reconstruction in Forensic Identification: Latest Progress and New Tendencies in the 21st Century. Journal of Forensic Science 50:12-17.

Demes B. 1982. The Resistance of Primate Skulls Against Mechanical Stresses. Journal of Human Evolution 11:687-691.

Demes B. 1987. Another look at an old face: biomechanics of the Neandertal facial skeleton reconsidered. Journal of Human Evolution 16:297-303.

Demes B, Creel N. 1988. Bite force, diet, and cranial morphology of fossil hominids. Journal of Human Evolution 17:657-670.

De Villiers H. 1968. The skull of the South African Negro: A biometrical and morphological study. Johannesburg: Witwatersrand University Press.

DiGangi EA, Moore MK (ed). 2013. Research Methods in Human Skeletal Biology. Academic Press, Waltham, MA.

d'Incau E, Couture C, Maureille B.2012. Human tooth wear in the past and the present: Tribological mechanisms, scoring systems, dental and skeletal compensations Review Article *Archives of Oral Biology*, *Volume 57, Issue 3*, *Pages 214-229.*

Du Brul EL. 1977. Early hominid Feeding Mechanisms. American Journal of Physical Anthropology 47:305-320.

Dumont ER, Grosse IR, Slater GJ. 2009. Requirements for comparing the performance of finite element models of biological structures. Journal of Theoretical Biology 256:96-103.

Dumont ER, Piccirillo J, Grosse IR. 2005. Finite-Element Analysis of Biting Behaviour and Bone Stress in the Facial Skeletons of Bats. The Anatomical Record Part A 283A:319-330.

El-Najjar MY, McWilliams KR. 1978. Forensic Anthropology: The structure, morphology, and variation of human bone and dentition. Springfield, Illinois: Charles C. Thomas.

Endo B. 1966. Experimental studies on the mechanical significance of the form of the human facial skeleton. Journal of the Faculty of science University of Tokyo III:1-101.

Endo B. 1970. Analysis of stresses around the orbit due to masseter and temporalis muscles respectively. American Journal of the Anthropological Society of Nippon 78:251-266.

Enlow DH. 1966a. A Comparative Study of Facial Growth in Homo and Macaca. American Journal of Physical Anthropology 24:293-303.

Enlow DH. 1966b. A morphogenetic analysis of facial growth. American Journal of Orthodontics 52:283-299.

Enlow DH, Bang S. 1965. Growth and remodelling of the human maxilla. American Journal of Orthodontics 51:446-464.

Esclassan R, Grimoud AM, Ruas MP, Donat R, Sevin A, Astie F, Lucas S, Crubezy E. "Dental caries, tooth wear and diet in an adult medieval (12th–14th century) population from Mediterranean France," Archives of Oral Biology, vol. 54, pp. 287– 297, 2009.

FEBio Finite Elements for Biomechanics version 1.1.7 (University of Utah, Musculoskeletal Research Laboratories, Salt Lake City, Utah. Available at http://mrl.sci.utah.edu)

Fehrenbach MJ, Herring SW. 1996. Illustrated Anatomy of the Head and Neck. Philadelphia: W.B. Saunders Company.

Fehrenbach MJ, Herring SW. 2007. Anatomy of the Head and Neck. St. Louis, Missouri: Saunders Elsevier.

Ferrante L, Cameriere R 2009. Statistical methods to assess the reliability of measurements in the procedures for forensic age estimation. International Journal of Legal Medicine 123:277-283.

Francisus RG and Trinkaus E. 1988. The Neandertal nose. American Journal of Physical Anthropology 75 (Suppl.):209-210.

Franklin D, Oxnard CE, O'Higgins P and Dadour I. 2007. Sexual dimorphism in the subadult mandible: quantification using geometric morphometrics*. *Journal of forensic sciences*, *52*(1), 6-10.

Freidline SE, Gunz P, Harvati K, Hublin, J. 2012. Middle Pleistocene human facial morphology in an evolutionary and developmental context. Journal of Human Evolution 63:723-740.

Fried LA. 1980. Anatomy of the Head, Neck, Face, and Jaws. Philadelphia: Lea and Febiger.

Frost HM. 2003. Bone's Mechanostat: A 2003 Update. The Anatomical Record Part A 275A:1081-1101.

García LV. 2004. Escaping the Bonferroni iron claw in ecological studies. OIKOS 105(3): 657-663.

Geng J, Tan K, Liu G. 2001. Application of finite element analysis in implant dentistry: A review of the literature. Journal of Prosthetic Dentistry 85:585-598.

Gill GW. 1998. Craniofacial criteria in the skeletal attribution of race. In: Reichs KJ, editor. Advances in the identification of human remains. Springfield, IL: Charles C. Thomas. p 293-317.

Gill GW, Gilbert BM. 1990. Race identification from the mid-facial skeleton: American blacks and whites. In: Gill GW and Rhine S, editors. Skeletal Attributions of Race Methods for Forensic Anthropology. Albuquerque, New Mexico: Maxwell Museum of Anthropology. p 47-53.

Gionhaku N, Lowe AA. 1989. Relationship Between Jaw Muscle Volume and Craniofacial Form. Journal Dental Research 68:805-809.

Glanville EV. 1969. Nasal Shape, Prognathism and Adaptation in Man. American Journal of Physical Anthropology 30:29-38.

Gonzalez PN, Bernal V and Perez SI. 2009. Geometric morphometric approach to sex estimation of human pelvis. *Forensic science international*, *189*(1), 68-74.

Goto TK, Nishida S, Yahagi M, Langenbach GEJ, Nakamura Y, Tokumori K, Sakai S, Yabuuchi H, Yoshiura K. 2006. Size and Orientation of Masticatory Muscles in Patients with mandibular Laterognathism. Journal Dental Research 85:552-556.

Grant JCB. 1972. Grant's Atlas of Anatomy. Baltimore: The Williams and Wilkins Co.

Green JO, Wang J, Diab T, Vidakovic B, Guldberg RE. 2011. Age-related differences in morphology of microdamage propagation in trabecular bone Journal of Biomechanics 44(15):2659-2666.

Grine, FE. 1981. Trophic differences between 'gracile' and 'robust' australopithecines: a scanning electron microscope analysis of occlusal events. *S. Afr. J. Sci.* 77:203–230.

Gröning F, Liu J, Fagan MJ, O'Higgins P. 2009. Validating a voxel-based finite element model of a human mandible using digital speckle patter interferometry. Journal of Biomechanics 42:1224-1229.

Gross MD, Arbel G, Hershkovitz I. 2001. Three-dimensional finite element analysis of the facial skeleton on simulated occlusal loading. *Journal of Oral Rehabilitation*, *28*(7), 684-694.

Hanihara T. 1996. Comparison of Craniofacial Features of Major Human Groups. American Journal of Physical Anthropology 99:389-412.

Hannam AG, Wood WW. 1989. Relationships Between the Size and Spatial Morphology of Human Masseter and Medial Pterygoid Muscles, the Craniofacial Skeleton, and Jaw Mechanics. American Journal of Physical Anthropology 80:429-445.

Harvati K, Weaver TD. 2006. Human Cranial Anatomy and the Differential Preservation of Population History and Climate Signatures. The Anatomical Record Part A 288A:1225-1233.

Hefner JT. 2009. Cranial non-metric variation and estimating ancestry. J. Forensic Sci. 54: 985-959.

Helgason B, Taddei F, Pálsson H, Schileo E, Cristofolini L, Wiceconti M, Brynjólfsson S. 2008. A modified method for assigning material properties to FE models of bones. Medical Engineering and Physics 30:444-453.

Hennessy RJ and Stringer CB. 2002. Geometric Morphometric Study of the Regional Variation of Modern Human Craniofacial Form. American Journal of Physical Anthropology 117:37-48.

Herrel A, Schaerlaeken V, Mayers JJ, Metzger KA, Ross CF. 2007. The evolution of cranial design and performance in squamates: Consequences of skull-bone reduction on feeding behavior. Integrative and Comparative Biology1-11.

Herring SW. 2007. Masticatory Muscles and the Skull: A Comparative Perspective. Archives of Oral Biology 52:296-299.

Herring SW, Ochareon P. 2005. Bone- special problems of the craniofacial region. Orthod Craniofacial Res 8:174-182.

Hilloowala RA, Trent RB. 1988. Supraorbital ridge and masticatory aparatus II: humans (Eskimos). Human Evolution 3(5):351-356.

Hillson S, FitzGerald C, Flinn H. 2005. Alternative Dental Measurements: Proposals and Relationships with Other Measurements. American Journal of Physical Anthropology 126:413-426.

Holton NE, Francisus RG. 2008. The paradox of a wide nasal aperture in cold-adapted Neandertals: a causal assessment. Journal of Human Evolution 55:942-951.

Howells W. 1973. Cranial Variation in Man. A Study by Multivariate Analyses of Patterns of Difference Among Recent Human Populations. Cambridge, MA: Harvard University.

Howells WW. 1989. Skull shapes and the map: craniometric analyses in the dispersion of modern Homo. Papers of the Peabody Museum No. 79. Cambridge, MA: Peabody Museum.

Howells WW. 1995. Who's who in skulls: ethnic identification of crania from measurements. Papers of the Peabody Museum No. 82. Cambridge, MA: Peabody Museum.

Howells WW. 1996. Howells' craniometric data on the internet. American Journal of Physical Anthropology 101:441–442.

Hylander WL. 1975. The Human Mandible: Lever or Link? American Journal of Physical Anthropology 43:227-242.

Hylander WL. 1977. The adaptive significance of Eskimo craniofacial morphology. In: Dahlberg AA, Graber TM, editors. Oralfacial growth and development. The Hague: Mouton. p 129–170.

Hylander WL. 1987. Loading patterns an jaw movements during mastication in *Macaca fasicularis*: a bone-strain, electromyographic, and cineradiographic analysis. American Journal of Physical Anthropology 72:287-314.

Hylander WL, Johnson KR. 1997. In Vivo Bone Strain Patterns in the Zygomatic Arch of Macaques and the Significance of These Patterns for Functional Interpretations of Craniofacial form. American Journal of Physical Anthropology 102:203-232.

Hylander WL, Picq PG, Johnson KR. 1991a. Function of the Supraorbital region of Primates. Archives of Oral Biology 36:273-281.

Hylander WL, Picq PG, Johnson KR. 1991b. Masticatory-Stress Hypotheses and the Supraorbital Region of Primates. American Journal of Physical Anthropology 86:1-36.

Ichim I, Sawin M, Kieser JA. 2006. Mandibular Biomechanics and Development of the Human Chin. Journal Dental Research 85:638-642.

Ingervall B. 1976. Facial Morphology and Activity of Temporal and Lip Muscles during Swallowing and Chewing. The Angle Orthodontist 46:372-380.

İşcan MY, Steyn M. 1999. Craniometric determination of population affinity in South Africans. Journal of Legal Medicine 112:91-97.

İşcan MY, Loth SR, Steyn M. 2000. Determination of Racial Affinity. In: Siegel JA, Saukko PJ, and Knupfer GC, editors. Encyclopedia of Forensic Sciences. London: Academic Press. p 227-235.

Jantz RL, Owsley DW. 2001. Variation Among Early North American Crania. American Journal of Physical Anthropology 114:146-155.

Jacobson A. 1982. The Dentition of the South African Negro. Anniston, Alabama: Higginbotham Inc.

Johnson DR, Moore WJ. 1997. Anatomy for Dental Students. New York: Oxford University Press.

Jolly C J. 1970. The seed eaters: a new model for hominid differentiation based on a baboon analogy. *Man* 5:5–26.

*Jungers WL (1978) On canine reduction in early hominids. Curr Anthropol **19**, 155–156.*

Kaifu Y, Baba H, Sutikna T, Morwood MJ, Kubo D, Saptomo EW, Jatmiko, Awe RD,

Djubiantono T. 2011. Craniofacial morphology of *Homo floresiensis*: Description, taxonomic affinities, and evolutionary implication. Journal of Human Evolution. 61:644-682.

Kay RF. 1985. Dental evidence for the diet of *Australopithecus*. A. Rev. Anthrop. 14, 315–341.

Keen JA. 1950. A study of the differences between male and female skulls. American Journal of Physical Anthropology 8:64-80.

Kerley ER. 1965. The micrscopic determination of age in human bone. American Journal of Physical Anthropology 23(2):149-163.

Kieser J. 1990. Human Adult Odontometrics. Cambridge: Cambridge University Press.

Kieser J. 1999. Biomechanics of masticatory force production. Journal of Human Evolution 36:575-579.

Kiliaridis S. 1995. Masticatory muscle influence on craniofacial growth. Acta Odontological Scand 53:196-202.

Kitai N, Fujii Y, Murakami S, Furukawa S, Kreiborg S, Takada K. 2002. Human masticatory Muscle Volume and Zygomatico-mandibular Form in Adults with Mandibular Prognathism. Journal Dental Research 81:752-756.

Kleiven S and von Holst H. 2002. Consequences of head size following trauma to the human head. Journal of Biomechanics 35:153-160.

Knußman R. 1988. Anthropologie Handbuch der vergleichenden Biologie des Menschen. Stuttgart: Gustav Fischer Verlag.

Koolstra JH. 2003. Number Crunching with the Human Masticatory System. Journal Dental Research 82:672-676.

Koolstra JH, van Eijden TMGJ. 1992. Application and Validation of a Three-Dimensional mathematical Model of the Human Masticatory System In Vivo. Journal of Biomechanics 25:175-187.

Koolstra JH, van Eijden TMGJ. 1995. Biomechanical Analysis of Jaw-closing Movement. Journal Dental Research 74:1564-1570.

Koolstra JH, van Eijden TMGJ, Weijs WA, Naeije M. 1988. A Three-Dimensional Mathematical Model of the Human Masticatory System Predicting Maximum Possible Bite Force. Journal of Biomechanics 21:563-576.

Korioth TWP, Romilly DP, Hannam AG. 1992. Three dimensional finite element stress analysis of the dentate human mandible. American Journal of Physical Anthropology, 88, 69.

Krogman WM, İşcan MY. 1986. The Human Skeleton in Forensic Medicine 2nd ed. Springfield, Illinois: Charles C. Thomas.

Kubota M, Nakano H, Sanjo I, Satoh K. 1998. maxillofacial morphology and masseter muscle thickness in adults. European Journal of Orthodontics 20:535-542.

Kupczik K, Dobson CA, Fagan MJ, Crompton RH, Oxnard CE, O'Higgins P. 2007. Assessing mechanical function of the zygomatic region in macaques: validation and sensitivity testing of finite element models. Journal of Anatomy 210:41-53.

L'Abbe´ EN, Loots M, and Meiring JM. 2005. The Pretoria Bone Collection: A modern South African skeletal sample. HOMO - Journal of Comparative Human Biology 56:197-205.

L'Abbé EN, Van Rooyen C, Nawrocki SP, Becker, PJ. 2011. An evaluation of non-metric cranial traits used to estimate ancestry in a South African sample, Forensic Science International, Volume 209, Issues 1–3, 15 June, Pages 195.e1-195.e7.

Lahr MM, Wright RVS. 1996. The question of robusticity and the relationship between cranial size and shape in Homo sapiens. Journal of Human Evolution 31:157-191.

Larsen CS. 1995. Biological changes in human populations with agriculture. Annual Review of Anthropology, vol. 24, pp. 185-213.

Lefort R, Tessier DP (translated from French).1972. Experimental study of fractures of the upper jaw. *Plastic and Reconstructive Surgery*, *50*(5), 497-506.

Lewis JH. 1942. The Biology of the Negro. Chicago: University of Chicago Press.

Liao S-H, Tong R-F., Dong J-X. 2007. Anisotropic finite element modeling for patient-specific mandible. Computer Methods and Programs in Biomedicine 88:197-209.

Lieberman DE. 1998. Sphenoid shortening and the evolution of modern human cranial shape. Nature 393, 158–162.

Lieberman DE. 1996. How and why humans grow thin skulls: experimental evidence for systemic cortical robusticity. Am J Phys Anthropol 101:217–236.

Lieberman D.E. 2000. Ontogeny, homology, and phylogeny in the Hominid craniofacial skeleton: the problem of the browridge. In: O'Higgins, P., Cohn, M. (Eds.), Development, Growth and Evolution: Implications for the Study of Hominid Skeletal Evolution. Academic Press, London, pp. 85–122.

Lieberman DE, McBratney BM, Krovitz G. 2002. The evolution and development of cranial form in Homo sapiens. Proc. Natl. Acad. Sci. 99, 1134e1139.

Lieberman DE, Krovitz GE, Yates FW, Devlin M, St.Claire M. 2004. Effects of food

processing on masticatory strain and craniofacial growth in a retrognathic face. Journal of Human Evolution 46:655-677.

Lieberman DE. 2008. Speculations About the Selective Basis for Modern Human Craniofacial Form. Evolutionary Anthropology 17:55-68.

Lieberman DE . 2011. Complexity, Modularity, and Integration in the Human Head. The Evolution of the Human Head. Cambridge, Mass: The Belknap Press of Harvard University Press.

Liao S-H, Tong R-F., and Dong J-X. 2007. Anisotropic finite element modeling for patient-specific mandible. Computer Methods and Programs in Biomedicine 88:197-209.

Low IM, Duraman N, Mahmood U. 2008. Mapping the structure, composition and mechanical properties of human teeth. Materials Science and Engineering C 28:243-247.

Lucas PW, Corlett RT, Luke DA. 1985. Plio-Pleistocene Hominid Diets: an Approach Combining Masticatory and Ecological Analysis. Journal of Human Evolution 14:187-202.

Magee L. 1990. R2 Measures Based on Wald and Likelihood Ratio Joint Significance Tests. The American Statistician 44:250-253.

Matshes EW, Burbridge B, Sher B, Mohamed A, Juurlink BH. 2005. Human Osteology and Skeletal Radiology An Atlas and Guide. Boca Raton, Florida: CRC Press.

McDowell JL, L'Abbé EN and Kenyhercz MW. 2012. Nasal aperture shape evaluation between black and white South Africans. *Forensic Science International*, *222*(1), 397-e1.

McElhaney JH, Fogle JL, Melvin JW, Haynes RR, Roberts VL, Alem NM. 1970. Mechanical Properties of Cranial Bone. Journal of Biomechanics 3:495-511.

McMinn RMH, Hutchings RT. 1988. A Colour Atlas of Human Anatomy. Weert, Netherlands: Wolfe Medical Publications Ltd.

Meijer HJA, Starmans FJM, Bosman F, Steen WHA. 1993. A comparison of three finite element models of an edentulous mandible provided with implants. Journal of Oral Rehabilitation, 20, 147.

Meijer HJA, Starmans FJM, Steen WHA, Bosman F. 1996. Loading conditions of endosseous implants in anedentulous human mandible: a three-dimensional finite-element study. Journal of Oral Rehabilitation, 23, 757.

Merdji A, Mootanah R, Bouiadjra BAB, Benaissa A, Aminallah L, Chikh EBO, Mukdadi S. 2013. Stress analysis in single molar tooth, Materials Science and Engineering: C, Volume 33, Issue 2, 1 March, Pages 691-698.

Mitteroecker P and Gunz P. 2009. Advances in geometric morphometrics. Evolutionary Biology, 36(2), 235-247.

Moore-Jansen PM, Ousley SD, Jantz RL. 1994. Data Collection Procedures for Forensics Skeletal Material: Report of Investigations no. 48. Knoxville: The University of Tennessee Department of Anthropology.

Moran MD. 2003. Arguments for rejecting the sequential Bonferroni in ecological studies. Oikos, 1*00*(2), 403-405.

Moss ML, Young RW. 1960. A Functional Approach to Craniology. American Journal of Physical Anthropology 18:281-292.

Mota A, Klug WS, Ortiz M, Pandolfi A. 2003. Finite-Element simulation of firearm injury to the human cranium. Computational Mechanics 31:115-121.

Motoyoshi M, Shimazaki T, Sugai T, Namura S. 2002. Biomechanical influences of head posture on occlusion: an experimental study using finite element analysis. European Journal of Orthodontics 24:319-326.

Nakagawa S. 2004. A farewell to Bonferroni: the problems of low statistical power and publication bias. Behavioral Ecology, Volume 15, No 6: 1044-1045.

Neves WA, Hubbe M, Pilo LB. 2007. Early Holocene human skeletal remains from Sumidouro Cave, Lagoa Santa Brazil: History of discoveries, geological and chronological context, and comparative cranial morphology. Journal of Human Evolution 52:16-30.

Nie Q, Kanno Z, Xu T, Lin J, Soma K. 2010. Clinical study of frontal chewing patterns in various crossbite malocclusions. American Journal of Orthodontics and Dentofacial Orthopedics, Volume 138, Issue 3, September, Pages 323-329.

Niinimäki S. 2011. What do muscle marker ruggedness scores actually tell us?. Int. J. Osteoarchaeol., 21: 292–299.

Nott JC, Gliddon GR, Morton SG, Agassiz JLR, Usher W, Patterson HS. 1854. *Types of Mankind: Or Ethnological Researches, Based Upon the Ancient Monuments, Paintings, Sculptures, and Crania of Races, and Upon Their Natural, Geographical, Philological, and Biblical History: Illustrated by Selections from the Inedited Papers of Samuel George Morton, and by Additional Contributions from L. Agassiz, W. Usher, and HS Patterson*. Lippincott, Grambo & Company.

O'Connor CF, Francisus RG, Holton NE. 2005. Bite Force Production Capability and Efficiency in Neandertals and Modern Humans. American Journal of Physical Anthropology 127:129-151.

Oettle, AC, Becker PJ, de Villiers E, Steyn M. 2009. The influence of age, sex, population group, and dentition on the mandibular angle as measured on a South African sample. *American Journal of Physical Anthropology*, *139*(4), 505-511.

Osborn JW. 1996. Features of Human Jaw Design Which Maximize the Bite Force. Journal of Biomechanics 29:589-595.

Osborn JW, Baragar FA. 1985. Predicted Pattern of Human Muscle Activity During Clenching Derived From a Computer Assisted Model: Symmetric Vertical Bite Force. Journal of Biomechanics 18:599-612.

Ostermann AC, Dowdy JD, Lindemann S, Türp JC, Swales JM. 1999. Patterns in self-reported illness experiences: letters to a TMJ support group. Language and Communication, Volume 19, Issue 2, April, Pages 127–147

Oyen OJ,Walker AC, Rice RW. 1979. Craniofacial growth in olive baboons (*Papio cynocephalus anubis*): browridge formation. Growth 43:174-187.

O'Higgins P, Bastir M, Kupczik K. 2006. Shaping the Human Face. International Congress Series 1296:55-73.

Palubeckaitė Ž, Jankauskas R, Ardagna Y, Macia Y, Rigeade C, Signoli M, Dutour O. 2006. Dental status of Napoleon's Great Army's (1812) mass burial of soldiers in Vilnius: childhood peculiarities and adult dietary habits. Int. J. Osteoarchaeol., 16: 355–365.

Paphangkorakit J, Osborn JW. 1998. Effects of human maximum bite force of biting on a softer or harder object. Archives of Oral Biology 43:833-839.

Park MA. 1996. Biological Anthropology. London: Mayfield Publishing Company.

Patriquin ML, Loth SR, Steyn M. 2003. Sexually dimorphic pelvic morphology in South African whites and blacks. HOMO - Journal of Comparative Human Biology 53:255-262.

Pearson OM, Lieberman DE. 2004. The Aging of Wolff's "Law": Ontogeny and Responses to Mechanical Loading in Cortical Bone. Yearbook of Physical Anthropology 47:63-99.

Perez SI, Bernal V and Gonzalez PN. 2006. Differences between sliding semi-landmark methods in geometric morphometrics, with an application to human craniofacial and dental variation. *Journal of anatomy*, *208*(6), 769-784.

Perneger TV. 1998. What's Wrong with Bonferroni Adjustments. British Medical Journal. 316:1236-1238.

Petersen HC. 2000. Comment on ‘‘Activity, climate, and postcranial robusticity implications for modern human origins and scenarios of adaptive change,’’ by O.M. Pearson. Curr Anthropol 41:596–597.

Peterson J, Dechow PC. 2003. Material Properties of the Human Cranial Vault and Zygoma. The Anatomical Record Part A 274 A:785-797.

Pfeiffer S. 1980. Age changes in the external dimensions of adult bone. American Journal of Physical Anthropology. 52(4):529-532.

Picq PG, Hylander WL. 1989. Endo's stress analysis of the primate skull and the functional significance of the supraorbital region. American Journal of Physical Anthropology 79:393-398.

Picq P. 1990. The diet of *Australopithecus afarensis*: an attempted reconstruction. C. R. Acad. Sci. Ser. II 311, 725–730.

Pileicikiene G, Surna A. 2004. The Masticatory System From A Biomechanical Perspective: A Review. Stomatologija, Baltic Dental and Maxillofacial Journal 6:81-84.

Poiate IA, de Vasconcellos AB, de Santana RB, Poiate Jr E. 2009. Three-dimensional stress distribution in the human periodontal ligament in masticatory, parafunctional, and trauma loads: finite element analysis. Journal of Periodontology 80:1859-1867.

PostView Finite Element Post Processing (University of Utah, Musculoskeletal Research Laboratories, Salt Lake City, Utah. Available at http://mrl.sci.utah.edu/software)

Predan J, Gubeljak N, and Kolednik O. 2007. On the local variation of the crack driving force in a double mismatched weld. Engineering Fracture Mechanics 74:1739-1757.

Preuschoft H and Witzel U. 2005. Functional Shape of the Skull in Vertebrates: Which Forces Determine Skull Morphology in Lower Primates and Ancestral Synapsids. The Anatomical Record Part A 283A:402-413.

PreView Finite Element Pre-Processing software (University of Utah, Musculoskeletal Research Laboratories, Salt Lake City, Utah. Available at http://mrl.sci.utah.edu/software)

Proffit WR, Fields HW, Nixon WL. 1983. Occlusal forces in Normal and long-face Adults. Journal Dental Research 62:566-571.

Provatidis C, Georgiopoulos B, Kotinas A, McDonald JP. 2007. On the FEM modeling of craniofacial changes during rapid maxillary expansion. Medical Engineering and Physics 29:566-579.

Provatidis C, Georgiopoulos B, Kotinas A, McDonald JP. 2008. Evaluation of craniofacial effects during rapid maxillary expansion through combined *in vivo* / *in vitro* and finite element studies. European Journal of Orthodontics 30:437-448.

Raadsheer MC, Kiliaridis S, van Eijden TMGJ, van Ginkel FC, Prahl-Andersen B. 1996. Masseter muscle thickness in growing individuals and its relation to facial morphology. Archives of Oral Biology 41:323-332.

Raghavan ML, Vorp DA, Federle MP, Makaroun MS, Webster MW. 2000. Wall stress distribution on three-dimensionally reconstructed models of human abdominal aortic aneurysm. *Journal of Vascular Surgery*, *31*(4), 760-769.

Rak Y. 1983. The Australopithecine Face. New York: Academic Press.

Rak Y. 1986. The Neandertal: A New Look at an Old Face. Journal of Human Evolution 15:151-164.

Rak Y. 1985. Australopithecine taxonomy and phylogeny in light of facial morphology. *Am J. Phys. Anthropol.* 66:281–287.

Ravosa MJ. 1991a. Interspecific perspective on mechanical and nonmechanical models of primate circumorbital morphology. Am. J. Phys. Anthropol. 86, 369–396.

Ravosa, MJ. 1991b. Ontogenetic perspective on mechanical and non-mechanical models of primate circumorbital morphology. Am. J. Phys. Anthropol. 85:95–112.

Rayfield EJ. 2007. Finite Element Analysis and Understanding the Biomechanics of Evolution of Living and Fossil Organisms. Annual Review of Earth and Planetary Sciences 35:541-576.

Reina JM, García-Aznar JM, Domínguez J, Doblaré M. 2007. Numerical estimation of bone density and elastic constants distributions in a human mandible. Journal of Biomechanics 40:828-836.

Reina JM, García-Aznar JM, Domínguez J, Doblaré M. 2007. Numerical estimation of bone density and elastic constants distributions in a human mandible. Journal of Biomechanics 40:828-836.

Rhine S. 1990. Non-metric skull sexing. In: Gill GW and Rhine S, editors. Skeletal Attributions of Race Methods for Forensic Anthropology. Albuquerque, New Mexico: Maxwell Museum of Anthropology. p 9-18.

Rho J-Y, Kuhn-Spearing L, Zioupos P. 1998. Mechanical properties and the hierarchial structure of bone. Medical Engineering and Physics 20(2):92-102.

Richmond BG, Wright BW, Grosse IR, Dechow PC, Ross CF, Spencer MA, Strait DS. 2005. Finite Element Analysis in Functional Morphology. The Anatomical Record Part A 283A:259-274.

Richtsmeier JT. Burke Deleon V and Lele SR. 2002. The promise of geometric morphometrics. American Journal of Physical Anthropology, 119(S35), 63-91.

Ringqvist M. 1973. Isometric bite force and its relation to dimensions of the facial skeleton. Acta Odontological Scand35-42.

Robertson JH. 1979. More on Skeletal Analysis and the Race Concept. Current Anthropology 20:617-619.

Robinson JT. 1954. Prehominid dentition and hominid evolution. Evolution 8:324-334.

Robinson JT. 1962. The origin and adaptive radiation of the australopithecines. In: Kurth, G. (Ed.) *Evolution und Hominisation.* Stuttgart, Fischer, pp. 120–140.

Robinson JT. 1963. Adaptive radiation in the Australopithecines and the origin of man. In Howell, F. C. and Boulière, F. (Eds.) *African Ecology and Human Evolution.* Cambridge, Cambridge University press, pp. 385–416.

Robinson JT. 1967. Variation and the taxonomy of the early hominids. In: Dobzhansky, T, Hecht, MK, and Steere, WC. *Evolutionary Biology.* New York, Meredith, pp. 69–100.

Rohlf FJ. 1998. On applications of geometric morphometrics to studies of ontogeny and phylogeny. Systematic Biology, 47(1), 147-158.

Röhrle O, Pullan AJ. 2007. Three-dimensional finite element modelling of muscle forces during mastication. Journal of Biomechanics 40:3363-3372.

Rogers GM, Allen RC. 2012. "Le Fort Fractures". Smith and Nesi's Ophthalmic Plastic and Reconstructive Surgery 3rd ed. Black, E.H.; Nesi, F.A.; Gladstone, G.J.; Levine, M.R.; Calvano, C.J. (Eds.). Springer. pp 283-295.

Roseman CC, Weaver TD. 2004. Multivariate Apportion of Global Human Craniofacial Diversity. American Journal of Physical Anthropology 125:257-263.

Ross CF, Patel BA, Slice DE, Strait DS, Dechow PC, Richmond BG, Spencer MA. 2005. Modeling Masticatory Muscle Force in Finite Element Analysis: Sensitivity Analysis Using Principal Coordinates Analysis. The Anatomical Record Part A 283A:288-299.

Ross CF. 1999. How to Carry Out Functional Morphology. Evolutionary Anthropology: Issues, News, and Reviews. Volume 7, Issue 6: 217-22.

Ross CF. 2005. Finite Element Analysis in Vertebrate Biomechanics. The Anatomical Record Part A 283A:253-258.

Ross CF, Metzger KA. 2004. Bone strain gradients and optimization in vertebrate skulls. Annuals of Anatomy 186:387-396.

Ross CF, Patel BA, Slice DE, Strait DS, Dechow PC, Richmond BG, Spencer MA. 2005. Modeling Masticatory Muscle Force in Finite Element Analysis: Sensitivity Analysis Using Principal Coordinates Analysis. The Anatomical Record Part A 283A:288-299.

Rowe NC, Killey H. 1955. Fractures of the Facial Skeleton. Baltimore, MD Williams and Wilkins. pp205-233.

Rubin CT, McLeod KJ, Bain SD. 1990. Functional strains and cortical bone adaptation: Epigenetic assurance of skeletal integrity, Journal of Biomechanics, Volume 23, Supplement 1, Pages 43-49,51-54.

Ruff C, Holt B, Trinkaus E. 2006. Who's Afraid of the Big Bad Wolff?: "Wolff's Law" and Bone Functional Adaptation. American Journal of Physical Anthropology 129:484-498.

Russell MD. 1982. Tooth Eruption and Browridge Formation. American Journal of Physical Anthropology 58:59-65.

Russell MN. 1985. The supraorbital torus7: "a most remarkable peculiarity". Current Anthropology 26(3):337-360.

Sarraj M, Burgess IW, Davison JB, Plank RJ. 2007. Finite element modelling of steel fin plate connections in fire. Fire Safety Journal 42:408-415.

Savoldelli C, Bouchard PO, Manière-Ezvan A, Bettega G, Tillier Y. 2012. Comparison of stress distribution in the temporomandibular joint during jaw closing before and after symphyseal distraction: a finite element study. International Journal of Oral and Maxillofacial Surgery, Volume 41, Issue 12, Pages 1474-1482.

Scholtz Y, Steyn M and Pretorius E. 2010. A geometric morphometric study into the sexual dimorphism of the human scapula. *HOMO-Journal of comparative human biology*, *61*(4), 253-270.

Scott RS, Ungar PS, Bergstrom TS, Brown CA, Grine FE, Teaford MF, Walker A. 2005. Dental microwear texture analysis shows within-species diet variability in fossil hominins. *Nature* 436:693–695.

Sellers WI, Crompton RH. 2004. Using sensitivity analysis to validate the predictions of a biomechanical model of bite forces. Annuals of Anatomy 186:89-95.

Sertgoz A, Guvener S. 1996. Finite element analysis of the effect of cantilever and implant length on stress distribution in an implant-supported prosthesis. Journal of Prosthetic Dentistry, 76, 165.

Shearer BM, Sholts SB, Garvin HM, Wärmländer SKTS. 2012. Sexual dimorphism in human browridge volume measured from 3D models of dry crania: A new digital morphometrics approach. *Forensic Science International*, *Volume 222, Issues 1–3*, *Pages 400.e1-400.e5.*

Silverthorn, DU. 2007. Human Physiology An integrated Approach 4th Edition. Pearson Education, Inc. San Francisco, USA.

Simpson, S. W., Lovejoy, C. O., & Meindl, R. S. (1991). Relative dental development in hominoids and its failure to predict somatic growth velocity. *American Journal of Physical Anthropology*, *86*(2), 113-120

Singh M, Detamore MS. 2009. Biomechanical properties of the mandibular condylar cartilage and their relevance to the TMJ disc. *Journal of Biomechanics*, *Volume 42, Issue 4*, *11 March*, *Pages 405-417*.

Slice DE. 2007. Geometric morphometrics. *Annu. Rev. Anthropol.*, *36*, 261-281.

Smith BH. 1984. Patterns of molar wear in hunter-gatherers and agriculturalists. *American Journal of Physical Anthropology*, vol. 63, pp. 39-56.

Smith RJ, Josell SD. 1984. The plan of the human face: A test of three general concepts. American Journal of Orthodontics 85:103-108.

Smith HF, Terhune CE, Lockwood CA. 2007. Genetic, Geographic, and Environmental Correlates of Human Temporal Bone Variation. American Journal of Physical Anthropology 134:312-322.

Smith JB, Suggs CW. 1976. Dynamic Properties of the Human Head. Journal of Sound and Vibration 48:35-43.

Solberg WK, Bibb CA, Nordström BB, Hansson TL. 1986. Malocclusion associated with temporomandibular joint changes in young adults at autopsy, American Journal of Orthodontics, Volume 89, Issue 4, April, Pages 326-330.

Spears IR, Macho GA. 1998. Biomechanical Behaviour of Modern Human Molars: Implications for Interpreting the Fossil Record. American Journal of Physical Anthropology 106:467-482.

Spencer MA. 1998. Force production in the primate masticatory system: electromyographic tests of biomechanical hypotheses. Journal of Human Evolution 34:25-54.

Spencer MA, Demes B. 1993. Biomechanical Analysis of Masticatory System Configuration in Neandertals and Inuits. American Journal of Physical Anthropology 91:1-20.

Standring S. 2004. *Gray's Anatomy: The Anatomical Basis of Clinical Practice*. In: London: Elsevier.

Stanley Jr, RB. 1995. Buttress fixation with plates, Operative Techniques in Otolaryngology-Head and Neck Surgery, Volume 6, Issue 2. Pages 97-103.

Steele DG, Bramblett CA. 1988. The anatomy and biology of the human skeleton. College Station: Texas AandM University Press.

Steyn M, Pretorius E, Hutten L. 2004. Geometric morphometric analysis of the greater sciatic notch in South Africans. Homo 54(3), 197-206.

Strait PT. 1989. A First Course in Probability and Statistics with Applications. San Diego: Harcourt Brace Jovanovich.

Strait DS, Richmond BG, Spencer MA, Ross CF, Dechow PC, Wood BA. 2007. Masticatory biomechanics and its relevance to early hominid phylogeny: An examination of palatal thickness using finite-element analysis. Journal of Human Evolution 52:585-599.

Strait DS, Richmond BG, Spencer MA, Ross CF, Dechow PC, Wood BA. 2007. Masticatory biomechanics and its relevance to early hominid phylogeny: An examination of palatal thickness using finite-element analysis. Journal of Human Evolution 52:585-599.

Strait DS, Wang Q, Dechow PC, Ross CF, Richmond BG, Spencer MA, Patel BA. 2005. Modeling Elastic Properties in Finite-Element Analysis: How Much Precision Is Needed to Produce an Accurate Model? The Anatomical Record Part A 283A:275-287.

Strait DS, Weber GW, Neubauer S, Chalk J, Richmond BG, Lucas PW, Spencer MA, Schrein CA, Dechow PC, Ross CF, Grosse IR, Wright BW, Constantino P, Wood BA, Lawn B, Hylander WL, Wang Q, Byron C, Slice DE, Smith AL. 2009. The feeding biomechanics and dietary ecology of Australopithecus africanus. Proceedings of the National Academy of Sciences of the United States of America 106:2124-2129.

Strait DS, Wright BW, Richmond BG, Ross CF, Dechow PC, Spencer MA, Wang Q. 2008. Craniofacial strain patterns during premolar loading: implications for human evolution. *Primate Craniofacial Function and Biology*, 173-198.

Stringer C. 2002. Modern human origins: progress and prospects. Phil. Trans. R. Soc. Lond. B. 357, 563e579.

Taddei F, Pancanti A, Viceconti M. 2004. An improved method for the automatic mapping of computed tomography numbers onto finite element models. Medical Engineering and Physics 26:61-69.

Tanne K, Miyasaka J, Yamagata Y, Sachdeva R, Tsutsumi S. 1988. Three-dimensional model of the human craniofacial skeleton: method and preliminary results using finite element analysis. Journal of Biomedical Engineering 10:246-252.

Tanne K, Hiraga J, Kakiuchi K, Yamagata Y, Sakuda M. 1989a. Biomechanical effect of anteriorly directed extraoral forces on the craniofacial complex: a study using the fi nite elements method . American Journal of Orthodontics and Dentofacial Orthopedics 95:200-207.

Tanne K, Hiraga J, Sakuda M. 1989b. Effects of directions of maxillary forces on biomechanical changes in craniofacial complex. European Journal of Orthodontics 11:382-391.

Tanne K, Sakuda M. 1991. Biomechanical and clinical changes of the craniofacial complex from orthopedic maxillary protraction. Angle Orthodontist 61:145-152.

Teaford MF, Ungar PS. 2000. Diet and the evolution of the earliest human ancestors. *Proc. Nat. Acad. Sci.* 97:13506–13511.

Teaford MF, Ungar PS, Grine FE. 2002. Paleontological evidence for the diets of African Plio-Pleistocene hominins with special reference to early *Homo*. In: Ungar, P.S., Teaford, M.F. (Eds.), Human Diet: Its Origins and Evolution. Bergin and Garvey Publishers, Westport, CT, pp. 143–166.

TetGen (Numerical Mathematics and Scientific Computing, Berlin, Germany. Available from http://tetgen.berlios.de/)

Trinkaus E. 1983. Bodies, brawn, brains and noses: human ancestors and human predation. In: Nitecki MH and Nitecki DV, editors. The Evolution of Human Hunting. New york: Plenum. p 107-145.

Trinkaus E. 1987. The Neandertal face: evolutionary and functional perspectives on a recent hominid face. Journal of Human Evolution 16:429-443.

Trinkaus E. 2003. Neandertal faces were not long; modern human faces are short. Proc. Natl. Acad. Sci. 100, 8142e8145.

Tuxen A, Bakke M, Pinholt EM. 1999. Comparative data from young men and women on masseter muscle fibres, function and facial morphology. Archives of Oral Biology 44:509-518.

Ungar PS, Teaford, MF. 2001. The dietary split between apes and the earliest human ancestors. In: Tobias, P.V., Raath, M.A., Moggi-Chcchi, J., Doyle, G.A. (Eds.), Humanity from African Naissance to Coming Millennia. Firenze University Press, Florence, pp. 337–354.

Ungar P. 2004. Dental topography and diets of *Australopithecus afarensis* and early *Homo*. Journal of Human Evolution 46:605-622.

Usui T, Maki K, Toki Y, Yoshinobu S, Takanobu H, Takanishi A, Miller AJ. 2004. Mechanical strain on the human skull in a humanoid robotic model. American Journal of Orthodontics and Dentofacial Orthopedics 126:421-431.

Vance VL and Steyn M. 2013. Geometric morphometric assessment of sexually dimorphic characteristics of the distal humerus. *HOMO-Journal of Comparative Human Biology*.

Van Der Bilt A, Engelen L, Pereira LJ, van der Glas HW, Abbink JH. 2006. Oral physiology and mastication. Physiology and Behavior 89:22-27.

Vargervik K. 1997. Relationship between bone muscles of mastication in hemifacial microsomia. Plastic and Reconstructive Surgery 99:998-999.

Viðarsdóttir US, O'Higgins P, Stringer C. 2002. A geometric morphometric study of regional differences in the ontogeny of the modern human facial skeleton. Journal of Anatomy 201:211-229.

Voo L, Kumaresan S, Pintar FA, Yoganandan N, Sances A. 1996. Finite-element models of the human head. *Medical and Biological Engineering and Computing*, *34*(5), 375-381.

VRMesh Studio (VirtualGrid, Seattle City, WA. Available from http://www.vrmesh.com/)

Lotika Wadhwa, Ashok Utreja, Amrit Tewari. 1993. A study of clinical signs and symptoms of temporomandibular dysfunction in subjects with normal occlusion, untreated, and treated malocclusions . *American Journal of Orthodontics and Dentofacial Orthopedics*, *Volume 103, Issue 1*, *January*, *Pages 54-61.*

Wang Q, Dechow PC. 2006. Elastic Properties of External Cortical Bone in the Craniofacial Skeleton of the Rhesus Monkey. American Journal of Physical Anthropology 131:402-415.

Wang Q, Strait DS, Dechow PC. 2006. A comparison of cortical elastic properties in the craniofacial skeletons of three primate species and its relevance to the study of human evolution. Journal of Human Evolution 51:375-382.

Ward SC, Molnar S. 1980. Experimental Stress Analysis of Topographic Diversity in Early Hominid Gnathic Morphology. American Journal of Physical Anthropology 53:383-395.

Weaver TD, Roseman CC, Stringer CB. 2007. Were Neandertal and modern human cranial differences produced by natural selection or genetic drift. Journal of Human Evolution 53:135-145.

Wei SHY. 1969. Craniofacial Variations, Sex Differences and the Nature of Prognathism in Chinese Subjects. Angle Orthodontist 39:303-315.

Weidenreich F. 1941. The brain and its role in the phylogenetic transformation of the human skull. Trans. Am. Phil. Soc. 31, 328–442.

Weijs WA, Hillen B. 1984. Relationships between Masticatory Muscle Cross-section and Skull Shape. Journal Dental Research 63:1154-1157.

Weijs WA, Hillen B. 1986. Correlations between the cross-sectional area of the jaw muscles and craniofacial size and shape. American Journal of Physical Anthropology 70:423-431.

Weiner S, Wagner HD. 1998. The Material Bone: Structure-Mechanical Function Relations. Annual Review of Material Science 28:271-298.

Weiner S, Traub W, Wagner HD. 1999. Lamellar Bone: Structure-Function Relations. Journal of Structural Biology 126(3): 241-255.

Weiss E. 2003. Understanding muscle markers: Aggregation and construct validity. Am. J. Phys. Anthropol., 121: 230–240.

White TD. 2000. Human Osteology. San Diego, California: Academic Press.

Wolff J. 1892. Das gaesetz der transformation der knochen. Berlin: Published with support from the Royal Academy of Sciences.

Wolpoff MH. 1996. Human Evolution. New York: McGraw-Hill Companies, Inc.

Wood B. 2006. Human Evolution: A Very Short Introduction (Very Short Introductions). Oxford University Press Inc. New York.

Wroe S, Moreno K, Clausen P, Mchenry C, Curnoe D. 2007. High-resolution three-dimensional computer simulation of hominid cranial mechanics. Anatomical Record 290:1248-1255.

Yamada H. (1970) Strength of Biological Materials. Williams and Wilkins, Baltimore.

Yokley TR. 2006. The functional and adaptive significance of anatomical variation in recent and fossil human nasal passages. Duke University. Ref Type: Dissertation

Young B, Lowe JS, Stevens A, Heath JW. 2006. Wheater's Functional Histology A text and Colour Atlas 5th ed. Elsevier Limited, China.

Zannoni C, Mantovani R, Viceconti M. 1998. Material properties assignment to finite element models of bone structures: a new method. Medical Engineering and Physics 20:735-740.

Zienkiewicz OC, Taylor RL. 2000. The Finite Element Method Volume 2 Solid Mechanics. Oxford: Butterworth-Heinemann.

Zelditch ML, Swiderski DL and Sheets HD. 2004. Geometric morphometrics for biologists: a primer. Academic Press.

Zong Z, Lee HP, Lu C. 2006. A three-dimensional human head finite element model and power flow in a human head subject to impact loading. Journal of Biomechanics 39:284-292.

Zumwalt A. 2005. A new method for quantifying the complexity of muscle attachment sites. Anat. Rec., 286B: 21–28.

APPENDIX

APPENDIX A. Relationship between Gnathic Index (GI) and facial parameter for all individuals in the data set and within the orthognathic (1) mesognathic (2) and prognathic (3) groups.

Variable (x)	Group	Pearson Correlation Coefficient	R^2 x 100% Coefficient of Determination	Linear relationship	p-Value
Max cranial length	All	-0.0598	0.36	GI= 106.02 -0.028 (X)	0.4495
	1	-0.2096	4.39	GI= 101.50 -0.029(x)	0.1398
	2	0.0890	0.79	GI= 97.34 + 0.019 (x)	0.4989
	3	0.0430	0.18	GI= 102.61 + 0.016(x)	0.7646
Max cranial breadth	All	0.0017	0.00	GI=100.60 + 0.001 (x)	0.9832
	1	0.2554	6.52	GI= 84.89 + 0.09(x)	0.0704
	2	0.0938	0.88	GI= 96.61 + 0.032(x)	0.4757
	3	0.0225	0.05	GI= 104.25 + 0.009(x)	0.8769
Bizygomatic breadth	All	-0.0998	1.00	GI=110.47 – 0.75(x)	0.2079
	1	-0.1717	2.95	GI=101.66- 0.04(x)	0.2283
	2	0.0789	0.62	GI=96.88 + 0.03(x)	0.5524
	3	-0.1962	3.85	GI= 115.20 – 0.76(x)	0.1677
Basion- bregma	All	-0.2273	5.17	GI= 118.16 – 0.131(x)	**0.0037**
	1	-0.2997	8.98	GI= 107.53 – 0.086(x)	**0.0327**
	2	-0.0417	0.17	GI=101.97 – 0.009(x)	0.7538
	3	-0.1633	2.67	GI= 112.99 – 0.058(x)	0.2522
Basion-nasion	All	-0.1908	3.64	GI =119.469-0.184(x)	**0.0150**
	1	-0.3401	11.57	GI =107.275-0.110(x)	**0.0146**
	2	-0.1008	1.02	GI =105.766-0.048(x)	0.4435
	3	-0.0577	0.33	GI =108.768-0.033(x)	0.6876
Basion-prosthion	All	0.6040	36.48	GI =53.935+0.460(x)	**0.0001**
	1	0.0131	0.02	GI =95.69+0.004(x)	0.9271
	2	0.3695	13.66	GI =83.75+0.164(x)	**0.0037**
	3	0.3951	15.61	GI =86.518+0.181(x)	**0.0041**
Max alveolar breadth	All	0.0905	0.82	GI= 94.26+ 0.102(x)	0.2518
	1	-0.2873	8.25	GI= 102.85 – 0.106(x)	**0.0409**
	2	0.0783	0.61	GI= 98.15 + 0.041(x)	0.5519
	3	0.0880	0.78	GI=101.74 + 0.058(x)	0.5390
Max alveolar length	All	0.5809	33.75	GI=64.43 + 0.632(x)	**0.0001**
	1	-0.0844	0.71	GI=98.28 – 0.039(x)	0.5601
	2	0.2216	4.91	GI= 92.57 + 0.14(x)	0.0889
	3	0.3559	12.67	GI=89.95 + 0.259(x)	**0.0112**
Upper facial height	All	0.0118	0.01	GI=100.14+ 0.009(x)	0.8814
	1	-0.2144	4.60	GI= 100.72- 0.068(x)	0.1309
	2	-0.1497	2.24	GI= 104.80 – 0.058(x)	0.2537
	3	0.1182	1.40	GI= 102.32 + 0.047(x)	0.4086

Min frontal breadth	All	-0.1240	1.54	GI= 111.49 – 0.110(x)	0.1159
	1	0.0733	0.54	GI= 93.70 + 0.025(x)	0.6091
	2	-0.0992	0.98	GI=104.5 – 0.039(x)	0.4507
	3	-0.496	0.25	GI=107.66 – 0.023(x)	0.7298
Nasal height	All	-0.0084	0.01	GI= 101.34 – 0.011(x)	0.9153
	1	-0.2754	7.58	GI= 102.56 – 0.13(x)	0.0505
	2	-0.0441	0.19	GI= 101.94 – 0.023(x)	0.7382
	3	0.2288	5.24	GI= 96.82 + 0.176(x)	0.1063
Nasal breadth	All	-0.0567	0.32	GI= 103.63 – 0.105(x)	0.4733
	1	-0.2472	6.11	GI= 100.64 – 0.167(x)	0.0804
	2	-0.0268	0.07	GI=101.35 – 0.020(x)	0.0804
	3	0.1029	1.06	GI= 102.59 + 0.109(x)	0.4726
Interorbital breadth	All	-0.2130	4.54	GI= 110.70 – 0.350(x)	**0.0067**
	1	-0.0490	0.24	GI= 97.02 – 0.030(x)	0.7328
	2	-0.0372	0.14	GI= 101.61 – 0.027(x)	0.7797
	3	-0.2768	7.66	GI= 112.08 – 0.241(x)	**0.0493**
Mandibular body breadth	All	0.1989	3.95	GI= 93.89 + 0.567(x)	**0.0112**
	1	-0.1156	1.34	GI= 97.82 – 0.141(x)	0.4191
	2	0.1744	3.04	GI= 98.26 + 0.206(x)	0.1826
	3	0.0675	0.46	GI= 104.22 + 0.100(x)	0.6379
Bigonial width	All	-0.1148	1.32	GI= 108.66 – 0.083(x)	0.1459
	1	-0.1450	2.10	GI= 99.76 – 0.038(x)	0.3100
	2	0.0144	0.02	GI= 100.30 + 0.005(x)	0.9129
	3	-0.0946	0.89	GI= 108.61 – 0.03(x)	0.5093
Min ramus breadth	All	0.2102	4.42	GI= 90.81 + 0.280(x)	**0.0074**
	1	-0.2711	7.35	GI= 10.99 – 0.140(x)	0.0543
	2	0.2919	8.52	GI= 94.51 + 0.72(x)	**0.0249**
	3	0.2347	5.51	GI= 99.38 + 0.170(x)	0.0974
Max ramus breadth	All	0.0073	0.01	GI= 100.39 + 0.009(x)	0.9270
	1	-0.3555	12.64	GI= 102.98 – 0.168(x)	**0.0105**
	2	-0.0375	0.14	GI= 101.76 – 0.024(x)	0.7780
	3	0.1703	2.90	GI= 100.33 + 0.126(x)	0.2322
Max ramus height	All	0.0802	0.64	GI= 97.09 + 0.064(x)	0.3103
	1	-0.2404	5.78	GI= 99.54 – 0.060(x)	0.0892
	2	0.0106	0.01	GI= 100.50 + 0.004(x)	0.9360
	3	-0.1350	1.82	GI= 108.88 – 0.058(x)	0.3451
Mandibular projection	All	0.2282	5.21	GI= 84.90 + 0.194(x)	0.3451
	1	-0.1500	2.25	GI= 99.91 – 0.046(x)	0.2936
	2	0.2868	8.23	GI= 90.74 + 0.121(x)	**0.0263**
	3	0.1046	1.09	GI= 101.85 + 0.043(x)	0.4651
Mandibular angle	All	-0.0020	0.00	GI= 100.84 – 0.001(x)	0.9795
	1	0.2783	7.75	GI= 94.15 + 0.061(x)	**0.0480**
	2	-0.2224	4.95	GI= 102.67 – 0.060(x)	0.0876
	3	0.0195	0.04	GI= 105.29 + 0.005(x)	0.8921
Orbital breadth	All	-0.2217	4.92	GI= 116.45 – 0.423(x)	**0.0046**

	1	-0.3636	13.22	GI= 105.19 – 0.243(x)	**0.0087**
	2	-0.0781	0.61	GI= 103.17 – 0.064(x)	0.5530
	3	-0.1990	3.96	GI= 113.82 – 0.229(x)	0.1615
Orbital height	All	-0.1879	3.53	GI= 112.55 – 0.351(x)	**0.0167**
	1	-0.2571	6.61	GI= 101.68 – 0.162(x)	0.0686
	2	-0.0713	0.51	GI= 102.85 – 0.062(x)	0.5880
	3	-0.1005	1.01	GI= 108.93 – 0.103(x)	0.4827
Zygomatic arch height	All	0.1067	1.14	GI= 96.96 + 0.192(x)	0.1768
	1	-0.2339	5.47	GI= 99.29 – 0.161(x)	0.0986
	2	-0.1555	2.42	GI= 103.25 – 0.122(x)	0.2355
	3	0.1997	3.99	GI= 101.61 + 0.191(x)	0.1599
Temporal fossa height	All	-0.1022	1.05	GI= 106.23 – 0.067(x)	0.1969
	1	-0.1568	2.46	GI= 98.89 – 0.034(x)	0.2719
	2	-0.0992	0.98	GI= 103.27 – 0.030(x)	0.4549
	3	-0.0566	0.32	GI= 107.16 – 0.021(x)	0.6932

[a]p≤0.05
[b]p≤0.01
[c]p≤0.001

APPENDIX B. Relationship between Gnathic Index (GI) and dental measurements of maxilla and mandible right and left sides for all individuals in the data set and orthognathic (1) mesognathic (2) and prognathic (3) groups.

Variable (x)	Group	Pearson Correlation Coefficient	R^2 x 100% Coefficient of Determination	Linear relationship	p- Value
Meso-Distal					
RT maxilla first molar	All	0.1111	1.23	GI= 93.54 + 0.721(x)	0.1716
	1	-0.1249	1.56	GI= 98.99 – 0.286(x)	0.4083
	2	0.0300	0.09	GI= 99.74 + 0.098(x)	0.8247
	3	0.0973	0.95	GI= 102.35 + 0.308(x)	0.5016
RT maxilla canine	All	0.1901	3.61	GI= 88.83 + 1.545(x)	**0.0225**
	1	0.0910	0.83	GI= 93.99 + 0.286(x)	0.5431
	2	-0.0687	0.47	GI= 102.34 – 0.176(x)	0.6247
	3	0.3326	11.06	GI= 92.65 + 1.651(x)	**0.0274**
Rt maxilla second incisor	All	0.2692	7.25	GI= 89.48 + 1.67(x)	**0.0041**
	1	0.1539	2.37	GI= 93.58 + 0.411(x)	0.3775
	2	-0.0898	0.81	GI= 102.46 – 0.225(x)	0.5868
	3	0.1778	3.16	GI= 102.14 + 0.455(x)	0.2855
Right maxilla first incisor	All	0.3579	12.81	GI= 84.98 + 1.80(x)	**0.0008**
	1	-0.0221	0.05	GI= 96.53 – 0.0388(x)	0.9061
	2	0.1826	3.33	GI= 96.38 + 0.525(x)	0.3341
	3	0.3472	12.06	GI= 97.38 + 0.889(x)	0.0964
Lt maxilla first incisor	All	0.1524	2.32	GI= 93.95 + 0.767(x)	0.1744
	1	-0.1683	2.83	GI=98.75 – 0.327(x)	0.3829
	2	0.1049	1.10	GI= 97.67 + 0.345(x)	0.6177
	3	0.1195	1.43	GI=103.38 + 0.202(x)	0.5527
Lt maxilla second incisor	All	0.2328	5.42	GI= 89.98 + 1.559(x)	**0.0185**
	1	0.1573	2.47	GI= 93.39 + 0.420(x)	0.3819
	2	0.0258	0.07	GI= 99.96 + 0.088(x)	0.8831
	3	0.2196	4.82	GI= 100.82 + 0.659(x)	0.2121
Lt maxilla canine	All	0.2541	6.45	GI= 82.96 + 2.293(x)	**0.0031**
	1	0.1476	2.18	GI= 92.48 + 0.482(x)	0.3391
	2	0.0363	0.13	GI= 99.41 + 0.161(x)	0.8067
	3	0.2488	6.19	GI= 96.26 + 1.191(x)	0.1121
Lt maxilla first molar	All	0.0917	0.84	GI= 94.62 + 0.612(x)	0.2613
	1	-0.1783	3.18	GI= 100.41 – 0.424(x)	0.2358
	2	0.0807	0.65	GI= 98.22 + 0.245(x)	0.5543
	3	0.1225	1.50	GI= 101.23 + 0.416(x)	0.3969
Rt mandible first molar	All	0.1741	3.03	GI= 88.64 + 1.126(x)	**0.0356**
	1	-0.1156	1.34	GI= 99.13 – 0.266(x)	0.4661
	2	0.0571	0.33	GI= 98.80 + 0.182(x)	0.6817
	3	0.2891	8.36	GI= 94.94 + 0.931(x)	**0.0417**
Rt mandible canine	All	0.1895	3.59	GI= 89.31 + 1.588(x)	**0.0329**
	1	0.3348	11.21	GI= 88.63 + 1.063(x)	**0.0302**
	2	0.1237	1.53	GI= 97.40 + 0.439(x)	0.4184

	3	0.2230	4.97	GI= 97.83 + 1.083(x)	0.1667
Rt mandible second incisor	All	0.1688	2.85	GI= 92.93 + 1.330(x)	0.0867
	1	0.2414	5.83	GI= 92.35 + 0.630(x)	0.1832
	2	-0.1164	1.36	GI= 103.56 – 0.532(x)	0.4989
	3	0.3855	14.86	GI= 96.73 + 1.487(x)	**0.0202**
Rt mandible first incisor	All	0.2508	6.29	GI= 91.76 + 1.756(x)	**0.0142**
	1	0.4258	0.1813	GI= 90.27 + 1.117(x)	**0.0151**
	2	-0.1247	1.55	GI= 102.82 – 0.445(x)	0.5355
	3	0.1066	1.14	GI= 103.91 + 0.353(x)	0.5359
Lt mandible first incisor	All	0.1788	3.20	GI= 93.31 + 1.451(x)	0.0782
	1	0.2781	7.74	GI= 92.13 + 0.753(x)	0.1232
	2	0.1543	2.38	GI= 97.86 + 0.513(x)	0.4155
	3	0.1429	2.04	GI= 101.77 + 0.719(x)	0.4056
Lt mandible second incisor	All	0.275	7.59	GI= 89.25 + 1.939(x)	**0.0041**
	1	0.1819	3.31	GI= 93.05 + 0.533(x)	0.2957
	2	0.2440	5.95	GI= 95.24 + 0.853(x)	0.1578
	3	0.3285	10.79	GI= 99.05 + 1.090(x)	**0.0471**
Lt mandible canine	All	0.1305	1.70	GI= 92.74 + 0.120(x)	0.1344
	1	0.2252	5.07	GI= 91.04 + 0.710(x)	0.1465
	2	0.0544	0.30	GI= 98.96 + 0.242(x)	0.7164
	3	0.1652	2.73	GI= 100.65 + 0.677(x)	0.2897
Lt mandible first molar	All	0.2088	4.36	GI= 86.15 + 1.309(x)	**0.0112**
	1	-0.0098	0.01	GI= 96.29 – 0.020(x)	0.9498
	2	0.3010	9.06	GI= 90.27 + 0.922(x)	0.0255
	3	0.2726	7.43	GI= 95.42 + 0.889(x)	0.0608
Bucco-Lingual					
Rt maxilla first molar	All	0.1505	2.26	GI= 89.36 + 1.015(x)	0.0634
	1	0.1232	1.52	GI= 92.86 + 0.290(x0	0.4146
	2	0.0715	0.51	GI= 97.91 + 0.246(x)	0.5971
	3	0.1906	3.63	GI= 97.95 + 0.665(x)	0.1850
Rt maxilla canine	All	0.2386	5.69	GI= 87.52 + 1.527(x)	**0.0039**
	1	0.0499	0.25	GI= 95.10 0.127(x)	0.7392
	2	0.1906	3.63	GI= 96.84 + 0.467(x)	0.1675
	3	0.2413	5.82	GI= 98.86 + 0.761(x)	0.1146
Rt maxilla second incisor	All	0.1894	3.59	GI= 91.35 + 1.413(x)	**0.0427**
	1	0.0121	0.01	GI= 95.99 + 0.037(x)	0.9433
	2	0.3130	9.80	GI= 94.16 + 1.001(x)	**0.0492**
	3	0.2764	7.64	GI= 100.01 + 0.787(x)	0.0929
Rt maxilla first incisor	All	0.3172	10.06	GI= 78.94 + 2.984(x)	0.0019
	1	-0.1264	1.60	GI= 99.62 – 0.482(x)	0.4904
	2	0.0560	0.31	GI= 98.37 + 0.338(x)	0.7607
	3	0.0939	0.88	GI= 103.02 + 0.298(x)	0.6280
Lt maxilla first incisor	All	0.2143	4.59	GI= 86.26 + 1.981(x)	**0.0450**
	1	-0.2240	5.02	GI= 102.76 – 0.960(x)	0.2256
	2	-0.3832	14.68	GI= 117.02 – 2.23(x)	**0.0485**
	3	0.3759	14.13	GI= 96.89 + 1.122(x)	**0.0406**
Lt maxilla second incisor	All	0.1295	1.68	GI= 93.79 + 1.035(x)	0.1924

	1	-0.0382	0.15	GI= 97.01 – 0.120(x)	0.8300
	2	0.0791	0.62	GI= 98.06 + 0.364(x)	0.6517
	3	0.1241	1.54	GI= 102.87 + 0.389(x)	0.4844
Lt maxilla canine	All	0.1795	3.22	GI= 91.10 + 1.110(x)	**0.0359**
	1	0.0206	0.04	GI= 95.76 + 0.044(x)	0.8945
	2	0.1859	3.45	GI= 94.43 + 0.703(x)	0.1962
	3	0.0682	0.47	GI= 103.81 + 0.199(x)	0.6637
Lt maxilla first molar	All	0.2485	6.18	GI= 81.26 + 1.709(x)	**0.0020**
	1	0.0300	0.09	GI= 95.31 + 0.070(x)	0.8429
	2	0.0242	0.06	GI= 99.70 + 0.090(x)	0.8595
	3	-0.0172	0.03	GI= 106.21 – 0.059(x)	0.9058
Rt mandible first molar	All	0.1087	1.18	GI= 91.36 + 0.913(x)	0.1914
	1	0.1014	1.03	GI= 92.74 + 0.324(x)	0.5230
	2	0.0131	0.02	GI= 100.31 + 0.049(x)	0.9250
	3	-0.0431	0.19	GI= 107.52 – 0.187(x)	0.7663
Rt mandible canine	All	0.1242	1.54	GI= 93.26 + 0.945(x)	0.1482
	1	-0.0634	0.40	GI= 97.33 – 0.155(x)	0.6789
	2	0.0959	0.92	GI= 97.81 + 0.355(x)	0.5169
	3	0.1472	2.17	GI= 100.43 + 0.639(x)	0.3403
Rt mandible second incisor	All	0.1711	2.93	GI= 90.52 + 1.672(x)	0.0780
	1	0.0829	0.69	GI= 94.11 + 0.319(x)	0.6465
	2	0.0568	0.32	GI= 98.86 + 0.234(x)	0.7422
	3	0.0105	0.01	GI= 105.45 + 0.060(x)	0.9499
Rt mandible first incisor	All	0.2578	6.64	GI= 85.27 + 2.651(x)	**0.0104**
	1	-0.0481	0.23	GI= 97.27 – 0.226(x)	0.7869
	2	-0.3585	12.85	GI= 108.85 – 1.427(x)	0.0663
	3	0.2183	4.76	GI= 98.03 + 1.286(x)	0.1943
Lt mandible first incisor	All	0.1307	1.71	GI = 95.36 + 0.937(x)	0.1996
	1	-0.2078	4.32	GI= 100.84 – 0.831(x)	0.2460
	2	0.1410	1.99	GI= 97.82 + 0.454(x)	0.4574
	3	-0.0313	0.10	GI= 106.23 – 0.094(x)	0.8582
Lt mandible second incisor	All	0.1662	2.76	GI= 90.77 + 1.611(x)	0.0785
	1	-0.0256	0.07	GI= 96.75 – 0.098(x)	0.8824
	2	0.1560	2.43	GI= 95.04 + 0.841(x)	0.3636
	3	0.2981	8.89	GI= 97.44 + 1.282(x)	0.0584
Lt mandible canine	All	0.1306	1.71	GI= 92.41 + 1.043(x)	0.1227
	1	0.0387	0.15	GI= 95.28 + 0.104(x)	0.7986
	2	0.1276	1.63	GI= 96.37 + 0.528(x)	0.3773
	3	0.3209	10.30	GI= 95.11 + 1.310(x)	**0.0316**
Lt mandible first molar	All	0.0471	0.22	GI= 96.97 + 0.364(x)	0.5708
	1	0.1129	1.28	GI= 92.61 + 0.325(x)	0.4655
	2	0.1203	1.45	GI= 96.09 + 0.427(x)	0.3816
	3	0.0112	0.01	GI= 105.00 + 0.045(x)	0.9397

[a] $p \leq 0.05$
[b] $p \leq 0.01$
[c] $p \leq 0.001$

APPENDIX C. Relationship between Gnathic Index (GI) cranial indices and molar areas for all individuals in the data set and orthognathic (1) mesognathic (2) and prognathic (3) groups.

Variable (x)	Group	Pearson Correlation Coefficient	R^2 x 100% Coefficient of Determination	Linear relationship	p- Value
Nasal index	All	-0.0426	0.18	GI= 102.81 – 0.036(x)	0.5902
	1	-0.0217	0.05	GI= 96.52 – 0.006(x)	0.8800
	2	-0.0013	0.00	GI= 100.84 – 0.0(x)	0.9923
	3	-0.0788	0.62	GI= 107.66 – 0.040(x)	0.5825
Orbital index	All	-0.0142	0.02	GI= 101.60 – 0.008(x)	0.8572
	1	0.0272	0.07	GI= 95.62 + 0.005(x)	0.8495
	2	-0.0067	0.00	GI= 100.95 – 0.001(x)	0.9596
	3	0.0464	0.22	GI= 104.10 + 0.015(x)	0.7463
Cranial index	All	-0.0526	0.28	GI= 104.70 – 0.055(x)	0.5075
	1	0.0176	0.03	GI= 95.57 + 0.008(x)	0.9026
	2	0.1774	3.15	GI= 93.37 + 0.104(x)	0.1751
	3	-0.1550	2.40	GI= 110.11 – 0.065(x)	0.2825
Cranial height index	All	-0.1306	1.71	GI= 109.26 – 0.118(x)	0.0986
	1	-0.4065	16.52	GI= 104.49 – 0.115(x)	**0.0031**
	2	0.0568	0.32	GI= 98.34 + 0.034(x)	0.691
	3	-0.0747	0.56	GI= 107.74 – 0.031(x)	0.6025
Vertical index	All	-0.0769	0.59	GI= 105.99 – 0.052(x)	0.3337
	1	-0.4107	16.86	GI= 104.52 – 0.082(x)	**0.0028**
	2	-0.1129	1.28	GI= 104.89 – 0.041(x)	0.3944
	3	0.1179	1.39	GI= 100.95 + 0.044(x)	0.4147
Frontoparietal index	All	0.0264	0.07	GI= 98.51 + 0.030(x)	0.7393
	1	0.0063	0.00	GI= 95.97 + 0.002(x)	0.9652
	2	-0.2774	7.69	GI= 112.42 – 0.157(x)	**0.0319**
	3	-0.1509	2.28	GI= 112.55 – 0.095(x)	0.2954
Zygomaticofrontal index	All	0.1040	1.08	GI= 91.19 + 0.127(x)	0.1890
	1	0.2290	5.24	GI= 89.02 + 0.095(x)	0.1060
	2	-0.1221	1.49	GI= 105.74 – 0.066(x)	0.3570
	3	-0.2503	6.26	GI= 119.23 – 0.180(x)	0.0765
Upper facial index	All	0.1673	2.80	GI= 91.47 + 0.176(x)	**0.0339**
	1	-0.1647	2.71	GI= 99.26 – 0.060(x)	0.2781
	2	0.1136	1.29	GI= 97.86 + 0.054(x)	0.3916
	3	-0.0054	0.00	GI= 105.66 – 0.003(x)	0.9702
Maxilla molar area Rt	All	0.1582	2.50	GI= 94.12 + 0.058(x)	0.0508
	1	-0.0056	0.00	GI= 96.12 – 0.0007(x)	0.9704
	2	0.0554	0.31	GI= 99.46 + 0.010(x)	0.6826
	3	0.1570	2.47	GI= 102.21 + 0.028(x)	0.2761
Maxilla molar area Lt	All	0.1825	3.33	GI= 92.69 + 0.069(x)	**0.0244**
	1	-0.0885	0.78	GI= 97.44 – 0.011	0.5586
	2	0.0640	0.41	GI= 99.29 + 0.012(x)	0.6391
	3	0.0797	0.64	GI= 103.69 + 0.015(x)	0.5821

Mandible molar Area Rt	All	0.1690	2.86	GI= 93.03 + 0.067(x)	**0.0414**
	1	-0.0238	0.06	GI= 96.56 – 0.003(x)	0.8808
	2	0.0401	0.16	GI= 9.96 + 0.007(x)	0.7732
	3	0.1809	3.27	GI= 100.87 + 0.038(x)	0.2087
Mandible molar area Lt	All	0.1489	2.22	GI= 94.50 + 0.052(x)	0.0719
	1	0.0592	0.35	GI= 95.18 + 0.007(x)	0.7026
	2	0.2382	5.67	GI= 95.90 + 0.039(x)	0.0799
	3	0.1661	2.76	GI= 101.71 + 0.031(x)	0.2591

[a]p≤0.05
[b]p≤0.01
[c]p≤0.001